

Doctoral Thesis

Species Delimitation in

Assassin Bug Genera *Biasticus*, *Rhynocoris*, and *Sphedanolestes*

(Hemiptera: Heteroptera: Reduviidae)

Known from Vietnam and Surrounding Areas.

ベトナムおよび周辺地域に生息する

Biasticus 属、*Rhynocoris* 属、*Sphedanolestes* 属 サシガメ類

(半翅目：異翅亜目：サシガメ科) の種判別 (英文)

Ha Ngoc Linh

2023

Abstract

The family Reduviidae Latreille, 1807, also known as assassin bugs, is the second most species-rich group assigned to the true bug suborder Heteroptera (Insecta: Hemiptera), with approximately 6,800 valid named species. This family is currently subdivided into 30 subfamilies by their morphology, dietary, and predation strategies. Among them, Harpactorinae is the most species-rich subfamily, with more than 2,700 species assigned to 7 tribes and more than 300 genera. They usually exhibit broader habitat and prey preferences. Some species are also dominant in cultivated lands of rice, soybean, peanut, coffee, tea, etc. Because reduviid species are active predators and some species are common in and around ecosystems, they are considered potential agents for biological control (pest control using natural enemies).

Although the idea of scaling up the use of reduviids in biological control has been proposed and taken experiments in laboratories for many years, there are still many obstacles and challenges. The species-level and higher classification of Harpactorinae species are far from complete and, therefore, basic knowledge on their distribution, habitat preference, prey preference, life history, reproduction, natural enemies, physiological and biochemical characteristics, etc. has not been accumulated for most species including potential biological control agents.

So far, 70 species in 35 genera of the subfamily Harpactorinae have been recognized in Indo-China. However, the number accounts just for approximately 2.4% of the total number of the validly named species of the subfamily, and it is likely that species diversities of Harpactorinae have been still underestimated in Indo-China, as well as other terrestrial invertebrate taxa.

As the first case study of revising the classification of the subfamily Harpactorinae, the present study aimed to reveal the species of the three genera *Biasticus* Stål, 1867, *Sphedanolestes* Stål, 1867, and *Rhynocoris* Hahn, 1834 from Vietnam and adjacent areas. The unclear boundaries among the species-rich genus *Biasticus* and its related genera *Sphedanolestes* and *Rhynocoris* seem to be

sources of taxonomic confusion at the species level. Therefore, by focusing on *Biasticus* and its close genera, *Sphedanolestes* and *Rhynocoris*, I aimed to clarify the boundary of the genera and discriminate the species of each genus by using a combination of morphological examination and molecular phylogenetic analyses.

In Chapter 3, as a result of this study, the three problematic genera, *Biasticus*, *Sphedanolestes*, and *Rhynocoris*, were assigned to six genera. The validity of the genus *Biasticus* was confirmed. On the other hand, the genus *Sphedanolestes* was proposed to be subdivided into at least three genera, and the genus *Rhynocoris* into at least two genera.

In Chapter 4, a total of 222 *Biasticus* and *Biasticus*-like specimens from Indo-China and surrounding areas were examined and assigned to 33 male-based and 58 female-based morphospecies based on their external and genital morphological characteristics. Of them, 15 male-based and 28 female-based morphospecies were involved in molecular phylogenetic analyses. As the results of the present integrative approach, 31 independent monophyletic lineages or singleton lineages were recovered with long basal branches and high supporting values and could be reasonably considered as “fully-recognized species.” Conspecific male and female combinations were also confirmed in 12 of the 31 species. In addition, there remain 18 male-based and 30 female-based morphospecies, of which at least some will be able to be confirmed as “fully-recognized species” through my future studies.

In Chapter 5, a total of 59 *Sphedanolestes* and *Sphedanolestes*-like specimens from Vietnam and Japan were examined, and four “fully-recognized species” were discriminated. As shown in Chapter 3, they were divided into three genera: the genus *Sphedanolestes* sensu stricto consisting of *S. impressicollis* with two intraspecific morphological forms which are distributed allopatrically (Vietnam and Japan), genus C consisting of “*S.*” *pubinotus* and one fully-recognized species (“gen. C” sp. HNL002), and genus D consisting of “*S.*” *xiongi*. Furthermore, two species, “*S.*” *gularis* and

“*S.*” *annulipes*, were proposed to be allocated to the genus *Blasticus* sensu stricto as mentioned in Chapter 4.

In Chapter 6, a total of 96 *Rhynocoris* and *Rhynocoris*-like specimens from Vietnam and surrounding areas were examined, and nine “fully-recognized species” were discovered. As shown in Chapter 3, the genus *Rhynocoris* was divided into two genera: genus E consisting of “*Rhynocoris*” *mendicus* with two intraspecific morphological forms, “*R.*” *marginellus* complex, and three other fully-recognized species, and genus F consisting of “*R.*” *fuscipes*. “*R.*” *marginellus* complex consists of four morphologically similar species.

This study highlighted that the species diversity of Harpactorinae in Indo-China seems to be still underestimated, and the present integrative taxonomy has great potential to solve the problems and obscurities involved in the current classification of Harpactorinae. Furthermore, it is also suggested that male genitalia have many morphological features useful for discriminating taxa in different taxonomic ranks such as genus and species. However, it is noted that there might be cases in which morphological examination based on male genitalia was not helpful to discriminate in species level, for example, genus D.

CONTENTS

Chapter 1: General Introduction	9
1.1.An Overview of the Assassin Bug Family Reduviidae Latreille, 1807	10
1.2.An Overview of the Sticky Trap Bugs Subfamily Harpactorinae Amyot and Serville, 1843	12
1.3.The Role of the Subfamily Harpactorinae as Natural Enemies in Cultivated Lands	13
1.4.Incomplete Classification of the Family Reduviidae and the Subfamily Harpactorinae in Indo- China	14
1.5. Purposes of the present study.....	16
References	17
Chapter 2: Materials And Methods	31
2.1. An Overview of the Subfamily Harpactorinae	32
2.2. An Overview of the Three Genera <i>Biasticus</i> , <i>Sphedanolestes</i> , and <i>Rhynocoris</i>	33
2.2.1. <i>Synopsis of the Genus Biasticus Stål, 1867 in Indo-China</i>	33
2.2.2. <i>Synopsis of the Genus Sphedanolestes Stål, 1867 in Indo-China</i>	34
2.2.3. <i>Synopsis of the Genus Rhynocoris Hahn, 1834 in Indo-China</i>	35
2.3. An Overview of the Research Area, the Indochinese Peninsula	36
2.4. Outline of the Research: How to Discriminate and Identify the Species.....	37
2.5. Specimen Preparation.....	38
2.6. Morphological Examination and Imaging	39
2.7. Molecular Data Preparation	40
2.8. Molecular Phylogenetic Analyses	41

2.9. Species Delimitation Analyses	41
2.10. Final Identification	42
References	42
Chapter 3: The Boundary of the Three Genera <i>Biasticus</i>, <i>Sphedanolestes</i>, And <i>Rhynocoris</i> and the Validity of Each Genus	83
3.1. Introduction	84
3.2. Material and Methods	84
3.2.1. <i>Specimens Examined</i>	84
3.2.2. <i>Molecular Phylogenetic Analyses</i>	85
3.3. Results	86
3.3.1. <i>Phylogenetic Analyses and DNA Barcoding</i>	86
3.3.2. <i>Evaluation of Examination of External and Genital Morphological Features in Female and the Male Adults</i>	86
3.4. Discussions	92
3.4.1. <i>Reclassification of the Genera <i>Biasticus</i>, <i>Sphedanolestes</i>, and <i>Rhynocoris</i></i>	92
3.4.2. <i>Usefulness of Integrated Taxonomy for Re-classifying the Inner Taxa of Harpactorinae</i>	94
References	95
Appendix: Definitions of the Six Genera Recognized by the Present Integrated Taxonomy .	112
<i>Biasticus</i> Stål, 1867	112
<i>Sphedanolestes</i> Stål, 1867, sensu stricto	113
Genus C	114
Genus D	116
Genus E	117

Genus F.....	119
Chapter 4: Discrimination of the Species of the Genus <i>Blasticus</i> (Hemiptera: Heteroptera: Reduviidae) Known from Vietnam and Surrounding Areas	121
4.1. Introduction.....	122
4.2. Material and Methods	122
4.3. Results.....	125
4.3.1. <i>Morphological Examination in the Male and Female Adults</i>	125
4.3.2. <i>Identities of the Morphospecies Based on the 16S + COI Phylogenetic Trees</i>	126
4.3.3. <i>Identities of the Morphospecies Based on the Uni-Minibar Phylogenetic Trees</i>	127
4.4. Discussion.....	127
4.4.1. <i>Full Recognition of the Species and Identification</i>	127
4.4.2. <i>Morphological Diagnostic Characteristics Reliable for Discriminating Species</i> ...	129
4.4.3. <i>Distribution and Biogeographical Criteria</i>	132
4.4.4. <i>The Future Prospect of This Study</i>	133
References	134
Appendix: Taxonomic accounts of the genus <i>Blasticus</i> found in Vietnam and surrounding areas	164
Chapter 5: Discrimination of the Species of the Genus <i>Sphedanolestes</i> sensu lato (Hemiptera: Heteroptera: Reduviidae) Known from Vietnam and Surrounding Areas	201
5.1. Introduction.....	202
5.2. Material and Methods	202
5.3. Results.....	206
5.3.1. <i>Morphological Examination in the Male and Female Adults</i>	206
5.3.2. <i>Identities of the Morphospecies Based on the 16S + COI Phylogenetic Trees</i>	206

5.4. Discussion	207
5.4.1. <i>Full Recognition of the Species and Identification</i>	207
5.4.2. <i>Distribution and Biogeographical Criteria</i>	209
5.4.3. <i>The Future Prospect of This Study</i>	209
References	209
Appendix: Taxonomic accounts of <i>Sphedanolestes</i> sensu lato found in Vietnam and surrounding areas.....	225
1. Taxonomic accounts of the genus <i>Sphedanolestes</i> Stål, 1867, sensu stricto found in Vietnam and surrounding areas	225
2. Taxonomic accounts of the genus C found in Vietnam and surrounding areas	226
3. Taxonomic accounts of the genus D found in Vietnam and surrounding areas	227
Chapter 6: Discrimination of the Species of the Genus <i>Rhynocoris</i> sensu lato (Hemiptera: Heteroptera: Reduviidae) Known from Vietnam and Surrounding Areas	229
6.1. Introduction	230
6.2. Material and methods	230
6.3. Results	233
6.3.1. <i>Morphological Examination in the Male and Female Adults</i>	233
6.3.2. <i>Identities of the Morphospecies Based on the 16S + COI Phylogenetic Trees</i>	234
6.4. Discussion	235
6.4.1. <i>Full Recognition of the Species and Identification</i>	235
6.4.2. <i>The Problem of Using Morphological Examination in Discrimination of Genus E</i> 237	
6.4.3. <i>Distribution and Biogeographical Criteria</i>	237
6.4.4. <i>The Future Prospect of This Study</i>	238
References	239

Appendix: Taxonomic accounts of the genus <i>Rhynocoris</i> sensu lato found in Vietnam and surrounding areas	258
1. Taxonomic accounts of the genus E found in Vietnam and surrounding areas	258
2. Taxonomic accounts of the genus F found in Vietnam and surrounding areas.....	264
Chapter 7: General Discussion	265
7.1. The Validity of the Three Genera <i>Biasticus</i> , <i>Sphedanolestes</i> , and <i>Rhynocoris</i>	266
7.2. Morphological Characters Useful in the Classification of Harpactorinae	266
7.3. Notes on the Diversification of Genital Morphology in the Examined Genera.....	268
7.4. Distribution Pattern of Indo-Chinese Species of the Three Genera <i>Biasticus</i> , <i>Sphedanolestes</i> , and <i>Rhynocoris</i>	269
7.5. The Male and Female Imbalance among Harpactorinae Species.....	271
7.6. Prospects of the Taxonomy of Harpactorinae and Other Reduviids	272
References	274

CHAPTER 1:
GENERAL INTRODUCTION

1.1. An Overview of the Assassin Bug Family Reduviidae Latreille, 1807

The family Reduviidae Latreille, 1807, also known as assassin bugs, is the second most species-rich group assigned to the true bug suborder Heteroptera (Insecta: Hemiptera), with approximately 6,800 valid named species (Maldonado 1990; Froeschner et al. 1989; Hwang and Weirauch 2012). This family has been recorded worldwide and is exceptionally species-rich in the tropical regions of Palearctic, Afrotropical, Oriental, Sino-Japanese realms of the Old World and Nearctic, Panamanian, and Neotropical realms of the New World (Maldonado 1990; Weirauch et al. 2014). According to the current classification of Heteroptera (Panizzi and Grazia 2015), the members of the family Reduviidae can be distinguished from others by the combination of the following characteristics: elongated head; three-segmented labium that the apical segment fits into stridulatory sulcus, which is a central groove on the prosternum; raptorial front legs covered with setose and spines for catching prey; abdomen wider than the rest of the body and extend beyond the width of the wings (Figs 1.1-1.2). The unique behavioral characteristic of the family is the vibroacoustic signal produced by rubbing the third visible labial segment to the stridulatory sulcus, often used for discouraging enemies and /or disrupting prey's movement (Schmidt 1994; Roces & Manrique 1996; Reyes-Lugo et al. 2006; Goula 2008; Quiroga et al. 2019).

Regarding the classification of Reduviidae, the family Reduviidae is currently subdivided into 30 subfamilies by their morphology, dietary, and predation strategies. The subfamilies are listed as the following: Apiomerinae Amyot and Serville 1843, Bactrodinae Stål, 1866, Centrocnemidinae Miller, 1956, Cetherinae Jeannel, 1919, Chryxinae Champion, 1898, Ectinoderinae Stål, 1866, Ectrichodiinae Amyot and Serville, 1843, Elasmodeminae Lethierry and Severin, 1896, Emesinae Amyot and Serville, 1843 (spider web-inhabiting thread-legged bugs), Epiroderinae Distant, 1904, Hammacerinae Stål, 1859, Harpactorinae Amyot and Serville, 1843 (sticky trap bugs), Holoptilinae Lepeletier and Serville, 1825 (ant-luring feather-legged bugs), Manangocorinae Miller, 1954,

Microtominae Schumacher, 1924, Peiratinae Amyot and Serville, 1843, Phimophorinae Handlirsch, 1897, Phonolibinae Miller, 1952, Phymatinae Laporte, 1832 (ambush bugs), Physoderinae Miller, 1954, Pseudocetherinae Villiers, 1963, Reduviinae Latreille, 1807, Saicinae Stål, 1859, Salyavatinae Amyot and Serville, 1843 (termite-feeding), Sphaeridopinae Pinto, 1927, Stenopodainae Amyot and Serville, 1843, Triatominae Jeannel, 1919 (kissing bugs or blood-feeding bugs), Tribelocephalinae Stål, 1866, Vesciinae Fracker and Bruner, 1924, Visayanocorinae Miller, 1952 (Maldonado 1990).

Reduviid species exhibit diversity in habitats, dietary (prey items), and predation strategies. Assassin bugs exist in various terrestrial ecosystems and microhabitats, ranging from forests and agricultural and industrial fields to human settlements. While almost all Harpactorinae (Reduviidae) and Salyavatinae (Reduviidae) can be easily found in shrubbery and understory levels, and most species are active in the daytime, members of Physoderinae (Reduviidae) are found in the forest floor, especially under leaf litters, under or inside the decaying woods and some species are active at night (Hwang and Weirauch 2017).

Most species and lineages are considered generalists, which feed on a variety of insects (Ambrose 1999; Ambrose 2003; Hwang and Weirauch 2012; Truong and Ha 2017), while some species lineages exhibit prey specialization in association with their habitat preference. For example, some thread-legged bugs (Reduviidae: Emesinae) prefer to steal spiders' prey from spider webs (Soley et al. 2011). Hundreds of Ectrichodiinae species appear to be specialized millipede predators; numerous species of Peiratinae are fond of beetles and grasshoppers; many Harpactorinae species are partial to caterpillars, termites and some other insect groups with soft cuticles; several Reduviinae species have a preference with ants, bees, and termites; and many Emesinae species prey mainly on flies (Ambrose 2003; Wang et al. 2020). Besides, one of the most infamous groups of assassin bugs is Triatominae, which is widely known as conenose bugs, kissing bugs, or sucking bugs. They feed on vertebrate blood; some species feed on human blood (Lent and Wygodzinsky 1979) and mediate

Trypanosoma cruzi, the parasite that causes Chagas disease (Bern et al. 2011).

The diverse predator strategies and predatory behaviors of reduviid species are also pronounced by many previous studies. For instance, many members of the subfamilies Apiomerinae and Ectrichodiinae have been reported with a strategy of sticky-trapping prey by extending their resin-coated fore tibia toward the prey; some species of Emesinae spy and capture the prey by their front thread-legs which are covered by spines and tubercles; species of Reduviinae, Salyavatinae, and Stenopodainae watch and grab their prey when appropriate; species of Harpactorinae pin and jab the prey by their long and sturdy labium; while some species of Peiratinae, Reduviinae, and Ectrichodiinae pursue and capture the prey by their well-developed tibial pads (Ambrose 1999, 2003; Claver and Ambrose 2001b).

1.2. An Overview of the Sticky Trap Bugs Subfamily Harpactorinae Amyot and Serville, 1843

Among the subfamilies of Reduviidae, Harpactorinae Amyot et Serville, 1843 is the most species-rich subfamily with more than 2,700 species assigned to 7 tribes, i.e., Apiomerini, Diaspidiini, Dicrotelini, Ectinoderini, Harpactorini, Rhaphidosomini, and Tegeini, and more than 300 genera (Davis 1969; Schuh and Slater 1995; Miller 1954; Tomokuni and Cai 2002; Weirauch et al. 2014). Ishikawa (2003) and Weirauch et al. (2014) define the subfamily by a combination of the following characteristics: antecular area of head dorsomedially with short, longitudinal sulcus posteriorly; postocular area of head cylindrical, often globose in anterior part; ocelli located dorsally; antennae generally long, with scape longest of all segments and usually longer than head; labium curved inwards with 3 visible segments; second visible labial segment never curved outwards; quadrate cell on the corium formed by the cubitus; membranes of hemelytra generally glossy; well-developed subapical spur on the foretibia that carries the foretibial comb; tarsi 2 or 3-segmented; paramere simple in form, sometimes rod-shaped, rarely lacking (Fig. 1.3).

Harpactorinae has been known from the five continents (except Antarctica) and from major terrestrial ecosystems and is especially species-rich in tropical and subtropical regions. They usually exhibit a broader habitat preference and prey on a wide range of animals. Some species are also dominant in cultivated lands of rice, soybean, peanut, coffee, tea, etc., and thus have the potentials to be used as native natural enemies of agricultural pests (Ambrose 1999, 2003).

1.3. The Role of the Subfamily Harpactorinae as Natural Enemies in Cultivated Lands

Because reduviid species are active predators and some species are common in and around ecosystems, they are considered to be potential biocontrol agents with the following valuable features: a limited range of plants (and crops) on which the bugs ambush to capture their prey; positive functional and numerical response to pests; good host-searching efficiency; multiply faster with a high fecundity; short life cycle; female-biased population; possess good pest suppression efficacy; amenable for mass-culturing in the laboratory; adaptability to new environmental condition; and primarily free from parasites or parasitoids (Ambrose 2003).

Numerous studies have elucidated the preferences in prey taxa and their stages for nearly 200 reduviid species (Ambrose 1999, Ambrose 2003). Among them, many species of the harpactorine genera *Coranus* Curtis, 1883, *Rhynocoris* Hahn, 1834, e.g., *R. fuscipes* (Fabricius, 1787), *R. kumarii* Ambrose et Livingstone, 1986 and *R. marginatus* (Fabricius, 1794), *Sphedanolestes* Stål, 1866 and *Sycanus* Amyot et Serville, 1843, as well as the peiratine *Ectomocoris tibialis* Distant, 1904 and the reduviine *Acanthaspis pedestris* Stål, 1863 prey upon a broader range of agricultural pests on cotton, vegetables, castor, groundnut, and cereals. Furthermore, it is also known that assassin bugs can also exhibit positive functional and numeral responses to the various conditions of prey density and spatial structure (heterogeneity) by controlling their intensity of assassinating the number of prey or by changing their population size (Ambrose 1999, 2003; Omkar, 2016). Such a response represents

the high adaptability of reduviids and the potential to use in biological control (Ambrose 2003). Therefore, the idea of scaling up the use of reduviids in biological control has been proposed and taken experiments in laboratories for many years.

There are, however, still many obstacles and challenges (Edwards 1962; Van den Bosch and Telford 1964; Ables 1978; Ambrose 1980, 1987, 1988, 1991, 1995, 1996, 1999, 2000, 2002; Abasa 1981; Tawfik et al. 1983a, 1983b; Lakkundi and Parshad 1987; Babu et al. 1995; Grundy 2007; Tomson et al. 2017; etc.). The species-level and higher classification of the family Reduviidae are far from complete and, therefore, basic knowledge on their distribution, habitat preference, prey preference, life history, reproduction, natural enemies, physiological and biochemical characteristics, etc. has not been accumulated for most species including potential biological control agents. In other words, taxon names do not function as keywords for information storage and retrieval.

Some “species” are known to exhibit remarkable variations or flexibilities in biological features relevant to their potential uses as biological control agents (Ambrose 2003). For example, the brownish orange form of *Rhynocoris marginatus* (Fabricius, 1794) has more hunting efficiency and a higher ability to be insecticide-resisting than the sanguineous and the blackish red form (Sahayaraj and Ambrose 1996a; Ambrose 1999, 2003; George 1999a, 1999b, 2000a, 2000b). However, the conspecificity of such forms or the existence of unnoticed species currently assigned to a single valid species name needs to be confirmed by further studies.

1.4. Incomplete Classification of the Family Reduviidae and the Subfamily Harpactorinae in Indo-China

Despite the usefulness and fascination of Reduviidae and Harpactorinae as potential biological control agents in agriculture and forestry, the less-developed species-level and higher classifications are a significant obstacle to basic and applied research of reduviids. The current classification of

Reduviidae species is still largely morphology-based and poorly and less comprehensively revised by modern approaches such as phylogenetics and species delimitation analyses using DNA sequence data. Thus, taxonomic obscurities and confusions in species recognition have been caused by cases of the cryptic species complex (Panzera et al. 2015; Zhao et al. 2021) (see also Chapter 6), male-female dimorphism in a single species (Kwadjo et al. 2010; Forthman 2017; Gil-Santana 2017; Weirauch et al. 2017; Chen et al. 2021), and remarkable morphological polymorphism or variation among conspecific populations or seasonal generations (Stål 1867; Distant 1903; Moreno et al. 2006; Rivas et al. 2021; Vilaseca et al. 2021). Moreover, recent studies using molecular phylogenetic analyses have provided phylogenetic hypotheses or presumptions that claim the necessity of reexaminations of the boundaries of many genera and subfamilies in the current classification of the family (Weirauch and Munro 2009; Hwang and Weirauch 2012). For example, according to Weirauch and Munro (2009), it is remarkable that the monophyly of subfamilies Reduviinae, Stenopodainae, and Emesinae were not supported. Ignore the case of insufficient sampling, there were at least three subfamilies that should be re-examined (Fig. 1.4). Therefore, future studies with more representatives of subfamilies and genera might recognize more issues of the current taxonomy of Reduviidae.

With the subfamily Harpactorinae, the boundaries of genera, intergeneric relationships, and species recognition in each genus also need to be revised with comprehensive phylogenetic analyses (Zhang and Weirauch 2013; Hwang and Weirauch 2017). Taxonomic over-splitting of a single phenotypically diverse species might remain (Nascimento et al. 2019), while many species have not yet been discovered or taxonomically recognized, especially in the world's tropics and subtropics (Hwang and Weirauch 2017).

The Indo-Chinese peninsula is located on the boundary between the Oriental and Sino-Japanese realms (Chen et al. 2008; Holt et al. 2013) and involves various bioclimate zones, such as

tropical, subtropical, and temperate zones characterized by different levels of rainfall and seasonality, because of its up-down topology (Phan et al. 2009). Meta-analyses of geological, paleoclimatic, and phylogeographic data sets revealed that Indo-China and Borneo had produced new lineages of animals and plants and supplied them to the surrounding areas since the early Miocene (de Bruyn et al. 2014). Especially, Truong Son Mountain Range and Tay Nguyen Plateau laid on the border between Vietnam and Laos/Cambodia is thought to be one of the centers of species diversity, endemism, and relictness of terrestrial organisms in the Oriental realm (Mittermeier et al. 2011; de Bruyn et al. 2014).

So far, 70 species in 35 genera of the subfamily Harpactorinae have been recognized in Indo-China (Stål 1863; Truong et al. 2015; Truong et al. 2020; Ha et al. 2022). However, the number accounts just for approximately 2.4% of the total number of the validly named species of the subfamily, and it is likely that species diversities of Harpactorinae have been still underestimated in Indo-China, as well as other terrestrial invertebrate taxa. Therefore, the author sets a long-term project for revising the classification of the family Reduviidae in Indo-China, which has been established primarily based on morphological information.

1.5. Purposes of the present study

As the first case study of the long-term project of revising the classification of the family Reduviidae, the present study aimed to reveal the species of the three harpactorine genera *Biasticus* Stål, 1867, *Sphedanolestes* Stål, 1867, and *Rhynocoris* Hahn, 1834 from Indo-China and adjacent areas by using a combination of conventional morphological examination and molecular phylogenetic analyses.

The present thesis is comprised of seven chapters, including this one (Chapter 1). In Chapter 2, an overview of the subfamily Harpactorinae and the three target genera, and the research area are

given; and the materials and methods used in the present study are also explained in detail. In Chapter 3, the boundaries of the three target genera are revised using a combination of molecular phylogenetic analyses and conventional morphological examination. In Chapters 4 to 6, the species of each target genus from Vietnam and surrounding areas are revised by an integrative taxonomic approach. Finally, Chapter 7 summarize the validity of the three genera, some useful morphological features for the classification of the subfamily Harpactorinae and distribution patterns of species in Indo-China.

References

1. Abasa RO (1981) *Harpactor tibialis* Stål (Hemiptera) insect pests and their arthropod parasites and predators. Biology and management of rice insects. Wiley Eastern Ltd., New Delhi, India, 13–359.
2. Ables JR (1978) Feeding behaviour of an assassin bug, *Zelus renardii*. Annals of the Entomological Society of America 71: 476–478.
3. Ambrose DP (1980) Bioecology, ecophysiology and ethology of reduviids (Heteroptera) of the scrub jungles of Tamil Nadu, India. Ph.D. Thesis, University of Madras, Madras, India.
4. Ambrose DP (1987) Assassin bugs of Tamil Nadu and their role in biological control (Insecta: Heteroptera: Reduviidae). Advances in biological control research in India. Department of Zoology, University of Calicut, Calicut, India. 16–28.
5. Ambrose DP (1988) Biological control of insect pests by augmenting assassin bugs (Insecta; Heteroptera: Reduviidae). Bicovas II, Loyola College, Madras, India, 25–40.
6. Ambrose DP (1991) Conservation and augmentation of predaceous bugs and their role in biological control. Advanced in Management and conservation of soil fauna. Oxford & IBH Publication Co. Pvt. Ltd., New Delhi, India, 225–257.

7. Ambrose DP (1995) Reduviids as predators: Their role in biological control. Biological control of social forests and plantation crop insects. Oxford & IBH Publication Co. Pvt. Ltd., New Delhi, India, 153–170.
8. Ambrose DP (1996) Assassin bugs (Insecta: Heteroptera-Reduviidae) in biocontrol: success and strategies, a review. Biological and cultural control of insect pests, an India scenario, Adeline Publishers, 262–284.
9. Ambrose DP (1999) Assassin Bugs. Science Publishers, Enfield, NH.
10. Ambrose DP (2000) Assassin bugs (Reduviidae excluding Triatominae). In: Heteroptera of economic importance. CRC Press, LLC, Florida, U.S.A.
11. Ambrose DP (2002) Assassin bugs (Heteroptera: Reduviidae) in Intergrated pest management programme: Success and strategies. Strategies in intergrated pest management: current trends and future prospects. Phoenix Publishing House, New Delhi, India, 73–85.
12. Ambrose DP (2003) Biocontrol potential of assassin bugs (Hemiptera: Reduviidae). J. Exp. Zool. India. Vol 6, No. 1: 1–44.
13. Amyot CJB, Serville A (1843) Histoire naturelle des insectes; Hemipteres. Histoire naturelle des insectes Hemipteres. Paris: Fain et Thunot., 675 pp.
14. Babu A, Seenivasagam R, Karuppasamy C (1995) Biological control resources in social forest stands. Biological control of social forest and plantation crop insects. Oxford & IBH Publication Co. Pvt. Ltd., New Delhi, India, 7–24.
15. Bern C, Kjos S, Yabsley ML, Montgomery SP (2011) *Trypanosoma cruzi* and Chagas' Disease in the United States. Clinical microbiology reviews, Oct. 2011, p. 655–681. <https://doi.org/10.1128%2FCMR.00005-11>
16. Chen L, Song Y, Xu S (2008) The boundary of palaeartic and oriental realms in western China. Progress in Natural Science 18: 833–841. <https://doi.org/10.1016/j.pnsc.2008.02.004>

17. Chen Z, Liu Y, Cai W (2021). Taxonomic review of *Xenorhyncocoris* Miller (Heteroptera: Reduviidae: Ectrichodiinae), with description of *X. attractivus* sp. nov. and notes on sexual dimorphism of the genus. *European Journal of Taxonomy* 746(1): 26–49. <https://doi.org/10.5852/ejt.2021.746.1315>
18. Claver MA, Ambrose DP (2001) Impact of antennectomy, eye blinding and tibia comb coating on the predatory behaviour of *Rhynocoris kumarii* Ambrose and Livingstone (Het., Reduviidae) on *Spodoptera litura* Fabr. (Lep., Noctuidae). *Journal of Applied Entomology* 125: 519–525.
19. Davis NT (1969) Contribution to the morphology and phylogeny of the Reduvidae (Hemiptera: Heteroptera). Part IV. The harpactoroid complex. *Annals of the Entomological Society of America*, 62, 74–94.
20. de Bruyn M, Stelbrink B, Morley RJ, Hall R, Carvalho GR, Cannon CH, van den Bergh G, Meijaard E, Metcalfe I, Boitani L, Maiorano L, Shoup R, von Rintelen T (2014) Borneo and Indochina are major evolutionary hotspots for Southeast Asian biodiversity. *Systematic Biology* 63: 879–901. <https://doi.org/10.1093/sysbio/syu047>
21. Distant WL (1903) Rhynchotal notes. XVI. Heteroptera: Family Reduviidae (continued). *The Annals and Magazine of Natural History* (7)11: 203–213.
22. Du Z, Ishikawa T, Liu H, Kamitani S, Tadauchi O, Cai W, Li H (2019) Phylogeography of the assassin bug *Sphedanolestes impressicollis* in East Asia inferred from mitochondrial and nuclear gene sequences. *International Journal of Molecular Sciences*, 20: 1234. <https://doi.org/10.3390/ijms20051234>
23. Edwards JS (1962) Observations on the development and predatory habits of two reduviids (Heteroptera), *Rhynocoris carmelita* Stål and *Platrymeris rhadamanthus* Gerst. *Proceedings of the Royal Entomological Society of London (A)* 37: 89–98.

26. Forthman M, Weiwauch C (2017) Millipede assassins and allies (Heteroptera: Reduviidae: Ectrichodiinae, Tribelocephalinae): total evidence phylogeny, revised classification and evolution of sexual dimorphism. *Systematic Entomology* 42(3):575–595. <https://doi.org/10.1111/syen.12232>
27. Froeschner RC, Kormilev NA (1989) Phymatidae or ambush bugs of the world: a synonymic list with keys to species, except *Lophoscutus* and *Phymata* (Hemiptera). *Entomography* 6: 1–76.
28. George PJE (1999a) Development, life table and intrinsic rate of natural increase of three morphs of *Rhynocoris marginatus* (Fabricius) (Heteroptera: Reduviidae) on cotton leaf worm *Spodoptera litura* (Fabricius) (Lepidoptera: Noctuidae). *Entomon* 24: 339–343.
29. George PJE (1999b) Biology and life table studies of the reduviid *Rhynocoris marginatus* (Fabricius) (Heteroptera: Reduviidae) on three lepidopteran insect pests. *Journal of Biological Control* 13: 33–38.
30. George PJE (2000a) Life tables and intrinsic rate of natural increase of three morphs of *Rhynocoris marginatus* (Fabricius) (Heteroptera: Reduviidae) on *Corcyra cephalonica* Stainton. *Journal of Experimental Zoology India* 3: 59–63.
31. George PJE (2000b) Polymorphic adaptation in reproductive strategies of *Rhynocoris marginatus* (Fabricius) on *Earias vitelli* (Fabricius). *Journal of Biological Control* 14: 35–39.
32. Gil-Santana HR, Salomão AT, Oliveira J (2017) First description of the male and redescription of the female of *Parahiranetis salgadoi* Gil-Santana (Hemiptera, Reduviidae, Harpactorinae). *ZooKeys* 671: 19–48. <https://doi.org/10.3897/zookeys.671.11985>
33. Goula M (2008) Acoustical Communication in Heteroptera (Hemiptera: Heteroptera). In: Capinera, J.L. (eds) *Encyclopedia of Entomology*. Springer, Dordrecht. https://doi.org/10.1007/978-1-4020-6359-6_34

34. Grundy, P. (2007). Utilizing the assassin bug, *Pristhesancus plagipennis* (Hemiptera: Reduviidae), as a biological control agent within an integrated pest management programme for *Helicoverpa* spp. (Lepidoptera: Noctuidae) and *Creontiades* spp. (Hemiptera: Miridae) in cotton. *Bulletin of Entomological Research*, 97(3), 281–290.
<https://doi.org/10.1017/s0007485307004993>
35. Ha NL, Truong XL, Ishikawa T, Jaitrong W, Lee CF, Chouangthavy B, Eguchi K (2022) Three new species of the genus *Biasticus* Stål, 1867 (Insecta, Heteroptera, Reduviidae, Harpactorinae) from Central Highlands, Vietnam. *ZooKeys* 1118: 133–180.
<https://doi.org/10.3897/zookeys.1118.83156>
36. Holt BG, Lessard JP, Borregaard MK, Fritz SA, Araújo MB, Dimitrov D, Fabre PH, Graham CH, Graves GR, Jønsson KA, Nogués-Bravo D, Wang Z, Whittaker RJ, Fjeldså J, Rahbek C (2013) An Update of Wallace’s Zoogeographic Regions of the World. *Science* 339: 74–78.
<https://doi.org/10.1126/science.1228282>
37. Hwang WS, Weirauch C (2012) Evolutionary History of Assassin Bugs (Insecta: Hemiptera: Reduviidae): Insights from Divergence Dating and Ancestral State Reconstruction. *PLoS ONE* 7(9): e45523. <https://doi.org/10.1371/journal.pone.0045523>
38. Hwang WS, Weirauch C (2017) Uncovering hidden diversity: phylogeny and taxonomy of Physoderinae (Reduviidae, Heteroptera), with emphasis on *Physoderes* Westwood in the Oriental and Australasian regions. *European Journal of Taxonomy* 341: 1–118.
<https://doi.org/10.5852/ejt.2017.341>
39. Kwadjo KE, Doumbia M, Haubruge E, Kra KD, Tano Y (2010) Sexual dimorphism in adults of *Rhynocoris albopilosus* Signoret (Heteroptera: Reduviidae). *Journal of Applied Biosciences* 2010 Vol.30: 1873–1877.

40. Lakkundi NH, Parshad B (1987) A technique for mass multiplication of predator with sucking type of mouth parts with special reference to reduviids. *Journal of Soil Biology and Ecology* 7: 65–69.
41. Latreille PA (1807) *Genera crustaceorum et insectorum: secundum ordinem natrualem in familias disposita, iconibus exemplisque plurimis explicata. Tomus tertius. Amand Koenig, Parisiis et Argentorati, Paris. Vol. 3: 1–399.*
42. Lent H, Wygodzinsky P (1979) Revision of the Triatominae (Hemiptera, Reduviidae), and their significance as vectors of Chagas' disease. *Bulletin of the American Museum of Natural History* 163: 123–520.
43. Maldonado-Capriles J (1990) Systematic catalogue of the Reduviidae of the world (Insecta: Heteroptera). A special edition of *Caribbean Journal of Science*, Puerto Rico.
44. Miller N. C. E. (1954) New genera and species of Reduviidae from Indonesia and the description of a new subfamily (Hemiptera-Heteroptera). *Tijds. Ent.*, 97: 75–114.
45. Mittermeier RA, Turner WR, Larsen FW, Brooks TM, Gascon C (2011) *Global Biodiversity Conservation: The Critical Role of Hotspots. Biodiversity Hotspots. Springer, Berlin, Heidelberg.*
http://dx.doi.org/10.1007/978-3-642-20992-5_1
46. Moreno ML, Gorla D, Catalá S (2006) Association between antennal phenotype, wing polymorphism and sex in the genus *Mepraia* (Reduviidae: Triatominae). *Infection, Genetics and Evolution* Vol. 6, Issue 3: 228–234. <https://doi.org/10.1016/j.meegid.2005.06.001>
47. Nascimento JD, da Rosa JA, Salgado-Roa FC, Hernández C, Pardo-Diaz C, Alevi KCC, Ravazi A, de Oliveira J, de Azeredo Oliveira MTV, Salazar C, Ramírez JD (2019) Taxonomical over splitting in the *Rhodnius prolixus* (Insecta: Hemiptera: Reduviidae) clade: Are *R. taquarussuensis* (da Rosa et al., 2017) and *R. neglectus* (Lent, 1954) the same species? *PLoS One* 14 (2): e0211285. <https://doi.org/10.1371/journal.pone.0211285>

48. Omkar O (2016) Ecofriendly Pest Management for Food Security. Elsevier Science, Netherland.
<https://doi.org/10.1016/C2014-0-04228-1>
49. Panizzi AR, Garzia J (2015) Chapter 1: Introduction to True Bugs (Heteroptera) of the Neotropics. In: Panizzi AR, Garzia J (Eds.), True bugs (Heteroptera) of the Neotropics, Vol. 2 (pp. 3–20). Dordrecht, the Netherlands: Springer Science+Business Media.
50. Panzera F, Pita S, Nattero J, panzera Y, Galvão C, Chavez T, Rojas De Arias A, Téllez LC, Noireau F (2015) Cryptic speciation in the *Triatoma sordida* subcomplex (Hemiptera, Reduviidae) revealed by chromosomal markers. *Parasites Vectors* **8**, 495 (2015).
<https://doi.org/10.1186/s13071-015-1109-6>
51. Phan VT, Ngo-Duc T, Ho TMH (2009) Seasonal and interannual variations of surface climate elements over Vietnam. *Climate Research* 40(1): 49–60. <http://dx.doi.org/10.3354/cr00824>
52. Reyes-Lugo M, Díaz-Bello Z, Abate T, Avilán A (2006) Stridulatory sound emission of *Panstrongylus rufotuberculatus* Champion, 1899, (Hemiptera: Reduviidae: Triatominae). *Brazilian Journal of Biology* 66 (2a): 443–446. <https://doi.org/10.1590/S1519-69842006000300009>
53. Rivas N, Sánchez-Cordero V, Camacho AD, Alejandre-Aguilar R (2021) Morphological and Chromatic Variation in Four Populations of *Triatoma mexicana* (Hemiptera: Reduviidae). *Journal of Medical Entomology* Vol. 58, Issue 1: 274–285. <https://doi.org/10.1093/jme/tjaa176>
54. Roces F, Manrique G (1996) Different stridulatory vibrations during sexual behaviour and disturbance in the blood-sucking bug *Triatoma infestans* (Hemiptera: Reduviidae). *Journal of Insect Physiology* Volume 42, Issue 3: 231–238. [https://doi.org/10.1016/0022-1910\(95\)00099-2](https://doi.org/10.1016/0022-1910(95)00099-2)

55. Sahayaraj K, Ambrose DP (1996) Biocontrol potential of the reduviid predator *Neohaematorrhophus therasii* Ambrose and Livingstone (Heteroptera: Reduviidae). *Journal Of Advanced Zoology* 17: 49–53.
56. Schaefer CW (1988) Reduviidae (Hemiptera: Heteroptera) as agents of biological control. In: K.S. Ananthasubramanian, P. Venkatesan and S. Sivaraman, [eds.], *Bicovas I*, Loyola College, Madras. 22–33.
57. Schmidt JM (1994) Encounters between adult spined assassin bugs, *Sinea diadema* (F.) (Hemiptera: Reduviidae): The occurrence and consequences of stridulation. *Journal of Insect Behavior* 7 (6): 811–828. <https://doi.org/10.1007/BF01997128>
58. Schuh RT, Slater JA (1995) *True Bugs of the World (Hemiptera: Heteroptera): Classification and Natural History*. Comstock Pub. Associates, Ithaca. 336.
59. Soley FG, Jackson RR, Taylor PW (2011) Biology of *Stenolemus giraffa* (Hemiptera: Reduviidae), a web invading, araneophagic assassin bug from Australia. *New Zealand Journal of Zoology* 38: 297–316. <https://doi.org/10.1080/03014223.2011.604092>
60. Stål C (1863) *Formae speciesque novae Reduviidum*. *Annales de la Société entomologique de France* 3: 38.
61. Stål C (1867) *Bidrag till Reduviidarnas kaennedom. Öfversigt af Kongl. Vetenskaps-akademiens forhandlingar* 23, 235–302.
62. Tawfik MFS, Awadallah KT, Abdullah MMH (1983a) Effect of prey on various stages of the predator, *Alloeocranum biannulipes* (Montr. et Sign.) (Hemiptera: Reduviidae). *Bulletin of the Entomological Society of Egypt* 64: 251–258.
63. Tawfik MFS, Awadallah KT, Abozeid NA (1983b) The biology of the reduviid *Alloeocranum biannulipes* (Montr. et Sign.) a predator of stored-product insects. *Bulletin of the Entomological Society of Egypt* 64: 231–237.

64. Tomokuni M, Cai W (2002) Type materials of the Reduviidae (Heteroptera) described by S. Matsumura, with notes on their taxonomy and nomenclature. *Insecta matsumurana*. New series: journal of the Faculty of Agriculture Hokkaido University, series entomology, 59: 101–108.
65. Tomson M, Sahayaraj K, Kumar V, Avery PB, McKenzie CL, Osborne LS. Mass rearing and augmentative biological control evaluation of *Rhynocoris fuscipes* (Hemiptera: Reduviidae) against multiple pests of cotton. *Pest Manag Sci*. 2017 Aug;73(8):1743–1752. <https://doi.org/10.1002/ps.4532>.
66. Truong XL, Cai WZ, Tomokuni M, Ishikawa T (2015) The assassin bug subfamily Harpactorinae (Hemiptera: Reduviidae) from Vietnam: an annotated checklist of species. *Zootaxa*, ISSN: 1175-5326:101–116. <https://doi.org/10.11646/zootaxa.3931.1.7>
67. Truong XL, Ha NL (2017) Composition and diversity of assassin bugs belong subfamily Harpactorinae (Heteroptera: Reduviidae) in some habitats in Kon Chu Rang natural reserve, Gia Lai province. *Proceedings of the 7th National Scientific Conference on Ecology and Biological Resources*. Hanoi 2017: 763.
68. Truong XL, Bui TQH, Ha NL, Cai W (2020) A new species of the assassin bug genus *Rihirbus* (Hemiptera: heteroptera: Reduviidae) from Vietnam. *Zootaxa* 4780 (3): 587–593. <https://doi.org/10.11646/zootaxa.4780.3.10>
69. Van den Bosch R, Telford AD (1964) Environmental modification and biological control. In: P. DeBach [ed.], *Biological control of insect pests and weeds*. Chapman and hall, Ltd. London, UK, 8–44.
70. Vilaseca C, Méndez MA, Pinto CF, Lemic D, Benítez HA (2021) Unraveling the Morphological Variation of *Triatoma infestans* in the Peridomestic Habitats of Chuquisaca Bolivia: A Geometric Morphometric Approach. *Insect* 12(2):185. <https://doi.org/10.3390/insects12020185>

71. Wang Y, Zhang J, Wang W, Brozek J, Dai W (2020) Unique Fine Morphology of Mouthparts in *Haematoloecha nigrorufa* (Stål) (Hemiptera: Reduviidae) Adapted to Millipede Feeding. *Insects* 2020, 11, 386. <https://doi.org/10.3390/insects11060386>
72. Weirauch C, Bérenger JM, Berniker L, Forero D, Forthman M, Frankenberg S, Freedman A, Gordon E, Hoey-Chamberlain R, Hwang WS, Marshall SA, Michael A, Paiero SM, Udah O, Watson C, Yeo M, Zhang G, Zhang J (2014) An Illustrated Identification Key to Assassin Bug Subfamilies and Tribes (Hemiptera: Reduviidae). *Canadian Journal of Arthropod Identification* No. 26: 1–115. <https://dx.doi.org/10.3752/cjai.2014.26>
73. Weirauch C, Forthman M, Grebennikov V, Baňář P (2017) From Eastern Arc Mountains to extreme sexual dimorphism: systematics of the enigmatic assassin bug genus *Xenocaucus* (Hemiptera: Reduviidae: Tribelocephalinae). *Organisms Diversity & Evolution* 17: 421–445. <https://doi.org/10.1007/s13127-016-0314-2>
74. Weirauch C, Munro JB (2009) Molecular phylogeny of the assassin bugs (Hemiptera: Reduviidae), based on mitochondrial and nuclear ribosomal genes. *Molecular Phylogenetics and Evolution* 53: 287–299. <https://doi.org/10.1016/j.ympev.2009.05.039>
75. Zhang G, Weirauch C (2013) Molecular phylogeny of Harpactorini (Insecta: Reduviidae): correlation of novel predation strategy with accelerated evolution of predatory leg morphology. *Cladistics* (2013): 1-13. <https://doi.org/10.1111/cla.12049>
76. Zhao P, Du Z, Zhao Q, Li D, Shao X, Li H, Cai W (2021) Integrative Taxonomy of the Spinous Assassin Bug Genus *Scloмина* (Heteroptera: Reduviidae: Harpactorinae) Reveals Three Cryptic Species Based on DNA Barcoding and Morphological Evidence. *Insects* 2021 12(3): 251. <https://doi.org/10.3390/insects12030251>

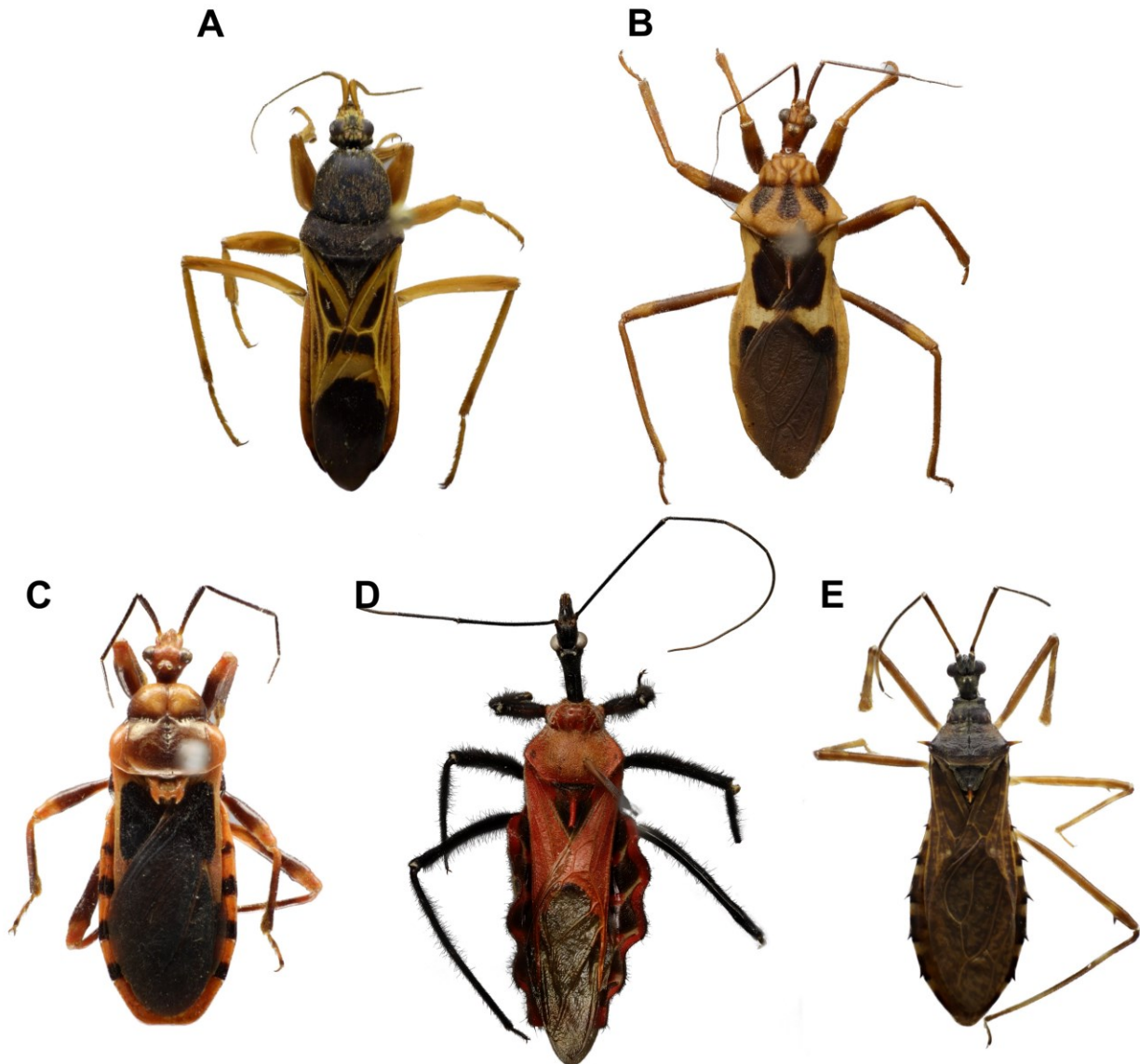


Figure 1.1. Habitus of some representatives of Reduviidae. **A**, TXL2004-051, ♀, *Ectomocoris elegans* (Fabricius, 1803), subfamily Peiratinae; **B**, TXL2004-081, *Acanthaspis ruficeps* Hsiao, 1976, subfamily Reduviinae; **C**, TXL2003-061, *Ectrichotes comottoi* Lethierry, 1883, subfamily Ectrichodiinae; **D**, TXI2019-821, ♂, *Sycanus falleni* Stål, 1863, subfamily Harpactorinae; **E**, HNL2018-187, subfamily Salyavatinae.



Figure 1.2. Morphological characters of some representatives of Reduviidae. A–E, head in lateral view; F–I, third visible labial segment and stridulatory sulcus; J–N, front legs. A, J, TXL2004-051, ♀, *Ectomocoris elegans* (Fabricius, 1803), subfamily Peiratinae; B, F, K, TXL2004-081, *Acanthaspis ruficeps* Hsiao, 1976, subfamily Reduviinae; C, G, L, TXL2003-061, *Ectrichotes comottoi* Lethierry, 1883, subfamily Ectrichodiinae; D, H, M, TXL2019-821, ♂, *Sycanus falleni* Stål, 1863, subfamily Harpactorinae; E, I, N, HNL2018-187, subfamily Salyavatinae.

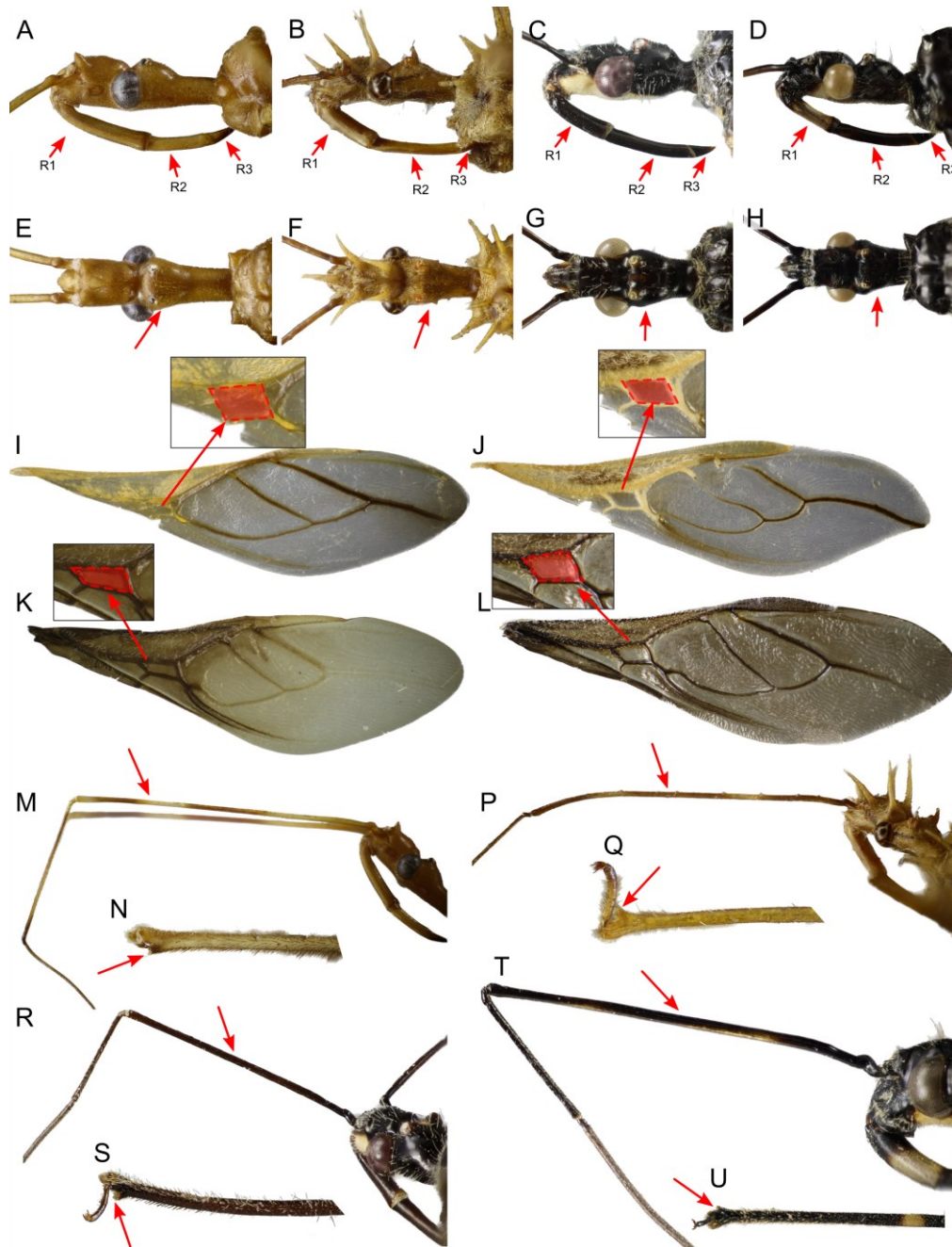


Figure 1.3. Morphological characters of some representatives of Harpactorinae. **A–D**, head in lateral view; **E–H**, head in dorsal view; **I–L**, Right hemelytron; **M, P, R, S**, Scape; **N, Q, S, U**, apical half of front tibia which demonstrates the developed spur. **A, E, I, M, N**, HNL2018-276, ♀, *Epidaurus* sp.; **B, F, J, P, Q**, AY2015-001, ♀, *Sclomina erinacea* Stål, 1861; **C, G, K, R, S**, HNL2018-007, *Biasticus griseocapillus* Ha, Truong et Ishikawa, 2022; **D, H, L, T, U**, AD2020-033, ♀, *Sphepanolestes impressicollis* (Stål, 1861).

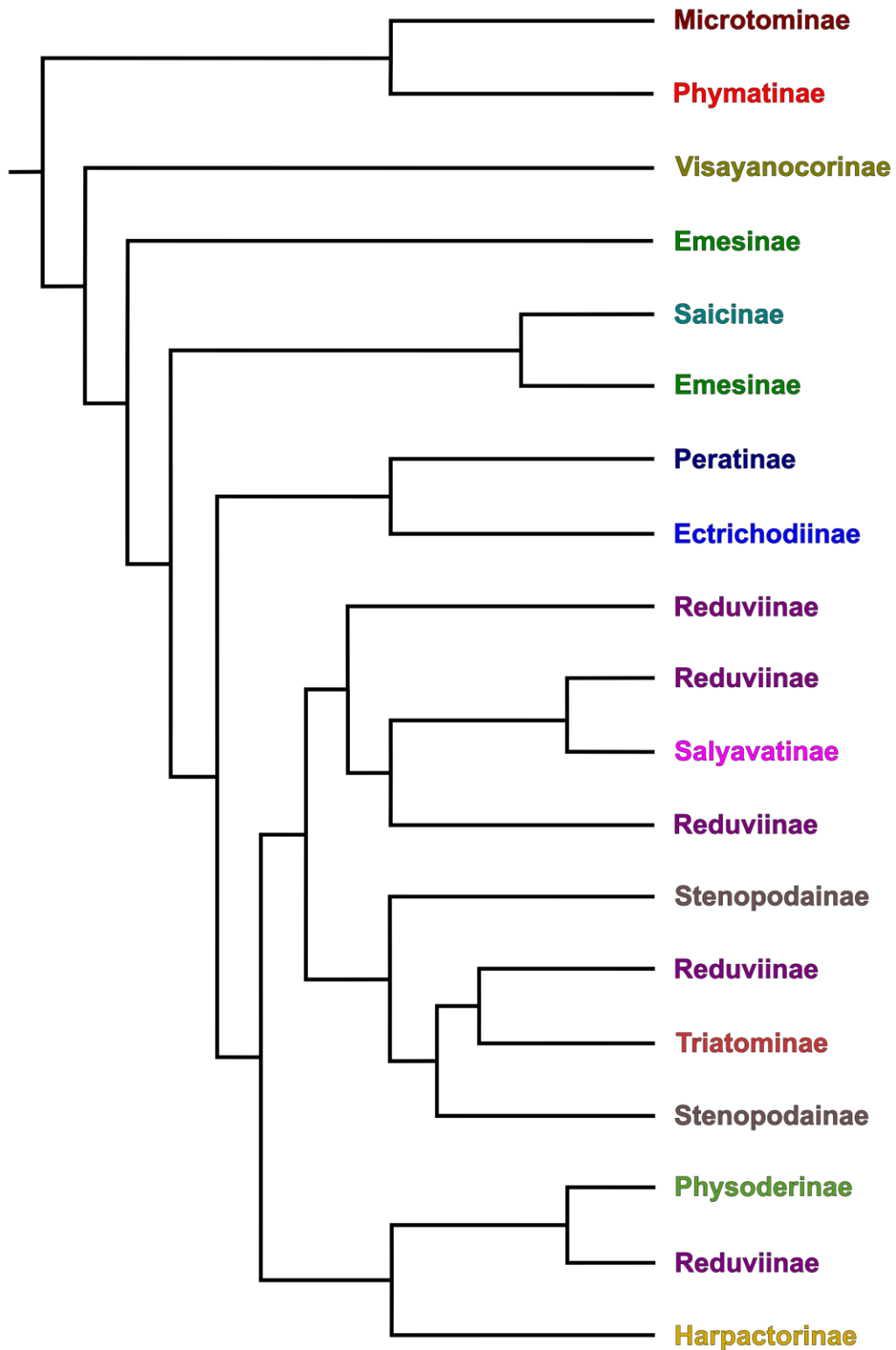


Figure 1.4. Strict consensus tree of some representative subfamilies of Reduviidae, modified from Weirauch and Munro (2009).

CHAPTER 2:
MATERIALS AND METHODS

2.1. An Overview of the Subfamily Harpactorinae

Among the 30 subfamilies of Reduviidae, the most species-rich subfamily is Harpactorinae. It consists of approximately 2,700 species (about 40% of the total species number of Reduviidae) assigned to more than 300 genera of seven tribes (Schuh and Slater, 1995; Forero, 2011), species-rich in the world's tropics and subtropics, and is found in various types of terrestrial habitats, i.e., from tropical rainforests to grasslands and shrubs, and agricultural habitats, and from lowland to highland (Ambrose, 1999; Omkar, 2016; Siti et al., 2017).

The subfamily Harpactorinae is considered a monophyletic group (Weirauch, 2008; Weirauch and Munro, 2009) with diagnostic characteristics as follows: quadrate discal cell in the corium, reduction of the vermiform gland on the bursa copulatrix of the female genitalia, absence of the dorsal connexival suture, and absence of the metathoracic scent gland and its opening (Weirauch, 2008).

Most species of Harpactorinae are founded on vegetation, while some live on the ground surface or tree shanks, under loose barks or stones, and inside termite nests as an exception (Miller, 1971; Schuh & Slater, 1995). Furthermore, Harpactorinae species are usually associated with plants (Bérenger and Pluot-Sigwalt, 1997) for hunting, oviposition, or obtaining sticky resin, as mentioned below (Bérenger and Pluot-Sigwalt, 1997; Choe and Rust, 2007; Forero et al., 2011; Dejean et al., 2013). Harpactorinae species feed on a wide range of arthropods (Ambrose, 1999; Ambrose, 2003; Truong and Ha, 2017) and phytophagy has been rarely found (Bérenger and Pluot-Sigwalt, 1997). Some tribes, such as Apiomerini, Ectinoderini, and Diaspidiini have special hunting strategies, i.e., they coat their fore tibiae with sticky resins of plants for capturing the prey (Forero et al., 2011), while some members of the tribe Harpactorini secrete the sticky substance from their tibia for the same predatory purpose (Zhang and Weirauch, 2011).

With their nature of active wandering predators and dominance in various types of vegetation,

hundreds of species of Harpactorinae, such as the species of *Coranus* Curtis, 1883, *Rhynocoris* Hahn, 1834, *Sphedanolestes* Stål, 1866 and *Sycanus* Amyot and Serville, 1843, were documented as natural enemies of agricultural and forestry pests, and potentially usable as biocontrol agents because they prey a wide range of pests and exhibit functional and numerical responses when the density or the structure of agricultural pest population varies (Ambrose, 1999; Ambrose, 2003; Omkar, 2016).

2.2. An Overview of the Three Genera *Biasticus*, *Sphedanolestes*, and *Rhynocoris*

2.2.1. Synopsis of the Genus *Biasticus* Stål, 1867 in Indo-China

Biasticus Stål, 1867 was established by monotypy with *Reduvius impiger* Stål, 1863, and recently has been allocated to the tribe Harpactorini, subfamily Harpactorinae of the family Reduviidae (Stål 1863, 1867; Maldonado 1990). The following definition of the genus *Biasticus* which was slightly revised by Distant (1904) and the present study was herein used as the initial working hypothesis: body elongated; head sub-elongated, almost as long as pronotum; postocular a little longer than anteocular area; labium with the first visible segment shorter than second, a little longer than anteocular area of head; scape a little longer than pronotum; anterior lobe of pronotum longitudinally impressed; posterior lobe with a distinct, central, anterior, longitudinally elevation; scutellum not apically produced; hemelytra passing the abdominal apex; legs moderately long and slender; femora apically moderately nodulose; anterior femora very slightly incrassated (Fig. 2.1).

The genus currently comprised 23 valid named species distributing exclusively from the Oriental and Sino-Japanese realms (Stål 1863; Reuter 1887; Distant 1903; Bergroth 1913; Matsumura 1913; Miller 1941, 1948, 1949, 1954a, 1954b; Hsiao 1979; Hsiao and Ren 1981; Cai and Yang 2002; Ishikawa 2003; Afzal and Ahmad 2019; Ha et al. 2022) (Fig. 2.2). Among them, six species have been recorded and described from Indo-China, i.e., *B. confusus* Hsiao et al., 1979, *B. flavinotus* (Matsumura, 1913), *B. flavus* (Distant, 1903), *B. griseocapillus* Ha, Truong et Ishikawa,

2022, *B. luteicollis* Ha, Truong et Ishikawa, 2022, and *B. taynguyenensis* Ha, Truong et Ishikawa, 2022.

2.2.2. Synopsis of the Genus *Sphedanolestes* Stål, 1867 in Indo-China

Sphedanolestes Stål, 1867 was established with *Reduvius impressicollis* Stål, 1861 as the type species of the genus. The genus has been allocated to the tribe Harpactorini, subfamily Harpactorinae of the family Reduviidae (Stål 1861, 1867; Maldonado 1990). The following definition of the genus *Sphedanolestes* which was slightly revised by Ishikawa (2003) and the present study was herein used as the initial working hypothesis: body elongated elliptic; head elongated elliptic, nearly as long as pronotum; anteocular area of head as long as or shorter than postocular area; postocular area of head globose in anterior half and constricted in posterior half; scape as long as or longer than head; first visible labial segment as long as or shorter than second segment, reaching level of middle of compound eye; compound eye prominent; pronotum shorter than humeral width, with prominent anterolateral angles; anterior lobe shorter than posterior lobe, with median sulcus posteriorly; median sulcus reaching posterior lobe; posterior lobe depressed along meson, rounded at humeral angles; scutellum triangular, triangularly elevated discally; hemelytra reaching or exceeding apex of abdomen; femora nodular or not; tarsi 3-segmented; abdomen elliptic, wider than hemelytra, with lateral margins gently curved; genital capsule dorsodistally with a pair of tubercles or bifurcate projection; paramere rod-shaped (Fig. 2.3).

The genus currently comprises 185 validly named species distributing widely in Afrotropical, Palearctic, Sino-Japanese, Oriental, and Oceanic Realms (Maldonado 1990; Livingstone and Ravichandran 1990; Cai and Yang 2002; Cai et al. 2004; Zhao et al. 2015) (Fig. 2.4). Among them, ten species have been recorded and described from Indo-China, i.e., *S. annulipes* Distant, 1903, *S. femoralis* Distant, 1919, *S. flaviventris* Distant, 1919, *S. gularis* Hsiao, 1979, *S. impressicollis* (Stål,

1861), *S. marginiventris* Distant, 1919, *S. pubinotus* Reuter, 1881, *S. sericatus* Breddin, 1903, *S. trichrous* Stål, 1874, and *S. xiongi* Cai et al., 2004 (Breddin 1903; Distant 1919; Truong et al. 2015).

2.2.3. Synopsis of the Genus *Rhynocoris* Hahn, 1834 in Indo-China

Rhynocoris Hahn, 1834 was established Poda, 1761 (syn. with *Cimex iracundus* Poda, 1761 (syn. *Reduvius cruentus* Fabricius, 1787) as the type species of the genus. The genus has been allocated currently to the tribe Harpactorini, subfamily Harpactorinae of the family Reduviidae (Fabricius 1787; Hahn 1834; Maldonado 1990). The following definition of the genus *Rhynocoris* which was slightly revised by Ishikawa (2003) and the present study was herein used as the initial working hypothesis: body elongated, elliptic; head elongated and elliptic, nearly as long as pronotum; anteocular area of head as long as or shorter than postocular area; postocular area of head gradually narrowed posteriorly; scape longer than head; first visible labial segment shorter than second segment, reaching level of middle of eye; compound eye prominent; pronotum shorter than humeral width, prominent at anterolateral angles; anterior pronotal lobe shorter than posterior pronotal lobe, with median sulcus posteriorly; median sulcus not reaching posterior lobe; posterior lobe rounded at humeral angles, with reflexed posterolateral margins; scutellum triangular, reflexed in apical part, triangularly elevated discally; hemelytra reaching or exceeding apex of abdomen; abdomen elliptic, wider than hemelytra, with gently curved lateral margins; genital capsule with a process dorsoapically; parameres rod-shaped (Fig. 2.5).

The genus currently comprises 144 validly named species distributing widely in Afrotropical, Palearctic, Sino-Japanese, Oriental, and Nearctic Realms (Stål 1867; Distant 1903; Ambrose and Livingstone 1986; Linnavuori 1989; Maldonado 1990; Truong et al. 2015) (Fig. 2.6). Among them, four species have been recorded and described from Indo-China, i.e., *R. fuscipes* (Fabricius, 1787), *R. marginellus* (Fabricius, 1803), *R. mendicus* (Stål, 1867), and *R. tristicolor* (Reuter, 1881).

2.3. An Overview of the Research Area, the Indochinese Peninsula

This study was conducted with specimens mainly obtained from Vietnam and Laos, which are also known as the Indochinese Peninsula or Indo-China, and surrounding areas. The geography of this region is briefly described below.

The Indochinese Peninsula is located in the mainland of Southeast Asia, which is widely known as the region of Vietnam, Laos, and Cambodia. Geologically, Indo-China, the Malay peninsula, Sumatra, the western part of Java, Kalimantan, Sulawesi, and Sunda shelf connects and forms a primary geomorphological unit of mainland Southeast Asia. Among them, the Sunda shelf, which is a shallow oceanic area of the Gulf of Thailand and the South China Sea, was exposed many times during Mesozoic to glacial periods of Pleistocene of Cenozoic (2.52–0.11 MYA) (Rundell 1999; Averyanov et al. 2003). The region of the Indochinese Peninsula can be subdivided into several tectonic units, i.e., northeastern montane geomorphologic region of Vietnam (southern extension of South China terrane), Truong Son Fold Belt, Dalat-Kratie Belt, Khorat Basin, Loei Fold Belt, Sukhothai Belt, and Chiang Mai Belt (Sirisokha et al. 2019).

The Indochinese Peninsula is close to the boundary between the Oriental and Sino-Japanese realms (Chen et al., 2008; Holt et al., 2013), and involves various bioclimate zones, such as tropical, subtropical, and temperate zones characterized by the regular winter and summer monsoons, different levels of rainfall and seasonality, and the complicated orography of the region and the specific configuration of the eastern coastal line of Indo-China which shift the directions of the monsoon winds, and affect the time of dry and rainy seasons and the amount of precipitation (Averyanov 2003; Phan et al. 2009; Beck et al. 2018) (Fig. 2.7).

Meta-analyses of geological, paleoclimatic, and phylogenetic data sets revealed that the Indochinese Peninsula and Borneo has produced new lineages of animals and plants, and supplied them to the surrounding areas since at least the early Miocene (de Bruyn et al., 2014). Indo-China,

especially the border of Vietnam and Laos, is expected to be one of the centers of species diversity, endemism, and relictness of terrestrial organisms in the Oriental realm (Mittermeier et al., 2011; de Bruyn et al., 2014).

However, only 70 species in 35 genera of the subfamily Harpactorinae have so far been recognized in the Indo-China peninsula (Stål 1863; Truong et al. 2015; Truong et al. 2020; Ha et al. 2022), accounting for only about 2.4% of the total number of the validly named species of the subfamily. Therefore, species diversity is likely to be underestimated, and a lot of species have not yet been found or taxonomically recognized.

2.4. Outline of the Research: How to Discriminate and Identify the Species

The specimens (male and female adults) of *Biasticus*, *Sphedanolestes*, and *Rhynocoris* obtained from Vietnam and surrounding areas were discriminated at the species level by a combination of morphological examination, molecular phylogenetic analyses, and morphometry.

- (0) *Evaluation of the validity of the genus Biasticus.* The validity of the genus *Biasticus*, i.e., the targets of the present study, was evaluated by morphological examination and phylogenetic and morphometric analyses. Based on the results, male and female adult specimens of each genus were selected as the targets of the present study (Steps 1 to 5).
- (1) *Preliminary recognition of morphospecies.* Specimens were sorted into morphospecies based on external morphology and genital morphology.
- (2) *Evaluation by molecular phylogenetic analyses.* Morphospecies delimitation was evaluated based on the monophyly and the degree of divergence from each other and, if available, phylogeographic information, i.e., sympatric occurrence of multiple distinct phylogenetic lineages suggesting the presence of reproductive isolations among them.

- (3) *Confirmation of species delimitation.* In the case where a morphospecies was discriminated from the others consistently by steps (1) and (2), then it will be treated here as an independent species. In the case where multiple morphospecies were not discriminated from each other by step (2), they will be treated as morphological variants of a single species. On the other hand, in the case where a morphospecies was further subdivided into multiple units by step (2), it will be treated as a cryptic species complex.
- (4) *Final identification of species.* Independent species recognized by the above steps were identified by referring to the taxonomic articles and the images of the type materials of several species. The species (including cryptic species) unable to be identified were tentatively treated as new species. Formal taxonomic treatments, such as the description of new species and solution of synonymies, will be done in a separate paper(s).

2.5. Specimen Preparation

Specimens were labeled with their specimen IDs and locality information before being pinned or individually preserved in vials containing 99% ethanol. Each specimen's right hindlimb was cut off in the lab and used for DNA extraction (then for molecular phylogenetic examination and DNA barcoding). The rest of the corpse was pinned or preserved in 99% ethanol for morphological and morphometric study. The voucher samples of this investigation are housed in the following institutions:

IEBR—Institute of Ecology and Biological Resources, Vietnam Academy of Science and Technology, Vietnam

BNHM—British Natural History Museum collection, UK

HU—Hokkaido University, Japan

NRM— Swedish Museum of Natural History, Sweden

NSMT—National Museum of Nature and Science, Tokyo, Japan

NSM—Department of Entomology, Zoological Research Division, Office of Natural Science Research, National Science Museum, Thailand

TARI—Taiwan Agricultural Research Institute Insect Collection, Taiwan Agricultural Research Institute, Taiwan

NUOL—Faculty of Agriculture, National University of Laos, Laos P.D.R.

TMU-SZL—Systematic Zoology Laboratory, Tokyo Metropolitan University, Tokyo, Japan

UCR—Entomology Research Museum, the University of California, Riverside, U.S.A

2.6. Morphological Examination and Imaging

External morphological characteristics were examined for dry-mounted specimens using a Nikon SMZ1270 stereomicroscope. The genitalia were prepared for examination as described below. Firstly, each male specimen was relaxed by soaking for 3 days in 70 % ethanol. After that, the male genitalia were detached from the body and soaked in hot 10 % KOH for five minutes until body fat and muscle were released. The endosoma was pulled out from the phallosoma by fine tweezers after removing the phallus from the pygophore. All parts of male genitalia were preserved in a tiny vial filled with propylene glycol and subsequently associated with the pinned specimens. Next, the female genitalia were inspected without being detached from the body. A Nikon SMZ1270 stereomicroscope was used to examine the male and female genital morphology.

Focus stacking was executed using Helicon Focus Pro 8.2.0 software (Helicon Soft Ltd., Ukraine) based on a sequence of the source pictures photographed by a Canon EOS Kiss X10 digital camera connected to a Nikon AZ100 stereomicroscope, and artifacts were removed using the retouch function of the software. After that, the contrast, brightness, color balance, and intensity were adjusted using Adobe Photoshop Elements 10.0 software (Adobe Systems Incorporated, San Jose,

CA, USA) and a color corresponding sticker (CASMATCH, Bear Medic Corporation, Japan).

Morphological terminology followed Schuh and Weirauch (2020), Forero and Weirauch (2012), Rosa et al. (2005), and Ha et al. (2022).

2.7. Molecular Data Preparation

DNA was isolated from each specimen's left leg/legs by the Chelex-TE-ProK protocol (Satria et al. 2015). The mitochondrial 16S and COI gene fragments were examined using the primers presented in Table 2. Polymerase chain reaction (PCR) amplification, cycle sequencing reaction, sequencing using ABI PRISM 3130xl (Applied Biosystems), and sequence assembly using ChromasPro 1.7.6 (Technelysium Pty Ltd., Australia) were executed using the methods of Satria et al. (2015), Kessing et al. (1989), Shekhovtsov et al. (2013), Bely and Wray (2004), and Zhang & Weirauch (2013). The PCR thermal situation for the two gene fragments, 16S and COI, comprised of initial denaturation at 94 °C (2 min), denaturation at 94 °C (30 s), annealing at appropriate annealing temperature (30 s) (Table 2), and extension at 72 °C (45 s) for 35 cycles, with final extension at 72 °C (7 min). COI and 16S sequences were effectively obtained from 29 of the 61 *Blasticus* samples.

Test for association was performed using MUSCLE implemented in MEGA X (Kumar et al. 2018) with default setting (Gap Open = -400.00; Gap Extend = 0.00; Cluster Method [Iterations 1,2 and Other iterations] = UPGMA; Min Diag Length [Lambda] = 24) for COI and 16S sequences while including and excluding outgroups (OG⁺ or OG⁻): 16S^(OG⁺) (479 bp), 16S^(OG⁻) (479 bp), COI^(OG⁺) (606 bp), and COI^(OG⁻) (606 bp) datasets. The 16S^(OG⁺) and COI^(OG⁺) datasets were aggregated to produce a concatenated 16S + COI dataset (1085 bp). The FASTA-configured files derived from MEGA X were then converted to NEXUS layout or PHYLIP design, which were suitable input layouts for molecular phylogenetic examination and estimation of genetic distances

and species delimitation analysis by ClustalX 2.0.11 (Larkin et al. 2007).

2.8. Molecular Phylogenetic Analyses

Molecular phylogenetic analyses were done based on the concatenated 16S + COI dataset. The substitution models were selected respectively for the 16S^(OG⁺), COI^(OG⁺), and the concatenated 16S + COI datasets by Model Finder (Kalyaanamoorthy et al. 2017) executed in IQ-TREE 2.1.2 (Minh et al. 2020). Maximum likelihood (**ML**) examinations were then carried out using IQ-TREE 2.1.2 (Chernomor et al. 2016; Minh et al. 2020); bootstrap values (**BP**) were estimated from 1,000 replications. The generalized time-reversible (**GTR**) + Gama model was chosen for the 16S + COI dataset using Model Finder (Kalyaanamoorthy et al. 2017) under the Bayesian information criterion. The Bayesian inference (**BI**) evaluations were then executed for the data using MrBayes v. 3.2.7 (Ronquist and Huelsenbeck 2003) with 20,000,000 production and statutory parameter configuration (examining every 500 generations and tuning constraints every 100 generations, with a burn-in of 25 %). The effective sampling size (ESS) of each constraint was verified to be > 200 using Tracer 1.7.2 (Rambaut et al. 2018). The nodes were designated as “well supported” when posterior probability (**PP**) ≥ 0.95 and BP ≥ 80 .

2.9. Species Delimitation Analyses

To create species partitions, two different protocols, i.e., Assemble Species by Automatic Partitioning (**ASAP**) (Puillandre et al. 2021) and Bayesian implementation of the Poisson Tree Processes model (**bPTP**) for species delimitation (Zhang et al. 2013), were used with pairwise genetic distances. For ASAP, the FASTA-configured files of 16S^(OG⁻) and COI^(OG⁻) datasets were used and executed on the ASAP website (<https://bioinfo.mnhn.fr/abi/public/asap>), with two replacement samples to estimate the distances, i.e., simple p-distance model and K2P model. The

bPTP were executed in the bPTP online server (<https://species.h-its.org>) based on the NEXUS formatted BI trees of 16S^(OG⁻) and COI^(OG⁻) datasets, with default values (100,000 Markov chain Monte Carlo [MCMC] generations, thinning = 100, burn-in = 0.1, and Seed = 123). The NEXUS formatted BI trees used in bPTP were converted from TREE formatted by TreeGraph 2.15.0-887 (Stöver and Müller 2010).

2.10. Final Identification

In step (4), the species were identified by referring to taxonomic articles, species descriptions and identification keys and images of the type specimens (Table. 1). The images were provided by Dr. Wei Song Hwang (National University of Singapore) or provided in official websites of some museums. The species unable to be identified were tentatively labeled with species codes such as “*B.* sp. HNL001”.

References

1. Afzal H, Ahmad I (2019) A new record of the predatory bug *Biasticus flavus* (Distant) (Hemiptera: Reduviidae: Harpactorinae) from Pakistan and its redescription with reference to its unknown male and female genitalia. *International Journal of Biology and Biotechnology* 16 (1): 205–210.
2. Ambrose DP (1999) *Assassin Bugs*. Science Publishers, Enfield, NH.
3. Ambrose, D.P. (2003) Biocontrol potential of assassin bugs (Hemiptera: Reduviidae). *J. Exp. Zool. India*. Vol 6, No. 1, pp. 1–44.
4. Ambrose DP, Livingstone D (1986) A new species of *Rhynocoris* (Fabricius) from Southern India (Heteroptera-Reduviidae-Harpactorinae). *Journal of Bombay Natural History Society* 83: 173–177.

5. Averyanov LV, Phan KL, Nguyen TH, Harder DK (2003) Phytogeographic review of Vietnam and adjacent areas of Eastern Indochina. *Komarovia* 3: 1–83.
6. Beck H, Zimmermann N, McVicar T, Vergopolan N, Berg A, Wood EF (2018) Present and future Köppen-Geiger climate classification maps at 1-km resolution. *Sci Data* 5, 180214. <https://doi.org/10.1038/sdata.2018.214>
7. Bely AE, Wray GA (2004) Molecular phylogeny of naidid worms (Annelida: Clitellata) based on cytochrome oxidase I. *Molecular Phylogenetics and Evolution* 30: 50–63. [https://doi.org/10.1016/S1055-7903\(03\)00180-5](https://doi.org/10.1016/S1055-7903(03)00180-5)
8. Bérenger JM, Pluot-Sigwalt D (1997) Relations privilégiées de certains Heteroptera: Reduviidae prédateurs avec les végétaux. Premier cas connu d'un Harpactorinae phytophage. *Comptes Rendus de l'Académie des Sciences, Series III, Sciences de la Vie* 320: 1007–1012.
9. Bergroth E (1913) New genera and species of Reduviidae from Borneo. *The Sarawak Museum Journal* 3: 25–38.
10. Cai W, Yang S (2002) Insect from Maolan landscape. Guizhou Science and Technology Publishing House, Guiyang, 208–230.
11. Cai W, Cai X, Wang Y (2004) Notes on the genus *Sphecanolestes* Stål (Heteroptera: Reduviidae: Harpactorinae) from China, with the description of three new species. *The Raffles bulletin of Zoology* 2004, 52(2): 379–388.
12. Chen L, Song Y, Xu S (2008) The boundary of palaeartic and oriental realms in western China. *Progress in Natural Science* 18: 833–841. <https://doi.org/10.1016/j.pnsc.2008.02.004>
13. Chernomor O, Haeseler von A, and Minh BQ (2016) Terrace aware data structure for phylogenomic inference from supermatrices. *Systematic Biology* 65: 997–1008. <https://doi.org/10.1093/sysbio/syw037>

14. Choe DH, Rust MK (2007) Use of plant resin by a bee assassin bug *Apiomerus flaviventris* (Hemiptera: Reduviidae). *Annals of the Entomological Society of America* 100: 320–326. [https://doi.org/10.1603/0013-8746\(2007\)100\[320:UOPRBA\]2.0.CO;2](https://doi.org/10.1603/0013-8746(2007)100[320:UOPRBA]2.0.CO;2)
15. Dejean A, Revel M, Azémar F, Roux O (2013) Altruism during predation in an assassin bug. *Naturwissenschaften*, vol. 100 (n° 10). pp. 913–922. ISSN 0028-1042. <https://doi.org/10.1007/s00114-013-1091-9>
16. Distant WL (1903) Rhynchotal notes. XVI. Heteroptera: Family Reduviidae (continued). *Apiomerinae, Harpactorinae and Nabidae*. *The Annals and Magazine of Natural History* (7)11: 203–213.
17. Distant WL (1904) Rhynchotal notes. XXII. Heteroptera from North Queensland. *The Annals and Magazine of Natural History* (7)18: 286–293.
18. Fabricius JC (1787) *Mantissa Insectorum*. Hafniae, II: 312.
19. Forero D, Choe DH, Weirauch C (2011) Resin Gathering in Neotropical Resin Bugs (Insecta: Hemiptera: Reduviidae): Functional and Comparative Morphology. *Journal of Morphology* 272: 204–229. <https://doi.org/10.1002/jmor.10907>
20. Forero D, Weirauch C (2012) Comparative genitalic morphology in the New World resin bugs *Apiomerini* (Hemiptera, Heteroptera, Reduviidae, Harpactorinae). *Deutsche entomologische Zeitschrift* 59 (1) 2012, 5–41. <http://dx.doi.org/10.1002/mmnd.201200001>
21. Ha NL, Truong XL, Ishikawa T, Jaitrong W, Lee CF, Chouangthavy B, Eguchi K (2022) Three new species of the genus *Biasticus* Stål, 1867 (Insecta, Heteroptera, Reduviidae, Harpactorinae) from Central Highlands, Vietnam. *ZooKeys* 1118: 133–180. <https://doi.org/10.3897/zookeys.1118.83156>
22. Hahn CW (1834) *Die Wanzenartigen Insecten*. Nurnberg: C. H. Zeh'schen Buchhandlung 2: 20.

23. Holt BG, Lessard JP, Borregaard MK, Fritz SA, Araújo MB, Dimitrov D, Fabre PH, Graham CH, Graves GR, Jønsson KA, Nogués-Bravo D, Wang Z, Whittaker RJ, Fjeldså J, Rahbek C (2013) An Update of Wallace's Zoogeographic Regions of the World. *Science* 339: 74. <http://dx.doi.org/10.1126/science.1228282>
24. Hsiao TY (1979) New species of Harpactorinae from China. II. (Hemiptera: Reduviidae). *Acta Zootaxonomica Sinica* 4: 238–295.
25. Hsiao TY, Ren SZ (1981) Reduviidae. In: Hsiao et al., A handbook for the determination of the Chinese Hemiptera-Heteroptera (II). Science Press, Beijing, 390–538.
26. Ishikawa T (2003) Taxonomic study on the Tribe Harpactorini (Heteroptera, Reduviidae) from Indochina, with Zoogeographical considerations. Ph.D. Thesis, Tokyo University of Agriculture, Kanagawa, Japan.
27. Kalyanamoorthy S, Minh BQ, Wong T, Haeseler von A, Jermini LS (2017) ModelFinder: fast model selection for accurate phylogenetic estimates. *Nature Methods* 14: 587–589. <https://doi.org/10.1038/nmeth.4285>
28. Kassambara A, Mundt F (2020) Package 'factoextra': Extract and Visualize the Results of Multivariate Data Analyses. Version 1.0.7. <https://cran.r-project.org/package=factoextra>
29. Kessing B, Croom H, Martin A, McIntosh C, McMillan WO, Palumbi SP (1989) The simple fool's guide to PCR, version 1.0. Special Publication of the Dept. of Zoology, Univ. of Hawaii, Honolulu, HI.
30. Kumar S, Stecher G, Li M, Knyaz C, Tamura K (2018) MEGA X: Molecular Evolutionary Genetics Analysis across Computing Platforms. *Molecular Biology and Evolution* 35: 1547-9. <https://doi.org/10.1093/molbev/msy096>

31. Livingstone D and Ravichandran G (1990) Two new species of Harpactoraria from Southern India (Heteroptera: Reduviidae: Harpactorinae). *The journal of the Bombay Natural History Society*, 86: 422–424.
32. Larkin MA, Blackshields G, Brown NP, Chenna R, McGettigan PA, McWilliam H, Valentin F, Wallace IM, Wilm A, Lopez R, Thompson JD, Gibson TJ, Higgins DG (2007) Clustal W and Clustal X version 2.0. *Bioinformatics* 23: 2947-2948.
<https://doi.org/10.1093/bioinformatics/btm404>
33. Maldonado J (1990) Systematic catalogue of the Reduviidae of the World. *Caribbean Journal of Science*, Special publication No. 1: 171–172.
34. Matsumura S, (1913) Additions to Thousand Insects of Japan. 1: 1–184.
35. Meusnier I, Singer GAC, Landry JF, Hickey DA, Hebert PDN, Hajibabaei M (2008) A universal DNA mini-barcode for biodiversity analysis. *BMC Genomics* 9(1): 214.
<https://doi.org/10.1186/1471-2164-9-214>
36. Miller NCE (1941) New genera and species of Malaysian Reduviidae (continued). Part II. *Journal of the Federated Malay States Museums* 18: 601–773.
37. Miller NCE (1948) New genera and species of Reduviidae from the Philippines, Celebes, and Malaysia. *Transactions of the Entomological Society of London* 99: 411–473.
38. Miller NCE (1949) A new genus and new species of Malaysian Reduviidae. *Proceedings of the Royal Entomological Society of London (B)*18: 229–237.
39. Miller NCE (1954a) Reduviidae (Hemiptera-Heteroptera). Synonymic notes and corrections. *The Annals and Magazine of Natural History* (12)7: 639–640.
40. Miller NCE (1954b) New genera and species of Reduviidae from Indonesia and the description of a new subfamily (Hemiptera-Heteroptera). *Tijdschrift voor entomologie* 97: 75–114.

41. Miller NCE (1971) *The Biology of the Heteroptera* (2nd rev. ed.). E.W. Classey, London, xiii + 206, 5.
42. Minh BQ, Schmidt HA, Chernomor O, Schrempf D, Woodhams MD, von Haeseler A, Lanfear R (2020) IQ-TREE 2: new models and efficient methods for phylogenetic inference in the genomic era. *Molecular Biology and Evolution* 37: 1530–1534. <https://doi.org/10.1093/molbev/msaa015>
43. Omkar O (2016) *Ecofriendly Pest Management for Food Security*. Elsevier Science, Netherland. <https://doi.org/10.1016/C2014-0-04228-1>
44. Olson DM, Dinerstein E, Wikramanayake ED, Burgess ND, Powell GV, Underwood EC, D'amico JA, Itoua I, Strand HE, Morrison JC, and Loucks CJ (2001) Terrestrial Ecoregions of the World: A new map of life on Earth. A new global map of terrestrial ecoregions provides an innovative tool for conserving biodiversity. *BioScience* 51(11): 933 – 938. [https://doi.org/10.1641/0006-3568\(2001\)051\[0933:TEOTWA\]2.0.CO;2](https://doi.org/10.1641/0006-3568(2001)051[0933:TEOTWA]2.0.CO;2)
45. Phan V. T., Ngo-Duc T., Ho T. M. H. (2009) Seasonal and interannual variations of surface climate elements over Vietnam. *Clim Res* 40: 49-60. <https://doi.org/10.3354/cr00824>
46. Puillandre N, Brouillet S, Achaz G (2021) ASAP: Assemble species by automatic partitioning. *Molecular Ecology Resources* 21(2): 609–620. <https://doi.org/10.1111/1755-0998.13281>
47. Rambaut A, Drummond AJ, Xie D, Baele G, Suchard MA (2018) Posterior summarisation in Bayesian phylogenetics using Tracer 1.7. *Systematic Biology*. syy032. <https://doi.org/10.1093/sysbio/syy032>
48. Reuter OM (1887) *Reduviidae novae et minus cognitae descriptae*. *Revue d'entomologie* 6: 149–167.
49. Rosa JA, Mendonça VJ, Rocha CS, Gardim S, Cilense M (2005) Characterization of the external female genitalia of six species of Triatominae (Hemiptera: Reduviidae) by scanning electron

- microscopy. Memórias do Instituto Oswaldo Cruz, Rio de Janeiro, Vol. 105(3): 286–292.
<https://doi.org/10.1590/S0074-02762010000300007>
50. Ronquist F, Huelsenbeck JP (2003) MrBayes: Bayesian Phylogenetic Inference under Mixed Models. *Bioinformatics* 19 (12): 1572–1574. <https://doi.org/10.1093/bioinformatics/btg180>
51. Rundell PW (1999) Conservation priorities in Indochina – WWF Desk Study. Forest habitats and floral in Lao PDR, Cambodia, and Vietnam. Hanoi, World Wide Fund for Nature, Indochina Programme Office. 194.
52. Satria R, Kurushima H, Herwina H, Yamane Sk & Eguchi K (2015) The trap-jaw ant genus *Odontomachus* Latreille from Sumatra, with a new species description. *Zootaxa* 4048 (1): 1–36.
<http://dx.doi.org/10.11646/zootaxa.4048.1.1>
53. Schuh RT, Slater JA (1995) True Bugs of the World (Hemiptera: Heteroptera): Classification and Natural History. Comstock Pub. Associates, Ithaca. 336.
54. Schuh RT, Weirauch C (2020) True bugs of the world (Hemiptera: Heteroptera). Classification and natural history. 2nd Edition. Siri Scientific Press, Manchester, 767, 32 pls.
55. Shekhovtsov SV, Golovanova EV, Peltek SE (2013) Cryptic diversity within the Nordenskiöld's earthworm, *Eisenia nordenskioldi* subsp. *nordenskioldi* (Lumbricidae, Annelida). *European Journal of Soil Biology* 58: 13–18. <https://doi.org/10.1016/j.ejsobi.2013.05.004>
56. Sirisokha S, Yonezu K, Tindell T, Nakanishi T, Watanabe K and Pelletier J (2019) Lithogeochemistry of Intrusive Rocks in the Halo Porphyry Copper-Molybdenum Prospect, Northeast Cambodia. *Open Journal of Geology*, 9: 342–363.
<https://doi.org/10.4236/ojg.2019.97023>
57. Siti HZ, Hazali R, Abang F (2017) Systematics and distribution of the subfamily Harpactorinae Amyot & Serville, 1843 (Hemiptera: Heteroptera: Reduviidae) in Northern Sarawak. *Serangga* 22(1): 183–202.

58. Stål C (1861) *Miscellanea hemipterologica* - Entomologische Zeitung entomologischen Vereine zu Stettin, 22 Jahrgang, 4–6: 147.
59. Stål C (1863) *Formae speciesque novae Reduviidum*. *Annales de la Société entomologique de France* 3: 38.
60. Stål C (1867) *Bidrag till Reduviidernas Uennedom. Öfversigt af Kongliga Vetenskapsakademiens forhandlingar* 23: 290.
61. Stöver BC, Müller KF (2010) TreeGraph 2: Combining and visualizing evidence from different phylogenetic analyses. *BMC Bioinformatics* 11: 7. <https://doi.org/10.1186/1471-2105-11-7>
62. Truong XL, Bui TQH, Ha NL, Cai W (2020) A new species of the assassin bug genus *Rihirbus* (Hemiptera: heteroptera: Reduviidae) from Vietnam. *Zootaxa* 4780 (3): 587–593. <https://doi.org/10.11646/zootaxa.4780.3.10>
63. Truong XL, Cai WZ, Tomokuni M, Ishikawa T (2015) The assassin bug subfamily Harpactorinae (Hemiptera: Reduviidae) from Vietnam: an annotated checklist of species. *Zootaxa*, ISSN: 1175-5326:101–116. <https://doi.org/10.11646/zootaxa.3931.1.7>
64. Truong XL, Ha NL (2017) Composition and diversity of assassin bugs belong subfamily Harpactorinae (Heteroptera: Reduviidae) in some habitats in Kon Chu Rang natural reserve, Gia Lai province. *Proceedings of the 7th National Scientific Conference on Ecology and Biological Resources*. Hanoi 2017: 763.
65. Weirauch C (2008) Cladistic analysis of Reduviidae (Heteroptera: Cimicomorpha) based on morphological characters. *Systematic Entomology* 33: 229–274. <https://doi.org/10.1111/j.1365-3113.2007.00417.x>
66. Weirauch C, Munro JB (2009) Molecular phylogeny of the assassin bugs (Hemiptera: Reduviidae), based on mitochondrial and nuclear ribosomal genes. *Molecular Phylogenetics and Evolution* 53: 287–299. <https://doi.org/10.1016/j.ympev.2009.05.039>

67. Zhang G, Weirauch C (2011) Sticky predators: a comparative study of sticky glands in Harpactorine assassin bugs (Insecta: Hemiptera: Reduviidae). *Acta Zool.* 94: 1-10. <https://doi.org/10.1111/j.1463-6395.2011.00522.x>
68. Zhang G, Weirauch C (2013) Molecular phylogeny of Harpactorini (Insecta: Reduviidae): correlation of novel predation strategy with accelerated evolution of predatory leg morphology. *Cladistics* (2013): 1–13. <https://doi.org/10.1111/cla.12049>
69. Zhang J, Kapli P, Pavlidis P, Stamatakis A (2013) A general species delimitation method with applications to phylogenetic placements. *Bioinformatics* 29(22): 2869–2876. <https://doi.org/10.1093/bioinformatics/btt499>
70. Zhao P, Ren S, Wang B, Cai W (2015) A new species of the genus *Sphedanolestes* Stål 1866 (Hemiptera: Reduviidae: Harpactorinae) from China, with a key to Chinese species. *Zootaxa* 3985 (4): 591–599. <http://dx.doi.org/10.11646/zootaxa.3985.4.8>

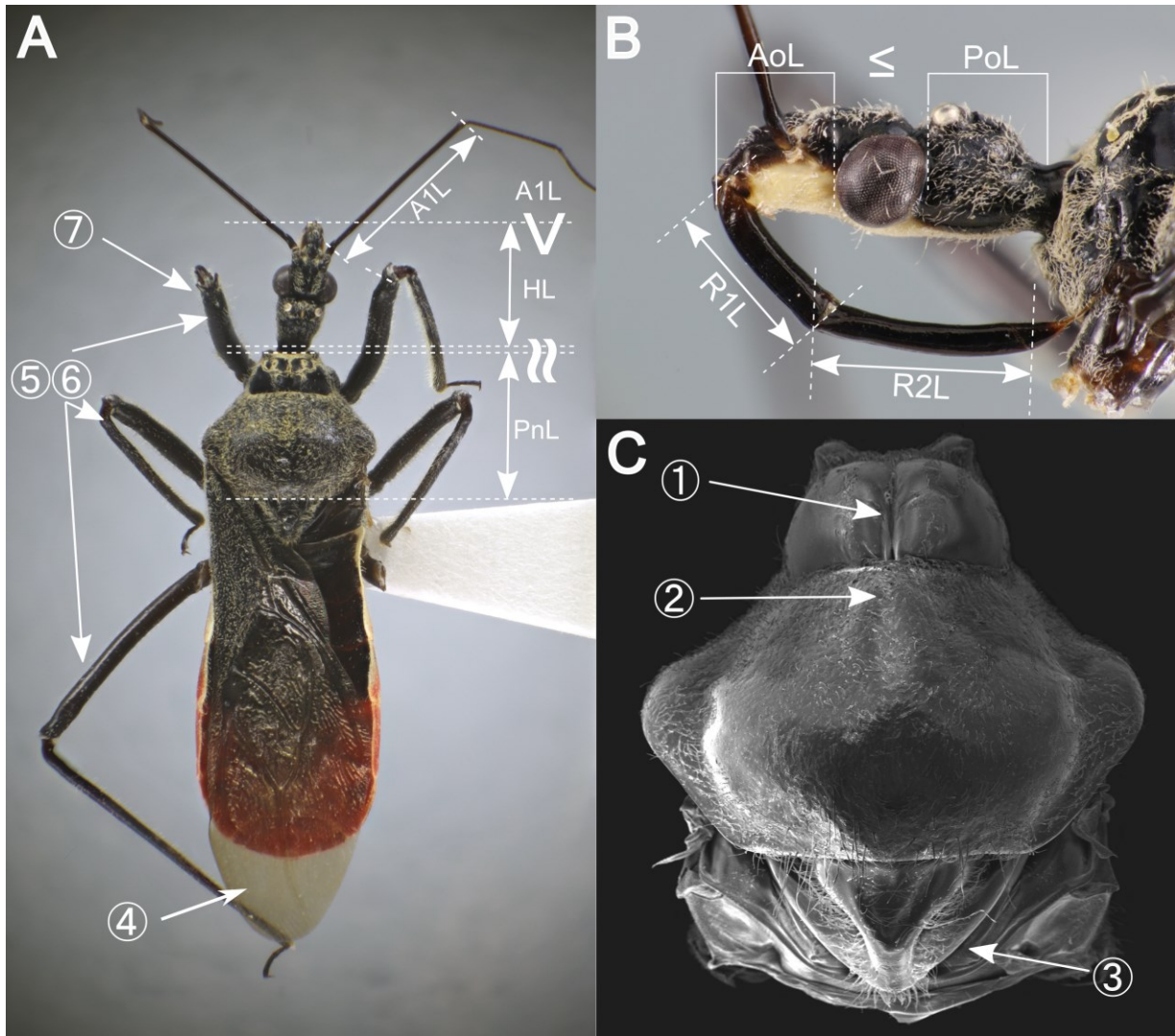


Figure 2.1. Diagnosis characters of the genus *Biasticus* Stål, 1867. **A, B, C,** *Biasticus griseocapillus* Ha, Truong, et Ishikawa, 2022, HNL2018-038, ♀. **A,** Body in dorsal view; **B,** Head in lateral view; **C,** Pronotum in dorsal view. Body elongated; head sub-elongated, almost as long as pronotum; postocular area a little longer than anteocular area; rostrum with the first segment shorter than the second, a little longer than anteocular area of head; first antennal segment a little longer than pronotum; anterior lobe of pronotum longitudinally impressed (1); posterior lobe of pronotum with a distinct, central, anterior, longitudinally elevation (2); scutellum not apically produced (3); hemelytra passing the abdominal apex (4); legs moderately long and slender (5); femora apically moderately nodulose (6); anterior femora very slightly incrassated (7) (Distant 1904).

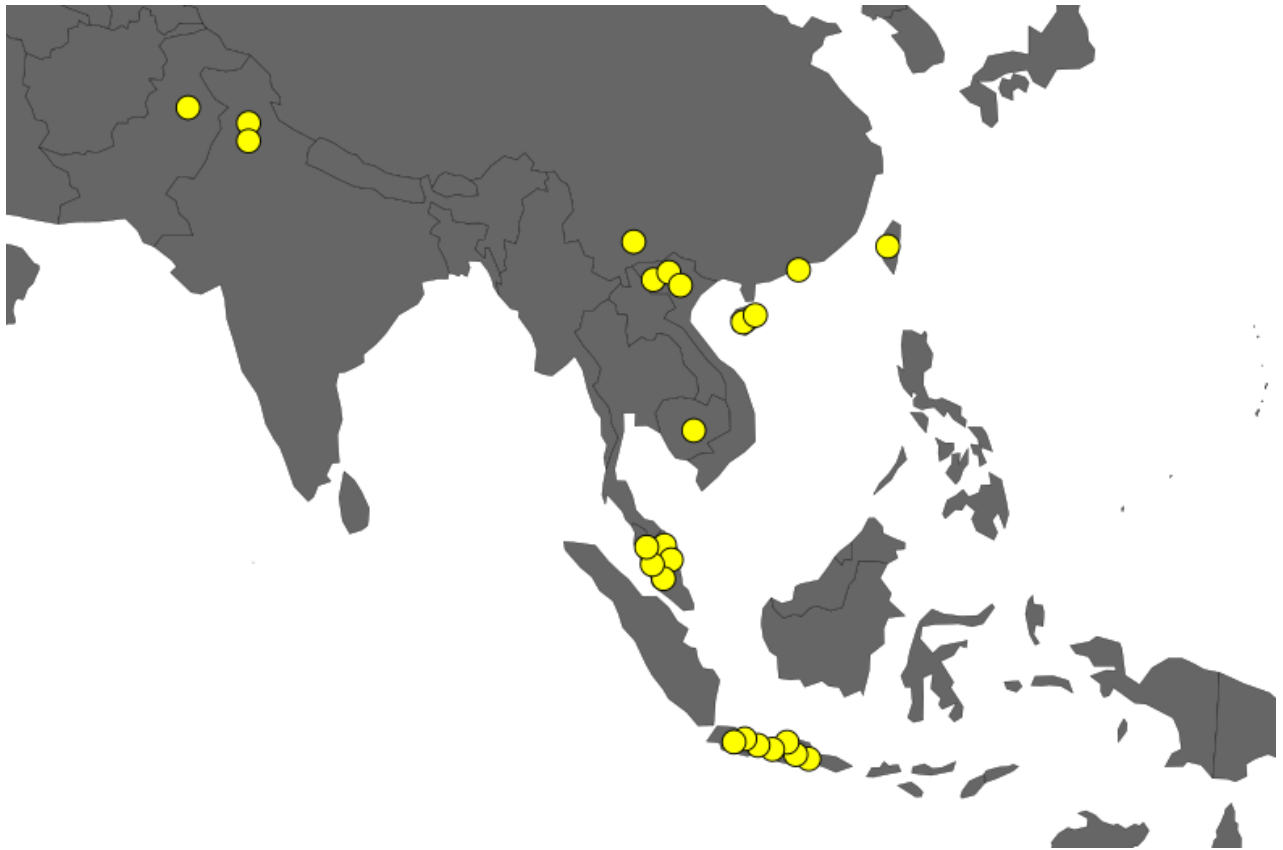


Figure 2.2. World distribution map of the genus *Biasticus* Stål, 1867.

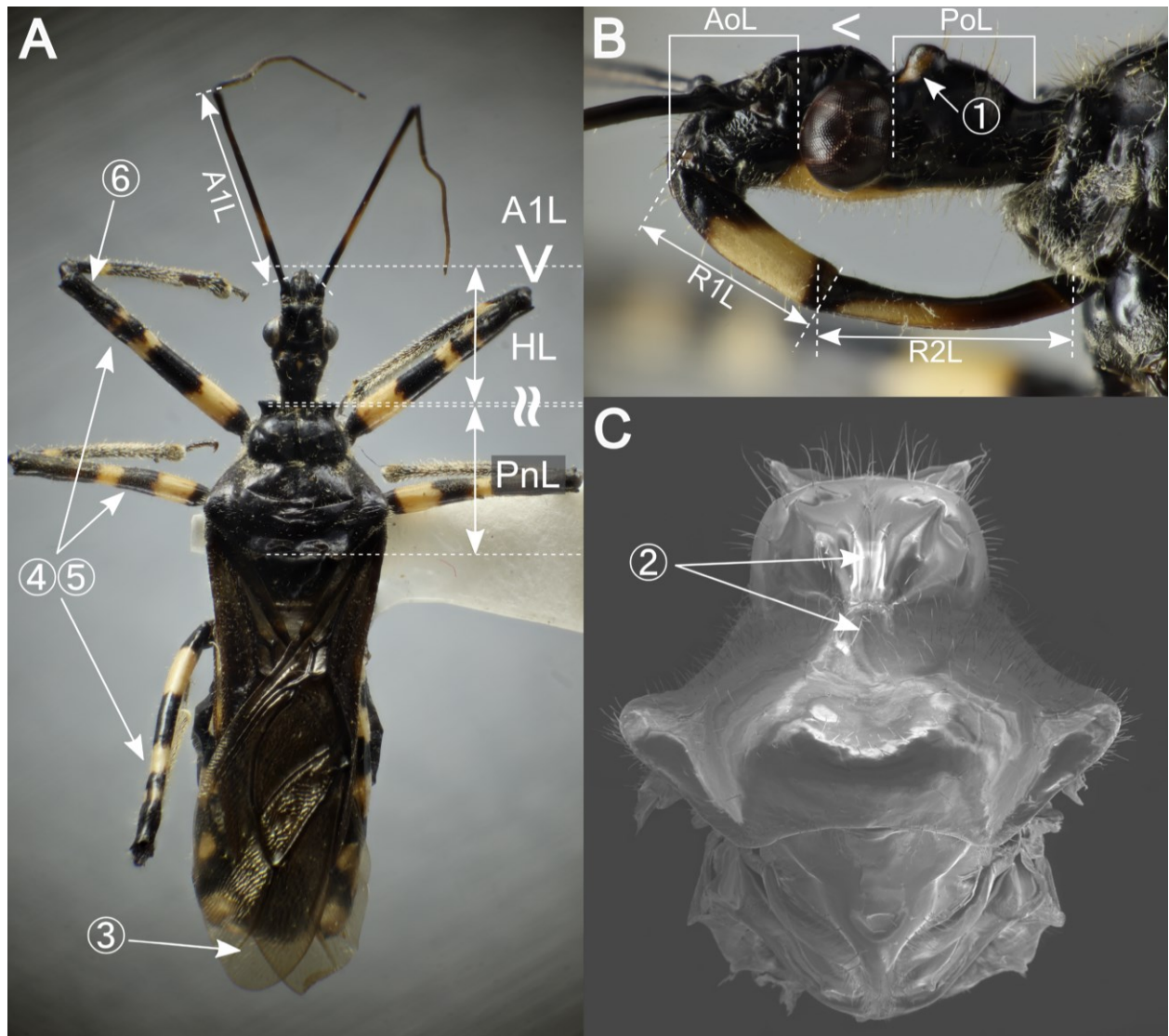


Figure 2.3. Diagnosis characters of the genus *Spheganolestes* Stål, 1867. **A, B, C,** *Spheganolestes impressicollis* (Stål, 1861), HNL2019-001, ♂. **A,** Body in dorsal view; **B,** Head in lateral view; **C,** Pronotum in dorsal view. Body oblong; head about equal to or very slightly longer than the pronotum, ante- and postocular areas about equally long, or the last a little the longer; area of the ocelli a little elevated (1); rostrum with the basal joint longer than the anteocular area of the head; antennae with the first joint subequal to the head or a little longer; pronotum with the anterior and posterior lobes conjointly longitudinally impressed (2); posterior lobe about twice as long as anterior; hemelytra not or very slightly passing abdominal apex (3); abdomen a little broader than hemelytra; legs of moderate size (4); femora near apices obsolete subnodulose (5); anterior femora not or slightly incrassated (6) (Distant 1904).

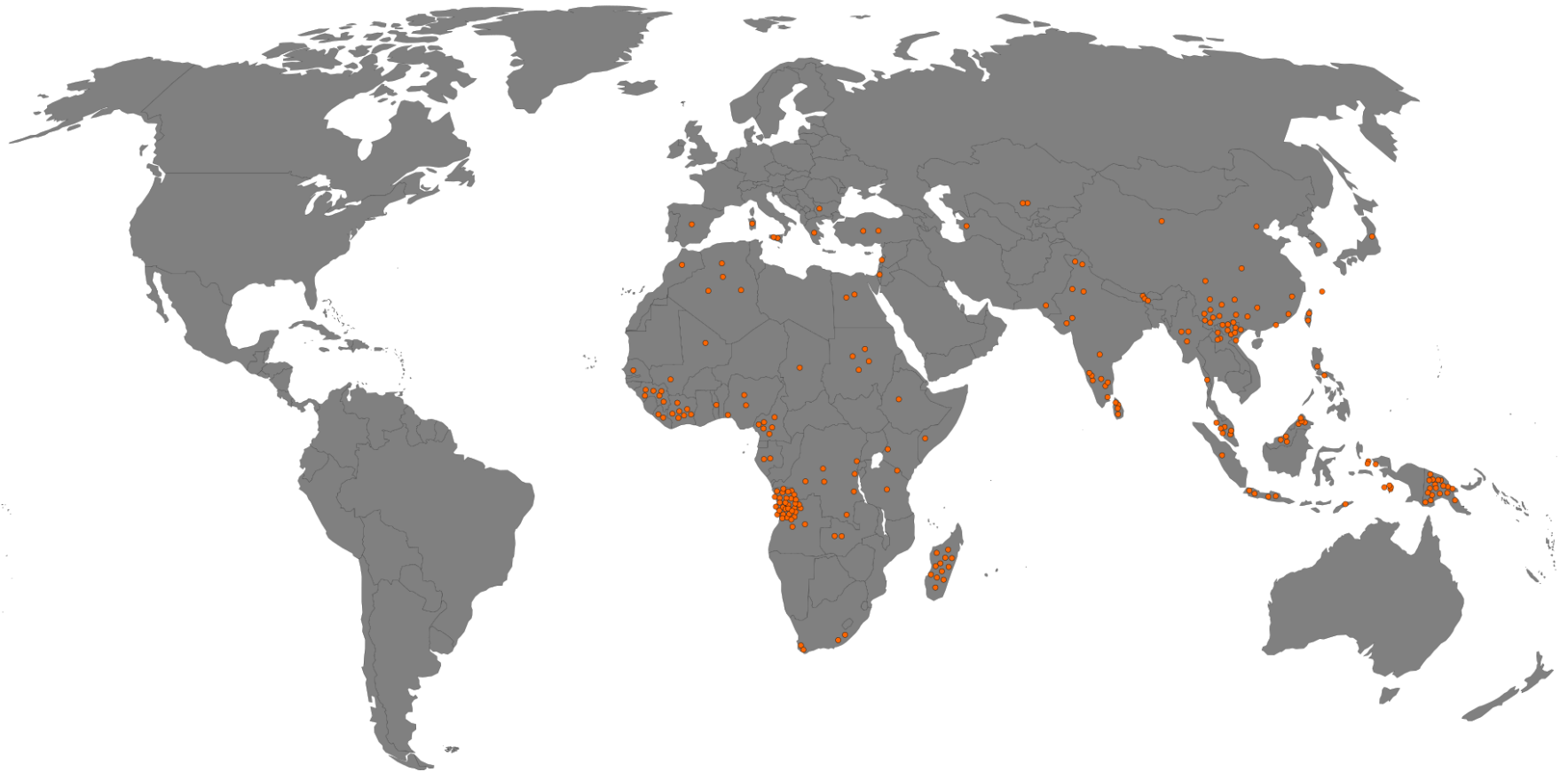


Figure 2.4. World distribution map of the genus *Spedanolestes* Stål, 1867.

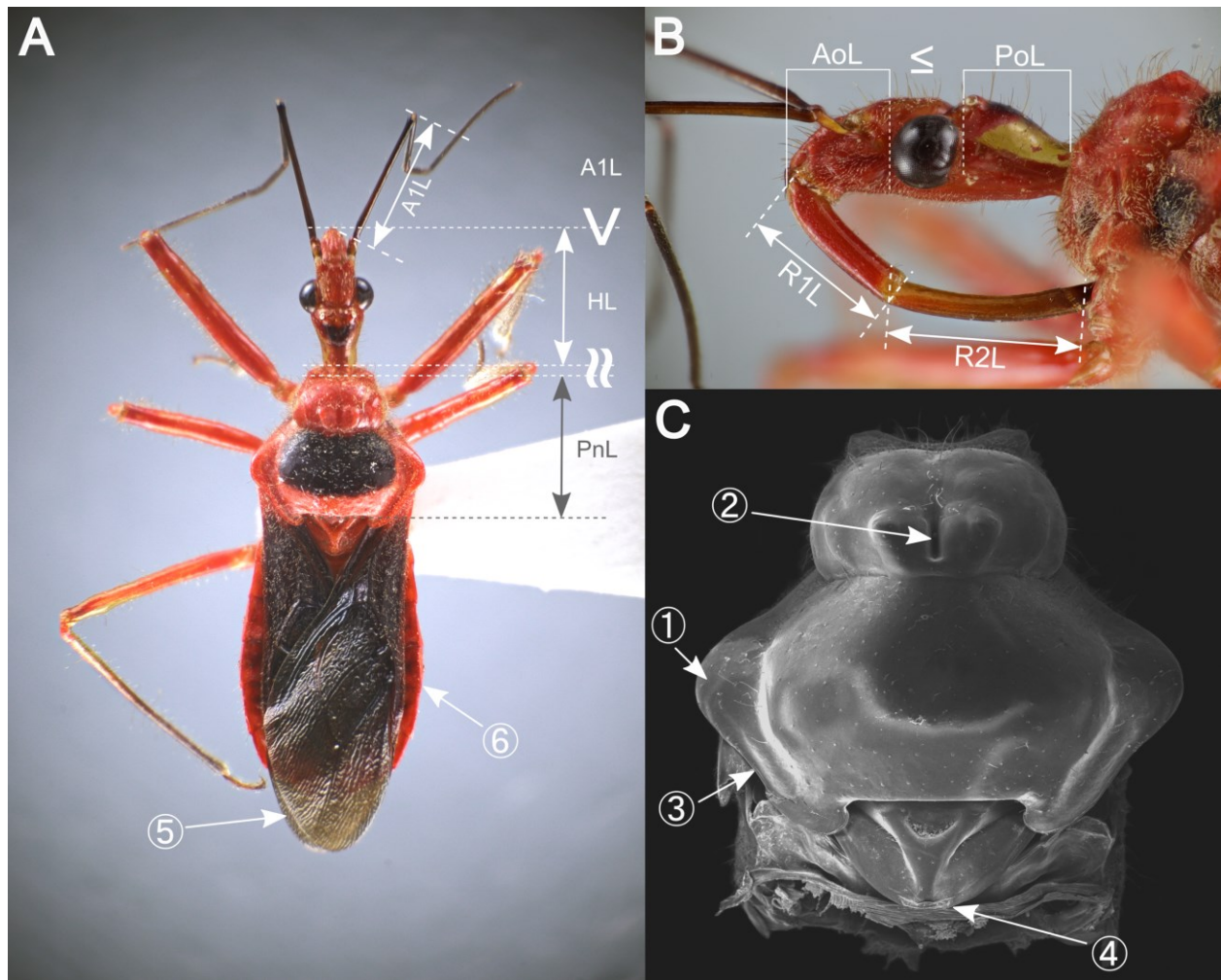


Figure 2.5. Diagnosis characters of the genus *Rhynocoris* Hahn, 1834. **A, B, C,** *Rhynocoris mendicus* (Stål, 1867), AD2019-001, ♂. **A,** Body in dorsal view; **B,** Head in lateral view; **C,** Pronotum in dorsal view. Body elongated, elliptic; head elongated and elliptic, nearly as long as pronotum; antecular area of head as long as or shorter than postocular area; postocular area of head gradually narrowed posteriorly; scape longer than head; first visible labial segment shorter than second segment, reaching level of middle of eye; compound eye prominent; pronotum shorter than humeral width, prominent at anterolateral angles (1); anterior pronotal lobe shorter than posterior pronotal lobe, with median sulcus posteriorly (2); median sulcus not reaching posterior lobe (2); posterior lobe rounded at humeral angles, with reflexed posterolateral margins (3); scutellum triangular, reflexed in apical part, triangularly elevated discally (4); hemelytra reaching or exceeding apex of abdomen (5); abdomen elliptic, wider than hemelytra, with gently curved lateral margins (6); genital capsule with a process dorsoapically; parameres rod-shaped (Ishikawa 2003).



Figure 2.6. World distribution map of the genus *Rhynocoris* Hahn, 1834.

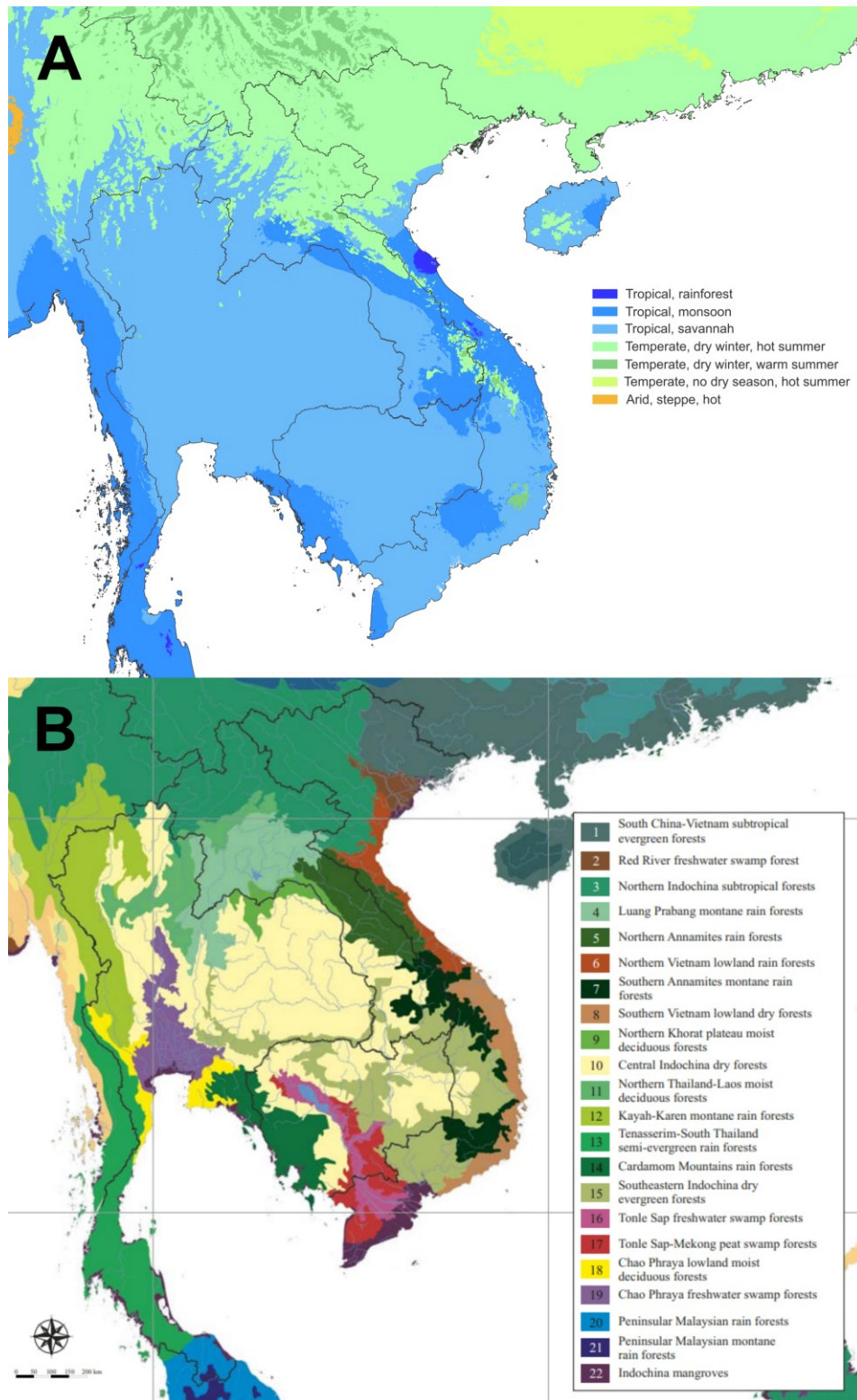


Figure 2.7. Climate and terrestrial ecoregion maps of Indo-China. **A**, combining with climate regions given by Beck et al. (2018); **B**, combining with terrestrial ecoregions given by Poyarkov et al. (2021) following Olson et al. (2001).

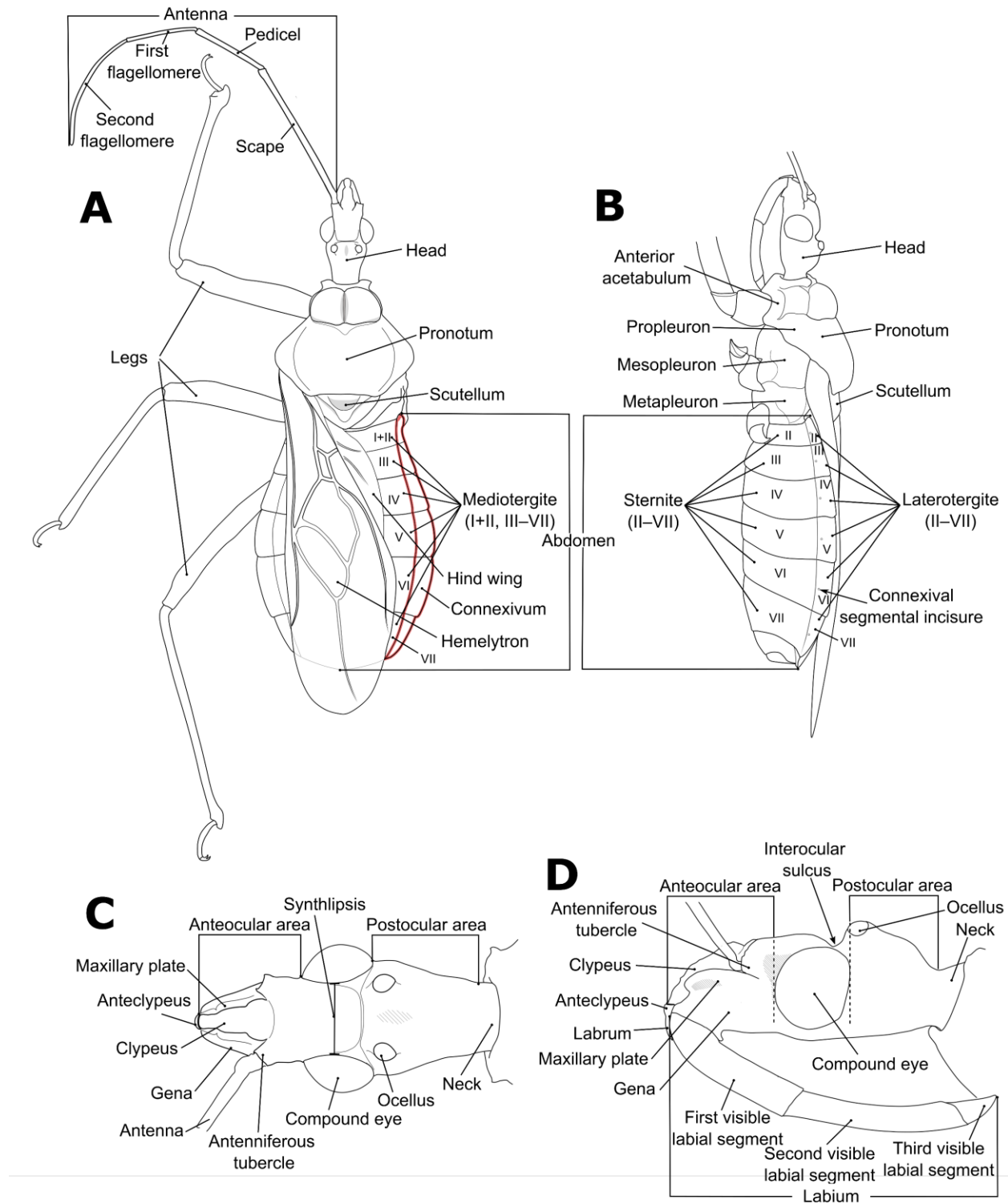


Figure 2.8. Structure and morphological terms of *Biasticus* species. Drawing based on *Biasticus luteicollis* Ha, Truong & Ishikawa, 2022, paratype, ♀, HNL2018-024. **A**, body in dorsal view; **B**, body in lateral view; **C**, head in dorsal view; **D**, head in lateral view.

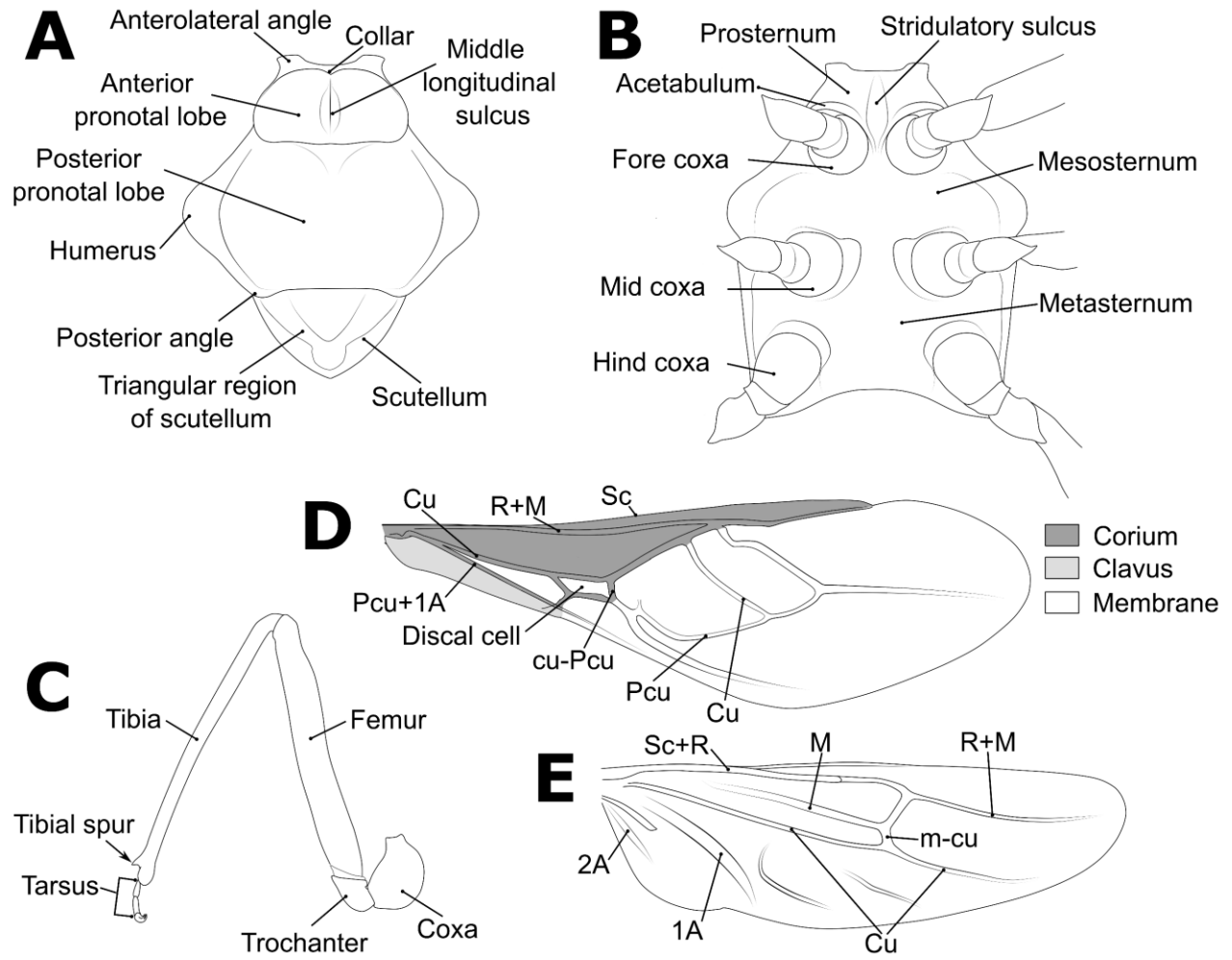


Figure 2.9. Structure and morphological terms of *Biasticus* species. Drawing based on *Biasticus luteicollis* Ha, Truong & Ishikawa, 2022, paratype, ♀, HNL2018-024. **A**, pronotum and scutellum in dorsal view; **B**, thorax in ventral view; **C**, right fore leg in anterior view; **D**, right hemelytron in dorsal view; **E**, right hind wing in dorsal view.

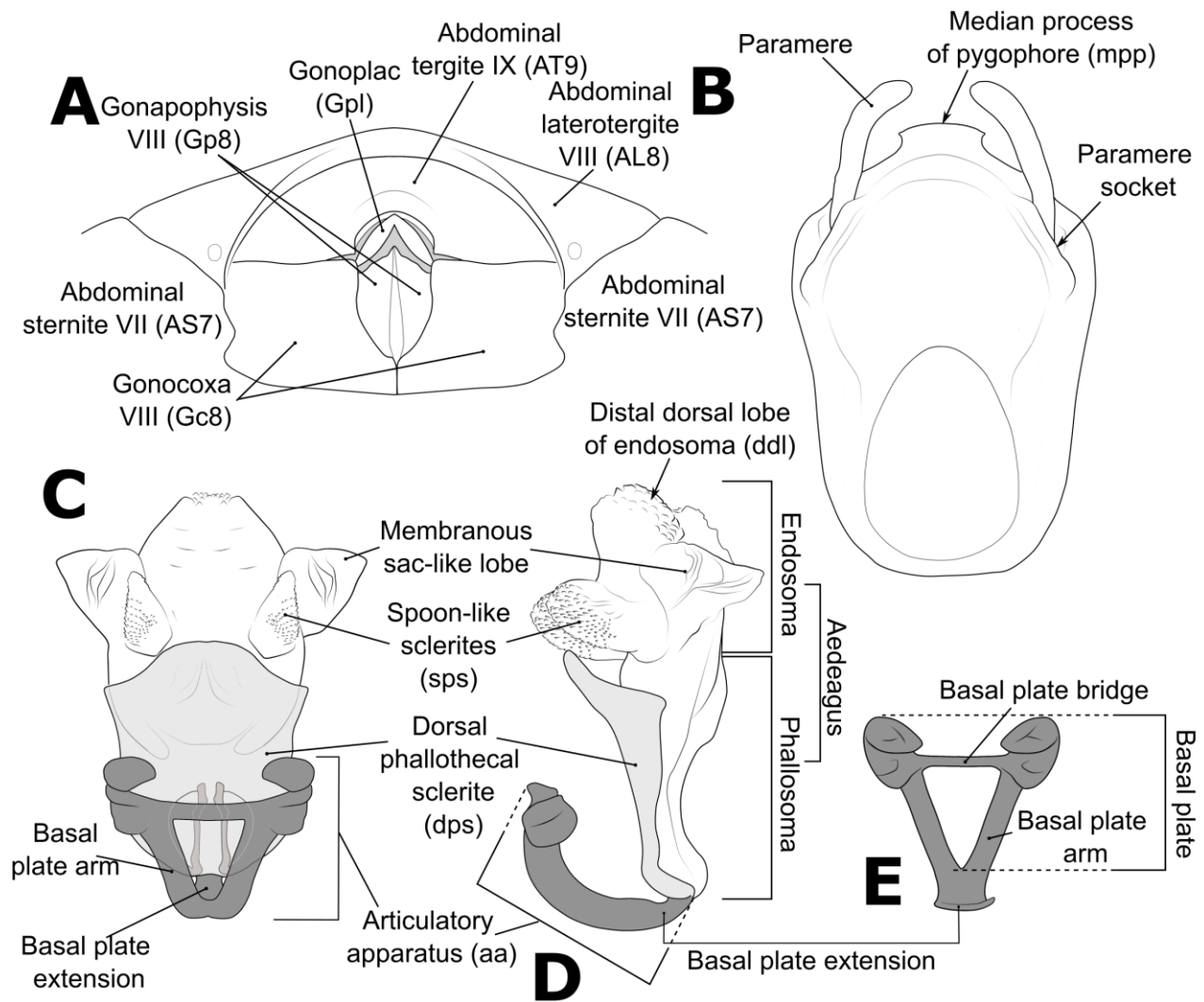


Figure 2.10. Structure and morphological terms of *Biasticus* species. Drawing based on *Biasticus luteicollis* Ha, Truong & Ishikawa, 2022. **A**, paratype, ♀, HNL2018-024; **B–E**, holotype, ♂, HNL2018-025. **A**, female external genitalia in ventral view; **B**, pygophore with parameres of male genitalia in dorsal view; **C**, phallus in dorsal view; **D**, phallus in lateral view; **E**, articulatory apparatus in ventral view.

Table 2.1. The data of the specimens used in this study. Abbreviations and symbols: S, success; N, failure; n/a: no data or not examined; BNHM, British Natural History Museum collection, UK; IEBR, Institute of Ecology and Biological Resources, Vietnam Academy of Science and Technology, Vietnam; NRM, Swedish Museum of Natural History, Sweden; NSMT, National Museum of Nature and Science, Tokyo, Japan; TARI, Taiwan Agricultural Research Institute Insect Collection, Taiwan Agricultural Research Institute, Taiwan; TMU-SZL, Systematic Zoology Laboratory, Tokyo Metropolitan University; UCR, Entomology Research Museum, University of California, Riverside, U.S.A; *, tentatively hold by Ha N. L. (first author).

No	Morpho-species/Species	Specimen code	Collecting date	Locality	Sex	Accession numbers			Depository
						16S	COI	Uni-Minibar	
Ingroups									
1	<i>B. sp.</i> HNL003	TXL2017-839	22. vii. 2017	Vietnam, Gia Lai	♀	S	N	N	IEBR
2	<i>B. sp.</i> HNL003	TXL2016-530	27. iv. 2016	Vietnam, Gia Lai	♀	S	S	S	IEBR
3	<i>B. sp.</i> HNL003	TXL2016-670	04. v. 2016	Vietnam, Dak Lak	♀	S	S	S	IEBR
4	<i>B. sp.</i> HNL003	TXL2016-558	29. iv. 2016	Vietnam, Gia Lai	♀	S	S	S	IEBR
5	<i>B. sp.</i> HNL003	TXL2016-671	04. v. 2016	Vietnam, Dak Lak	♀	S	S	S	IEBR
6	<i>B. sp.</i> HNL004	TXL2018-065	08. v. 2018	Vietnam, Dak Lak	♀	S	S	S	IEBR
7	<i>B. sp.</i> HNL004	TXL2018-067	08. v. 2018	Vietnam, Dak Lak	♀	S	S	S	IEBR
8	<i>B. sp.</i> HNL004	TXL2018-068	08. v. 2018	Vietnam, Dak Lak	♀	S	S	S	IEBR
9	<i>B. sp.</i> HNL005	HNL2019-061	27. iii. 2019	Vietnam, Thua Thien Hue	♀	S	S	S	IEBR*
10	<i>B. sp.</i> HNL006	TXL2016-621	11. vi. 2016	Vietnam, Thanh Hoa	♂	S	S	S	IEBR
11	<i>B. sp.</i> HNL007 (= <i>B. flavinotus</i> (Matsumura, 1913))	HU-TW-1928-001	iv-v.1928	Taiwan	♂	n/a	n/a	n/a	HU
12	<i>B. sp.</i> HNL007 (= <i>B. flavinotus</i> (Matsumura, 1913))			Taiwan, Gyochi (Yuechih)	♀	n/a	n/a	n/a	HU
13	<i>B. sp.</i> HNL007 (= <i>B. flavinotus</i> (Matsumura, 1913))	TW-Redu-2014-001	3. vii. 2014	Taiwan, Nantou	♀	S	N	S	TARI
14	<i>B. sp.</i> HNL007 (= <i>B. flavinotus</i>)	TW-Redu-2019-001	3. v. 2019	Taiwan, Taitung	♀	S	N	S	TARI

(Matsumura, 1913)

15	<i>B. sp.</i> HNL008	HNL2019-092	11. vi. 2019	Vietnam, Vinh Phuc	♀	S	S	N	IEBR*
16	<i>B. sp.</i> HNL009	TXL2019-680	06. v. 2019	Vietnam, Lao Cai	♂	S	S	N	IEBR
17	<i>B. sp.</i> HNL009	TXL2019-681	06. v. 2019	Vietnam, Lao Cai	♂	S	S	N	IEBR
18	<i>B. sp.</i> HNL009	TXL2019-011	06. v. 2019	Vietnam, Lao Cai	♂	n/a	n/a	n/a	IEBR
19	<i>B. sp.</i> HNL009	TXL2019-013	06. v. 2019	Vietnam, Lao Cai	♂	n/a	n/a	n/a	IEBR
20	<i>B. sp.</i> HNL009	TXL2019-015	06. v. 2019	Vietnam, Lao Cai	♂	n/a	n/a	n/a	IEBR
21	<i>B. sp.</i> HNL009	VN-HEM-2011- 007	24. v. 2011	Vietnam, Lao Cai	♀	S	N	S	IEBR*
22	<i>B. sp.</i> HNL009	VN-HEM-2011- 008	24. v. 2011	Vietnam, Lao Cai	♀	S	N	S	IEBR*
23	<i>B. sp.</i> HNL009	TXL2019-012	06. v. 2019	Vietnam, Lao Cai	♀	n/a	n/a	n/a	IEBR
24	<i>B. sp.</i> HNL010	TXL2019-700	15. v. 2019	Vietnam, Tuyen Quang	♀	S	S	N	IEBR
25	<i>B. sp.</i> HNL011 (= <i>B. taynguyenensis</i> Ha, Truong et Ishikawa, 2022)	HNL2018-036	09. v. 2018	Vietnam, Dak Lak	♀	OM908207	OM868188	ON542864	IEBR*
26	<i>B. sp.</i> HNL011 (= <i>B. taynguyenensis</i> Ha, Truong et Ishikawa, 2022)	HNL2018-072	08. v. 2018	Vietnam, Gia Lai	♀	OM908210	OM868178	ON542867	NSMT
27	<i>B. sp.</i> HNL011 (= <i>B. taynguyenensis</i> Ha, Truong et Ishikawa, 2022)	HNL2018-073	08. v. 2018	Vietnam, Gia Lai	♀	OM908211	OM868192	ON542868	IEBR*
28	<i>B. sp.</i> HNL011 (= <i>B. taynguyenensis</i> Ha, Truong et Ishikawa, 2022)	HNL2018-074	08. v. 2018	Vietnam, Gia Lai	♀	OM908212	OM868193	ON542869	VNMN
29	<i>B. sp.</i> HNL011 (= <i>B. taynguyenensis</i> Ha, Truong et Ishikawa, 2022)	HNL2018-075	08. v. 2018	Vietnam, Gia Lai	♀	OM908213	OM868194	ON542870	VNMN
30	<i>B. sp.</i> HNL011 (= <i>B. taynguyenensis</i> Ha, Truong et Ishikawa, 2022)	HNL2018-076	08. v. 2018	Vietnam, Gia Lai	♀	ON554765	N	ON542871	NSMT
31	<i>B. sp.</i> HNL011 (= <i>B. taynguyenensis</i> Ha, Truong et Ishikawa, 2022)	TXL2016-545	28. iv. 2016	Vietnam, Gia Lai	♂	OM908227	OM868177	ON542894	IEBR*
32	<i>B. sp.</i> HNL011 (= <i>B. taynguyenensis</i> Ha, Truong et Ishikawa, 2022)	TXLBX1	26. iii. 2022	Vietnam, Gia Lai	♂	S	S	N	IEBR
33	<i>B. sp.</i> HNL012 (= <i>B. griseocapillus</i> Ha, Truong et Ishikawa, 2022)	HNL2018-007	05. v. 2018	Vietnam, Gia Lai	♀	OM908197	OM868176	ON542854	NSMT

34	<i>B. sp.</i> HNL012 (= <i>B. griseocapillus</i> Ha, Truong et Ishikawa, 2022)	HNL2018-037	09.v.2018	Vietnam, Dak Lak	♀	OM908208	OM868189	ON542865	IEBR*
35	<i>B. sp.</i> HNL012 (= <i>B. griseocapillus</i> Ha, Truong et Ishikawa, 2022)	HNL2018-038	09. v. 2018	Vietnam, Dak Lak	♀	OM908209	OM868191	ON542866	IEBR*
36	<i>B. sp.</i> HNL012 (= <i>B. griseocapillus</i> Ha, Truong et Ishikawa, 2022)	AD2020-002	14. v. 2020	Vietnam, Phu Yen	♀	S	S	S	IEBR*
37	<i>B. sp.</i> HNL012 (= <i>B. griseocapillus</i> Ha, Truong et Ishikawa, 2022)	TXL2016-546	28. iv. 2016	Vietnam, Gia Lai	♂	OM908228	OM908228	OM908228	IEBR*
38	<i>B. sp.</i> HNL012 (= <i>B. griseocapillus</i> Ha, Truong et Ishikawa, 2022)	TXLBX17	4. v. 2022	Vietnam, Dak Lak	♂	S	S	S	IEBR
39	<i>B. sp.</i> HNL013 (= <i>B. luteicollis</i> Ha, Truong et Ishikawa, 2022)	HNL2018-022	09. v. 2018	Vietnam, Dak Lak	♂	OM908203	OM868184	ON542860	NSMT
40	<i>B. sp.</i> HNL013 (= <i>B. luteicollis</i> Ha, Truong et Ishikawa, 2022)	HNL2018-025	09. v. 2018	Vietnam, Dak Lak	♂	OM908206	OM868187	ON542863	IEBR*
41	<i>B. sp.</i> HNL013 (= <i>B. luteicollis</i> Ha, Truong et Ishikawa, 2022)	HNL2018-079	08. v. 2018	Vietnam, Gia Lai	♂	OM908215	OM868196	ON542873	NSMT
42	<i>B. sp.</i> HNL013 (= <i>B. luteicollis</i> Ha, Truong et Ishikawa, 2022)	HNL2018-083	08. v. 2018	Vietnam, Gia Lai	♂	OM908219	OM868200	ON542877	VNMN
43	<i>B. sp.</i> HNL013 (= <i>B. luteicollis</i> Ha, Truong et Ishikawa, 2022)	HNL2018-084	08. v. 2018	Vietnam, Gia Lai	♂	OM908220	OM868201	ON542878	NSMT
44	<i>B. sp.</i> HNL013 (= <i>B. luteicollis</i> Ha, Truong et Ishikawa, 2022)	HNL2018-085	08. v. 2018	Vietnam, Gia Lai	♂	OM908221	OM868202	ON542879	IEBR*
45	<i>B. sp.</i> HNL013 (= <i>B. luteicollis</i> Ha, Truong et Ishikawa, 2022)	HNL2018-086	08. v. 2018	Vietnam, Gia Lai	♂	OM908222	OM868203	ON542855	IEBR
46	<i>B. sp.</i> HNL013 (= <i>B. luteicollis</i> Ha, Truong et Ishikawa, 2022)	TXL2016-617	05, v, 2018	Vietnam, Dak Lak	♂	OM908230	OM868209	ON542857	NSMT
47	<i>B. sp.</i> HNL013 (= <i>B. luteicollis</i> Ha, Truong et Ishikawa, 2022)	HNL2018-017	09. v. 2018	Vietnam, Dak Lak	♀	OM908198	OM868179	ON542855	VNMN
48	<i>B. sp.</i> HNL013 (= <i>B. luteicollis</i> Ha, Truong et Ishikawa, 2022)	HNL2018-018	09. v. 2018	Vietnam, Dak Lak	♀	OM908199	OM868180	ON542856	IEBR*
49	<i>B. sp.</i> HNL013 (= <i>B. luteicollis</i> Ha,	HNL2018-019	09. v. 2018	Vietnam, Dak Lak	♀	OM908200	OM868181	ON542857	IEBR*

	Truong et Ishikawa, 2022)								
50	<i>B. sp.</i> HNL013 (= <i>B. luteicollis</i> Ha, Truong et Ishikawa, 2022)	HNL2018-020	09. v. 2018	Vietnam, Dak Lak	♀	OM908201	OM868182	ON542858	IEBR*
51	<i>B. sp.</i> HNL013 (= <i>B. luteicollis</i> Ha, Truong et Ishikawa, 2022)	HNL2018-021	09. v. 2018	Vietnam, Dak Lak	♀	OM908202	OM868183	ON542859	NSMT
52	<i>B. sp.</i> HNL013 (= <i>B. luteicollis</i> Ha, Truong et Ishikawa, 2022)	HNL2018-023	09. v. 2018	Vietnam, Dak Lak	♀	OM908204	OM868185	ON542861	NSMT
53	<i>B. sp.</i> HNL013 (= <i>B. luteicollis</i> Ha, Truong et Ishikawa, 2022)	HNL2018-024	09. v. 2018	Vietnam, Dak Lak	♀	OM908205	OM868186	ON542862	IEBR*
54	<i>B. sp.</i> HNL013 (= <i>B. luteicollis</i> Ha, Truong et Ishikawa, 2022)	HNL2018-078	08. v. 2018	Vietnam, Gia Lai	♀	OM908214	OM868195	ON542872	NSMT
55	<i>B. sp.</i> HNL013 (= <i>B. luteicollis</i> Ha, Truong et Ishikawa, 2022)	HNL2018-080	08. v. 2018	Vietnam, Gia Lai	♀	OM908216	OM868197	ON542874	IEBR*
56	<i>B. sp.</i> HNL013 (= <i>B. luteicollis</i> Ha, Truong et Ishikawa, 2022)	HNL2018-081	08. v. 2018	Vietnam, Gia Lai	♀	OM908217	OM868198	ON542875	IEBR*
57	<i>B. sp.</i> HNL013 (= <i>B. luteicollis</i> Ha, Truong et Ishikawa, 2022)	HNL2018-082	08. v. 2018	Vietnam, Gia Lai	♀	OM908218	OM868199	ON542876	VNMN
58	<i>B. sp.</i> HNL013 (= <i>B. luteicollis</i> Ha, Truong et Ishikawa, 2022)	TXL2016-616	05. v. 2018	Vietnam, Dak Lak	♀	OM908229	OM868208	ON542856	NSMT
59	<i>B. sp.</i> HNL016	TXL2017-666	19. ix. 2017	Vietnam, Tuyen Quang	♂	N	N	S	IEBR
60	<i>B. sp.</i> HNL017 (= " <i>Sphedanolestes</i> " <i>gularis</i> Hsiao, 1979)	TXL2018-843	22. vii. 2018	Vietnam, Gia Lai	♂	S	N	N	IEBR
61	<i>B. sp.</i> HNL017 (= " <i>Sphedanolestes</i> " <i>gularis</i> Hsiao, 1979)	AD2021-003	09. v. 2021	Vietnam, Cao Bang	♂	S	S	N	IEBR*
62	<i>B. sp.</i> HNL021	AD2022-001	01. v. 2022	Vietnam, Cao Bang	♀	S	S	S	IEBR*
63	<i>B. sp.</i> HNL021	AD2022-002	01. v. 2022	Vietnam, Cao Bang	♀	S	S	S	IEBR*
64	<i>B. sp.</i> HNL021	AD2022-003	01. v. 2022	Vietnam, Cao Bang	♀	S	S	S	IEBR*
65	<i>B. sp.</i> HNL021	AD2022-005	01. v. 2022	Vietnam, Cao Bang	♂	S	S	S	IEBR*
66	<i>B. sp.</i> HNL021	AD2022-006	01. v. 2022	Vietnam, Cao Bang	♂	S	S	S	IEBR*
67	<i>B. sp.</i> HNL021	NDD2022-246	17. iv.	Vietnam,	♂	S	S	S	IEBR*

			2022	Ha Giang					
68	<i>B. sp.</i> HNL022	HEM-TH-1998-001	16. iv. 1998	Thailand, Chiang Mai	♂	N	N	S	NSM
69	<i>B. sp.</i> HNL022	HEM-TH-1998-002	19. iv. 1998	Thailand, Chiang Mai	♂	N	N	S	NSM
70	<i>B. sp.</i> HNL022	HEM-TH-2002-003	13. v. 2002	Thailand, Chiang Mai	♂	N	N	S	NSM
71	<i>B. sp.</i> HNL022	HEM-TH-2000-001	18. iv. 2000	Thailand, Chiang Mai	♀	N	N	S	NSM
72	<i>B. sp.</i> HNL022	HEM-TH-2000-006	10. v. 2000	Thailand, Chiang Mai	♀	N	N	S	NSM
73	<i>B. sp.</i> HNL022	HEM-TH-2002-002	11. v. 2002	Thailand, Chiang Mai	♀	N	N	S	NSM
74	<i>B. sp.</i> HNL022	HEM-TH-2002-006	24. v. 2002	Thailand, Chiang Mai	♀	S	N	S	NSM
75	<i>B. sp.</i> HNL022	HEM-TH-2002-007	24. v. 2002	Thailand, Chiang Mai	♀	N	N	S	NSM
76	<i>B. sp.</i> HNL024	VN-Hem-2004-001	04. v. 2004	Vietnam, Ha Tinh	♀	N	N	S	IEBR*
77	<i>B. sp.</i> HNL024	VN-Hem-2004-002	04. v. 2004	Vietnam, Ha Tinh	♀	N	N	S	IEBR*
78	<i>B. sp.</i> HNL024	VN-Hem-2004-003	04. v. 2004	Vietnam, Ha Tinh	♀	N	N	S	IEBR*
79	<i>B. sp.</i> HNL024	VN-Hem-2004-004	04. v. 2004	Vietnam, Ha Tinh	♀	N	N	S	IEBR*
80	<i>B. sp.</i> HNL026	HEM-TH-2002-005	21. v. 2002	Thailand, Chiang Mai	♀	S	N	S	NSM
81	<i>B. sp.</i> HNL026	HEM-TH-2002-008	28. v. 2002	Thailand, Chiang Mai	♀	S	N	S	NSM
82	<i>B. sp.</i> HNL037 (= <i>B. confuses</i> Hsiao et al., 1979)	LA-Hem-2004-007	16. v. 2004	Laos, Houaphan	♀	S	N	S	NUOL
83	<i>B. sp.</i> HNL037 (= <i>B. confuses</i> Hsiao et al., 1979)	VN-Hem-1998-010	15. v. 1998	Vietnam, Cao Bang	♀	ON554779	N	ON542898	IEBR*
84	<i>B. sp.</i> HNL037 (= <i>B. confuses</i> Hsiao et al., 1979)	VN-Hem-1998-011	15. v. 1998	Vietnam, Cao Bang	♀	N	N	ON542899	IEBR*
85	<i>B. sp.</i> HNL037 (= <i>B. confuses</i> Hsiao et al., 1979)	VN-Hem-1998-012	22-27. v. 1998	Vietnam, Lao Cai	♀	N	N	ON542900	IEBR*
86	<i>B. sp.</i> HNL037 (= <i>B. confuses</i> Hsiao et al., 1979)	VN-HEM-2011-011	27. v. 2011	Vietnam, Lai Chau	♀	S	N	S	IEBR*
87	<i>B. sp.</i> HNL037 (= <i>B. confuses</i> Hsiao et al., 1979)	VN-HEM-2011-013	28. v. 2011	Vietnam, Cao Bang	♀	S	N	S	IEBR*

88	<i>B. sp.</i> HNL037 (= <i>B. confuses</i> Hsiao et al., 1979)	AD2021-002	09. v. 2021	Vietnam, Cao Bang	♀	S	N	S	IEBR*
89	<i>B. sp.</i> HNL037 (= <i>B. confuses</i> Hsiao et al., 1979)	NSMT-I-He-8263	15. v. 1998	Vietnam, Cao Bang	♂	n/a	n/a	n/a	NSMT
90	<i>B. sp.</i> HNL037 (= <i>B. confuses</i> Hsiao et al., 1979)	AD2020-027	06. vi. 2020	Vietnam, Cao Bang	♂	S	N	S	IEBR*
91	<i>B. sp.</i> HNL037 (= <i>B. confuses</i> Hsiao et al., 1979)	AD2021-001	09. v. 2021	Vietnam, Cao Bang	♂	S	N	S	IEBR*
92	<i>B. sp.</i> HNL043	HNL2018-117	12. vi. 2018	Vietnam, Lang Son	♀	S	S	S	IEBR
93	<i>B. sp.</i> HNL043	TXL2000-006	20. x. 2000	Vietnam, Son La	♀	N	N	N	IEBR
94	<i>B. sp.</i> HNL044	HEM-TH1999-002	25. iii. 1999	Thailand, Chiang Mai	♀	N	N	N	NSM
95	<i>B. sp.</i> HNL044	HEM-TH2004-022	3. vi. 2004	Thailand, Chiang Rai	♀	S	N	S	NSM
96	<i>B. sp.</i> HNL046	HEM-TH-2002-022	09. v. 2002	Thailand, Chiang Mai	♂	N	N	S	NSM
97	<i>B. sp.</i> HNL046	HEM-TH-2004-020	01. vi. 2004	Thailand, Chiang Rai	♀	N	N	S	NSM
98	<i>B. sp.</i> HNL048	TXL2016-547	28. iv. 2016	Vietnam, Gia Lai	♀	N	N	N	IEBR
99	<i>B. sp.</i> HNL049	NDD2022-062	06. v. 2022	Vietnam, Binh Dinh	♀	S	S	n/a	IEBR*
100	<i>B. sp.</i> HNL050	NDD2022-066	06. v. 2022	Vietnam, Binh Dinh	♂	S	S	n/a	IEBR*
101	<i>B. sp.</i> HNL051	NDD2022-014	01. v. 2022	Vietnam, Quang Nam	♀	S	S	n/a	IEBR*
102	<i>B. sp.</i> HNL053	NDD2022-015	02. v. 2022	Vietnam, Quang Nam	♂	S	S	n/a	IEBR*
103	<i>B. sp.</i> HNL053	NDD2022-020	02. v. 2022	Vietnam, Quang Nam	♂	N	S	n/a	IEBR*
104	<i>B. sp.</i> HNL053	NDD2022-025	02. v. 2022	Vietnam, Quang Nam	♂	S	S	n/a	IEBR*
105	<i>B. sp.</i> HNL053	NDD2022-017	02. v. 2022	Vietnam, Quang Nam	♀	S	S	n/a	IEBR*
106	<i>B. sp.</i> HNL053	NDD2022-019	02. v. 2022	Vietnam, Quang Nam	♀	S	S	n/a	IEBR*
107	<i>B. sp.</i> HNL054	NDD2022-002	29. iv. 2022	Vietnam, Quang Nam	♀	S	S	n/a	IEBR*
108	<i>B. sp.</i> HNL054	NDD2022-003	29. iv. 2022	Vietnam, Quang Nam	♀	S	S	n/a	IEBR*

109	<i>B. sp.</i> HNL054	NDD2022-005	29. iv. 2022	Vietnam, Quang Nam	♀	S	S	n/a	IEBR*
110	<i>B. sp.</i> HNL054	NDD2022-011	01. v. 2022	Vietnam, Quang Nam	♀	S	S	n/a	IEBR*
111	<i>B. sp.</i> HNL054	NDD2022-018	02. v. 2022	Vietnam, Quang Nam	♀	S	S	n/a	IEBR*
112	<i>B. sp.</i> HNL054	NDD2022-021	02. v. 2022	Vietnam, Quang Nam	♀	S	S	n/a	IEBR*
113	<i>B. sp.</i> HNL054	NDD2022-022	02. v. 2022	Vietnam, Quang Nam	♂	S	S	n/a	IEBR*
114	<i>B. sp.</i> HNL058	TXLBX16	26. v. 2022	Vietnam, Ha Giang	♀	S	S	S	IEBR
115	<i>B. sp.</i> HNL063 (= " <i>Sphedanolestes annulipes</i> Distant, 1903)	LA-Redu-2011-005	06. v. 2011	Laos, Xieng Khouang	♀	S	n/a	S	NUOL
116	<i>B. sp.</i> HNL063 (= " <i>Sphedanolestes annulipes</i> Distant, 1903)	LA-Redu-2011-006	06. v. 2011	Laos, Xieng Khouang	♂	S	n/a	S	NUOL
117	<i>B. sp.</i> HNL064	TXL2018-008	05. v. 2018	Vietnam, Gia Lai	♀	S	S	S	IEBR
118	<i>B. sp.</i> HNL067 (= <i>B. flavus</i> (Distant, 1903))	HEM-TH2004-016	24. v. 2004	Thailand, Chiang Mai	♂	ON554770	N	ON542887	NSM
119	<i>B. sp.</i> HNL067 (= <i>B. flavus</i> (Distant, 1903))	HEM-TH2004-018	25. v. 2004	Thailand, Chiang Mai	♂	ON554772	N	ON542889	NSM
120	<i>B. sp.</i> HNL067 (= <i>B. flavus</i> (Distant, 1903))	HEM-TH2004-019	25. v. 2004	Thailand, Chiang Mai	♂	ON554773	N	ON542890	NSM
121	<i>B. sp.</i> HNL067 (= <i>B. flavus</i> (Distant, 1903))	LA-Redu-2010-005	11. v. 2010	Laos, Xieng Khouang	♂	ON554769	N	ON542886	NUOL
122	<i>B. sp.</i> HNL067 (= <i>B. flavus</i> (Distant, 1903))	LA-Redu-2004-006	15. v. 2004	Laos, Houaphan	♀	ON554778	N	ON542883	NUOL
123	<i>B. sp.</i> HNL067 (= <i>B. flavus</i> (Distant, 1903))	HEM-TH2004-017	24. v. 2004	Thailand, Chiang Mai	♀	ON554771	N	ON542888	NSM
124	<i>B. sp.</i> HNL067 (= <i>B. flavus</i> (Distant, 1903))	LA-Redu-2004-011	21. v. 2004	Laos, Houaphan	♂	N	N	N	NUOL
125	<i>B. sp.</i> HNL067 (= <i>B. flavus</i> (Distant, 1903))	LA-Redu-2004-014	22. v. 2004	Laos, Houaphan	♂	N	N	N	NUOL
126	<i>B. sp.</i> HNL067 (= <i>B. flavus</i> (Distant, 1903))	HEM-TH2004-021	03. vi. 2004	Thailand, Chiang Rai	♀	ON554774	N	ON542891	NSM
127	<i>B. sp.</i> HNL067 (= <i>B. flavus</i> (Distant, 1903))	LA-Redu-2008-005	04. v. 2008	Laos, Xieng Khouang	♀	ON554767	N	ON542884	NUOL
128	<i>B. sp.</i> HNL067 (= <i>B. flavus</i> (Distant,	LA-Redu-2010-004	11. v. 2010	Laos, Xieng	♀	ON554768	N	ON542885	NUOL

1903))			Khouang						
129	<i>Blasticus</i> sp. M1	TXL2004-001	08. v. 2004	Vietnam, Ha Tinh	♂	N	N	N	IEBR
130	<i>B.</i> sp. M4	TXL2003-005	19. vii. 2003	Vietnam, Hai Phong	♂	N	N	N	IEBR
131	<i>B.</i> sp. M6	NSMT-I-He- 8268	21. v. 1997	Vietnam, Son La	♂	n/a	n/a	n/a	NSMT
132	<i>B.</i> sp. M6	TXL2004-003	26. v. 2004	Vietnam, Vinh Phuc	♂	N	N	N	IEBR
133	<i>B.</i> sp. M6	VN-Hem-2011- 017	30. v. 2011	Vietnam, Vinh Phuc	♂	S	N	S	IEBR*
134	<i>B.</i> sp. M6	VN-Hem-2011- 019	30. v. 2011	Vietnam, Vinh Phuc	♂	S	N	N	IEBR*
135	<i>B.</i> sp. M10	TXL2016-088	09. x. 2016	Vietnam, Son La	♂	S	N	N	IEBR
136	<i>B.</i> sp. M12	VN-Hem-1998- 005	22-27. v. 1998	Vietnam, Cao Bang	♂	N	N	N	IEBR*
137	<i>B.</i> sp. M12	VN-Hem-1998- 006	22-27. v. 1998	Vietnam, Cao Bang	♂	N	N	N	IEBR*
138	<i>B.</i> sp. M12	VN-Hem-1998- 007	22-27. v. 1998	Vietnam, Cao Bang	♂	N	N	N	IEBR*
139	<i>B.</i> sp. M12	VN-Hem-1998- 009	15. v. 1998	Vietnam, Cao Bang	♂	N	N	N	IEBR*
140	<i>B.</i> sp. M12	AD2020-030	07. vi. 2020	Vietnam, Cao Bang	♂	S	N	N	IEBR*
141	<i>B.</i> sp. M12	TXLBX20-1		Vietnam, Cao Bang	♂	S	N	N	IEBR
142	<i>B.</i> sp. M12	TXLBX20-3		Vietnam, Cao Bang	♂	N	N	N	IEBR
143	<i>B.</i> sp. M13	TXL2000-004	14. vii. 2000	Vietnam, Hoa Binh	♂	N	N	N	IEBR
144	<i>B.</i> sp. M16	HEM-TH-2000- 003	4-6. v. 2000	Thailand, Ching Dao	♂	N	N	N	NSM
145	<i>B.</i> sp. M16	HEM-TH-2000- 004	4-6. v. 2000	Thailand, Ching Dao	♂	N	N	N	NSM
146	<i>B.</i> sp. M16	HEM-TH-2000- 005	4-6. v. 2000	Thailand, Ching Dao	♂	N	N	N	NSM
147	<i>B.</i> sp. M17	NSMT-I-He- 73653	17. v. 2003	Vietnam, Lao Cai	♂	n/a	n/a	n/a	NSMT
148	<i>B.</i> sp. M18	NSMT-I-He- 8264	29. vi. 1997	Vietnam, Lao Cai	♂	n/a	n/a	n/a	NSMT
149	<i>B.</i> sp. M18	NSMT-I-He- 73785	18. v. 2003	Vietnam, Lao Cai	♂	n/a	n/a	n/a	NSMT
150	<i>B.</i> sp. M18	NSMT-I-He- 73786	18. v. 2003	Vietnam, Lao Cai	♂	n/a	n/a	n/a	NSMT
151	<i>B.</i> sp. M19	LA-Redu-2004- 005	15. v. 2004	Laos, Houaphan	♂	S	N	N	NUOL
152	<i>B.</i> sp. M19	LA-Redu-2004- 008	17. v. 2004	Laos, Houaphan	♂	N	N	N	NUOL
153	<i>B.</i> sp. M19	LA-Redu-2004- 013	21. v. 2004	Laos, Houaphan	♂	S	N	N	NUOL
154	<i>B.</i> sp. M20	VN-Hem-1997- 001	26. v. 1997	Vietnam, Lao Cai	♂	N	N	N	IEBR*

155	<i>B. sp. M21</i>	La-Redu-2004-015	22. v. 2004	Laos, Houaphan	♂	N	N	N	NUOL
156	<i>B. sp. M27</i>	LA-Redu-2008-004	30. iv. 2008	Laos, Xieng Khouang	♂	S	N	N	NUOL
157	<i>B. sp. M28</i>	VN-HEM-2011-012	27. v. 2011	Vietnam, Lao Cai	♂	S	N	N	IEBR*
158	<i>B. sp. M29</i>	LA-Redu-2011-003	04. v. 2011	Laos, Houaphan	♂	S	N	N	NUOL
159	<i>B. sp. M30</i>	VN-HEM-2011-016	28. v. 2011	Vietnam, Lai Chau	♂	S	N	S	IEBR*
160	<i>B. sp. M31</i>	NSMT-I-He-73776	21. vi. 2002	Vietnam, Lao Cai	♂	n/a	n/a	n/a	NSMT
161	<i>B. sp. M31</i>	NSMT-I-He-73777	21. vi. 2002	Vietnam, Lao Cai	♂	n/a	n/a	n/a	NSMT
162	<i>B. sp. F1</i>	TXL2004-002	14. v. 2004	Vietnam, Ha Tinh	♀	N	N	N	IEBR
163	<i>B. sp. F5</i>	VN-Hem-1998-003	22-27. v. 1998	Vietnam, Cao Bang	♀	N	N	N	IEBR*
164	<i>B. sp. F9</i>	NSMT-I-He-8267	19. v. 1997	Vietnam, Son La	♀	n/a	n/a	n/a	NSMT
165	<i>B. sp. F9</i>	NSMT-I-He-8265	21. v. 1997	Vietnam, Son La	♀	n/a	n/a	n/a	NSMT
166	<i>B. sp. F9</i>	LA-Redu-2004-009	20. v. 2004	Laos, Houaphan	♀	N	N	N	NUOL
167	<i>B. sp. F9</i>	LA-Redu-2004-010	20. v. 2004	Laos, Houaphan	♀	N	N	S	NUOL
168	<i>B. sp. F9</i>	VN-Hem-2011-010	25. v. 2011	Vietnam, Lao Cai	♀	S	N	S	IEBR*
169	<i>B. sp. F9</i>	VN-Hem-2011-018	30. v. 2011	Vietnam, Vinh Phuc	♀	S	N	N	IEBR*
170	<i>B. sp. F9</i>	TXL2021-010	v. 2021	Vietnam, Cao Bang	♀	S	N	S	IEBR
171	<i>B. sp. F9</i>	TXLBX8	19. v. 2022	Vietnam, Hoa Binh	♀	S	N	S	IEBR
172	<i>B. sp. F13</i>	HNL2018-077	08. v. 2018	Vietnam, Gia Lai	♀	N	N	N	IEBR
173	<i>B. sp. F14</i>	VN-Hem-1998-004	22-27. v. 1998	Vietnam, Cao Bang	♀	N	N	N	IEBR*
174	<i>B. sp. F14</i>	VN-Hem-1998-008	22-27. v. 1998	Vietnam, Cao Bang	♀	S	N	N	IEBR*
175	<i>B. sp. F14</i>	TXLBX20-2		Vietnam, Cao Bang	♀	N	N	N	IEBR
176	<i>B. sp. F15</i>	ZRC.HEM.50	28. i. 1975	Singapore	♀	n/a	n/a	n/a	ZRC
177	<i>B. sp. F15</i>	ZRC.HEM.244		Malaysia, Kuala Lumpur	♀	n/a	n/a	n/a	ZRC
178	<i>B. sp. F16</i>	ZRC.ENT00012353	31. viii. 2014	Singapore, Chestnut Avenue	♀	n/a	n/a	n/a	ZRC
179	<i>B. sp. F17</i>	TW-Redu-1980-001	10. viii. 1980	Taiwan, Taitung	♀	N	N	N	TARI
180	<i>B. sp. F21</i>	MMR-Hem-1987-001	21-22. ix. 1987	Myanmar, Shan	♀	N	N	N	IEBR*

181	<i>B. sp.</i> F23	HEM-TH-2004-023	04. vi. 2004	Thailand, Chiang Rai	♀	S	N	S	NSM
182	<i>B. sp.</i> F24	LA-Redu-2004-012	21. v. 2004	Laos, Houaphan	♀	S	N	N	NUOL
183	<i>B. sp.</i> F24	LA-Redu-2010-002	08. v. 2010	Laos, Xieng Khouang	♀	N	N	N	NUOL
184	<i>B. sp.</i> F24	VN-Hem-2011-001	26. v. 2011	Vietnam, Lao Cai	♀	N	N	N	IEBR*
185	<i>B. sp.</i> F25	VN-Hem-1997-002	27. v. 1997	Vietnam, Lao Cai	♀	N	N	S	IEBR*
186	<i>B. sp.</i> F26	VN-Hem-2000-007	06. v. 2000	Vietnam, Lao Cai	♀	N	N	N	IEBR*
187	<i>B. sp.</i> F26	VN-Hem-2000-008	06. v. 2000	Vietnam, Lao Cai	♀	N	N	N	IEBR*
188	<i>B. sp.</i> F26	VN-Hem-2000-009	06. v. 2000	Vietnam, Lao Cai	♀	N	N	N	IEBR*
189	<i>B. sp.</i> F26	VN-Hem-2000-010	06. v. 2000	Vietnam, Lao Cai	♀	N	N	N	IEBR*
190	<i>B. sp.</i> F27	VN-Hem-1999-001	20. vi. 1999	Vietnam, Lao Cai	♀	N	N	S	IEBR*
191	<i>B. sp.</i> F28	HEM-TH-2002-004	13. v. 2002	Thailand, Chiang Mai	♀	S	N	N	NSM
192	<i>B. sp.</i> F29	HEM-TH-2000-002	29. iv. 2000	Thailand, Chiang Mai	♀	N	N	S	NSM
193	<i>B. sp.</i> F30	VN-Hem-2011-002	28. v. 2011	Laos, Xieng Khouang	♀	N	N	N	IEBR*
194	<i>B. sp.</i> F31	LA-Redu-2010-001	07. v. 2010	Laos, Xieng Khouang	♀	S	N	N	NUOL
195	<i>B. sp.</i> F31	TXL2018-840	22. vii. 2018	Vietnam, Gia Lai	♀	N	N	N	IEBR
196	<i>B. sp.</i> F33	RCW_2681 (UCR_ENT00004467)	12. x. 2006	Thailand, Naykhon Nayok	♀	n/a	n/a	n/a	UCR
197	<i>B. sp.</i> F34	ZRC.HEM.55	04. v. 1974	Singapore, Bukit Timah forest	♀	n/a	n/a	n/a	ZRC
198	<i>B. sp.</i> F35	ZRC.HEM.49	23. xii. 1975	Malaysia, Pahang	♀	n/a	n/a	n/a	ZRC
199	<i>B. sp.</i> F36	ZRC.HEM.218		Malaysia, Kuala Lumpur	♀	n/a	n/a	n/a	ZRC
200	<i>B. sp.</i> F37	ZRC.ENT00012352	27. x. 2015	Singapore, Riffle Range Rd	♀	n/a	n/a	n/a	ZRC
201	<i>B. sp.</i> F40	TXL BX2	26. iii. 2022	Vietnam, Gia Lai	♀	N	N	N	IEBR
202	<i>B. sp.</i> F42	TXL BX18	14. v. 2022	Vietnam, Nghe An	♀	S	N	S	IEBR
203	<i>B. sp.</i> F48	LA-Redu-2008-002	28. iv. 2008	Laos, Xieng	♀	S	N	S	NUOL

				Khouang					
204	<i>B. sp.</i> F48	LA-Redu-2008-003	30. iv. 2008	Laos, Xieng Khouang	♀	S	N	S	NUOL
205	<i>B. sp.</i> F48	LA-Redu-2010-003	11. v. 2010	Laos, Xieng Khouang	♀	S	N	N	NUOL
206	<i>B. sp.</i> F49	VN-HEM-2011-014	28. v. 2011	Vietnam, Lai Chau	♀	S	N	S	IEBR*
207	<i>B. sp.</i> F49	VN-HEM-2011-015	28. v. 2011	Vietnam, Lai Chau	♀	S	N	S	IEBR*
208	<i>B. sp.</i> F51	TXL2021-009	v. 2021	Vietnam, Cao Bang	♀	S	N	N	IEBR
209	<i>B. sp.</i> F52	TXLBX19	14. v. 2022	Vietnam, Nghe An	♀	S	N	N	IEBR
210	<i>B. sp.</i> F53	TXLBXN3	28. iv. 2022	Vietnam, Gia Lai	♀	n/a	n/a	n/a	IEBR
211	<i>B. sp.</i> F54	TXL2002-065	20. vi. 2002	Vietnam, Thanh Hoa	♀	n/a	n/a	n/a	IEBR
212	<i>B. sp.</i> F59	TXL2002-064	22. iv. 2002	Vietnam, Hoa Binh	♀	n/a	n/a	n/a	IEBR
213	<i>B. abjectus</i> Miller, 1941 [Holotype]		07. viii. 1927	Borneo	♀	n/a	n/a	n/a	BNHM
214	<i>B. breddini</i> Miller, 1948 [Paratype]			Indonesia, Java	♀	n/a	n/a	n/a	BNHM
215	<i>B. chersonesus</i> (Distant, 1903) [Holotype]			Malaysia		n/a	n/a	n/a	BNHM
216	<i>B. eburneus</i> Miller, 1941 [Holotype]		12. ii. 1939	Borneo	♀	n/a	n/a	n/a	BNHM
217	<i>B. horfieldi</i> Distant, 1903 [Holotype]			Indonesia	♀	n/a	n/a	n/a	BNHM
218	<i>B. impiger</i> (Stål, 1863) [Holotype]			Cambodia	♀	n/a	n/a	n/a	NRM
219	<i>B. nigricollis</i> (Dallas, 1850) [Holotype]			Indonesia	♀	n/a	n/a	n/a	BNHM
220	<i>B. nigricollis</i> var. <i>rubescens</i> Miller [Paratype]			Indonesia, Java	♀	n/a	n/a	n/a	BNHM
221	<i>B. obfuscatus</i> Miller, 1949 [Holotype]		22. xi. 1940	Malay peninsula	♀	n/a	n/a	n/a	BNHM
222	<i>B. princeps</i> Miller, 1949 [Holotype]		29. ix. 1932	Malaysia, Selangor	♀	n/a	n/a	n/a	BNHM
223	<i>Sphedanolestes. sp.</i> HNL003 (=S. <i>impressicollis</i> (Stål, 1861))	TXL2018-842	22. vii. 2018	Vietnam, Gia Lai	♂	N	N	N	IEBR
224	<i>Sphedanolestes. sp.</i> HNL003 (=S. <i>impressicollis</i> (Stål, 1861))	NDD2013-001	15. v. 2013	Vietnam, Lang Son	♀	n/a	n/a	n/a	IEBR
225	<i>Sphedanolestes. sp.</i> HNL003 (=S. <i>impressicollis</i> (Stål, 1861))	TXL2011-509	20. v. 2011	Vietnam, Lao Cai	♀	S	N	N	IEBR

226	<i>Sphedanolestes</i> . sp. HNL003 (=S. <i>impressicollis</i> (Stål, 1861))	Eg2019-002	13. vii. 2019	Japan, Tokyo	♀	S	S	n/a	TMU-SZL
227	<i>Sphedanolestes</i> . sp. HNL003 (=S. <i>impressicollis</i> (Stål, 1861))	HNL2019-001	12. vii. 2019	Japan, Tokyo	♂	S	S	n/a	TMU-SZL
228	<i>Sphedanolestes</i> . sp. HNL003 (=S. <i>impressicollis</i> (Stål, 1861))	Eg2020-001	24. v. 2020	Japan, Tokyo	♂	S	S	n/a	TMU-SZL
229	<i>Sphedanolestes</i> . sp. HNL003 (=S. <i>impressicollis</i> (Stål, 1861))	Eg2020-002	24. v. 2020	Japan, Tokyo	♀	S	S	n/a	TMU-SZL
230	<i>Sphedanolestes</i> . sp. HNL003 (=S. <i>impressicollis</i> (Stål, 1861))	Eg2020-003	24. v. 2020	Japan, Tokyo	♂	S	S	n/a	TMU-SZL
231	<i>Sphedanolestes</i> . sp. HNL003 (=S. <i>impressicollis</i> (Stål, 1861))	Eg2020-004	24. v. 2020	Japan, Tokyo	♂	S	S	n/a	TMU-SZL
232	<i>Sphedanolestes</i> . sp. HNL003 (=S. <i>impressicollis</i> (Stål, 1861))	TXL2004-068	08. vii. 2004	Vietnam, Lao Cai	♂	n/a	n/a	n/a	IEBR
233	<i>Sphedanolestes</i> . sp. HNL003 (=S. <i>impressicollis</i> (Stål, 1861))	TXL2004-069	04. viii. 2004	Vietnam, Lao Cai	♀	n/a	n/a	n/a	IEBR
234	<i>Sphedanolestes</i> . sp. HNL003 (=S. <i>impressicollis</i> (Stål, 1861))	TXL2008-081	25. vi. 2008	Vietnam, Lao Cai	♂	n/a	n/a	n/a	IEBR
235	<i>Sphedanolestes</i> . sp. HNL003 (=S. <i>impressicollis</i> (Stål, 1861))	AD2020-033	07. vi. 2020	Vietnam, Cao Bang	♀	S	S	n/a	IEBR*
236	<i>Sphedanolestes</i> . sp. HNL003 (=S. <i>impressicollis</i> (Stål, 1861))	TXL2021-007	v. 2021	Vietnam, Cao Bang	♀	S	S	n/a	IEBR
237	<i>Sphedanolestes</i> . sp. HNL003 (=S. <i>impressicollis</i> (Stål, 1861))	TXL2021-008	v. 2021	Vietnam, Cao Bang	♀	S	S	n/a	IEBR
238	<i>Sphedanolestes</i> . sp. HNL003 (=S. <i>impressicollis</i> (Stål, 1861))	AD2022-004	1. v. 2022	Vietnam, Cao Bang	♀	S	S	n/a	IEBR*
239	<i>Sphedanolestes</i> . sp. HNL003 (=S. <i>impressicollis</i> (Stål, 1861))	NDD2022-075	15. iv. 2022	Vietnam, Ha Giang	♂	S	S	n/a	IEBR*
240	<i>Sphedanolestes</i> . sp. HNL003 (=S. <i>impressicollis</i> (Stål, 1861))	NDD2022-077	16. iv. 2022	Vietnam, Ha Giang	♂	S	S	n/a	IEBR*
241	<i>Sphedanolestes</i> . sp. HNL003 (=S.	NDD2022-078	17. iv. 2022	Vietnam, Ha Giang	♂	S	S	n/a	IEBR*

	<i>impressicollis</i> (Stål, 1861))								
242	<i>Sphedanolestes</i> sp. HNL003 (= <i>S. impressicollis</i> (Stål, 1861))	NDD2022-081	17. iv. 2022	Vietnam, Ha Giang	♂	S	S	n/a	IEBR*
243	“gen. C” sp. HNL001 (= <i>S. pubinotus</i> Reuter, 1881)	VN-HEM-2011-009	24. v. 2011	Vietnam, Lao Cai	♂	n/a	n/a	S	IEBR*
244	“gen. C” sp. HNL001 (= <i>S. pubinotus</i> Reuter, 1881)	HNL2019-002	11. iii. 2019	Vietnam, Quang Tri	♀	S	S	S	IEBR*
245	“gen. C” sp. HNL001 (= <i>S. pubinotus</i> Reuter, 1881)	TXL2021-006	v. 2021	Vietnam, Cao Bang	♀	S	S	S	IEBR
246	“gen. C” sp. HNL001 (= <i>S. pubinotus</i> Reuter, 1881)	TXL2021-012	09. v. 2021	Vietnam, Cao Bang	♀	S	S	S	IEBR
247	“gen. C” sp. HNL001 (= <i>S. pubinotus</i> Reuter, 1881)	NDD2022-007	30. iv. 2022	Vietnam, Quang Nam	♂	S	S	n/a	IEBR
248	“gen. C” sp. HNL001 (= <i>S. pubinotus</i> Reuter, 1881)	TXL BX11	26. iii. 2022	Vietnam, Gia Lai	♂	S	S	n/a	IEBR
249	“gen. C” sp. HNL001 (= <i>S. pubinotus</i> Reuter, 1881)	TXL2004-070	10. x. 2004	Vietnam, Lao Cai	♀	n/a	n/a	n/a	IEBR
250	“gen. C” sp. HNL001 (= <i>S. pubinotus</i> Reuter, 1881)	AD2020-003	14. v. 2020	Vietnam, Phu Yen	♀	S	S	n/a	IEBR*
251	“gen. C” sp. HNL002	TXL BX6	19. v. 2022	Vietnam, Hoa Binh	♂	S	S	S	IEBR
252	“gen. C” sp. M3	TXL2000-063	05. x. 2000	Vietnam, Son La	♂	n/a	n/a	n/a	IEBR
253	“gen. D” sp. HNL001 (= <i>S. xiongi</i> Cai et al., 2004)	NDD2019-276	18. ix. 2019	Vietnam, Dak Lak	♀	S	S	S	IEBR*
254	“gen. D” sp. HNL001 (= <i>S. xiongi</i> Cai et al., 2004)	NDD2019-281	19. ix. 2019	Vietnam, Dak Lak	♀	S	S	S	IEBR*
255	“gen. D” sp. HNL001 (= <i>S. xiongi</i> Cai et al., 2004)	NDD2019-282	19. ix. 2019	Vietnam, Dak Lak	♂	S	S	S	IEBR*
256	“gen. D” sp. HNL001 (= <i>S. xiongi</i> Cai et al., 2004)	NDD2019-283	19. ix. 2019	Vietnam, Dak Lak	♀	S	S	n/a	IEBR*
257	“gen. D” sp. HNL001 (= <i>S. xiongi</i> Cai et al.,	NDD2019-292	19. ix. 2019	Vietnam, Dak Lak	♂	S	S	n/a	IEBR*

	2004)								
258	“gen. D” sp. HNL001 (= <i>S.</i> <i>xiongi</i> Cai et al., 2004)	HNL2019-313	20. ix. 2019	Vietnam, Dak Lak	♀	n/a	n/a	n/a	IEBR*
259	“gen. D” sp. HNL001 (= <i>S.</i> <i>xiongi</i> Cai et al., 2004)	HNL2019-314	20. ix. 2019	Vietnam, Dak Lak	♀	S	S	n/a	IEBR*
260	“gen. D” sp. HNL001 (= <i>S.</i> <i>xiongi</i> Cai et al., 2004)	NDD2019-344	21. ix. 2019	Vietnam, Dak Lak	♀	S	S	n/a	IEBR*
261	“gen. D” sp. HNL001 (= <i>S.</i> <i>xiongi</i> Cai et al., 2004)	TXL2018-841	22. vii. 2018	Vietnam, Gia Lai	♀	S	S	n/a	IEBR
262	“gen. D” sp. HNL001 (= <i>S.</i> <i>xiongi</i> Cai et al., 2004)	TXL2003-066	16. viii. 2003	Vietnam, Nghe An	♀	n/a	n/a	n/a	IEBR
263	“gen. D” sp. HNL001 (= <i>S.</i> <i>xiongi</i> Cai et al., 2004)	TXL2003-067	16. viii. 2003	Vietnam, Nghe An	♂	n/a	n/a	n/a	IEBR
264		HNL2019-228	15. xi. 2019	Vietnam, Dong Nai	♂	S	n/a	S	IEBR*
265		ZRC.HEM.154	21. x. 1983	Singapore, Bukit Timah Forest	♀	n/a	n/a	n/a	ZRC
266		ZRC.HEM.259	10. iii. 1974	Singapore, Bukit Timah Forest	♀	n/a	n/a	n/a	ZRC
267	<i>S. bicolor</i> Schouteden, 1910 [Type]	n/a	n/a	Tanzania, Kilimandja ro	♀	n/a	n/a	n/a	NRM
268	<i>S. dromedarius</i> Reuter, 1881 [Type]	n/a	n/a	Guinea	♂	n/a	n/a	n/a	NRM
269	<i>S. fasciventris</i> (Stål, 1855) [Type]	n/a	n/a	South Africa, Eastern Cape	♀	n/a	n/a	n/a	NRM
270	<i>S. gulo</i> (Stål, 1863) [Type]	n/a	n/a	Indonesia, Mysool island	♀	n/a	n/a	n/a	NRM
271	<i>S. hemiochrus</i> (Stål, 1871) [Type]	n/a	n/a	Philippines	♂	n/a	n/a	n/a	NRM
272	<i>S. impressicollis</i> (Stål, 1861) [Type]	n/a	n/a	Hong Kong	♂	n/a	n/a	n/a	NRM
273	<i>S. indicus</i> Reuter, 1881 [Type]	n/a	n/a	Eastern India	♀	n/a	n/a	n/a	NRM
274	<i>S. jucundus</i> (Stål, 1866) [Type]	n/a	n/a	New Guinea	♀	n/a	n/a	n/a	NRM
275	<i>S. nanus</i> (Stål, 1855) [Type]	n/a	n/a	Zambia; Congo	♂	n/a	n/a	n/a	NRM
276	<i>S. politus</i> (Stål, 1870) [Type]	n/a	n/a	Philippines	♀	n/a	n/a	n/a	NRM

277	<i>S. pubinotus</i> Reuter, 1881 [Type]	n/a	n/a	India, Darjeeling	♀	n/a	n/a	n/a	NRM
278	<i>S. saucius</i> (Stål, 1861) [Type]	n/a	n/a	Indonesia, Aru islands	♂	n/a	n/a	n/a	NRM
279	<i>S. sjostedti</i> Villiers, 1948 [Type]	n/a	n/a	Cameroon	♀	n/a	n/a	n/a	NRM
280	<i>S. trichrous</i> Stål, 1874 [Type]	n/a	n/a	Eastern India	-	n/a	n/a	n/a	NRM
281	<i>S. verecundus</i> (Stål, 1863) [Type]	n/a	n/a	New Guinea	♂	n/a	n/a	n/a	NRM
282	“gen. E” sp. HNL001 (= <i>Rhynocoris mendicus</i> (Stål, 1867))	HNL2018-040	09. v. 2018	Vietnam, Gia Lai	♂	OP106592	S	OP103646	IEBR*
283	“gen. E” sp. HNL001 (= <i>Rhynocoris mendicus</i> (Stål, 1867))	TXL2016-592	04. v. 2016	Vietnam, Dak Lak	♂	S	S	n/a	IEBR
284	“gen. E” sp. HNL001 (= <i>Rhynocoris mendicus</i> (Stål, 1867))	TXL2016-593	04. v. 2016	Vietnam, Dak Lak	♂	S	S	n/a	IEBR
285	“gen. E” sp. HNL001 (= <i>Rhynocoris mendicus</i> (Stål, 1867))	TXL2016-594	04. v. 2016	Vietnam, Dak Lak	♂	S	S	n/a	IEBR
286	“gen. E” sp. HNL001 (= <i>Rhynocoris mendicus</i> (Stål, 1867))	TXL2016-595	04. v. 2016	Vietnam, Dak Lak	♂	S	S	n/a	IEBR
287	“gen. E” sp. HNL001 (= <i>Rhynocoris mendicus</i> (Stål, 1867))	TXL2016-596	04. v. 2016	Vietnam, Dak Lak	♂	S	S	n/a	IEBR
288	“gen. E” sp. HNL001 (= <i>Rhynocoris mendicus</i> (Stål, 1867))	TXL2016-597	04. v. 2016	Vietnam, Dak Lak	♂	S	S	n/a	IEBR
289	“gen. E” sp. HNL001 (= <i>Rhynocoris mendicus</i> (Stål, 1867))	TXL2016-598	04. v. 2016	Vietnam, Dak Lak	♂	S	S	n/a	IEBR
290	“gen. E” sp. HNL001 (= <i>Rhynocoris mendicus</i> (Stål, 1867))	TXL2016-599	04. v. 2016	Vietnam, Dak Lak	♂	S	S	n/a	IEBR
291	“gen. E” sp. HNL001 (= <i>Rhynocoris mendicus</i> (Stål, 1867))	AD2019-001	iii. 2019	Vietnam, Kon Tum	♂	S	S	n/a	IEBR*

292	“gen. E” sp. HNL001 (= <i>Rhynocoris mendicus</i> (Stål, 1867))	TXL2004-051	18. vii. 2004	Vietnam, Binh Dinh	♀	n/a	n/a	S	IEBR
293	“gen. E” sp. HNL001 (= <i>Rhynocoris mendicus</i> (Stål, 1867))	LA-Redu-2011-004	06. v. 2011	Laos, Xieng Khouang	♀	n/a	n/a	S	NUOL
294	“gen. E” sp. HNL001 (= <i>Rhynocoris mendicus</i> (Stål, 1867))	TXL2018-041	09. v. 2018	Vietnam, Gia Lai	♀	S	S	S	IEBR
295	“gen. E” sp. HNL001 (= <i>Rhynocoris mendicus</i> (Stål, 1867))	TXL2011-663	03. vii. 2011	Vietnam, Dong Nai	♂	S	S	n/a	IEBR
296	“gen. E” sp. HNL001 (= <i>Rhynocoris mendicus</i> (Stål, 1867))	HNL2019-174	12. xi. 2019	Vietnam, Dong Nai	♂	S	S	n/a	IEBR*
297	“gen. E” sp. HNL001 (= <i>Rhynocoris mendicus</i> (Stål, 1867))	NDD2019-229	13. ix. 2019	Vietnam, Gia Lai	♂	S	S	n/a	IEBR*
298	“gen. E” sp. HNL001 (= <i>Rhynocoris mendicus</i> (Stål, 1867))	NDD2019-233	13. ix. 2019	Vietnam, Gia Lai	♂	S	S	n/a	IEBR*
299	“gen. E” sp. HNL001 (= <i>Rhynocoris mendicus</i> (Stål, 1867))	NDD2019-234	13. ix. 2019	Vietnam, Gia Lai	♂	S	S	n/a	IEBR*
300	“gen. E” sp. HNL001 (= <i>Rhynocoris mendicus</i> (Stål, 1867))	NDD2019-239	13. ix. 2019	Vietnam, Gia Lai	♂	S	S	n/a	IEBR*
301	“gen. E” sp. HNL001 (= <i>Rhynocoris mendicus</i> (Stål, 1867))	NDD2019-244	13. ix. 2019	Vietnam, Gia Lai	♂	S	S	n/a	IEBR*
302	“gen. E” sp. HNL001 (= <i>Rhynocoris mendicus</i> (Stål, 1867))	NDD2019-245	13. ix. 2019	Vietnam, Gia Lai	♂	S	S	n/a	IEBR*
303	“gen. E” sp. HNL001 (= <i>Rhynocoris mendicus</i> (Stål, 1867))	NDD2019-246	13. ix. 2019	Vietnam, Gia Lai	♂	S	S	n/a	IEBR*
304	“gen. E” sp. HNL001 (= <i>Rhynocoris mendicus</i> (Stål,	TXL BX23	19. ix. 2021	Vietnam, Dak Lak	♀	S	S	n/a	IEBR

1867))

305	“gen. E” sp. HNL002	HNL2018-112	02. vi. 2018	Vietnam, Vinh Phuc	♂	S	S	S	IEBR*
306	“gen. E” sp. HNL002	TXL2018-115	12. vi. 2018	Vietnam, Lang Son	♂	S	S	S	IEBR
307	“gen. E” sp. HNL002	HNL2018-181	12. vi. 2018	Vietnam, Vinh Phuc	♂	S	S	n/a	IEBR*
308	“gen. E” sp. HNL002	HNL2018-185	12. vi. 2018	Vietnam, Vinh Phuc	♂	S	S	n/a	IEBR*
309	“gen. E” sp. HNL002	TTN2020-004	30. viii. 2020	Vietnam, Nghe An	♂	S	S	n/a	IEBR
310	“gen. E” sp. HNL002	TXL2021-001	10. iii. 2021	Vietnam, Vinh Phuc	♂	S	S	n/a	IEBR
311	“gen. E” sp. HNL002	TXL2021-002	10. iii. 2021	Vietnam, Vinh Phuc	♂	S	S	n/a	IEBR
312	“gen. E” sp. HNL002	TXL2021-003	30. iii. 2021	Vietnam, Vinh Phuc	♂	S	S	n/a	IEBR
313	“gen. E” sp. HNL002	HNL2018-113	02. vi. 2018	Vietnam, Vinh Phuc	♀	S	S	n/a	IEBR*
314	“gen. E” sp. HNL002	HNL2019-113	12. vi. 2019	Vietnam, Vinh Phuc	♀	S	S	n/a	IEBR*
315	“gen. E” sp. HNL002	HNL2019-136	16. vi. 2019	Vietnam, Tuyen Quang	♀	S	S	n/a	IEBR*
316	“gen. E” sp. HNL002	TXL2017-650	18. vii. 2017	Vietnam, Tuyen Quang	♀	S	S	n/a	IEBR
317	“gen. E” sp. HNL002	TXL2017-652	18. vii. 2017	Vietnam, Tuyen Quang	♀	S	S	n/a	IEBR
318	“gen. E” sp. HNL002	TXL2019-676	15. v. 2019	Vietnam, Tuyen Quang	♀	S	S	n/a	IEBR
319	“gen. E” sp. HNL002	NDD2019-232	13. ix. 2019	Vietnam, Dak Lak	♀	S	S	n/a	IEBR*
320	“gen. E” sp. HNL003	HNL2018-129	10. vi. 2018	Vietnam, Son La	♂	S	S	n/a	IEBR*
321	“gen. E” sp. HNL003	TXL2016-624	11. vi. 2016	Vietnam, Thanh Hoa	♂	S	N	n/a	IEBR
322	“gen. E” sp. HNL003	TXL2016-625	11. vi. 2016	Vietnam, Thanh Hoa	♂	S	N	n/a	IEBR
323	“gen. E” sp. HNL003	TXL2016-626	11. vi. 2016	Vietnam, Thanh Hoa	♂	S	N	n/a	IEBR
324	“gen. E” sp. HNL003	TXL2016-627	12. vi. 2016	Vietnam, Thanh Hoa	♂	S	S	n/a	IEBR
325	“gen. E” sp. HNL003	TXL2016-628	12. vi. 2016	Vietnam, Thanh Hoa	♂	S	S	n/a	IEBR
326	“gen. E” sp. HNL003	TXL2016-629	12. vi. 2016	Vietnam, Thanh Hoa	♂	S	S	n/a	IEBR
327	“gen. E” sp. HNL003	TXL2016-632	12. vi. 2016	Vietnam, Thanh Hoa	♂	S	S	n/a	IEBR
328	“gen. E” sp. HNL003	TXL2016-636	14. vi. 2016	Vietnam, Thanh Hoa	♀	S	S	n/a	IEBR
329	“gen. E” sp. HNL003	TXL2016-641	14. vi. 2016	Vietnam, Thanh Hoa	♂	S	S	n/a	IEBR

330	“gen. E” sp. HNL003	TXLBX15b	13. vi. 2016	Vietnam, Thanh Hoa	♂	n/a	n/a	n/a	IEBR
331	“gen. E” sp. HNL003	TXLBX15c	13. vi. 2016	Vietnam, Thanh Hoa	♂	n/a	n/a	n/a	IEBR
332	“gen. E” sp. HNL003	TXL2017-665	16. ix. 2017	Vietnam, Lang Son	♂	S	S	n/a	IEBR
333	“gen. E” sp. HNL003	TXL2018-836	12. vii. 2018	Vietnam, Gia Lai	♂	S	S	n/a	IEBR
334	“gen. E” sp. HNL003	TTN2020-003	30. viii. 2020	Vietnam, Nghe An	♂	S	S	n/a	IEBR
335	“gen. E” sp. HNL003	TTN2020-011	31. viii. 2020	Vietnam, Nghe An	♀	S	N	S	IEBR
336	“gen. E” sp. HNL003	TXL2016-622	11. vi. 2016	Vietnam, Thanh Hoa	♂	S	N	n/a	IEBR
337	“gen. E” sp. HNL003	TXL2016-623	11. vi. 2016	Vietnam, Thanh Hoa	♀	N	N	n/a	IEBR
338	“gen. E” sp. HNL003	TXL2016-630	12. vi. 2016	Vietnam, Thanh Hoa	♀	S	S	n/a	IEBR
339	“gen. E” sp. HNL003	TXL2016-631	12. vi. 2016	Vietnam, Thanh Hoa	♀	S	S	n/a	IEBR
340	“gen. E” sp. HNL003	TXL2016-635	12. vi. 2016	Vietnam, Thanh Hoa	♀	S	S	n/a	IEBR
341	“gen. E” sp. HNL003	TXL2016-637	14. vi. 2016	Vietnam, Thanh Hoa	♀	S	S	n/a	IEBR
342	“gen. E” sp. HNL003	TXL2016-643	15. vi. 2016	Vietnam, Thanh Hoa	♀	S	S	n/a	IEBR
343	“gen. E” sp. HNL003	TXLBX15	13. vi. 2016	Vietnam, Thanh Hoa	♀	S	S	n/a	IEBR
344	“gen. E” sp. HNL004	TXL2017-656	16. ix. 2017	Vietnam, Lang Son	♂	S	S	n/a	IEBR
345	“gen. E” sp. HNL004	TTN2020-002	30. viii. 2020	Vietnam, Nghe An	♂	S	S	n/a	IEBR
346	“gen. E” sp. HNL004	TTN2020-008	31. viii. 2020	Vietnam, Nghe An	♂	S	S	n/a	IEBR
347	“gen. E” sp. HNL006	DTH2022-001	13. iv. 2022	Vietnam, Dien Bien	♂	S	S	n/a	IEBR*
348	“gen. E” sp. HNL006	TXLBX7	19. v. 2022	Vietnam, Hoa Binh	♂	S	S	n/a	IEBR
349	“gen. E” sp. HNL005	NDD2019-277	18. ix. 2019	Vietnam, Dak Lak	♂	S	S	n/a	IEBR*
350	“gen. E” sp. HNL007	AD2020-035	19. x. 2020	Vietnam, An Giang		S	S	n/a	IEBR*
351	“gen. E” sp. HNL008	TXLBX24a	19. ix. 2020	Vietnam, Thua Thien Hue	♀	S	S	n/a	IEBR
355	“gen. E” sp. HNL008	TXLBX24b	19. ix. 2020	Vietnam, Thua Thien Hue	♂	n/a	n/a	n/a	IEBR
356	“gen. E” sp. HNL008	TXLBX24c	19. ix. 2020	Vietnam, Thua Thien Hue	♂	n/a	n/a	n/a	IEBR
357	“gen. E” sp. F5	AD2021-008	01. xi. 2021	Vietnam, Cao Bang	♀	S	S	n/a	IEBR*
358	“gen. E” sp. M9	LA-Redu-2010-006	11. v. 2010	Laos, Xieng	♂	N	n/a	S	NUOL

Khouang									
359	“gen. E” sp. M10	LA-Redu-2016-001	20-21. iii. 2016	Laos, Bolikhamxai	♂	n/a	n/a	n/a	NUOL
350		TXL1999-047	08. ix. 1999	Vietnam, Son La		n/a	n/a	n/a	IEBR
351		TXL2003-048	08. viii. 2003	Vietnam, Lang Son	♂	n/a	n/a	n/a	IEBR
352		TXL2004-049	24. v. 2004	Vietnam, Ha Tinh	♀	n/a	n/a	n/a	IEBR
353		TXL2004-050	24. viii. 2004	Vietnam, Vinh Phuc		n/a	n/a	n/a	IEBR
354		TXL2019-901	10. xii. 2019	Vietnam, Ha Giang	♀	S	N	S	IEBR
355		TXL2009-503	10. vi. 2009	Vietnam, Lao Cai	♀	S	N	N	IEBR
356		TTN2020-009	31. viii. 2020	Vietnam, Nghe An	♀	N	N	N	IEBR
357		TTN2020-010	31. viii. 2020	Vietnam, Nghe An	♂	N	N	S	IEBR
358		TXL2021-004	30. iv. 2021	Vietnam, Vinh Phuc		S	S	n/a	IEBR
359		TXL2021-005	v. 2021	Vietnam, Cao Bang		S	S	n/a	IEBR
360		LA-Redu-2009-001	18. vi. 2009	Laos, Xieng Khouang	♂	n/a	n/a	S	NUOL
361		LA-Redu-2009-002	18. vi. 2009	Laos, Xieng Khouang	♂	n/a	n/a	S	NUOL
362	“gen. F” sp. HNL001 (= <i>Rhynocoris fuscipes</i> (Fabricius, 1787))	TW-Redu-1982-001	14. vii. 1982	Taiwan, Nantou	♂	n/a	n/a	n/a	TARI
363	“gen. F” sp. HNL001 (= <i>Rhynocoris fuscipes</i> (Fabricius, 1787))	TXL1999-044	03. vii. 1999	Vietnam, Hoa Binh	♂	n/a	n/a	n/a	IEBR
364	“gen. F” sp. HNL001 (= <i>Rhynocoris fuscipes</i> (Fabricius, 1787))	TXL1999-046	08. ix. 1999	Vietnam, Son La	♂	n/a	n/a	n/a	IEBR
365	“gen. F” sp. HNL001 (= <i>Rhynocoris fuscipes</i> (Fabricius, 1787))	TXL2018-127	10. vi. 2018	Vietnam, Lang Son	♂	S	S	n/a	IEBR
366	“gen. F” sp. HNL001 (= <i>Rhynocoris fuscipes</i> (Fabricius, 1787))	TXL2019-692	14. vi. 2019	Vietnam, Hoa Binh	♂	S	S	n/a	IEBR
367	“gen. F” sp. HNL001 (= <i>Rhynocoris fuscipes</i> (Fabricius, 1787))	TXL2019-693	14. vi. 2019	Vietnam, Hoa Binh	♂	S	S	n/a	IEBR
368	“gen. F” sp. HNL001 (= <i>Rhynocoris fuscipes</i> (Fabricius, 1787))	AD2020-041	29. x. 2020	Vietnam, Vung Tau	♂	S	S	n/a	IEBR*

369	“gen. F” sp. HNL001 (= <i>Rhynocoris fuscipes</i> (Fabricius, 1787))	TXL1999-045	13. viii. 1999	Vietnam, Hoa Binh	♀	n/a	n/a	n/a	IEBR
370	“gen. F” sp. HNL001 (= <i>Rhynocoris fuscipes</i> (Fabricius, 1787))	LA-Redu-2008-001	22. iv. 2008	Laos, Vientiane	♀	n/a	n/a	n/a	NUOL
371	“gen. F” sp. HNL001 (= <i>Rhynocoris fuscipes</i> (Fabricius, 1787))	AD2020-040	29. x. 2020	Vietnam, Vung Tau	♀	S	S	n/a	IEBR*
372	<i>R. albopunctatus</i> (Stål, 1855) [Type]	n/a	n/a	Brazil, Natal	♂	n/a	n/a	n/a	NRM
373	<i>R. aulicus</i> (Stål, 1866) [Type]	n/a	n/a	Malaysia, Malacca	♂	n/a	n/a	n/a	NRM
374	<i>R. bellicosus</i> (Stål, 1865) [Type]	n/a	n/a	-	♀	n/a	n/a	n/a	NRM
375	<i>R. carmelita</i> (Stål, 1859) [Type]	n/a	n/a	Sierra Leone	♀	n/a	n/a	n/a	NRM
376	<i>R. cinctorius</i> (Stål, 1865) [Type]	n/a	n/a	South Africa, Eastern Cape	♂	n/a	n/a	n/a	NRM
377	<i>R. discoidalis</i> (Reuter, 1881) [Type]	n/a	n/a	Africa Meridionalis	♀	n/a	n/a	n/a	NRM
378	<i>R. erythrocnemis</i> (Germar, 1837) [Type]	n/a	n/a	Congo	♀	n/a	n/a	n/a	NRM
379	<i>R. fuscipes</i> (Fabricius, 1787)	n/a	n/a	India, Bengalia	♀	n/a	n/a	n/a	NRM
380	<i>R. illotus</i> Miller, 1941 [Holotype]	n/a	20. iv. 1926	Malaysia, Selangor	♀	n/a	n/a	n/a	BNHM
381	<i>R. illotus</i> Miller, 1941 [Paratype]	n/a	17. iv. 1926	Malaysia, Selangor	♀	n/a	n/a	n/a	BNHM
382	<i>R. kiritschenkoi</i> Popov, 1964 [Type]	n/a	n/a	Russia	♂	n/a	n/a	n/a	NRM
383	<i>R. latro</i> (Stål, 1855) [Type]	n/a	n/a	South Africa, Eastern Cape	♀	n/a	n/a	n/a	NRM
384	<i>R. leucospilus</i> (Stål, 1859) [Type]	n/a	n/a	Russia	♀	n/a	n/a	n/a	NRM
385	<i>R. longifrons</i> (Stål, 1874) [Type]	n/a	n/a	India, Pondichery	♀	n/a	n/a	n/a	NRM
386	<i>R. marginellus</i> Fabricius, 1803	n/a	n/a	Indonesia, Sulawesi, Bintan	♀	n/a	n/a	n/a	NRM
387	<i>R. mendicus</i> (Stål, 1867) [Type]	n/a	n/a	Malaysia, Malacca	♀	n/a	n/a	n/a	NRM
388	<i>R. monachus</i> Miller, 1941 [Holotype]	n/a	iv. 1929	Malaysia, Borneo	♀	n/a	n/a	n/a	BNHM
389	<i>R. nigripes</i> (Reuter, 1881) [Type]	n/a	n/a	Madagascar	♂	n/a	n/a	n/a	NRM
390	<i>R. nigronitens</i> (Reuter, 1881)	n/a	n/a	Siberia	♂	n/a	n/a	n/a	NRM

[Type]									
391	<i>R. rapax</i> (Stål, 1855) [Type]	n/a	n/a	South Africa, Eastern Cape	♀	n/a	n/a	n/a	NRM
392	<i>R. rufus</i> (Thunberg, 1822)	n/a	n/a	Cape	♀	n/a	n/a	n/a	NRM
393	<i>R. suspectus</i> Schouteden, 1910 [Type]	n/a	n/a	Tanzania, Kilimandjaro	♂	n/a	n/a	n/a	NRM
394	<i>R. tristicolor</i> (Reuter, 1881) [Type]	n/a	n/a	India	♂	n/a	n/a	n/a	NRM
395	<i>R. tristis</i> (Stål, 1855) [Type]	n/a	n/a	Brazil, Natal	♀	n/a	n/a	n/a	NRM
396	<i>R. venustus</i> (Stål, 1855) [Type]	n/a	n/a	Brazil, Natal; South Africa, Eastern Cape	♂	n/a	n/a	n/a	NRM
397	<i>R. vicinus</i> (Schouteden, 1910) [Type]	n/a	n/a	Tanzania, Kilimandjaro	♂	n/a	n/a	n/a	NRM
398	<i>R. violentus</i> (Germar, 1837)	n/a	n/a	-	♀	n/a	n/a	n/a	NRM
399	<i>R. vittiventris</i> (Stål, 1859) [Type]	n/a	n/a	Sierra Leone	♂	n/a	n/a	n/a	NRM
400	<i>R. vulneratus</i> (Germar, 1837)	n/a	n/a	Tanzania, Kilimandjaro	♀	n/a	n/a	n/a	NRM
401	<i>R. vulneratus</i> (Germar, 1837)	n/a	n/a	n/a	♀	n/a	n/a	n/a	NRM

Outgroups

402	<i>Coranus</i> sp.	HNL2019-050	21. iii. 2019	Vietnam, Thua Thien - Hue	♂	OM908226	OM868207	n/a	IEBR*
403	<i>Endochus singalensis</i> Distant, 1908	TXL2018-009	05. v. 2018	Vietnam, Gia Lai	♀	S	S	n/a	IEBR
404	<i>Cleptria corallina</i> Villiers, 1948	RCW014	n/a	Guinea-Bissau	n/a	FJ230388	JQ888569	n/a	UCR
405	<i>Triatoma recurva</i> (Stål, 1894)	RCW170	n/a	Mexico, Sonora	n/a	FJ230417	JQ888699	n/a	UCR
406	<i>Apiomerus lanipes</i> (Fabricius, 1803)	RCW281	n/a	Argentina, Santiago del Estero	n/a	FJ230435	JQ888546	n/a	UCR

Table 2.2. Primers used for PCR amplification and Sanger sequencing.

Gene	Forward	Reverse	Annealing temperature	Source
16S	16sa: 5'-CGC CTG TTT ATC AAA AAC AT-3'	16sb: 5'-CTC CGG TTT GAA CTC AGA TCA-3'	48 °C	Kessing et al. (1989)
COI	LCO1490m: 5'-TAC TCA ACA AAT CAC AAA GAT ATT GG-3'	3' COI-E: 5'-TAT ACT TCT GGG TGT CCG AAG AAT CA-3'	48.5 °C	Shekhovtsov et al. (2013) Bely & Wray (2004)
	COI_Harp_F: 5'-ATT GGA AAT GAY CAA ATY TAT A-3'	COI_Harp_R: 5'-GAD GTA TTA AAR TTW CGR TCW-3'	48.5 °C	Zhang & Weirauch (2013)
	Uni-Minibar (F1) 5'-TCC ACT AAT CAC AAR GAT ATT GGT AC-3'	Uni-Minibar (R) 5'-GAA AAT CAT AAT GAA GGC ATG AGC-3'	48.5 °C	Meusnier et al. (2008)

CHAPTER 3:
THE BOUNDARY OF THE THREE GENERA
BLASTICUS, SPHEDANOLESTES, AND RHYNOCORIS
AND THE VALIDITY OF EACH GENUS

Notification. The formal taxonomic actions will not be done in this thesis (disclaiming of taxonomic actions declared in the concerning work is supported by the International Code of Zoological Nomenclature: Article 8.3).

3.1. Introduction

The close relationship among the three genera *Biasticus* Stål, 1867, *Sphedanolestes* Stål, 1867, and *Rhynocoris* Hahn, 1834 (Insecta: Hemiptera: Heteroptera: Harpactorinae) was proposed by previous studies based on their high similarity in external morphology and phylogenetic positions (Zhang and Weirauch 2013; Chapter 1). However, due to the limited number of specimens and incomprehensive examination of morphology in the previous study, the phylogenetic relationships among the three genera and the boundaries among them have not yet been clarified.

Moreover, due to the lack of comprehensive morphological examination, the morphological definitions of the three genera *Biasticus*, *Sphedanolestes*, *Rhynocoris*, and probably many other genera of Harpactorinae and Reduviidae are usually obscure or problematic and might have caused misidentification and misassignment of the species.

Therefore, in this chapter, the genus-level classification of the three genera *Biasticus*, *Sphedanolestes*, and *Rhynocoris* is re-examined by involving newly collected materials in the phylogenetic analyses.

3.2. Material and Methods

3.2.1. Specimens Examined

Sampling sites, specimen depository, imaging, DNA sequencing, sequencing, and phylogenetic analyses were mentioned in Chapter 2.

A total of 214 *Biasticus* or “*Biasticus*-like” adult male and female specimens (146 specimens from Vietnam, 21 specimens from Laos, 26 specimens from Thailand, four specimens from Singapore, three specimens from Malaysia, three specimens from Taiwan, one specimen from Myanmar, ten holotype and 15 paratype specimens of *Biasticus* from Institute of Ecology and Biological Resources (IEBR), British Natural History Museum collection (BNHM), Swedish

Museum of Natural History (NRM), and Vietnam National Museum of Nature (VNMN), 100 *Rhynocoris* or “*Rhynocoris*-like” specimens (93 specimens from Vietnam, six specimens from Laos, and one specimen from Taiwan), 50 *Sphedanolestes* and “*Sphedanolestes*-like” specimens (41 specimens from Vietnam, two specimens from Laos, two specimens from Singapore, and six specimens from Japan) were analyzed as ingroups. Furthermore, a specimen of *Endochus singalensis* Distant, 1908 from Vietnam and a specimen of *Coranus* sp. and 16S and COI sequences of *Apiomerus lanipes* (Fabricius, 1803) (RCW281), *Cleptria corallina* Villiers, 1948 (RCW014), and *Triatoma recurva* (Stål, 1894) (RCW170) obtained from GenBank were involved in the analyses as outgroups (Table 2.1).

The initial definitions of the genus *Biasticus*, *Sphedanolestes*, and *Rhynocoris* used as working hypotheses are given in Chapter 2.

3.2.2. Molecular Phylogenetic Analyses

Molecular phylogenetic analyses were performed based on the concatenated 16S + COI dataset. The TPM3 + F + I + G4 and TIM2 + F + I + G4 models were selected for the 16S and COI subsets of the concatenated dataset, respectively, by Model Finder (Kalyaanamoorthy et al. 2017) executed in IQ-TREE 2.1.2 (Minh et al. 2020). Maximum likelihood (ML) examinations were then carried out using IQ-TREE 2.1.2 (Chernomor et al. 2016; Minh et al. 2020); bootstrap values (BP) were estimated from 1,000 replications. On the other hand, the generalized time-reversible (GTR) + Gamma model was chosen for the 16S + COI dataset using Model Finder (Kalyaanamoorthy et al. 2017) under the Bayesian information criterion. The Bayesian inference (BI) evaluations were then executed for the data using MrBayes v. 3.2.7 (Ronquist and Huelsenbeck 2003) with 20,000,000 production and statutory parameter configuration (examining every 500 generations and tuning constraints every 100 generations, with a burn-in of 25 %). The effective sampling size (ESS) of

each constraint was verified to be > 200 using Tracer 1.7.2 (Rambaut et al. 2018). The nodes were designated as “well supported” when posterior probability (PP) ≥ 0.95 and BP ≥ 80 .

3.3. Results

3.3.1. *Phylogenetic Analyses and DNA Barcoding*

Bayesian Inference (BI) and maximum likelihood (ML) consistently recovered seven clades (I–VII) which were deeply separated from each other and were well supported with high supporting values (PP = 1; BP ≥ 87) (Fig. 3.1).

The morphospecies initially identified as the member of “*Biasticus*” were subdivided into clades I (PP = 1; BP = 89) and II (PP = 0.98; BP = 87), which are sister to each other. The morphospecies of “*Sphedanolestes*” were subdivided into clades III (PP = 1; BP = 100), IV (PP = 1; BP = 94), and V (PP = 1; BP = 100), of which the relationship was not solved (those clades were shown as polytomy in Fig. 3.1). The morphospecies of “*Rhynocoris*” were subdivided into clades VI (PP = 1; BP = 100) and VII (PP = 1; BP = 100) which are sister to each other.

3.3.2. *Evaluation of Examination of External and Genital Morphological Features in Female and the Male Adults*

All ingroup specimens, i.e., 164 specimens of the seven clades shared the following external morphological characteristics: body elongated, somewhat robust; head sub-elongated and robust, shorter than pronotum; postocular area of head sub-globose, distinctly broader than anteocular area, approximately as long as anteocular area, constricted behind compound eyes, with a broad and deep interocular sulcus; neck short; compound eyes protruding laterally, nearly globose; lateral ocelli produced, elevated behind interocular sulcus, widely separated from each other; interspace between lateral ocelli wider than distance between compound eye and lateral ocellus; labium with three

visible segments; first visible labial segment shorter than second segment, longer than antecular area of head, almost extending beyond level of middle of compound eye when labium laid backward; antennae with four segments with scape often longest; collar very short in dorsal view, with anterolateral angle weakly and roundly produced; anterior pronotal lobe round and bulged, with middle longitudinal sulcus deep and narrow posteriorly, reach or not reach anterior margin of posterior lobe; anterior pronotal lobe short than posterior pronotal lobe; cutellum not apically produced; scutellum triangular, somewhat triangularly depressed basally, apically produced, and sloping downward; posterior apex blunt; femora thick, apically moderately nodulose; fore femora very slightly incrassated, thicker than mid and hind femora; hemelytra surpassing apex of abdomen when fully closed; discal cell of hemelytra nearly parallelogram-shaped (Figs 3.2, 3.3). That resemblance in morphology is the reason why there were many misidentifications among these targeted genera as well as other genera of Reduviidae.

The 164 ingroup specimens were subdivided into six morphological groups (morphogroups A–F which are mostly compatible with the seven clades recovered by phylogenetic analyses.

Clade I (= morphogroup A1) consisting of 37 specimens (16 males and 21 females) and clade II (= morphogroup A1) of 17 specimens (6 males and 11 females) showed no remarkable difference in external and genital morphology, except for some difference in size of both male and female genitalia (Figs 3.4, 3.6A–B, 3.6H–I, 3.7, 3.8A–B), and both share the following features: body medium-sized (body length (BL) = 8.9–12.0 mm in the male, 9.1–12.8 mm in the female); anterior pronotal lobe round and bulged, with middle longitudinal sulcus deep and narrow posteriorly, reach or nearly reach anterior margin of posterior lobe; lateral bulge of anterior pronotal lobe without produced tubercle centrally; posterior pronotal lobe with or without swollen anteromedial elevation, but never concave or sulcate; central disc of posterior pronotal lobe round and bulged; humerus roughly triangular, with round apex; scutellum triangular, triangularly depressed basally, apically

produced, and sloping downward, posterior margins not reflex (Fig. 3.5A, B, H, I); paramere rod-shape, somewhat slightly rough; pygophore ovoid; medial process of male pygophore (mpp) broad and with a convex or concave distal margin; endosoma ovoid with well-produced spoon-like sclerites (sps); distal dorsal lobe of endosoma round with membranous surface, some species with prickle(s); articular apparatus (aa) in dorsal view with slender basal plate arms that form a U-shape or V-shape, in lateral view arched intensively (Fig. 3.6A, B, H, I); abdominal laterotergite VIII (AL8) with thin and broad posterior margin; abdominal sternite VII (AS7) forming a semi-circular or broad sub-pentagonal median concavity, with posteromedian margin gently U-shaped, with inner posterolateral margin almost straight or slightly concave; gonocoxa VIII (Gc8) wider than length, gently slanting anteromesad along posterior margin, weakly produced mesad and forming an acute apex or tiny blunt apex at apical inner corner, and with inner margin weakly incurved; gonapophysis (Gp8) small and subtriangular, longer than width (Fig. 3.8A, B).

Clade III (= morphogroup B) consisting of 20 specimens (11 males and 9 females) were characterized by the following features: Body medium to large-sized (body length (BL) = 12.5–15.1 mm in the male, 14.7–16.8 mm in the female); anterior pronotal lobe round and bulged, with middle longitudinal sulcus deep and narrow posteriorly, reaching anterior margin of posterior lobe; lateral bulge of anterior pronotal lobe with produced tubercle centrally; posterior lobe depressed slightly anteromedially; central disc of posterior pronotal lobe round and bulged but slightly elevated latitudinally medially; humerus roughly triangular, with round apex; scutellum triangular, triangularly depressed basally, apically produced, and sloping downward, lateral margin convex; posterior apex posteriorly produced; posterior margins of scutellum not reflex (Fig. 3.5C, J); paramere rod-shaped, a small poor-produced tubercle near apex; pygophore ovoid; mpp narrow and posteriorly produced with bifurcate projection in distal margin; endosoma ovoid with well-produced sps; ddl round with membranous surface, and densely covered with small prickles; aa in dorsal view

with long slender basal plate arms that form a U-shape, in lateral view arched intensively (Fig. 3.6C, J); abdominal laterotergite VIII (AL8) with thin latero-posterior margin, center of posterior margin posteriorly produced; abdominal sternite VII (AS7) forming a semi-circular median concavity, with posteromedian margin gently V-shaped, with inner posterolateral margin concave; gonocoxa VIII (Gc8) wider than length, gently slanting anteromesad along posterior margin, weakly produced mesad and forming a little blunt apex at apical inner corner, and with inner margin weakly incurved; gonapophysis VIII (Gp8) small and subtriangular, longer than width (Fig. 3.8C).

Clade IV (= morphogroup C) consisting of 9 specimens (4 males and 5 females) was characterized by the following features: Body large-sized (body length (BL) = 12.3–13.2 mm in the male, 15.1–15.5 mm in the female); anterior pronotal lobe round and bulged, with middle longitudinal sulcus deep and narrow posteriorly, reaching anterior margin of posterior lobe; lateral bulge of anterior pronotal lobe without produced tubercle centrally; posterior lobe mildly elevated anteromedially, somewhat sulcate; transitional border of anterior and posterior pronotal lobes slightly unclear; central disc of posterior pronotal lobe round and bulged but elevated latitudinally medially; humerus roughly triangular, with round apex; scutellum triangular, triangularly depressed basally, apically produced, and sloping downward, posterior margins not reflex, posterior margin slightly convex and a little more convex at posterior apex (Fig. 3.5D, K); paramere rod-shaped; pygophore ovoid; mpp narrow and posteriorly produced with weakly concave distal margin; endosoma ovoid with well-produced sps; ddl round with membranous surface, and densely covered with tiny and faint prickles; aa in dorsal view with slender basal plate arms that form a U-shape or V-shape, in lateral view arched intensively (Fig. 3.6D, K); abdominal laterotergite VIII (AL8) with thin and broad posterior margin; abdominal sternite VII (AS7) forming a semi-circular or broad sub-pentagonal median concavity, with posteromedian margin gently U-shaped, with inner posterolateral margin concave; gonocoxa VIII (Gc8) wider than length, gently slanting anteromesad along posterior

margin, weakly produced mesad and forming a little blunt apex at apical inner corner, and with inner margin weakly incurved; gonapophysis (Gp8) small and subtriangular, longer than width (Fig. 3.8D).

Clade V (= morphogroup D) consisting of 10 specimens (3 males and 7 females) was characterized by the following features: Body medium-sized (body length (BL) = 9.9–10.2 mm in the male, 10.7–11.3 mm in the female); anterior pronotal lobe round and bulged, with middle longitudinal sulcus deep and narrow posteriorly, just reaching anterior margin of posterior lobe; lateral bulge of anterior pronotal lobe without produced tubercle centrally; posterior pronotal lobe with slightly swollen anteromedial elevation; central disc of posterior pronotal lobe round and bulged; humerus roughly triangular, with round apex; scutellum triangular, triangularly depressed basally, apically produced, and sloping downward, posterior margins not reflex (Fig. 3.5E, L); paramere rod-shaped, relatively slender and short, not exceed the distal margin of mpp; pygophore ovoid with posterolateral margin sinuous; mpp narrow and posteriorly produced with straight distal margin and apicolateral corner formed posterolaterad and blunt at the apex; endosoma ovoid with well-produced sps; ddl round with membranous surface, and covered with some rows of large prickles; aa in dorsal view with slender basal plate arms that form a V-shape, in lateral view arched intensively (Fig. 3.6 E, L); abdominal laterotergite VIII (AL8) with thin and broad posterior margin; abdominal sternite VII (AS7) forming a semi-circular or broad sub-pentagonal median concavity, with posteromedian margin gently U-shaped, with inner posterolateral margin gently concave; gonocoxa VIII (Gc8) wider than length, gently slanting anteromesad along posterior margin, weakly produced mesad and forming a little blunt apex at apical inner corner, inner margin weakly incurved with a weak sinuously longitudinal elevation beside inner margin; gonapophysis (Gp8) small and subtriangular, longer than width (Fig. 3.8E).

Clade VI (= morphogroup E) consisting of 61 specimens (53 males and 8 females) was characterized by the following features: Body medium to large-sized (body length (BL) = 10.0–13.5

mm in the male, 10.9–14.3 mm in the female); anterior pronotal lobe round and bulged, with middle longitudinal sulcus deep and narrow, far from reaching anterior margin of posterior lobe; lateral bulge of anterior pronotal lobe with produced tubercle in central of posterior 1/3; posterior lobe depressed slightly or not depressed anteromedially; central disc of posterior pronotal lobe round and bulged but slightly elevated latitudinally medially; humerus roughly triangular, with round apex, and slightly reflexed posterolateral margin; scutellum triangular, triangularly depressed basally, apically produced, and sloping downward, lateral margin convex; posterior apex posteriorly produced; posterior margin of scutellum slightly reflex (Fig. 3.5F, M); paramere rod-shaped; pygophore ovoid with posterolateral margin slight sinuous; mpp broad and posteriorly produced with slightly concave distal margin and apicolateral corner formed laterad; endosoma ovoid with produced sps; ddl with membranous surface, and centrally and dorsally covered with tiny prickles, and ventrally covered with large prickles; aa in dorsal view with slender basal plate arms that form a U-shape or V-shape, in lateral view arched intensively (Fig. 3.6F, M); abdominal laterotergite VIII (AL8) with thin posterior margin; abdominal sternite VII (AS7) forming a semi-circular or broad sub-pentagonal median concavity, with posteromedian margin gently U-shaped or V-shaped, with inner posterolateral margin almost straight or slightly concave; gonocoxa VIII (Gc8) usually subtriangular, wider than length with inner posterolateral margin bolded and elevated and posterior apex produced posteriorly; gonapophysis VIII (Gp8) small and subtriangular, longer than width (Fig. 3.8F).

Clade VII (= morphogroup F) consisting of 10 specimens (7 males and 3 females) was characterized by the following features: Body large-sized (body length (BL) = 11.6–12.2 mm in the male, 12.5–13.0 mm in the female); anterior pronotal lobe round and bulged, with middle longitudinal sulcus deep and narrow, far from reaching anterior margin of posterior lobe; lateral bulge of anterior pronotal lobe without tubercle; posterior lobe depressed slightly or not depressed anteromedially; central disc of posterior pronotal lobe round and bulged but slightly elevated

latitudinally medially; humerus roughly triangular, with round apex; scutellum triangular, triangularly depressed basally, apically produced, and sloping downward, lateral margin convex; posterior apex posteriorly produced; posterolateral margin of scutellum reflex (Fig. 3.5G, N); paramere rod-shaped, a small acute spike near apex; pygophore ovoid; mpp narrow and posteriorly well-produced with bifurcate projection in distal margin; endosoma small and ovoid with mall sps; ddl narrow with membranous surface; aa in dorsal view with long thick basal plate arms that form a V-shape, in lateral view arched intensively (Fig. 3.6G, N); abdominal laterotergite VIII (AL8) with thin and narrow posterior margin; abdominal sternite VII (AS7) forming a semi-circular or broad sub-pentagonal median concavity, with posteromedian margin gently U-shaped, with inner posterolateral margin slightly concave; gonocoxa VIII (Gc8) subtriangular, wider than length, gently slanting anteromesad along posterior margin, weakly produced mesad and forming blunt apex at apical inner corner, and with inner margin weakly incurved, and posterior apex reflexed; gonapophysis (Gp8) small and subtriangular, longer than width (Fig. 3.8G).

3.4. Discussions

3.4.1. Reclassification of the Genera *Biasticus*, *Sphedanolestes*, and *Rhynocoris*

The present phylogenetic analyses and morphological examination based on external and genital morphology of male and female adults recovered 7 clades (I–VII) or morphogroups (A–F). The two partitionings were mostly compatible with each other, except the division of clade I and clade II was not supported firmly by morphological examination (Fig. 3.9).

The two sister clades, I and II, were relatively deeply separated from each other in phylogenetic trees but were not distinct from each other by morphological examination of both external and genital morphology, except for the differences in the size of both male and female genitalia. Taken together, there is no sufficient concrete evidence to treat the clades I and II into different genus-level taxa,

even though the independence of the two clades is still debatable. Therefore, clades I and II are herein combined into genus “A”.

By examining the type materials and previous taxonomic knowledge on *Biasticus*, *Sphedanolestes*, *Rhynocoris* and other harpactorine genera, genus A (= clades I+II, morphogroup A) consists mostly of the morphospecies preliminarily determined as *Biasticus* and therefore can be reasonably determined as the genus *Biastics*, with minimal modifications in the genus definition (see Chapter 2). The revised definition of the genus is given in the Appendix of this chapter, and Indochinese species of the genus will be revised in the Chapter 4.

Clade III–VII were compatible with morphogroups B–F, respectively. Based on the compatibility, these clades are provisionally treated as independent genus-level taxa, genera B–F, and their taxonomic identities are discussed below. However, whether to treat the clades at the genus level or the species group level should be discussed by referring to the degree of discrimination in the phylogenetic tree based on further comprehensive taxon sampling.

Most of the morphospecies initially determined as “*Sphedanolestes*” are assigned to either of genera B, C or D. Genus B (= clades III, morphogroup B) consisted of *Sphedanolestes impressicollis* (Stål, 1861), the type species of the genus *Sphedanolestes* Stål, alone, 1867. Genus C (= clades IV, morphogroup C) consisted of *Sphedanolestes pubinotus* Reuter, 1881 and other morphospecies. Genus D (= clades V, morphogroup D) consisted of *Sphedanolestes xiongi* Cai et al., 2004 alone. Therefore, the three taxa B–D can be treated collectively by the genus *Sphedanolestes*. However, due to the remarkable distinction among the three taxa as examined above, it is quite reluctant to place the three taxa under the single genus *Sphedanolestes*. Therefore, I herein proposed to subdivide *Sphedanolestes* Stål, 1867 (or hereinafter referred to as *Sphedanolestes* sensu lato) into three independent genera, the genus *Sphedanolestes* sensu stricto (including the type species of the taxon name *Sphedanolestes*), genus C and genus D. The (revised) definitions of the genera are given in the

Appendix of this chapter, and Indochinese species of *Sphedanolestes* sensu lato will be revised in Chapter 5.

Most of the morphospecies initially determined as “*Rhynocoris*” are assigned to either Genera E or F. Genus E (= clades VI, morphogroup E) consisted of *Rhynocoris mendicus* (Stål, 1867), *R. marginellus* (Fabricius, 1803), and some morphospecies. Genus F (= clades VII, morphogroup F) consisted of *Rhynocoris fuscipes* (Fabricius 1787) alone. Therefore, the two taxa, E and F, can be treated collectively the genus *Rhynocoris*. Although genera E and F are sister to each other, they are genetically deeply separated and can be clearly discriminated by a combination of morphological features. Based on these facts, I herein treat these as different genera. The type species of genus *Rhynocoris*, *Rhynocoris iracundus* was not involved in this study. So, which of taxa E, F, or another genus might be the real *Rhynocoris* was not confirmed in this study. Therefore, I provisionally proposed to subdivide *Rhynocoris* Hahn, 1834 (or hereinafter referred to as *Rhynocoris* sensu lato) into three independent genera, *Rhynocoris* sensu stricto, genus E and genus F. The definitions of genera E and F are given in the Appendix of this chapter, and the Indochinese species of *Rhynocoris* sensu lato will be revised in Chapter 6.

3.4.2. Usefulness of Integrated Taxonomy for Re-classifying the Inner Taxa of Harpactorinae

The present study proposed the usefulness of “Integrated taxonomy”, which is the combination of morphological examination based on external morphology and male genital morphology, and molecular phylogenetic analyses, for revising the genus-level taxonomy of three closely related genera *Biasticus*, *Sphedanolestes*, and *Rhynocoris*. The taxonomic identities and ranks of the newly recognized genera (C, D, E, F) could be adequately resolved by further comprehensive integrative taxonomic analyses with larger samples, hopefully involving the specimens from the other zoogeographical realms. In addition, this approach may be useful for re-classifying genera and tribes

within the subfamily Harpactorinae, which is considered to have very high species diversity. Making definitions of higher taxa clear can accelerate the taxonomic elucidation of species diversity.

In the present study as well, I am ready to elucidate the taxonomic diversity of the species of *Biasticus*, *Sphedanolestes* sensu stricto, and *Rhynocoris* sensu stricto from Indo-China. These will be done in Chapters 4, 5, and 6 in order.

References

1. Dioli P (1990) *Rhynocoris iracundus* (Poda, 1761) e *Rhynocoris rubricus* (Germar, 1816) in Valtellina. (Insecta, Heteroptera, Reduviidae). Il naturalista valtellinese, Atti Mus. civo Stor. nat. Morbegno. I: 55–60.
2. Distant WL (1904) Rhynchotal notes. XXII. Heteroptera from North Queensland. Ann. Mag. Nat. Hist., (7)18: 286–293.
3. Ishikawa T (2003) Taxonomic study on the Tribe Harpactorini (Heteroptera, Reduviidae) from Indochina, with Zoogeographical considerations. Ph.D. Thesis, Tokyo University of Agriculture, Kanagawa, Japan.
4. Kalyaanamoorthy S, Minh BQ, Wong T, Haeseler von A, Jermin LS (2017) ModelFinder: fast model selection for accurate phylogenetic estimates. Nat Methods 14, 587–589. <https://doi.org/10.1038/nmeth.4285>
5. Minh BQ, Schmidt HA, Chernomor O, Schrempf D, Woodhams MD, von Haeseler A, Lanfear R (2020) IQ-TREE 2: new models and efficient methods for phylogenetic inference in the genomic era. Mol Biol Evol 37:1530–1534. <https://doi.org/10.1093/molbev/msaa015> Chernomor et al. 2016

6. Rambaut A, Drummond AJ, Xie D, Baele G, Suchard MA (2018) Posterior summarisation in Bayesian phylogenetics using Tracer 1.7. *Systematic Biology*. syy032. <https://doi.org/10.1093/sysbio/syy032>
7. Ronquist F, Huelsenbeck JP (2003) MrBayes: Bayesian Phylogenetic Inference under Mixed Models. *Bioinformatics*, 19 (12), 1572–1574. <https://doi.org/10.1093/bioinformatics/btg180>
8. Zhang G, Weirauch C (2013) Molecular phylogeny of Harpactorini (Insecta: Reduviidae): correlation of novel predation strategy with accelerated evolution of predatory leg morphology. *Cladistics* (2013): 1–13. <https://doi.org/10.1111/cla.12049>

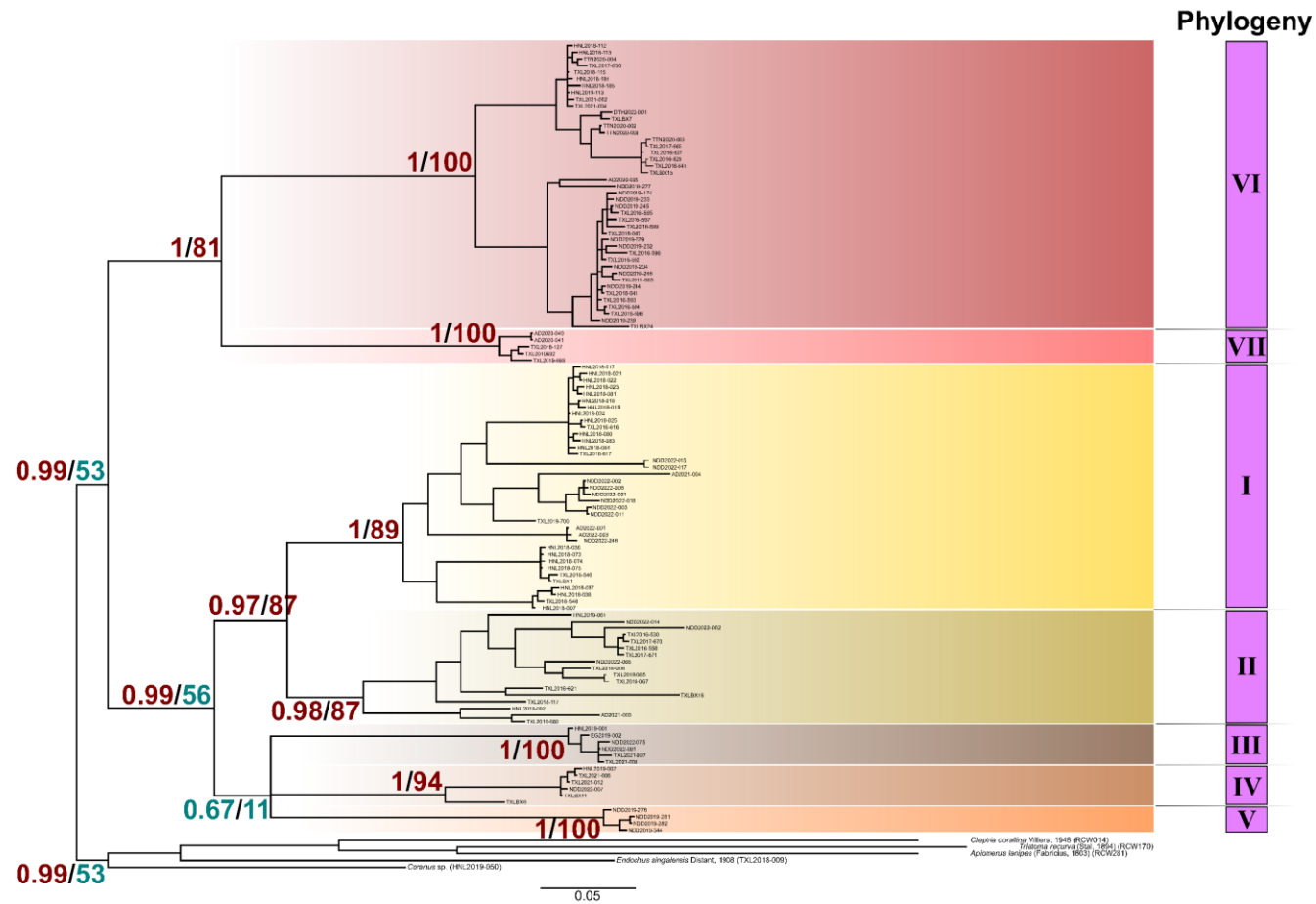


Figure 3.1. Bayesian inference phylogenetic trees based on the concatenated 16S + COI dataset (1083 bp) of the three genera *Biasticus*, *Sphecanolestes*, and *Rhynocoris*. Supports by posterior probability (PP) (left half) and bootstrap value (BP in %) (right half) are indicated in each node. Red is indicated for a high supporting value (PP \geq 0.95; BP \geq 80), and blue is indicated for a low or not supporting value (PP $<$ 0.95; BP $<$ 80).

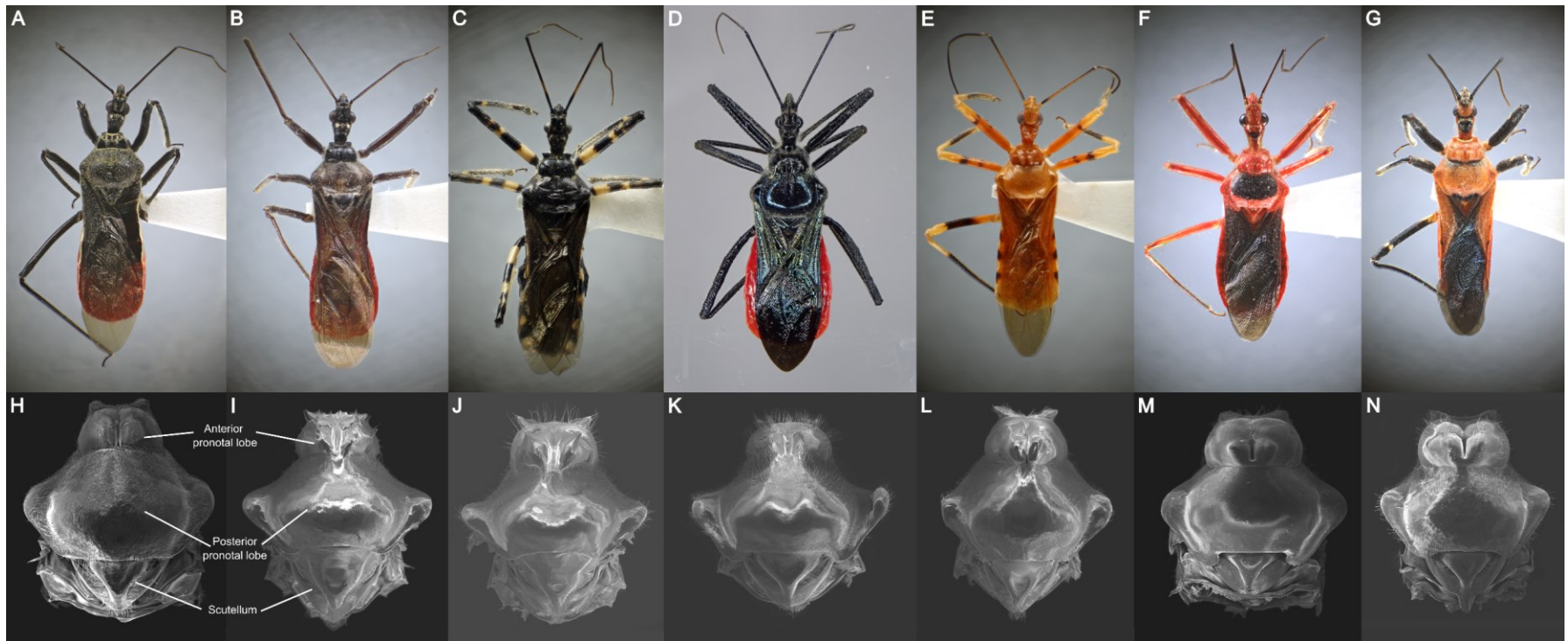


Figure 3.2. Shared morphological characters of the seven putative clades and lineages. **A–G**, body in dorsal view; **H–N**, SEM images of pronotum and scutellum in dorsal view. **A, H**, group A (= clade I), TXLBX1, ♂, *B. sp.* HNL011; **B, I**, group B (= clade II), TXL2018-843, ♂, *B. sp.* HNL017; **C, J**, group C (= lineage III), HNL2019-001, ♂, *S. sp.* HNL001; **D, K**, group D (clade IV), HNL2019-002, ♀, “A” sp. HNL001; **E, L**, group E (= lineage V), TXL2018-841, ♂, “B” sp. HNL001; **F, M**, group F (= clade VI), TXL2016-592, ♂, “gen. C” sp. HNL001; **G, N**, group G (= lineage VII), TXL2018-127, ♂, “gen. D” sp. HNL001.

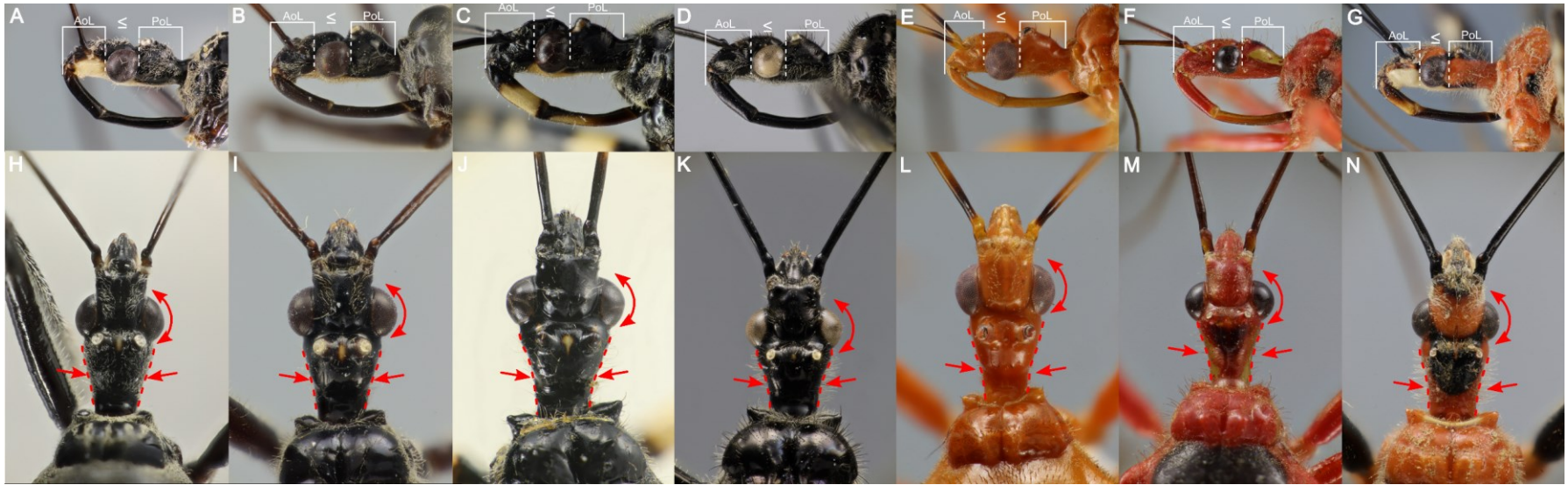


Figure 3.3. Shared morphological characters of the seven putative clades and lineages (cont.). **A–G**, head in lateral view; **H–N**, head in dorsal view. **A, H**, group A (= clade I), TXLBX1, ♂, *B. sp.* HNL011; **B, I**, group B (= clade II), TXL2018-843, ♂, *B. sp.* HNL017; **C, J**, group C (= lineage III), HNL2019-001, ♂, *S. sp.* HNL001; **D, K**, group D (clade IV), HNL2019-002, ♀, “A” sp. HNL001; **E, L**, group E (= lineage V), TXL2018-841, ♂, “B” sp. HNL001; **F, M**, group F (= clade VI), TXL2016-592, ♂, “gen. C” sp. HNL001; **G, N**, group G (= lineage VII), TXL2018-127, ♂, “gen. D” sp. HNL001.

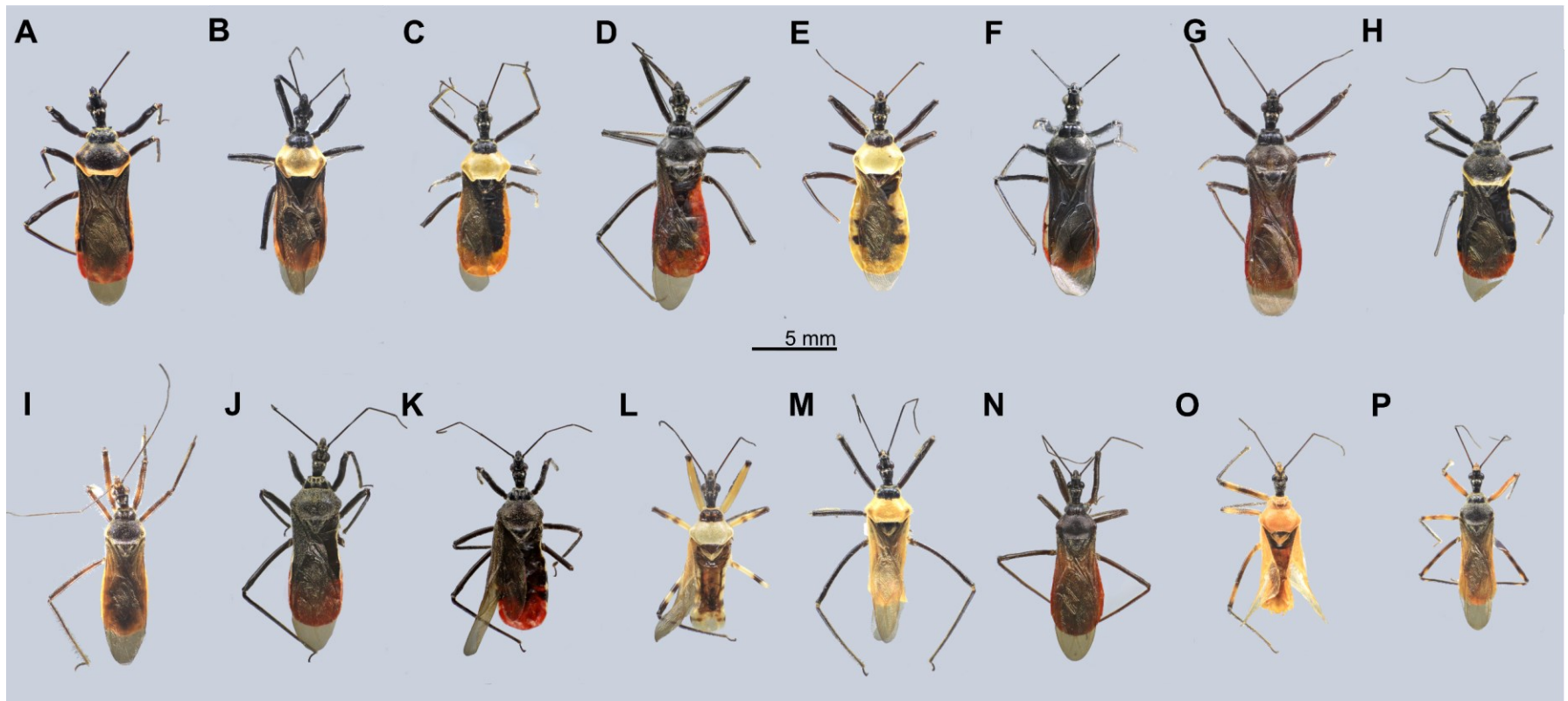


Figure 3.4. Morphospecies of groups A and B (= clades I and II). A–P, body in dorsal view. A–H, representatives of group A; I–P, representatives of group B.

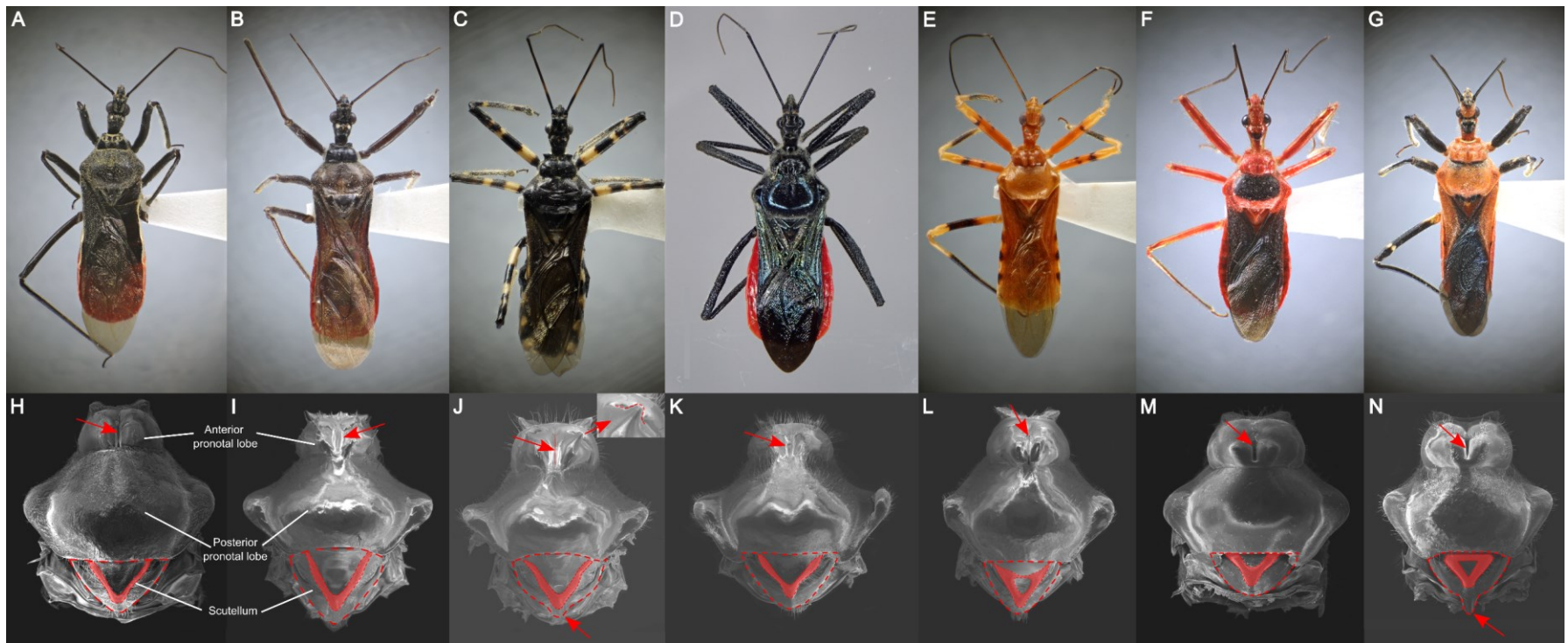


Figure 3.5. Distinct morphological characters of the seven putative clades and lineages. **A–G**, body in dorsal view; **H–N**, SEM images of pronotum and scutellum in dorsal view. **A, H**, group A (= clade I), TXLBX1, ♂, *B. sp.* HNL011; **B, I**, group B (= clade II), TXL2018-843, ♂, *B. sp.* HNL017; **C, J**, group C (= lineage III), HNL2019-001, ♂, *S. sp.* HNL001; **D, K**, group D (clade IV), HNL2019-002, ♀, “A” sp. HNL001; **E, L**, group E (= lineage V), TXL2018-841, ♂, “B” sp. HNL001; **F, M**, group F (= clade VI), TXL2016-592, ♂, “gen. C” sp. HNL001; **G, N**, group G (= lineage VII), TXL2018-127, ♂, “gen. D” sp. HNL001.

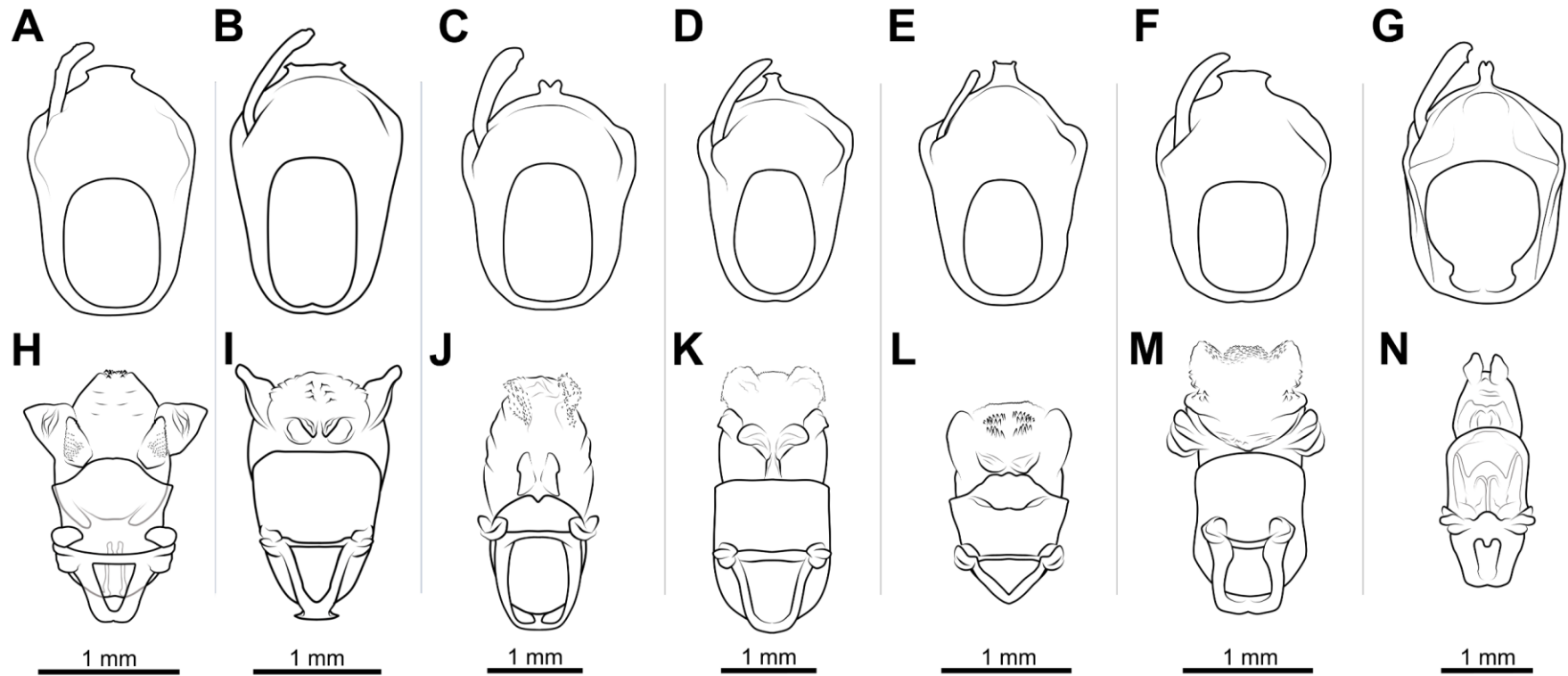


Figure 3.6. Genital morphology of male adults of the seven putative clades and lineages. **A–G**, pygophore in dorsal view; **H–N**, phallus in dorsal view. **A, H**, type mA (= group A) (= clade I), TXLBX1, ♂, *B. sp.* HNL011; **B, I**, type mB (= group B) (= clade II), TXL2018-843, ♂, *B. sp.* HNL017; **C, J**, type mC (= group C) (= lineage III), HNL2019-001, ♂, *S. sp.* HNL001; **D, K**, type mD (= group A) (clade IV), TXLBX11, ♂, “A” sp. HNL001; **E, L**, type mE (= group E) (= lineage V), TXL2018-841, ♂, “B” sp. HNL001; **F, M**, type mF (= group F) (= clade VI), TXL2016-592, ♂, “gen. C” sp. HNL001; **G, N**, type mG (= group G) (= lineage VII), TXL2018-127, ♂, “gen. D” sp. HNL001.

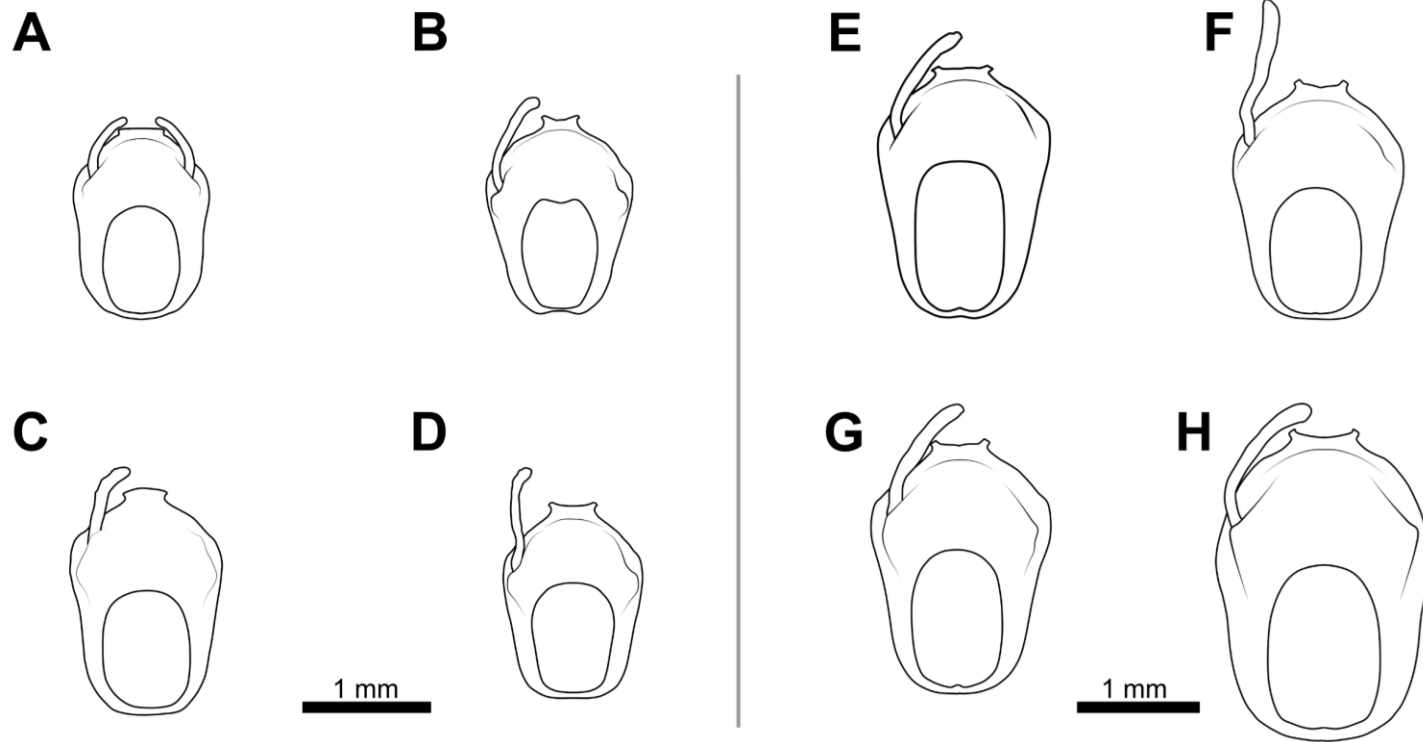


Figure 3.7. High similarity in genital morphology of male adults of the types mA and mB. **A–H**, pygophore in dorsal view. **A–D**, representatives of the type mA (= group A) (= clade I); **E–H**, representatives of the type mB (= group B) (= clade II); **A**, *B. sp.* HNL054, NDD2022-022, ♂; **B**, *B. sp.* HNL011, TXLBX11, ♂; **C**, *B. sp.* HNL013, HNL2018-025, ♂; **D**, *B. sp.* HNL021, AD2022-005, ♂; **E**, *B. sp.* HNL006, TXL2016-621, ♂; **F**, *B. sp.* HNL009, TXL2019-681, ♂; **G**, *B. sp.* HNL017, TXL2018-843, ♂; **H**, *B. sp.* HNL050, NDD2022-066, ♂.

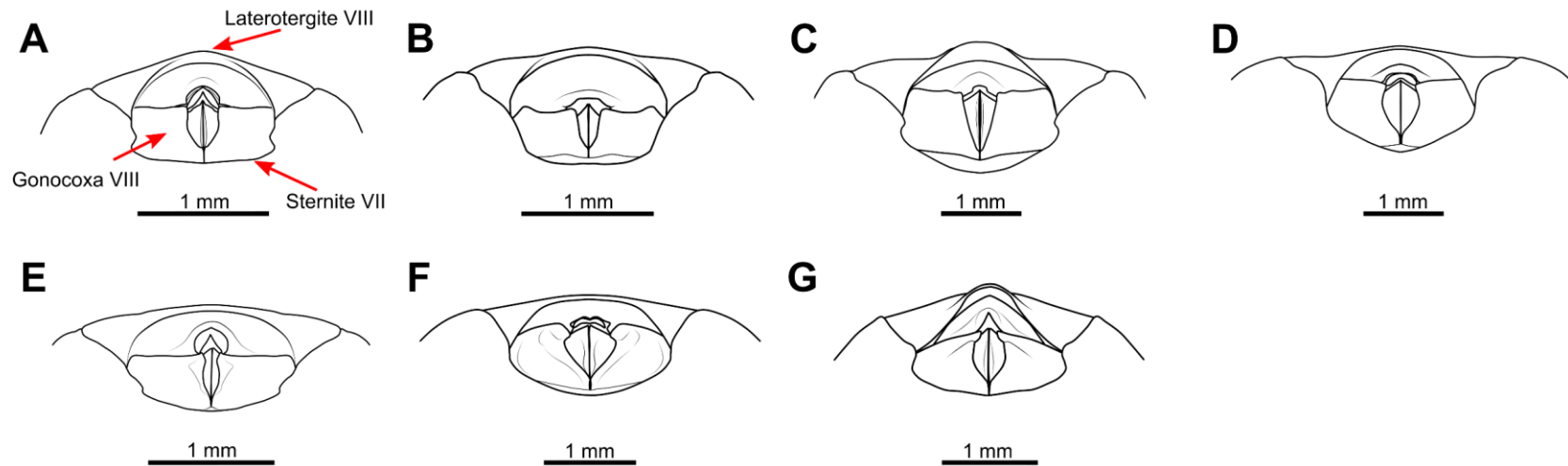


Figure 3.8. Genital morphology of female adults of the seven putative clades and lineages. **A–G**, external female genitalia in ventral view. **A**, type fA (= group A) (= clade I), HNL2018-024, ♀, *B. sp.* HNL013; **B**, type fB (= group B) (= clade II), HNL2019-061, ♀, *B. sp.* HNL005; **C**, type fC (= group C) (= lineage III), AD2020-030, ♀, *S. sp.* HNL001; **D**, type fD (= group D) (clade IV), HNL2019-002, ♀, “A” sp. HNL001; **E**, type fE (= group E) (= lineage V), NDD2019-276, ♀, “B” sp. HNL001; **F**, type fF (= group F) (= clade VI), TXL2018-041, ♀, “gen. C” sp. HNL001; **G**, type fG (= group G) (= lineage VII), LA-Redu-2008-001, ♀, “gen. D” sp. HNL001.

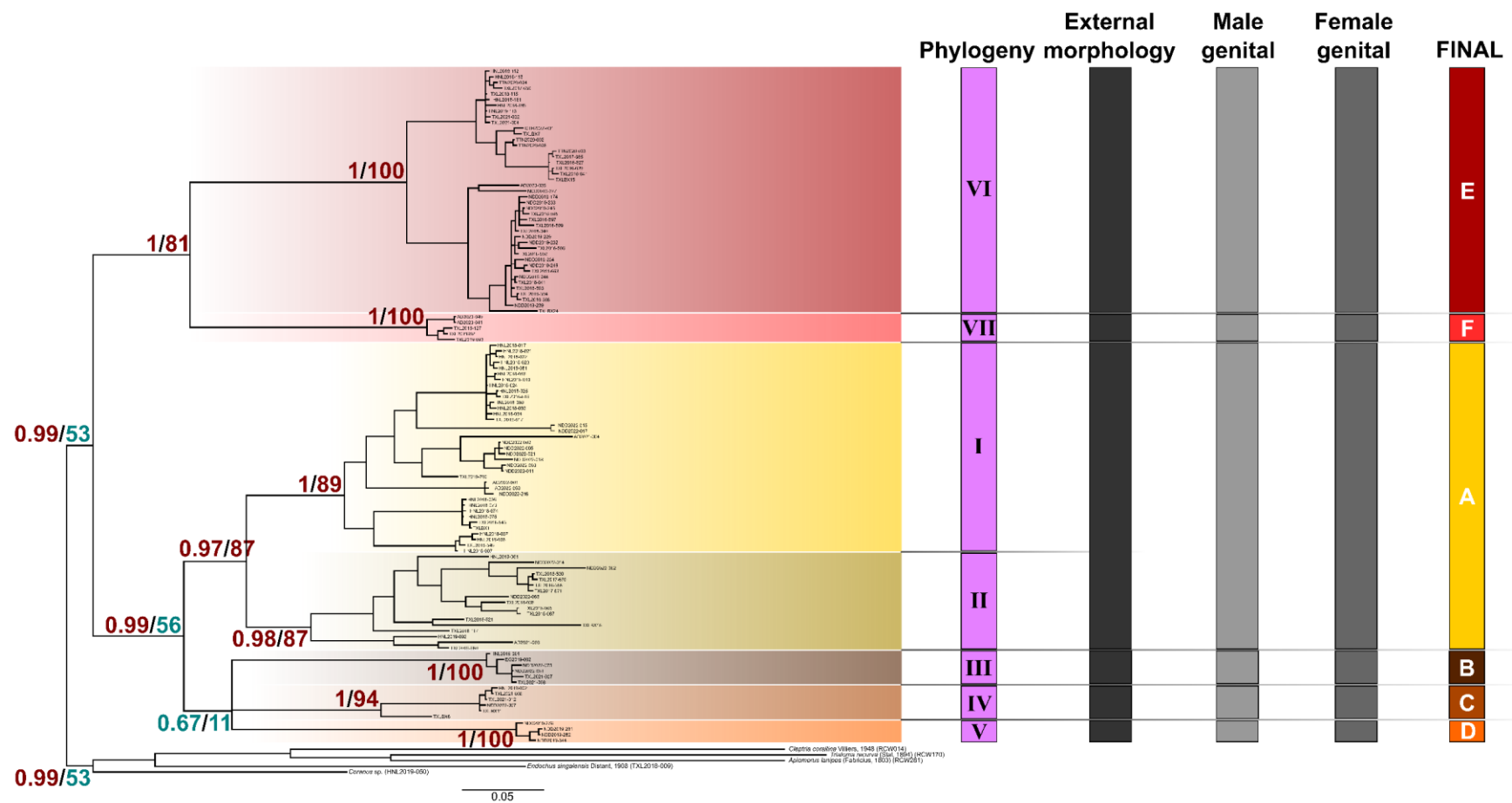


Figure 3.9. Bayesian inference phylogenetic trees based on the concatenated 16S + COI dataset (1083 bp) of the three genera combining with the results of morphological examination. Supports by posterior probability (PP) (left half) and bootstrap value (BP in %) (right half) are indicated in each node. Red is indicated for a high supporting value (PP \geq 0.95; BP \geq 80), and blue is indicated for a low or not supporting value (PP < 0.95; BP < 80).

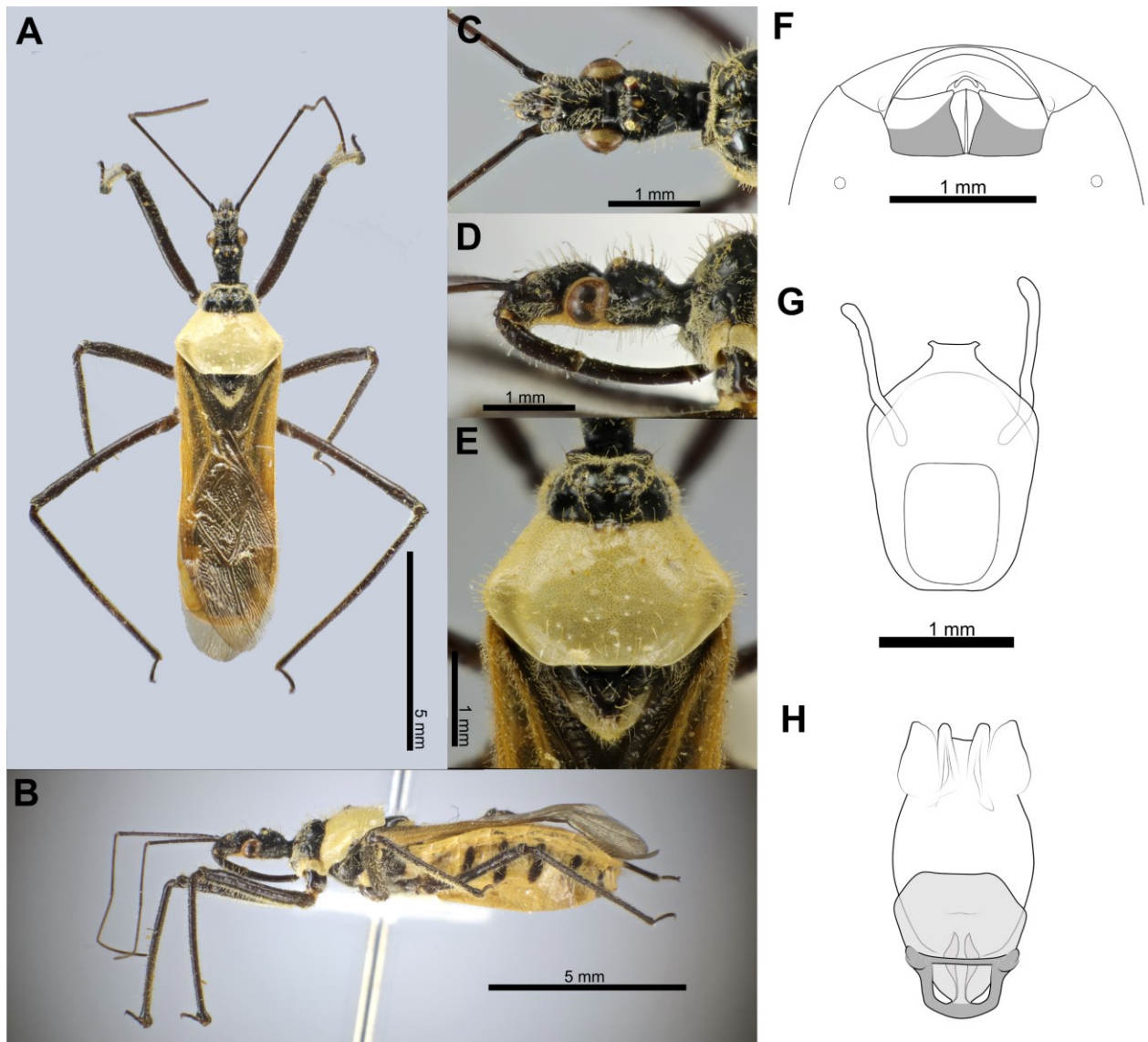


Figure 3.10. Morphology of the genus *Biasticus* (= Taxon A). **A–H**, *B. flavus* (Distant, 1903); **A–F**, LA-Redu-2004-006, ♀; **G, H**, HEM-TH2004-018, ♂. **A**, body in dorsal view; **B**, body in lateral view; **C**, head in dorsal view; **D**, head in lateral view; **E**, pronotum in dorsal view; **F**, female genital in ventral view; **G**, pygophore of male genital in dorsal view; **H**, phallus of male genital in dorsal view.

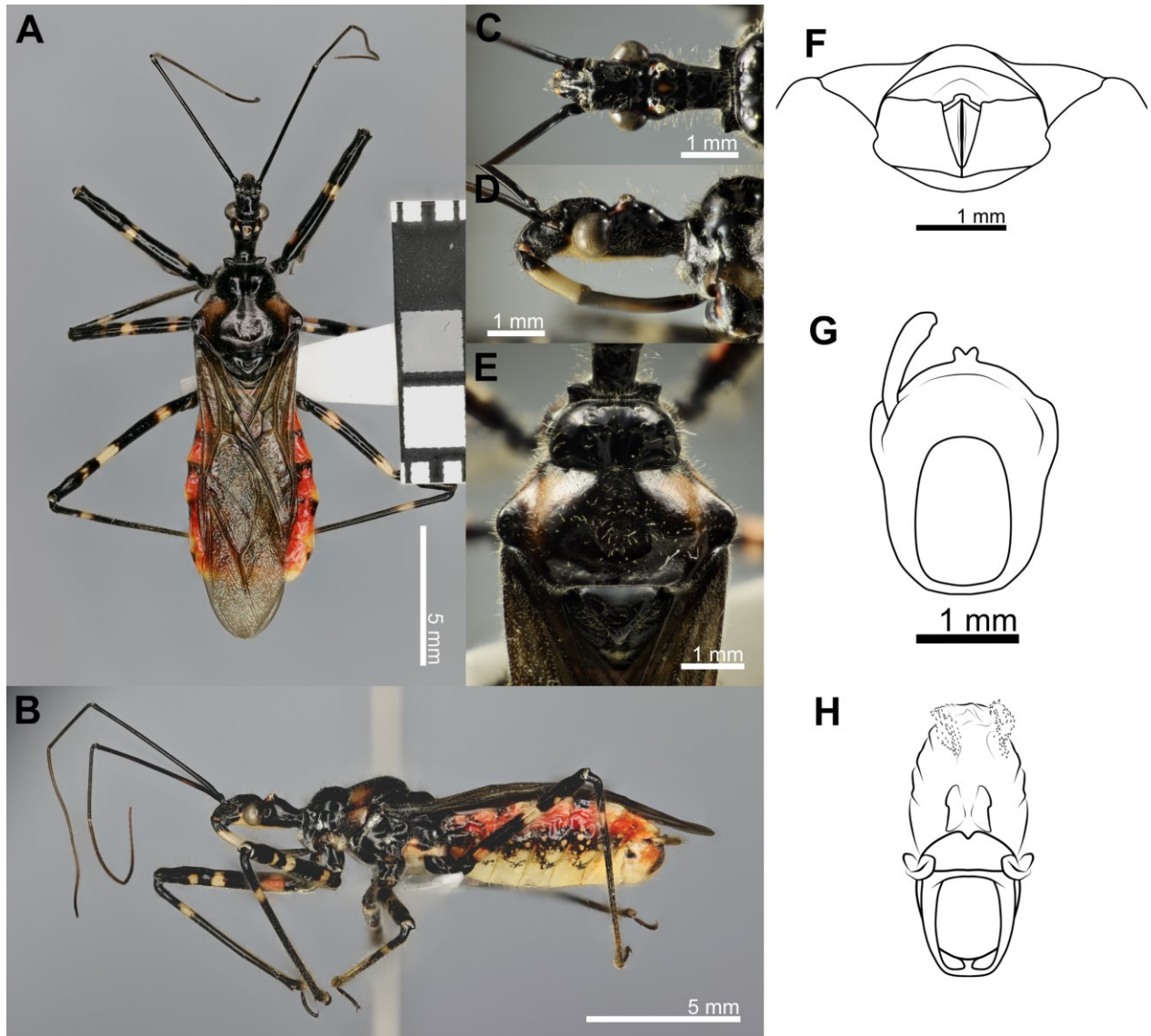


Figure 3.11. Morphology of the genus *Spedanolestes* (= taxon B). **A–H**, *S. impressicollis* (Stål, 1861). **A–E**, **G**, **H**, Eg2020-001, ♂; **E**, NDD2022-075, ♀. **A**, body in dorsal view; **B**, body in lateral view; **C**, head in dorsal view; **D**, head in lateral view; **E**, pronotum in dorsal view; **F**, female genital in ventral view; **G**, pygophore of male genital in dorsal view; **H**, phallus of male genital in dorsal view.

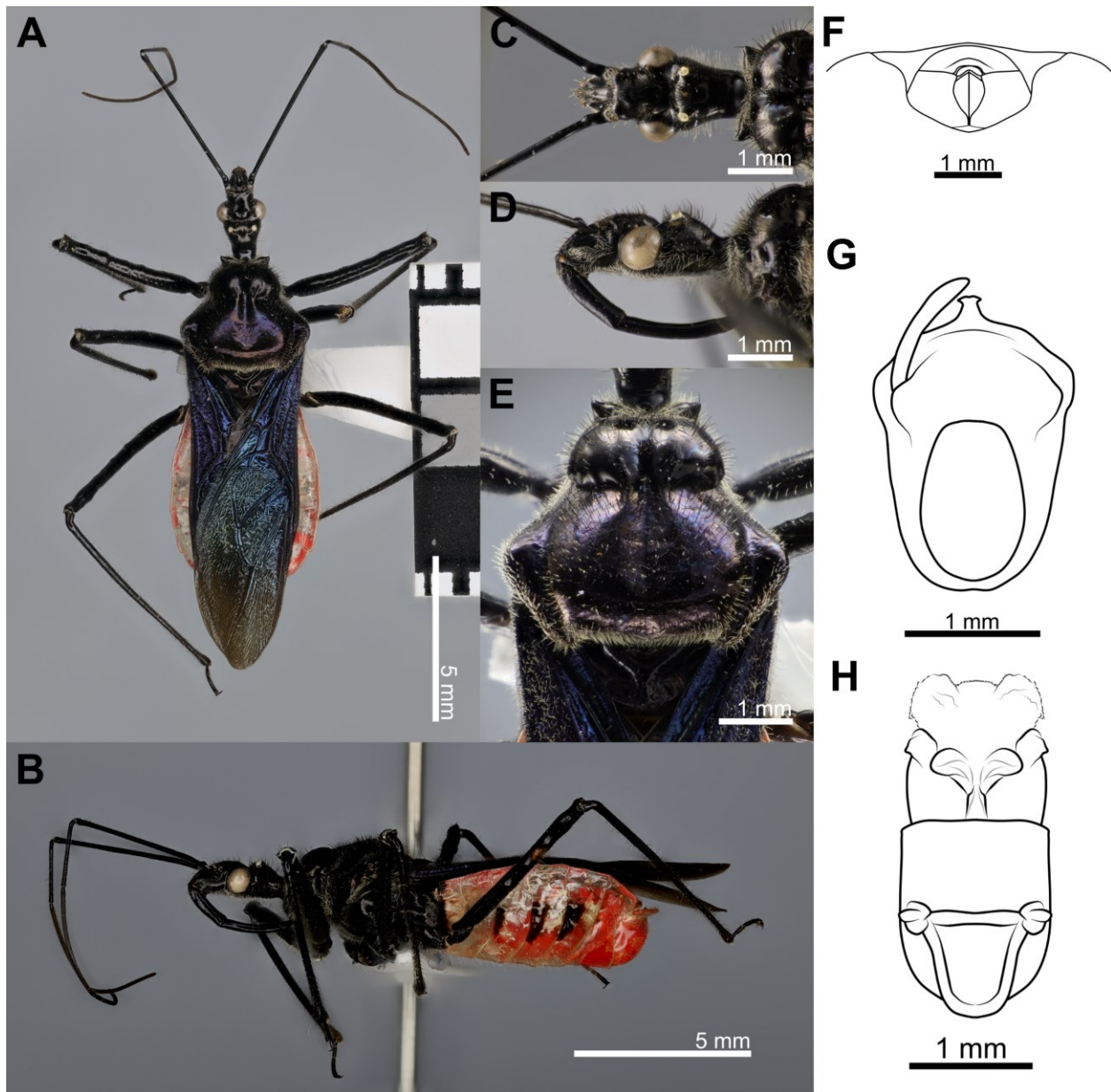


Figure 3.12. Morphology of the genus C (= taxon C). **A–H**, “*Sphedanolestes*” *pubinotus* Reuter, 1881. **A–E, G, H**, NDD2022-007, ♂; **E**, TXL2004-070, ♀. **A**, body in dorsal view; **B**, body in lateral view; **C**, head in dorsal view; **D**, head in lateral view; **E**, pronotum in dorsal view; **F**, female genital in ventral view; **G**, pygophore of male genital in dorsal view; **H**, phallus of male genital in dorsal view.

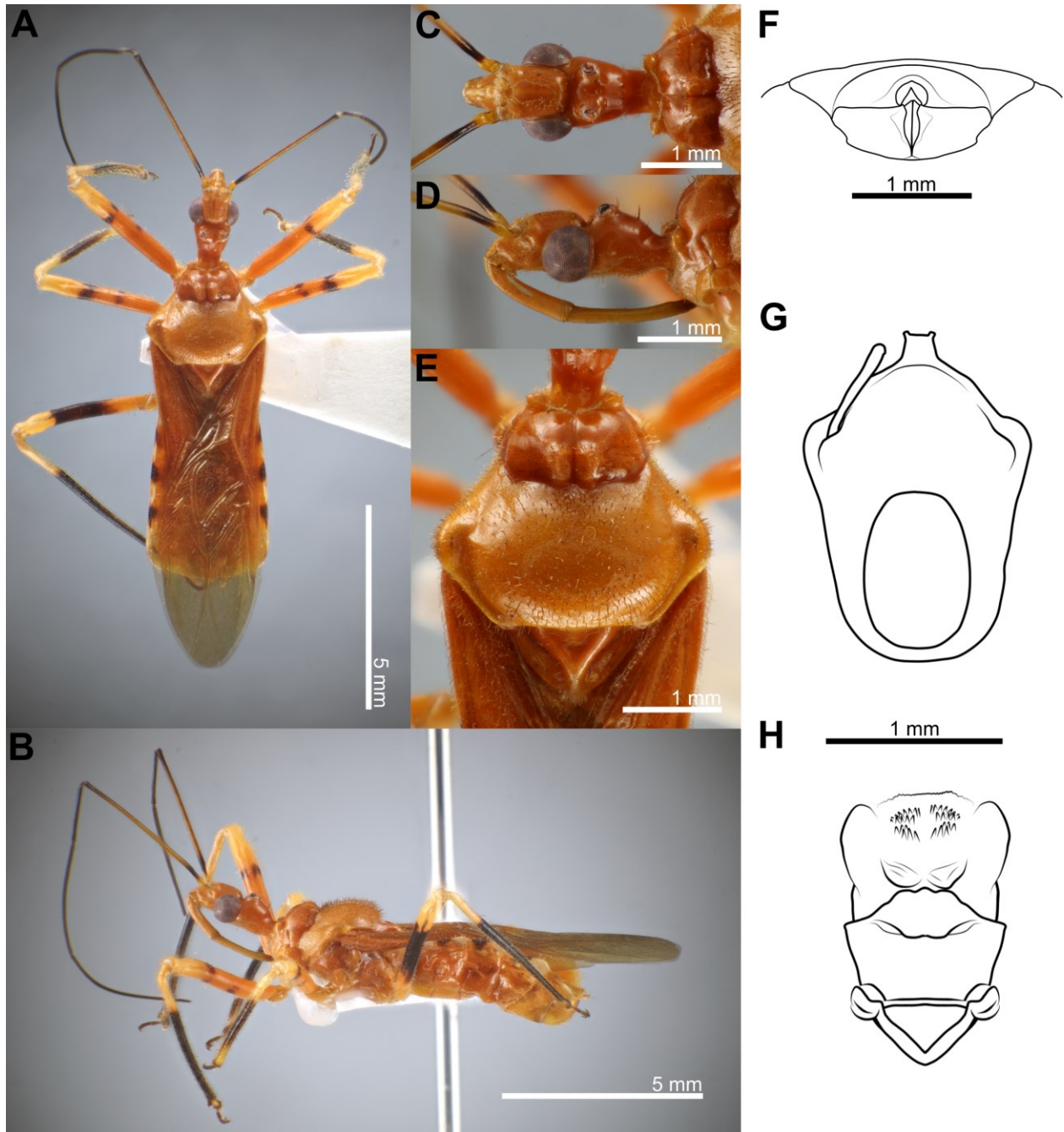


Figure 3.13. Morphology of the genus D (= taxon D). **A–H**, “*Spedanolestes*” *xiongi* Cai et al., 2004. **A–E, G, H**, NDD2019-292, ♂; **F**, NDD2019-276, ♀. **A**, body in dorsal view; **B**, body in lateral view; **C**, head in dorsal view; **D**, head in lateral view; **E**, pronotum in dorsal view; **F**, female genital in ventral view; **G**, pygophore of male genital in dorsal view; **H**, phallus of male genital in dorsal view.

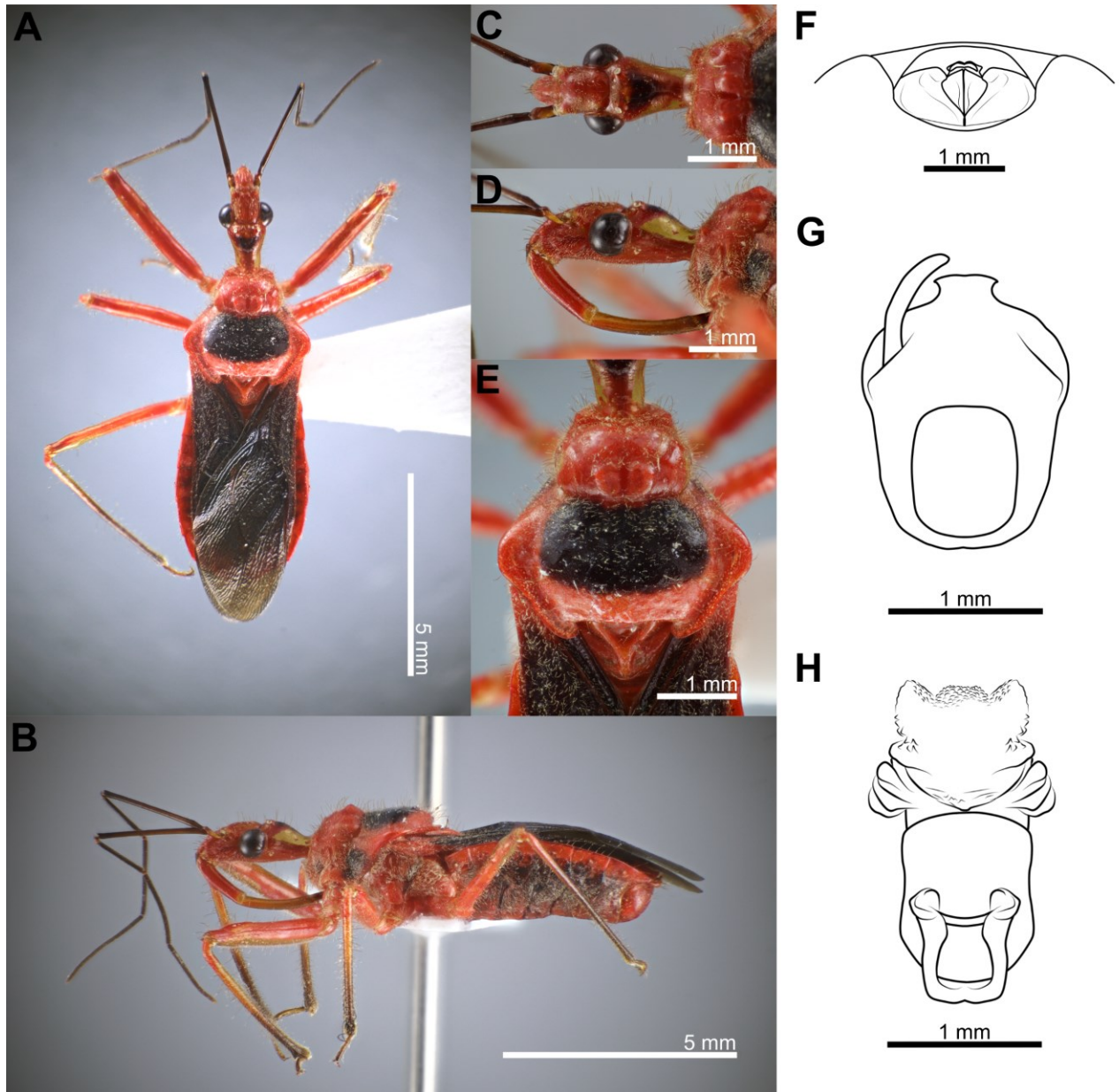


Figure 3.14. Morphology of the genus E (= taxon E). **A–H**, “*Rhynocoris*” *mendicus* (Stål, 1867). **A–E**, **G**, **H**, AD2019-001, ♂; **F**, LA-Redu-2011-004, ♀. **A**, body in dorsal view; **B**, body in lateral view; **C**, head in dorsal view; **D**, head in lateral view; **E**, pronotum in dorsal view; **F**, female genital in ventral view; **G**, pygophore of male genital in dorsal view; **H**, phallus of male genital in dorsal view.

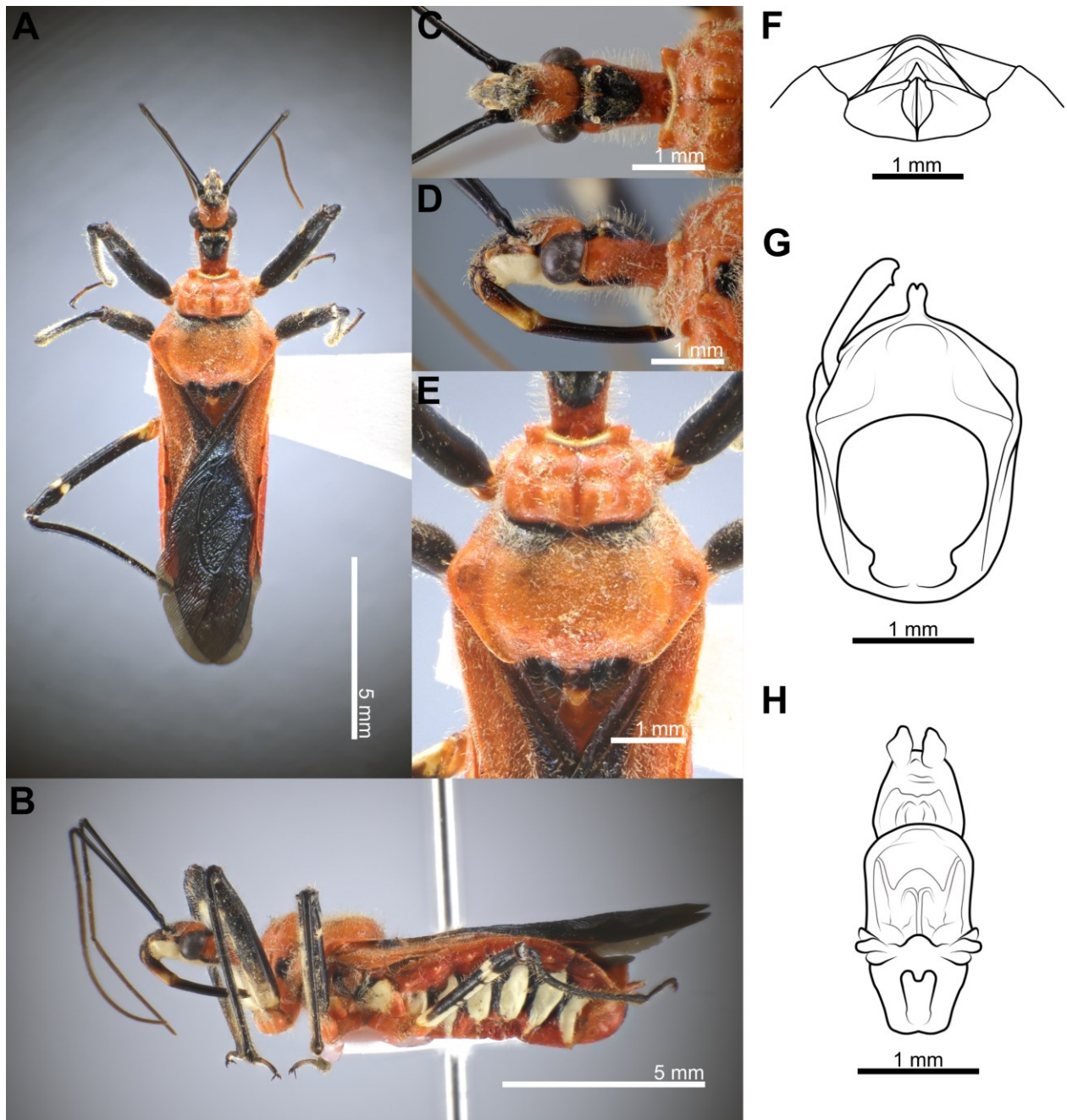


Figure 3.15. Morphology of the genus F (= taxon F). **A–H**, “*Rhynocoris*” *fuscipes* (Fabricius, 1787). **A–E, G, H**, TXL2019-692, ♂. **F**, LA-Redu-2008-001, ♀. **A**, body in dorsal view; **B**, body in lateral view; **C**, head in dorsal view; **D**, head in lateral view; **E**, pronotum in dorsal view; **F**, female genital in ventral view; **G**, pygophore of male genital in dorsal view; **H**, phallus of male genital in dorsal view.

Appendix: Definitions of the Six Genera Recognized by the Present Integrated Taxonomy

***Biasticus* Stål, 1867 (Fig. 3.10; Chapter 4)**

As proposed in 3.4.1, the cluster of the genus *Biasticus* Stål, 1867, was confirmed as an independent genus. The definition of the genus is revised as below.

Body medium to large-sized, elongated, and somewhat robust. Head sub-elongated and robust, shorter than pronotum; postocular area of head sub-globose, distinctly broader than antecular area, approximately as long as antecular area, constricted behind compound eyes, with a broad and deep interocular sulcus; neck short. Compound eyes protrude laterally, nearly globose; lateral ocelli produced, elevated behind interocular sulcus, widely separated from each other; interspace between lateral ocelli wider than distance between compound eye and lateral ocellus. Labium with three visible segments; first visible labial segment shorter than second segment, longer than antecular area of head, almost extending beyond level of middle of compound eye when labium laid backward; antennae with four segments with scape usually longest. Collar very short in dorsal view, with anterolateral angle weakly and roundly produced; anterior pronotal lobe round and bulged, with middle longitudinal sulcus deep and narrow posteriorly, reach or nearly reach anterior margin of posterior lobe; lateral bulge of anterior pronotal lobe without produced tubercle centrally; posterior pronotal lobe with or without swollen anteromedial elevation, but never concave or sulcate; central disc of posterior pronotal lobe round and bulged; humerus roughly triangular, with round apex. Scutellum triangular, triangularly depressed basally, apically produced, and sloping downward, posterior margins not reflex. Femora thick, apically moderately nodulose; fore femora very slightly incrassated, thicker than mid and hind femora. Hemelytra surpassing apex of abdomen when fully closed; discal cell nearly parallelogram-shaped, about twice as long as width. Connexivum slightly dilated and ascending with segmental incisures. Female genital with abdominal laterotergite VIII (AL8) with thin posterior margin; abdominal sternite VII (AS7) forming a semi-circular or broad

sub-pentagonal median concavity, with posteromedian margin gently U-shaped, with inner posterolateral margin almost straight; gonocoxa VIII (Gc8) wider than length, gently slanting anteromesad along posterior margin, weakly produced mesad and forming an acute apex or little blunt apex at apical inner corner, and with inner margin weakly incurved; gonapophysis (Gp8) small and subtriangular, longer than width. Male genital with paramere rod-shape, somewhat slightly rough; pygophore ovoid; medial process of male pygophore (mpp) broad and with a convex or concave distal margin; endosoma ovoid with well-produced spoon-like sclerites (sps); distal dorsal lobe of endosoma round with membranous surface, some species with prickle(s); articulatory apparatus (aa) in dorsal view with slender basal plate arms that form a U-shape or V-shape, in lateral view arched intensively.

***Sphedanolestes* Stål, 1867, sensu stricto (Fig. 3.11; Chapter 5)**

The genus *Sphedanolestes* sensu stricto is represented by the cluster of *Sphedanolestes impressicollis* (Stål, 1861), which is the type species of the genus. Definition of *Sphedanolestes* sensu stricto is given as below.

Body medium to large-sized, elongated, and somewhat robust. Head sub-elongated and robust, shorter than pronotum; postocular area of head sub-globose, distinctly broader than antecular area, longer than antecular area, constricted behind compound eyes, with a broad and deep interocular sulcus; neck short. Compound eyes protrude laterally, nearly globose; lateral ocelli produced, elevated behind interocular sulcus, widely separated from each other; interspace between lateral ocelli wider than distance between compound eye and lateral ocellus. Labium with three visible segments; first visible labial segment shorter than second segment, longer than antecular area of head, extending beyond level of middle of compound eye when labium laid backward; antennae with four segments with scape usually longest. Collar very short in dorsal view, with

anterolateral angle roundly produced with laterad apex; anterior pronotal lobe round and bulged, with middle longitudinal sulcus deep and narrow posteriorly, reaching anterior margin of posterior lobe; lateral bulge of anterior pronotal lobe with produced tubercle centrally; posterior lobe depressed slightly anteromedially; central disc of posterior pronotal lobe round and bulged but slightly elevated latitudinally medially; humerus roughly triangular, with round apex. Scutellum triangular, triangularly depressed basally, apically produced, sloping downward, lateral margin convex; posterior apex posteriorly produced; posterior margins of scutellum not reflex. Femora thick, apically moderately nodulose; fore femora very slightly incrassated, thicker than mid and hind femora. Hemelytra surpassing apex of abdomen when fully closed; discal cell nearly parallelogram-shaped, about twice as long as width. Connexivum slightly dilated and ascending with segmental incisures. Female genital with abdominal laterotergite VIII (AL8) with thin posterior margin; abdominal sternite VII (AS7) forming a semi-circular or broad sub-pentagonal median concavity, with posteromedian margin gently U-shaped, with inner posterolateral margin almost straight; gonocoxa VIII (Gc8) wider than length, gently slanting anteromesad along posterior margin, weakly produced mesad and forming an acute apex at apical inner corner, and with inner margin weakly incurved; gonapophysis (Gp8) small and subtriangular, longer than width. Male genital with paramere rod-shaped, a small poorly-produced tubercle near apex; ovoid pygophore; mpp narrow and posteriorly produced with bifurcate projection in distal margin; endosoma ovoid with well-produced spoon-like sclerites (sps); ddl round with membranous surface, and densely covered with small prickles; aa in dorsal view with slender basal plate arms that form a U-shape or V-shape, in lateral view arched intensively.

Genus C (Fig. 3.12; Chapter 5)

Genus C is represented by "*Sphedanolestes*" *pubinotus* Reuter, 1881 and "gen. C" sp.

HNL011. The definition of genus C is given below.

Body large-sized, elongated, and somewhat robust. Head sub-elongated and robust, shorter than pronotum; postocular area of head sub-globose, distinctly broader than anteocular area, slightly shorter or subequal in length to anteocular area, constricted behind compound eyes, with a broad and deep interocular sulcus; neck short. Compound eyes protrude laterally, nearly globose; lateral ocelli produced, elevated behind interocular sulcus, widely separated from each other; interspace between lateral ocelli wider than distance between compound eye and lateral ocellus. Labium with three visible segments; first visible labial segment shorter than second segment, longer than anteocular area of head, extending beyond level of middle of compound eye when labium laid backward; antennae with four segments, scape longest, first and second flagellomeres much longer than pedicel. Collar short in dorsal view, with anterolateral angle weakly and tubercle-shaped produced; anterior pronotal lobe round and bulged, with middle longitudinal sulcus deep and narrow posteriorly, reaching anterior margin of posterior lobe; lateral bulge of anterior pronotal lobe without produced tubercle centrally; posterior lobe mildly elevated anteromedially, somewhat sulcate; transitional border of anterior and posterior pronotal lobes slightly unclear; central disc of posterior pronotal lobe round and bulged but elevated latitudinally medially; humerus roughly triangular, with round apex. Scutellum triangular, triangularly depressed basally, apically produced, and sloping downward, posterior margins not reflex, posterior margin slightly convex and a little more convex at posterior apex. Femora thick, apically moderately nodulose, slightly incrassated. Hemelytra surpassing apex of abdomen when fully closed; discal cell nearly parallelogram-shaped, about twice as long as width. Connexivum slightly dilated and ascending with segmental incisures. Female genital with abdominal laterotergite VIII (AL8) with thin and broad posterior margin; abdominal sternite VII (AS7) forming a semi-circular or broad sub-pentagonal median concavity, with posteromedian margin gently U-shaped, with inner posterolateral margin concave; gonocoxa VIII (Gc8) wider than length, gently

slanting anteromesad along posterior margin, weakly produced mesad and forming a little blunt apex at apical inner corner, and with inner margin weakly incurved; gonapophysis (Gp8) small and subtriangular, longer than width. Male genital with paramere rod-shaped; pygophore ovoid and posterolateral margin slight sinuous; mpp narrow and posteriorly produced with weakly concave distal margin; endosoma ovoid with well-produced sps; ddl round with membranous surface, and densely covered with tiny and faint prickles; aa in dorsal view with slender basal plate arms that form a U-shape or V-shape, in lateral view arched intensively.

Genus D (Fig. 3.13; Chapter 5)

Genus D is represented by "*Sphedanolestes*" *xiongi* Cai et al., 2004. The definition of genus D is given below.

Body medium-sized, elongated, and somewhat robust. Head sub-elongated and robust, shorter than pronotum; postocular area of head sub-globose, distinctly broader than anteocular area, subequal in length or slightly longer than anteocular area, constricted behind compound eyes, with a broad and deep interocular sulcus; neck short. Compound eyes protrude laterally, nearly globose; lateral ocelli produced, elevated behind interocular sulcus, widely separated from each other; interspace between lateral ocelli wider than distance between compound eye and lateral ocellus. Labium with three visible segments; first visible labial segment shorter than second segment, longer than anteocular area of head, extending beyond level of middle of compound eye when labium laid backward; antennae with four segments, scape longest, first and second flagellomeres much longer than pedicel. Collar short in dorsal view, with anterolateral angle weakly and roundly produced; anterior pronotal lobe round and bulged, with middle longitudinal sulcus deep and narrow posteriorly, just reaching anterior margin of posterior lobe; lateral bulge of anterior pronotal lobe without produced tubercle centrally; posterior pronotal lobe with slightly swollen anteromedial elevation;

central disc of posterior pronotal lobe round and bulged; humerus roughly triangular, with round apex. Scutellum triangular, triangularly depressed basally, apically produced, and sloping downward, posterior margins not reflex. Femora thick, apically moderately nodulose; fore femora very slightly incrassated, thicker than mid and hind femora. Hemelytra surpassing apex of abdomen when fully closed; discal cell nearly parallelogram-shaped, about twice as long as width. Connexivum slightly dilated and ascending with segmental incisures. Female genital with abdominal laterotergite VIII (AL8) with thin and broad posterior margin; abdominal sternite VII (AS7) forming a semi-circular or broad sub-pentagonal median concavity, with posteromedian margin gently U-shaped, with inner posterolateral margin gently concave; gonocoxa VIII (Gc8) wider than length, gently slanting anteromesad along posterior margin, weakly produced mesad and forming a little blunt apex at apical inner corner, inner margin weakly incurved with a weak sinuously longitudinal elevation beside inner margin; gonapophysis (Gp8) small and subtriangular, longer than width. Male genital with paramere rod-shaped, relatively slender and short, not exceed the distal margin of mpp; pygophore ovoid with posterolateral margin sinuous; mpp narrow and posteriorly produced with straight distal margin and apicolateral corner formed posterolaterad and blunt at the apex; endosoma ovoid with well-produced sps; ddl round with membranous surface, and covered with some rows of large prickles; aa in dorsal view with slender basal plate arms that form a V-shape, in lateral view arched intensively.

Genus E (Fig. 3.14; Chapter 6)

Genus E is represented by "*Rhynocoris*" *mendicus* (Stål, 1867) and "*R*". *marginellus* (Fabricius, 1803). The definition of genus E is given below.

Body medium to large-sized, elongated, and somewhat robust. Head sub-elongated and robust, shorter than pronotum; postocular area of head sub-globose, distinctly broader than anteocular area, longer than anteocular area, constricted behind compound eyes, with a broad and

deep interocular sulcus; neck short. Compound eyes protrude laterally, nearly globose; lateral ocelli produced, elevated behind interocular sulcus, widely separated from each other; interspace between lateral ocelli wider than distance between compound eye and lateral ocellus. Labium with three visible segments; first visible labial segment shorter than second segment, longer than antecular area of head, extending beyond level of middle of compound eye when labium laid backward; antennae with four segments, scape and second flagellomere much longer than pedicel and first flagellomere. Collar short in dorsal view, with anterolateral angle weakly and roundly produced; anterior pronotal lobe round and bulged, with middle longitudinal sulcus deep and narrow, far from reaching anterior margin of posterior lobe; lateral bulge of anterior pronotal lobe somewhat with produced tubercle in central of posterior 1/3; posterior lobe depressed slightly or not depressed anteromedially; central disc of posterior pronotal lobe round and bulged but slightly elevated latitudinally medially; humerus roughly triangular, with round apex, and somewhat reflexed posterolateral margin. Scutellum triangular, triangularly depressed basally, apically produced, and sloping downward, lateral margin convex; posterior apex posteriorly produced; posterior margin of scutellum slightly reflex. Femora thick, apically moderately nodulose; fore femora very slightly incrassated, thicker than mid and hind femora. Hemelytra surpassing apex of abdomen when fully closed; discal cell nearly parallelogram-shaped, about twice as long as width. Connexivum slightly dilated and ascending with segmental incisures. Female genital with abdominal laterotergite VIII (AL8) with thin posterior margin; abdominal sternite VII (AS7) forming a semi-circular or broad sub-pentagonal median concavity, with posteromedian margin gently U-shaped or V-shaped, with inner posterolateral margin almost straight or slightly concave; gonocoxa VIII (Gc8) usually subtriangular, wider than length with inner posterolateral margin bolded and elevated and posterior apex produced posteriorly; gonapophysis VIII (Gp8) small and subtriangular, longer than width. Male genital with paramere rod-shaped; pygophore ovoid and posterolateral margin slight sinuous;

mpp broad and posteriorly produced with slightly concave distal margin and apicolateral corner formed laterad; endosoma ovoid with well-produced spoon-like sclerites (sps); ddl with membranous surface, and centrally and dorsally covered with tiny prickles, and ventrally covered with large prickles; aa in dorsal view with slender basal plate arms that form a U-shape or V-shape, in lateral view arched intensively.

Genus F (Fig. 3.15; Chapter 6)

Genus F is represented by "*Rhynocoris*" *fuscipes* (Fabricius, 1787). The definition of genus F is given below.

Body large-sized, elongated, and somewhat robust. Head sub-elongated and robust, shorter than pronotum; postocular area of head sub-globose, distinctly broader than antecular area, subequal in length to or longer than antecular area, constricted behind compound eyes, with a broad and deep interocular sulcus; neck short. Compound eyes protrude laterally, nearly globose; lateral ocelli produced, elevated behind interocular sulcus, widely separated from each other; interspace between lateral ocelli wider than distance between compound eye and lateral ocellus. Labium with three visible segments; first visible labial segment shorter than second segment, longer than antecular area of head, not extending beyond level of middle of compound eye when labium laid backward; antennae with four segments, scape and second flagellomere much longer than pedicel and first flagellomere. Collar short in dorsal view, with anterolateral angle weakly and roundly produced; anterior pronotal lobe round and bulged, with middle longitudinal sulcus deep and narrow, far from reaching anterior margin of posterior lobe; lateral bulge of anterior pronotal lobe without tubercle; posterior lobe depressed slightly or not depressed anteromedially; central disc of posterior pronotal lobe round and bulged but slightly elevated latitudinally medially; humerus roughly triangular, with round apex. Scutellum triangular, triangularly depressed basally, apically produced,

and sloping downward, lateral margin convex; posterior apex posteriorly produced; posterolateral margin of scutellum reflex. Femora thick, apically moderately nodulose; fore femora very slightly incrassated, thicker than mid and hind femora. Hemelytra surpassing apex of abdomen when fully closed; discal cell nearly parallelogram-shaped, about twice as long as width. Connexivum slightly dilated and ascending with segmental incisures. Female genital with abdominal laterotergite VIII (AL8) with thin and narrow posterior margin; abdominal sternite VII (AS7) forming a semi-circular or broad sub-pentagonal median concavity, with posteromedian margin gently U-shaped, with inner posterolateral margin slightly concave; gonocoxa VIII (Gc8) subtriangular, wider than length, gently slanting anteromesad along posterior margin, weakly produced mesad and forming blunt apex at apical inner corner, and with inner margin weakly incurved, and posterior apex reflexed; gonapophysis (Gp8) small and subtriangular, longer than width. Male genital with paramere rod-shaped, a small acute spike near apex; pygophore ovoid; mpp narrow and posteriorly well-produced with bifurcate projection in distal margin; endosoma small and ovoid with small sps; ddl narrow with membranous surface; aa in dorsal view with long thick basal plate arms that form a V-shape, in lateral view arched intensively.

CHAPTER 4:
**DISCRIMINATION OF THE SPECIES OF
THE GENUS *BLASTICUS*
(HEMIPTERA: HETEROPTERA: REDUVIIDAE)
KNOWN FROM VIETNAM AND SURROUNDING AREAS**

Notification. The formal taxonomic actions will not be done in this thesis (disclaiming of taxonomic actions declared in the concerning work is supported by the International Code of Zoological Nomenclature: Article 8.3).

Part of the contents of this chapter was published as below.

Ha NL, Truong XL, Ishikawa T, Jaitrong W, Lee CF, Chouangthavy B, Eguchi K (2022) Three new species of the genus *Biasticus* Stål, 1867 (Insecta, Heteroptera, Reduviidae, Harpactorinae) from Central Highlands, Vietnam. *ZooKeys* 1118: 133–180.

4.1. Introduction

Biasticus Stål, 1867 was established for *Reduvius impiger* Stål, 1863, and has been assigned to the tribe Harpactorini of the subfamily Harpactorinae in the current classification of the family Reduviidae (Stål 1863, 1867; Maldonado 1990).

Although the boundaries among *Biasticus* and its morphologically similar genera, such as *Sphedanolestes* and *Rhynocoris* have been unclear for a long time (Zhang and Weirauch 2013), the monophyly and the taxonomic validity of *Biasticus* were supported in the present study with a combination of the phylogenetic analyses and morphological examinations, and the morphological definition of *Biasticus* was partly updated from Distant (1904) and Ishikawa (2003), with a series of diagnostic characteristics (see Appendix of Chapter 3).

Biasticus currently comprised 23 valid named species known exclusively from the Oriental and Sino-Japanese realms (Stål 1863; Reuter 1887; Distant 1903; Bergroth 1913; Matsumura 1913; Miller 1941, 1948, 1949, 1954a, 1954b; Hsiao 1979; Hsiao and Ren 1981; Cai and Yang 2002; Ishikawa 2003; Afzal and Ahmad 2019; Ha et al. 2022) (Fig. 2.2). Among them, three species have been recorded and described from Vietnam, i.e., *B. confusus* Hsiao et al., 1979, *B. flavinotus* (Matsumura, 1913) and *B. flavus* (Distant, 1903), as of October 2018, when the present study was initiated (see Ha et al., 2022).

In the present study, the species-level classification of the Indo-Chinese and Indo-Malayan species of *Biasticus* is revised by the integrative approach, as explained in Chapter 2.

4.2. Material and Methods

The definition of the genus *Biasticus* follows the Appendix of Chapter 3. General information on sampling sites (Fig. 4.1), specimen depositories, and analytical methods (imaging, DNA sequencing, sequencing, and phylogenetic analyses) were given in Chapter 2. Additional information

for this chapter is given below.

This study included 222 *Biasticus* and *Biasticus*-like specimens (78 male and 144 female adults), of which 131 specimens were from Vietnam, 21 specimens from Laos, 26 specimens from Thailand, 4 specimens from Singapore, 3 specimens from Malaysia, 4 specimens from Taiwan, and 1 specimen from Myanmar. Among 222 specimens, there were 10 holotype and 15 paratype specimens from the Institute of Ecology and Biological Resources (IEBR), the British Natural History Museum collection (BNHM), Hokkaido University (HU), Swedish Museum of Natural History (NRM), and Vietnam National Museum of Nature (VNMN).

The following type specimens were also examined for identifying the species: *Biasticus abjectus* Miller, 1941 (a holotype specimen, BNHM), *B. breddini* Miller, 1948 (a paratype, BNHM), *B. chersonesus* (Distant, 1903) (a holotype, BNHM), *B. eburneus* Miller, 1941 (a holotype, BNHM), *B. flavinotus* (Matsumura, 1913) (a lectotype, HU), *B. griseocapillus* Ha, Truong et Ishikawa, 2022 (five include holotype and paratypes, IEBR and VNMN), *B. horfieldi* Distant, 1903 (a holotype, BNHM), *B. impiger* (Stål, 1863) (a holotype, NRM), *B. luteicollis* Ha, Truong et Ishikawa, 2022 (20 included holotype and paratypes, IEBR and VNMN), *B. nigricollis* (Dallas, 1850) (a holotype, BNHM), *B. nigricollis* var. *rubescens* Miller (a paratype, BNHM), *B. obfuscatus* Miller, 1949 (a holotype, BNHM), *B. princeps* Miller, 1949 (a holotype, BNHM) and *B. taynguyenensis* Ha, Truong et Ishikawa, 2022 (eight included holotype and paratypes, IEBR and VNMN) (Table 2.1).

Furthermore, specimens of *Sphedanolestes impressicollis* (Stål, 1861), “*Sphedanolestes*” *pubinotus* Reuter, 1881, and *Coranus* sp. collected from Vietnam were used as outgroups in molecular phylogenetic analyses (Table 2.1).

Morphological examination of the validly named species of the genus was conducted by referring to the original descriptions, other taxonomic publications, and type specimens where available (Stål 1863; Reuter 1887; Distant 1903; Bergroth 1913; Matsumura 1913; Miller 1941, 1948,

1949, 1954a, 1954b; Hsiao 1979; Hsiao and Ren 1981; Cai and Yang 2002; Ishikawa 2003; Afzal and Ahmad 2019; Ha et al. 2022) of the following congeners known from Vietnam and adjacent areas: *B. abdominalis* (Reuter, 1887), type location: India and Myanmar; *B. abjectus* Miller, 1941, Borneo; *B. breddin* Miller, 1948, Indonesia; *B. chersonesus* (Distant, 1903), Malaysia and Myanmar; *B. confusus* Hsiao et al., 1979, South China (see also Table 4.1); *B. dilectus* Miller, 1954, Indonesia; *B. eburneus* Miller, 1941, Borneo; *B. flavinotus* (Matsumura, 1913), Taiwan (see also Table 1); *B. flavus* (Distant, 1903), Hong Kong and Myanmar (see also Table 1); *B. fuliginosus* Reuter, 1887, North India; *B. gagatinus* Breddin, 1903, Indonesia; *B. griseocapillus* Ha, Truong et Ishikawa, 2022, Vietnam; *B. horfieldi* Distant, 1903, Indonesia; *B. impiger* (Stål, 1863), Cambodia; *B. insignis* (Miller, 1941), Indonesia; *B. luteicollis* Ha, Truong et Ishikawa, 2022, Vietnam; *B. lutescens* Breddin, 1903, Indonesia; *B. moultoni* Bergroth, 1913, Malaysia; *B. nigricollis* (Dallas, 1850), Indonesia; *B. obfuscatus* Miller, 1949, Malaysia; *B. princeps* Miller, 1949, Malaysia; *B. taynguyenensis* Ha, Truong et Ishikawa, 2022, Vietnam; *B. ventralis* Hsiao et al., 1979, South China.

The sexual dimorphism in external morphology of male and female adults is usually not very clear in the genus *Biasticus*, while female adults commonly showed larger body size, bigger abdomen, and more horizontally expanded connexivum than male adults (Kwadjo et al. 2010; Forthman 2017; Gil-Santana 2017; Weirauch et al. 2017; Chen et al. 2021) (Fig. 4.2). However, in order to take account of the importance of the sexual dimorphism, morphospecies recognition was made separately for males and females, and the male-based and female-based morphospecies are hereafter specified with unique codes such as “*B. sp. M1*” and “*B. sp. F1*” in which M and F mean the male-based species and the female-based species, respectively. Each morphospecies was characterized by the external and genitalia morphology of its sex.

The three-sequence dataset, i.e., mitochondrial 16S dataset (479 bp; 133 ingroup OTUs, 3 outgroup OTUs), the COI dataset (603 bp; 70 ingroup OTUs, 3 outgroup OTUs), the mini-barcode

of COI (= “Uni-Minibar” dataset, 177 bp, 106 ingroup OTUs, 3 outgroup OTUs) were successfully obtained (as listed in Table 2.1). Molecular phylogenetic analyses were done based on the concatenated 16S + COI dataset and the Uni-Minibar dataset. The substitution models, TPM3 + F + I + G4, TIM2 + F + I + G4, and TN + F + I + G4, were selected respectively for the 16S^(OG+), COI^(OG+), and Uni-Minibar^(OG+) datasets, respectively, by Model Finder (Kalyaanamoorthy et al. 2017) executed in IQ-TREE 2.1.2 (Minh et al. 2020). Maximum likelihood (ML) examinations were then carried out using IQ-TREE 2.1.2 (Chernomor et al. 2016; Minh et al. 2020); bootstrap values (BP) were estimated from 1,000 replications. The generalized time-reversible (GTR) + Gama model was chosen for both the 16S + COI dataset and the Uni-Minibar dataset using Model Finder (Kalyaanamoorthy et al. 2017) under the Bayesian information criterion. The Bayesian inference (BI) evaluations were then executed for the data using MrBayes v.3.2.7 (Ronquist and Huelsenbeck 2003) with 20,000,000 production and statutory parameter configuration (examining every 500 generations and tuning constraints every 100 generations, with a burn-in of 25 %). The effective sampling size (ESS) of each constraint was verified to be > 200 using Tracer 1.7.2 (Rambaut et al. 2018). The nodes were designated as “well supported” when posterior probability (PP) \geq 0.95 and BP \geq 80.

4.3. Results

4.3.1. Morphological Examination in the Male and Female Adults

A total of 77 males were grouped into 33 male-based morphospecies (*Biasticus* sp. M1–M33) based on characteristics presenting in external morphology, e.g., body coloration, anterior and posterior pronotal lobes, and scutellum (Fig 4.3) and characteristics presenting in male genitalia, e.g., distal margin of the median process of pygophore, dorsal outline of dorsal phallosomal sclerite, and spinulose processes on the distal dorsal lobe of endosoma (Figs 4.4–4.8).

On the other hand, 135 female *Blasticus* specimens were grouped into 59 female-based morphospecies (*Blasticus* sp. F1–F59) based on characteristics presenting in external morphology, e.g., body coloration, setation, anterior and posterior pronotal lobes, and scutellum (Fig 4.9) and features presenting in female genitalia, e.g., the posterior margin of abdominal sternite VII, the shape and structure of gonocoxa VIII, and the inner margin of abdominal laterotergite VIII (Figs 4.10–4.12).

4.3.2. Identities of the Morphospecies Based on the 16S + COI Phylogenetic Trees

For 10 male-based and 17 female-based morphospecies, mitochondrial 16S and COI sequences were successfully obtained.

In both ML and BI trees, twenty putative species were recovered as independent monophyletic lineages with high supporting values ($PP \geq 0.99$; $BP \geq 81$) or singleton lineages and deeply divergent well from each other with long basal branches (Fig. 4.13). It might be acceptable to interpret the following mismatch between morphospecies discrimination and phylogenetic topology as the result of DNA-based analyses successfully combining the male and female morphospecies of the same lineage together: M7 + F10, M8 + F11, M14 + F18, M25 + F46, M26 + F47, and M9 + F12. However, there is one remarkably incompatible case, i.e., three female-based morphospecies, namely, *B. sp.* F2, F56, and F57, recovered to constitute a well-supported monophyletic lineage in which further sub-lineages corresponding to the three morphospecies were not recognized.

The lineages recognized in the phylogenetic trees were mostly supported consistently by ASAP and bPTP (Fig. 4.13). As in the phylogenetic trees, *B. sp.* F2, F56, and F57 were not discriminated against in ASAP and bPTP. However, there is one except the case in the lineage consisting of *B. sp.* M26 and *B. sp.* F47. The lineage consisting of *B. sp.* M26 and *B. sp.* F47 was supported as an independent lineage in ASAP. On the other hand, the lineage was subdivided into two lineages in

bPTP, but the subdivision was not compatible with the separation of the morphospecies.

4.3.3. Identities of the Morphospecies Based on the Uni-Minibar Phylogenetic Trees

For 13 male-based and 24 female-based morphospecies, Uni-Minibar (COI) sequences were successfully obtained.

In both ML and BI trees, and ASAP and bPTP, mostly 26 putative species were recovered as independent monophyletic lineages with high supporting values ($PP \geq 0.91$; $BP \geq 87$) or singleton lineages and deeply divergent well from each other (Fig. 4.14), and the delimitation pattern is compatible well with the results of the analyses based on the 16S + COI datasets. DNA-based analyses successfully combined the male and female morphospecies of the same lineage together: M32 + F54, M22 + F32, M33 + F57, M15 + F19, M23 + F41, M26 + F47, M25 + F46, M14 + F18, M8 + F11, and M9 + F12. There is only an exceptional case of the lineage consisting of *B. sp. M7* and *B. sp. F10*, which was well supported in the ML tree ($BP = 89$) but lowly supported in the BI tree ($PP = 0.85$; PP is less than 0.95, which is the lower limit of “well supported” in the present study).

4.4. Discussion

4.4.1. Full Recognition of the Species and Identification

It is reasonable that the following 31 species, which correlated to 12 male-female combinations, 3 male-based, and 16 female-based morphospecies which were recovered independent units from each other by the present integrative approach, are treated as fully recognized species (or hereafter simply referred as species; abbreviation of each species is given as *Biasticus sp. HNL001* in which HNL is the initials of Ha Ngoc Linh) (Table 4.2; Figs 4.15–4.16).

The 31 species are listed as below, with the species of which both male and female were found

being highlighted in bold: *B. sp.* HNL003 (= *B. sp.* F2 + *B. sp.* F56 + *B. sp.* F57); *B. sp.* HNL004 (= *B. sp.* F3); *B. sp.* HNL005 (= *B. sp.* F4); *B. sp.* HNL006 (= *B. sp.* M2); *B. sp.* HNL007 (= *B. sp.* F6); *B. sp.* HNL008 (= *B. sp.* F7); ***B. sp.* HNL009** (= *B. sp.* M5 + *B. sp.* F8); *B. sp.* HNL010 (= *B. sp.* F9); ***B. sp.* HNL011** (= *B. sp.* M7 + *B. sp.* F10); ***B. sp.* HNL012** (= *B. sp.* M8 + *B. sp.* F11); ***B. sp.* HNL013** (= *B. sp.* M9 + *B. sp.* F12); *B. sp.* HNL016 (= *B. sp.* M11); *B. sp.* HNL017 (= *B. sp.* F14); ***B. sp.* HNL021** (= *B. sp.* M14 + *B. sp.* F18); ***B. sp.* HNL022** (= *B. sp.* M15 + *B. sp.* F19); *B. sp.* HNL024 (= *B. sp.* F22); *B. sp.* HNL026 (= *B. sp.* F22); ***B. sp.* HNL037** (= *B. sp.* M22 + *B. sp.* F32); *B. sp.* HNL043 (*B. sp.* F38); *B. sp.* HNL044 (= *B. sp.* F39); ***B. sp.* HNL046** (= *B. sp.* M23 + *B. sp.* F41); *B. sp.* HNL048 (= *B. sp.* F43); *B. sp.* HNL049 (= *B. sp.* F44); *B. sp.* HNL050 (= *B. sp.* M24); *B. sp.* HNL051 (= *B. sp.* F45); ***B. sp.* HNL053** (= *B. sp.* M25 + *B. sp.* F46); ***B. sp.* HNL054** (= *B. sp.* M26 + *B. sp.* F47); *B. sp.* HNL058 (= *B. sp.* F50); ***B. sp.* HNL063** (= *B. sp.* M32 + *B. sp.* F54); *B. sp.* HNL064 (= *B. sp.* F55); ***B. sp.* HNL067** (= *B. sp.* M33 + *B. sp.* F57).

Biasticus sp. M26 + *B. sp.* F47 is herein treated conservatively as a single species *B. sp.* HNL054, even if the monophyly is not “well” supported in the ML tree and subdivided in bPTP, since this species was supported consistently in morphological examination, ASAP, and their maximum intraspecific diversity was low (1.7% in p-distance and K2P-model) (see Section 4.3.2; Table 4.1).

There are two exceptional cases (incompatibility between the morphological examination and DNA-based phylogenetic and species delimitation analyses) that need to be explained. Firstly, *B. sp.* F2, F56, and F57, which were discriminated from each other by body color patterns, were not discriminated in phylogenetic analyses as well as ASAP and bPTP, and so they are herein concluded in intraspecific morphological forms of a single species *B. sp.* HNL003 (Fig. 4.17). Secondly, *B. sp.* M32 and *B. sp.* F54 were discriminated from each other by their body coloration (Fig. 4.18) but not discriminated against in phylogenetic analyses as well as ASAP and bPTP. Thus, they are herein

treated as an independent species with intraspecific morphological forms, and this species is coded as *B. sp.* HNL063.

By examining type material and taxonomic articles (including the original descriptions) of the valid named species of the genus *Biasticus* and species of some closed related genera (*Sphedanolestes* and *Rhynocoris*), the following eight species can be reasonably identified: *B. sp.* HNL037 = *B. confusus* Hsiao et al., 1979; *B. sp.* HNL007 = *B. flavinotus* (Matsumura, 1913); *B. sp.* HNL067 = *B. flavus* (Distant, 1903); *B. sp.* HNL012 = *B. griseocapillus* Ha, Truong et Ishikawa, 2022, *B. sp.* HNL013 = *B. luteicollis* Ha, Truong et Ishikawa, 2022; *B. sp.* HNL011 = *B. taynguyenensis* Ha, Truong et Ishikawa, 2022; *B. sp.* HNL063 = *Sphedanolestes annulipes* Distant, 1903; *B. sp.* HNL017 = *Sphedanolestes gularis* Hsiao et al., 1979 (Fig. 4.19). It is worth noting that *S. annulipes* and *S. gularis* need to be placed in *Biasticus* redefined in the Appendix of Chapter 3.

For the other 48 morphospecies (18 male-based and 30 female-based morphospecies), which were unable to involve in DNA sequencing, the status of the species and the conspecific male and female combination were not confirmed in the present study. Future studies based on further comprehensive sampling are necessary to solve the issues.

The morphological diagnosis and taxonomic remarks for each fully recognized species and the remaining morphospecies, and the synonymic list for the eight species identified above, will be provided in the Appendix of this chapter. These may be useful as the prior working hypotheses (= operational taxonomic units) in future integrative taxonomic studies. The formal taxonomic actions will not be done in this thesis (disclaiming of taxonomic actions declared in the concerning work is supported by the International Code of Zoological Nomenclature: Article 8.3).

4.4.2. Morphological Diagnostic Characteristics Reliable for Discriminating Species

The conspecific male and female were revealed for twelve of the thirty-one fully recognized

species. In these species, external morphology shows no remarkable conspecific sexual dimorphism. Therefore, external morphology has a certain usefulness as supporting evidence to infer conspecific male-female combinations when the molecular phylogenetic approach is not applicable. On the other hand, it should be noted that the present study revealed hidden intraspecific polymorphism, as in *B.* sp. HNL003. The same situation may be present in other species of the genus *Biasticus* as well as in other species of the genera of the family Reduviidae.

When only external morphological examination is allowed (e.g., target specimens in a certain collection are not permitted to be dissected for DNA extraction or high-draw observation), the following morphological characteristics commonly used in previous taxonomic studies of the family Reduviidae are unreliable and must be used with a special caution in species-level classification in subtle cases, such as species with high morphological similarity, phylogenetically close species, and sympatric species: coloration of pronotum, hemelytra, and abdominal sternites, body length, pronotal length and width (PnL and PnW), length of antennae segments (A1L–A4L, respectively), and the measurements of heads (head length (HL), length and width of antecular area of head (AoL and AoW), length and width of postocular area of head (PoL and PoW), maximum diameter of compound eye (ED), maximum diameter of left ocellus (OD), length of visible labial segments (R1L–R3L)). This is actually an important knowledge in taxonomy of *Biasticus*, because those characters have been repeatedly used as key species diagnostic characters in previous taxonomic articles of the genus (Stål 1863; Reuter 1887; Distant 1903; Bergroth 1913; Matsumura 1913; Miller 1941, 1948, 1949, 1954a, 1954b; Hsiao 1979; Hsiao and Ren 1981; Cai and Yang 2002; Ishikawa 2003; Afzal and Ahmad 2019; Ha et al. 2022).

However, from the detailed observation of the morphology of the 31 fully recognized species of *Biasticus*, even if DNA sequence information is unavailable, careful examinations of both external morphology and the genital morphology can provide a certain reliability in species discrimination

and identification, especially for the male. indicated that the reliability of identification should increase if both external morphology and the morphology of male and female copulatory organs can be observed. In particular, it is worth observing the following characters carefully. However, these characters may not be useful in the case of other genera, such as *Sphedanolestes* and *Rhynocoris* (see Chapters 5 and 6).

Median processes of pygophore (mpp), male — the posterior development of mpp, the shape of the distal margin of mpp and the apicolateral corner of male genitalia are hyper-diverse among similar species in general external morphology, the phylogenetically close species or sympatric species (e.g., *B. sp.* HNL011 and *B. sp.* HNL012, *B. sp.* HNL010 and *B. sp.* HNL054).

Spinulose processes on distal dorsal lobe of endosoma (ddl), male — the size, shape and arrangement of the spinulose processes on distal dorsal lobe of endosoma (ddl) of the male genitalia are hyper-diverse among similar species in general external morphology, the phylogenetically close species or sympatric species (e.g., *B. sp.* HNL011 and *B. sp.* HNL012, *B. sp.* HNL013 and *B. sp.* HNL046).

Surfaces of spoon-like sclerites (sps), male — The glabrous or spinulose surfaces of sps of the male genitalia are important in some cases of discriminating species (e.g., *B. sp.* HNL013 and *B. sp.* HNL046).

Dorsal outline of dorsal phallosclerite (dps) in lateral view, male — the dorsal outline of dps of the male genitalia are diverse among *Biasticus* species (e.g., *B. sp.* HNL021 and *B. sp.* HNL067).

Posterior margin of abdominal sternite VII (AS7), female — the concave, straight, or convex posterior margin of AS7 can be helpful characteristic for discriminating similar species in general external morphology, the phylogenetically close species or sympatric species (e.g., *B.*

sp. HNL007 and *B. sp.* HNL043, *B. sp.* HNL010 and *B. sp.* HNL054).

Apical inner corner and posterior and inner margins of gonocoxa VIII (Gc8), female — the shape of apical inner margin of Gc8 are diverse and helpful for discriminating similar species in general external morphology, the phylogenetically close species or sympatric species (e.g., *B. sp.* HNL007 and *B. sp.* HNL043, *B. sp.* HNL010 and *B. sp.* HNL054).

Length of antennae segments (A1L–A4L) — the length of scape, pedicel, first and second flagellomeres, and the proportional length of four antennae segments are useful characters for discriminating species of *Biasticus* (e.g., *B. sp.* HNL010 and *B. sp.* HNL054, *B. sp.* HNL013 and *B. sp.* HNL046). However, this characteristic might not be suitable in several cases, for instance, *B. sp.* HNL011 and *B. sp.* HNL012, or in the case of antennae, which is most fragile in reduviid body, missing.

Combination of color patterns in pronotum, hemelytra, abdominal mediotergites, laterotergites, and sternites — the differences in color patterns in external body organisms are useful for discriminating *Biasticus* species as well as other reduviid genera. However, as mentioned above, intraspecific polymorphisms are recorded in the genus *Biasticus*. Therefore, it suggested that these characteristics should be examined with other important features.

Length of femora and tibiae — the length of femora and tibiae varies in a wide range among species and was suggested as a set of useful characters for discriminating *Biasticus* species (Ha et al., 2022).

4.4.3. Distribution and Biogeographical Criteria

Among thirty-one species were discriminated in this study, eleven of them were only recorded from the Northern Indo-China, which is characterized by temperate climate. Other fourteen species were only recognized in the Middle and Southern Vietnam, which is characterized with tropical

climate. Moreover, three species are only found in the tropical savanna in Thailand. Therefore, the distribution patterns of *Biasticus* in Vietnam and surrounding areas roughly correspond to the climatic patterns. Besides, there are two exceptional species not being restricted in a climatic region, i.e., “*Sphedanolestes*” *gularis* widely distributing in both temperate and tropical climatic region of Vietnam and *Biasticus flavus* recorded in transitional border of the Northern temperate zone and Northern tropical savanna of Thailand.

On the other hand, among thirty-one species that were discriminated in this study, eleven of them were only recorded from Northern Indo-China, which comprised three terrestrial ecoregions, i.e., South China-Vietnam subtropical evergreen forests, Red River freshwater swamp forest, and Northern Indo-China subtropical forests. Other fourteen species were only recognized in Middle and Southern Vietnam, which included Northern and Southern Vietnam lowland rain forests, Northern Annamites and Southern Annamites montane rain forests, Southeastern Indo-China dry evergreen forests, and Central Indo-China dry forests. Moreover, three species are only found in the transitional regions of Kayah-Karen montane rain forests, Central Indo-China dry forests, and Northern Thailand-Laos moist deciduous forests in Northern Thailand. Therefore, the distribution patterns of *Biasticus* in Vietnam and surrounding areas roughly correspond to the climatic patterns. Besides, there are two exceptional species not being restricted in a climatic region, i.e., “*Sphedanolestes*” *gularis* widely distributed in both temperate and tropical climatic region of Vietnam and *Biasticus flavus* recorded in the transitional border of the Northern temperate zone and Northern tropical savanna of Thailand (Fig. 4.20). Therefore, it is suggested that the distribution patterns of *Biasticus* species are accordant to the climatic patterns of Indo-China rather than terrestrial ecoregions.

4.4.4. The Future Prospect of This Study

The present study highlighted that in the genus *Biasticus*, there are many undescribed species

and unsolved or unnoticed taxonomic problems, e.g., intraspecific polymorphism or variation, which may be associated with their life history and sexual dimorphism in morphology. Therefore, the species-level discrimination of the genus *Biasticus*, as well as other reduviid genera, should be appraised again by integrated taxonomy.

The usefulness of male genitalia for discriminating species of *Biasticus* was highlighted in this study. Nonetheless, there is a tendency of sexual imbalance observed in the species of *Biasticus*, i.e., 135 female specimens (58 female-based morphospecies) vs. 79 male specimens (33 male-based morphospecies) were available for the present study. Of 31 fully recognized species (31), the conspecific male and female pair was confirmed only for 12 species.

The utility of DNA-based phylogenetic and species delimitation analyses in the taxonomy of *Biasticus* and Reduviidae is no longer in doubt. However, mostly validly named *Biasticus* species were only discriminated by morphological examination, and there has been no available DNA barcode database of *Biasticus* yet. In addition, only 43 morphospecies (15 male-based morphospecies and 28 female-based morphospecies) over 91 morphospecies (33 male-based morphospecies and 58 female-based morphospecies) recorded in the present study (nearly 50%) were able to involve in molecular phylogenetic analyses. Thus, studies on more extensive collections of fresh or relatively newly collected specimens suitable for DNA sequencing should be done in the future.

Therefore, continuous research using integrated taxonomy, with a special effort to collect males, is necessary for fully elucidating the species diversity of *Biasticus* in Indo-China.

References

1. Afzal H, Ahmad I (2019) A new record of the predatory bug *Biasticus flavus* (Distant) (Hemiptera: Reduviidae: Harpactorinae) from Pakistan and its redescription with reference to its

- unknown male and female genitalia. *International Journal of Biology and Biotechnology* 16 (1): 205–210.
2. Beck H, Zimmermann N, McVicar T, Vergopolan N, Berg A, Wood FE (2018) Present and future Köppen-Geiger climate classification maps at 1-km resolution. *Scientific Data* 5, 180214. <https://doi.org/10.1038/sdata.2018.214>
 3. Bergroth E (1913) New genera and species of Reduviidae from Borneo. *J. Sarawak Mus.*, 3: 25–38.
 4. Cai W, Yang S (2002) *Insect from Maolan landscape*. Guizhou Science and Technology Publishing House, 208–230.
 5. Chen Z, Liu Y, Cai W (2021). Taxonomic review of *Xenorhyncocoris* Miller (Heteroptera: Reduviidae: Ectrichodiinae), with description of *X. attractivus* sp. nov. and notes on sexual dimorphism of the genus. *European Journal of Taxonomy* 746(1): 26–49. <https://doi.org/10.5852/ejt.2021.746.1315>
 6. Chernomor O, Haeseler von A, and Minh BQ (2016) Terrace aware data structure for phylogenomic inference from supermatrices. *Syst. Biol.*, 65: 997–1008. <https://doi.org/10.1093/sysbio/syw037>
 7. Distant WL (1903) Rhynchotal notes. XVI. Heteroptera: Family Reduviidae (continued). Apiomerinae, Harpactorinae and Nabidae. *The Annals and Magazine of Natural History* (7)11: 203–213.
 8. Distant WL (1904) Rhynchotal notes. XXII. Heteroptera from North Queensland. *Ann. Mag. Nat. Hist.*, (7)18: 286–293.
 9. Forthman M, Weiwauch C (2017) Millipede assassins and allies (Heteroptera: Reduviidae: Ectrichodiinae, Tribelocephalinae): total evidence phylogeny, revised classification and

evolution of sexual dimorphism. *Systematic Entomology* 42(3):575–595.
<https://doi.org/10.1111/syen.12232>

10. Gil-Santana HR, Salomão AT, Oliveira J (2017) First description of the male and redescription of the female of *Parahiranetis salgadoi* Gil-Santana (Hemiptera, Reduviidae, Harpactorinae). *ZooKeys* 671: 19–48. <https://doi.org/10.3897/zookeys.671.11985>
11. Ha NL, Truong XL, Ishikawa T, Jaitrong W, Lee CF, Chouangthavy B, Eguchi K (2022) Three new species of the genus *Biasticus* Stål, 1867 (Insecta, Heteroptera, Reduviidae, Harpactorinae) from Central Highlands, Vietnam. *ZooKeys* 1118: 133–180.
<https://doi.org/10.3897/zookeys.1118.83156>
12. Hsiao TY (1979) New species of Harpactorinae from China. II. (Hemiptera: Reduviidae). *Acta Zootaxon.Sinica.*, 4: 238–295.
13. Hsiao TY, Ren SZ (1981) Reduviidae. In: Hsiao et al., A handbook for the determination of the Chinese Hemiptera-Heteroptera (II). Science Press, Beijing, pp. 390–538.
14. Ishikawa T (2003) Taxonomic study on the Tribe Harpactorini (Heteroptera, Reduviidae) from Indochina, with Zoogeographical considerations. Ph.D. Thesis, Tokyo University of Agriculture, Kanagawa, Japan.
15. Kalyaanamoorthy S, Minh BQ, Wong T, Haeseler von A, Jermini LS (2017) ModelFinder: fast model selection for accurate phylogenetic estimates. *Nat Methods* 14, 587–589.
<https://doi.org/10.1038/nmeth.4285>
16. Kwadjo KE, Doumbia M, Haubruge E, Kra KD, Tano Y (2010) Sexual dimorphism in adults of *Rhynocoris albopilosus* Signoret (Heteroptera: Reduviidae). *Journal of Applied Biosciences* 2010 Vol.30: 1873–1877.
17. Matsumura S (1913) Additions to Thousand Insects of Japan. 1: 1–184.

18. Miller NCE (1941) New genera and species of Malaysian Reduviidae (continued). Part II. *Journal of the Federated Malay States Museums*, 18: 601–773.
19. Miller NCE (1948) New genera and species of Reduviidae from the Philippines, Celebes, and Malaysia. *Transactions of the Entomological Society of London*, 99: 411–473.
20. Miller NCE (1949) A new genus and new species of Malaysian Reduviidae. *Proc. R. Entomol. Soc. London*, (B)18: 229–237.
21. Miller NCE (1954a) Reduviidae (Hemiptera-Heteroptera). Synonymic notes and corrections. *Ann. Mag. Nat. Hist.*, (12) 7: 639–640.
22. Miller NCE (1954b) New genera and species of Reduviidae from Indonesia and the description of a new subfamily (Hemiptera-Heteroptera). *Tijds. Ent.*, 97: 75–114.
23. Minh BQ, Schmidt HA, Chernomor O, Schrempf D, Woodhams MD, von Haeseler A, Lanfear R (2020) IQ-TREE 2: new models and efficient methods for phylogenetic inference in the genomic era. *Mol Biol Evol* 37:1530–1534. <https://doi.org/10.1093/molbev/msaa015>
24. Olson DM, Dinerstein E, Wikramanayake ED, Burgess ND, Powell GV, Underwood EC, D'amico JA, Itoua I, Strand HE, Morrison JC, and Loucks CJ (2001) Terrestrial Ecoregions of the World: A new map of life on Earth. A new global map of terrestrial ecoregions provides an innovative tool for conserving biodiversity. *BioScience* 51(11): 933 – 938. [https://doi.org/10.1641/0006-3568\(2001\)051\[0933:TEOTWA\]2.0.CO;2](https://doi.org/10.1641/0006-3568(2001)051[0933:TEOTWA]2.0.CO;2)
25. Park DS, Foottit R, Maw E, Hebert PDN (2011) Barcoding Bugs: DNA-Based Identification of the True Bugs (Insecta: Hemiptera: Heteroptera). *PLoS ONE* 6(4): e18749. <https://doi.org/10.1371/journal.pone.0018749>
26. Poyarkov NA, Nguyen VT, Popov SE, Geissler P, Pawangkhanant P, Neang T, Suwannapoom C, Orlov LN (2021) Recent progress in taxonomic studies, biogeographic analysis, and revised

- checklist of amphibians in Indochina. *Russian Journal of Herpetology* Vol. 28, No. 3A, 202: 1–110. <http://dx.doi.org/10.30906/1026-2296-2021-28-3A-1-110>
27. Rambaut A, Drummond AJ, Xie D, Baele G, Suchard MA (2018) Posterior summarization in Bayesian phylogenetics using Tracer 1.7. *Systematic Biology*. Syy032. <https://doi.org/10.1093/sysbio/syy032>
28. Reuter OM (1887) Reduviidae novae et minus cognitae descriptae. *Rev. Entomol.*, 6: 149–176.
29. Ronquist F, Huelsenbeck JP (2003) MrBayes: Bayesian Phylogenetic Inference under Mixed Models. *Bioinformatics*, 19 (12), 1572–1574. <https://doi.org/10.1093/bioinformatics/btg180>
30. Stål C (1863) *Formae speciesque novae Reduviidum*. *Annales de la Société entomologique de France* 3: 38.
31. Weirauch C, Forthman M, Grebennikov V, Baňář P (2017) From Eastern Arc Mountains to extreme sexual dimorphism: systematics of the enigmatic assassin bug genus *Xenocaucus* (Hemiptera: Reduviidae: Tribelocephalinae). *Organisms Diversity & Evolution* 17: 421–445. <https://doi.org/10.1007/s13127-016-0314-2>
32. Zhang G, Weirauch C (2013) Molecular phylogeny of Harpactorini (Insecta: Reduviidae): correlation of novel predation strategy with accelerated evolution of predatory leg morphology. *Cladistics* (2013): 1–13. <https://doi.org/10.1111/cla.12049>

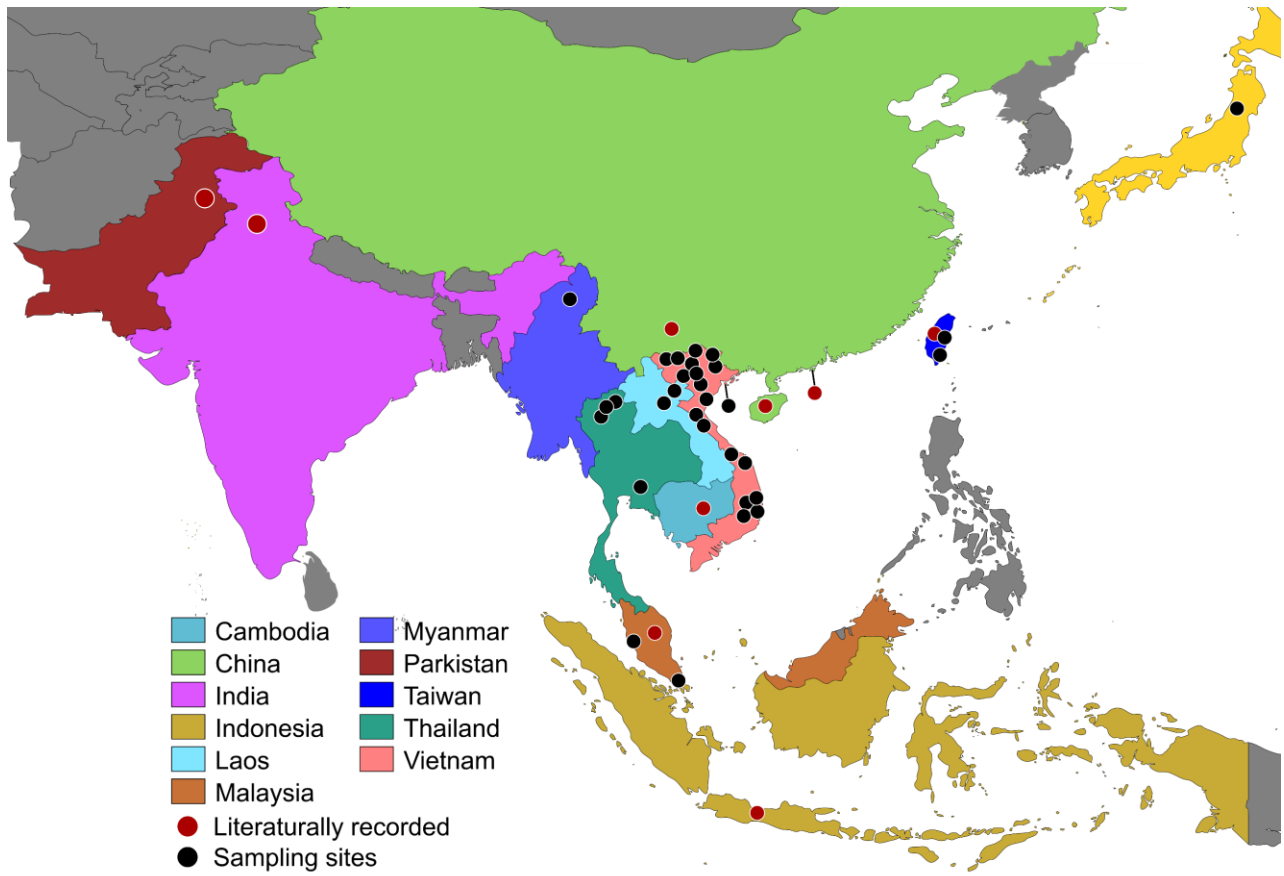


Figure 4.1. Sampling sites.

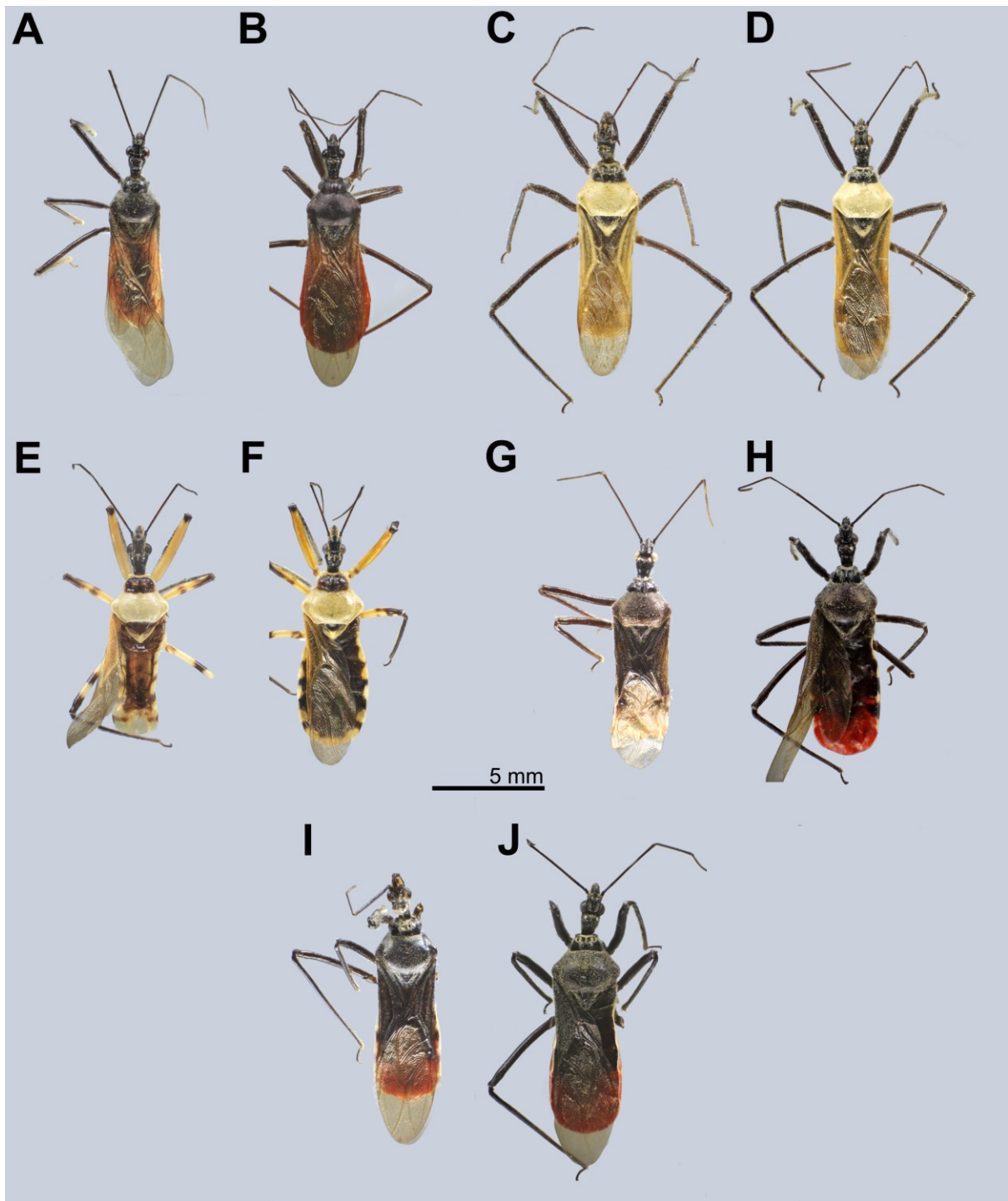


Figure 4.2. Sexual dimorphism in external morphology of male and female adults of *Biastiscus* species. A–J, body in dorsal view. A, B, *Biastiscus confusus* Hsiao et al, 1979; C, D, *B. flavus* Distant, 1903; E, F, *B. luteicollis* Ha, Truong et Ishikawa, 2022; G, H, *B. griseocapillus* Ha, Truong et Ishikawa, 2022; I, J, *B. taynguyenensis* Ha, Truong et Ishikawa, 2022. A, AD2021-001, ♂; B, VN-Hem-1998-012, ♀; C, HEM-TH2004-016, ♂; D, LA-Redu-2004-006, ♀; E, HNL2018-025, ♂; F, HNL2018-024, ♀; G, TXBX17, ♂; H, HNL2018-073, ♀; I, TXLBX1, ♂; J, HNL2018-073, ♀.

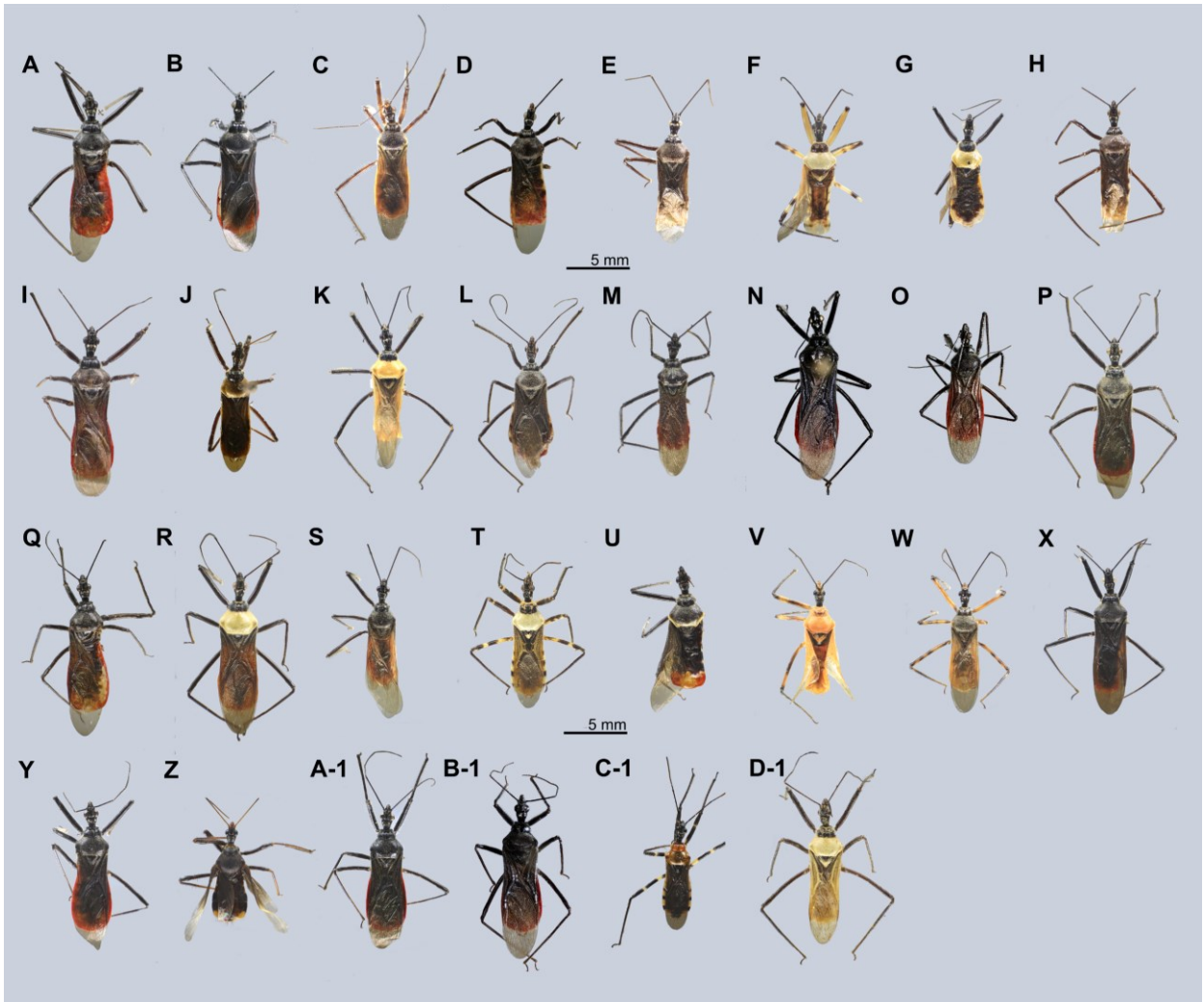


Figure 4.3. Body in dorsal view of male-based morphospecies. **A**, *Biasticus* sp. M2, TXL2016-621, ♂; **B**, *B. sp.* M5, TXL2019-680, ♂; **C**, *B. sp.* M6, VN-Hem-2011-017, ♂; **D**, *B. sp.* M7, TXL2016-545, ♂; **E**, *B. sp.* M8, TXL2016-546, ♂; **F**, *B. sp.* M9, HNL2018-025, ♂; **G**, *B. sp.* M10, TXL2016-088, ♂; **H**, *B. sp.* M11, TXL2017-666, ♂; **I**, *B. sp.* M12, TXL2018-843, ♂; **J**, *B. sp.* M13, TXL2000-004, ♂; **K**, *B. sp.* M14, AD2022-005, ♂; **L**, *B. sp.* M15, HEM-TH-2002-003, ♂; **M**, *B. sp.* M16, HEM-TH-2000-004, ♂; **N**, *B. sp.* M17, NSMT-I-He-73653, ♂; **O**, *B. sp.* M18, NSMT-I-He-8264, ♂; **P**, *B. sp.* M19, LA-Redu-2004-008, ♂; **Q**, *B. sp.* M20, VN-Hem-1997-001, ♂; **R**, *B. sp.* M21, La-Redu-2004-015, ♂; **S**, *B. sp.* M22, AD2021-001, ♂; **T**, *B. sp.* M23, HEM-TH-2002-022, ♂; **U**, *B. sp.* M24, NDD2022-066, ♂; **V**, *B. sp.* M25, NDD2022-015, ♂; **W**, *B. sp.* M26, NDD2022-022, ♂; **X**, *B. sp.* M27, LA-Redu-2008-004, ♂; **Y**, *B. sp.* M28, VN-HEM-2011-012, ♂; **Z**, *B. sp.* M29, LA-Redu-2011-003, ♂; **A-1**, *B. sp.* M30, VN-HEM-2011-016, ♂; **B-1**, *B. sp.* M31, NSMT-I-He-73776, ♂; **C-1**, *B. sp.* M32, LA-Redu-2011-006, ♂; **D-1**, *B. sp.* M33, HEM-TH2004-018, ♂.

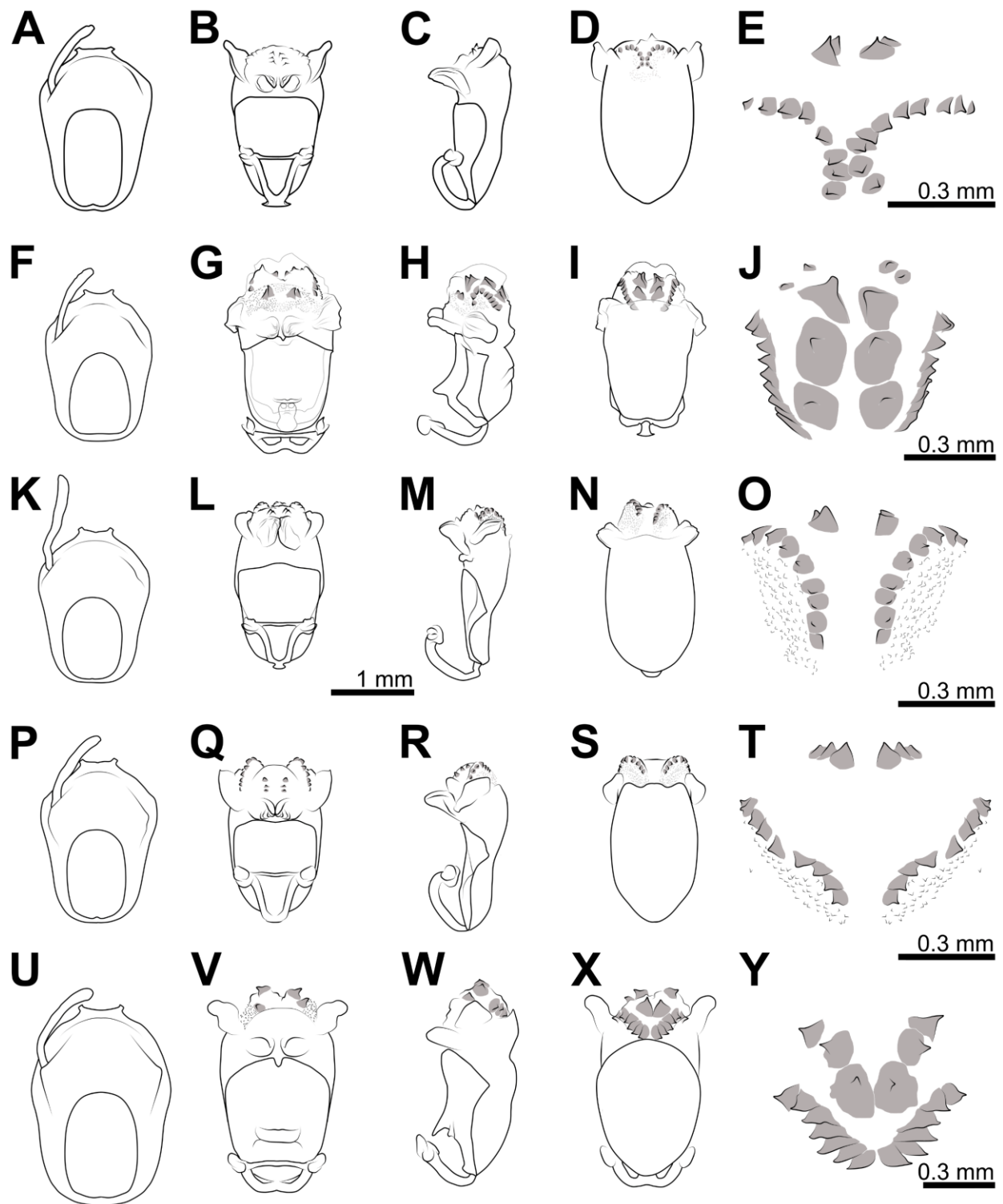


Figure 4.4. Genital morphology of male-based morphospecies of *Biasticus*. **A–E**, TXL2016-621, ♂, *B. sp. M2*; **F–J**, TXL2003-005, ♂, *B. sp. M4*; **K–O**, TXL2019-681, ♂, *B. sp. M5*; **P–T**, TXL2018-843, ♂, *B. sp. M12*; **U–Y**, NDD2022-066, ♂, *B. sp. M24*; **A, F, K, P, U**, pygophore in dorsal view; **B, G, L, Q, V**, phallus in dorsal view; **C, H, M, R, W**, phallus in lateral view; **D, I, N, S, X**, phallus in ventral view; **E, J, O, T, Y**, distal dorsal lobe of endosoma (ddl).

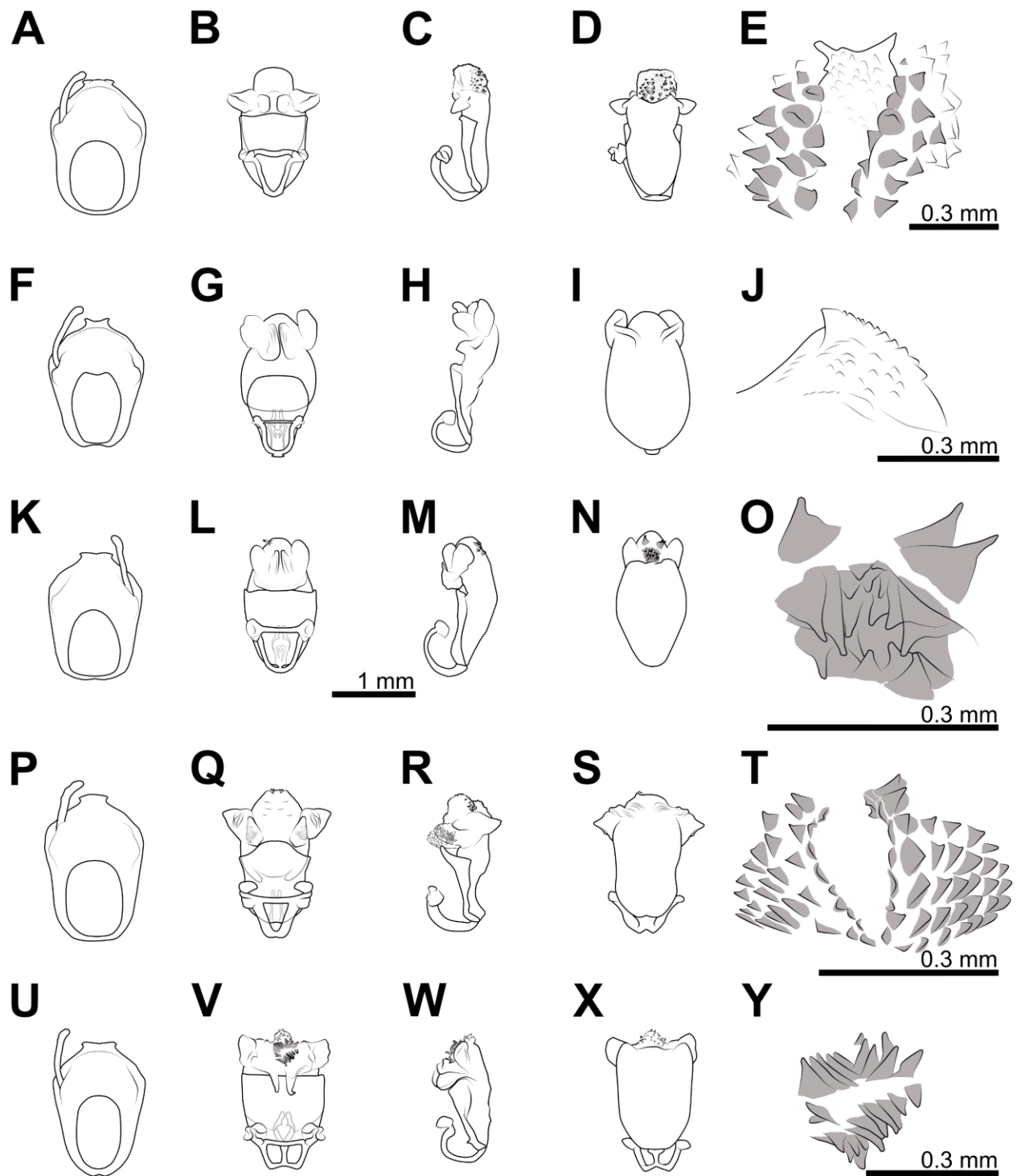


Figure 4.5. Genital morphology of male-based morphospecies of *Biasticus* (cont.). **A–E**, VN-HEM-2011-017, ♂, *B. sp. M6*; **F–J**, TXL2016-545, ♂, *B. sp. M7*; **K–O**, TXL2016-546, ♂, *B. sp. M8*; **P–T**, HNL2018-025, ♂, *B. sp. M9*; **U–Y**, TXL2017-666, ♂, *B. sp. M11*. **A, F, K, P, U**, pygophore in dorsal view; **B, G, L, Q, V**, phallus in dorsal view; **C, H, M, R, W**, phallus in lateral view; **D, I, N, S, X**, phallus in ventral view; **E, J, T, Y**, distal dorsal lobe of endosoma (ddl).

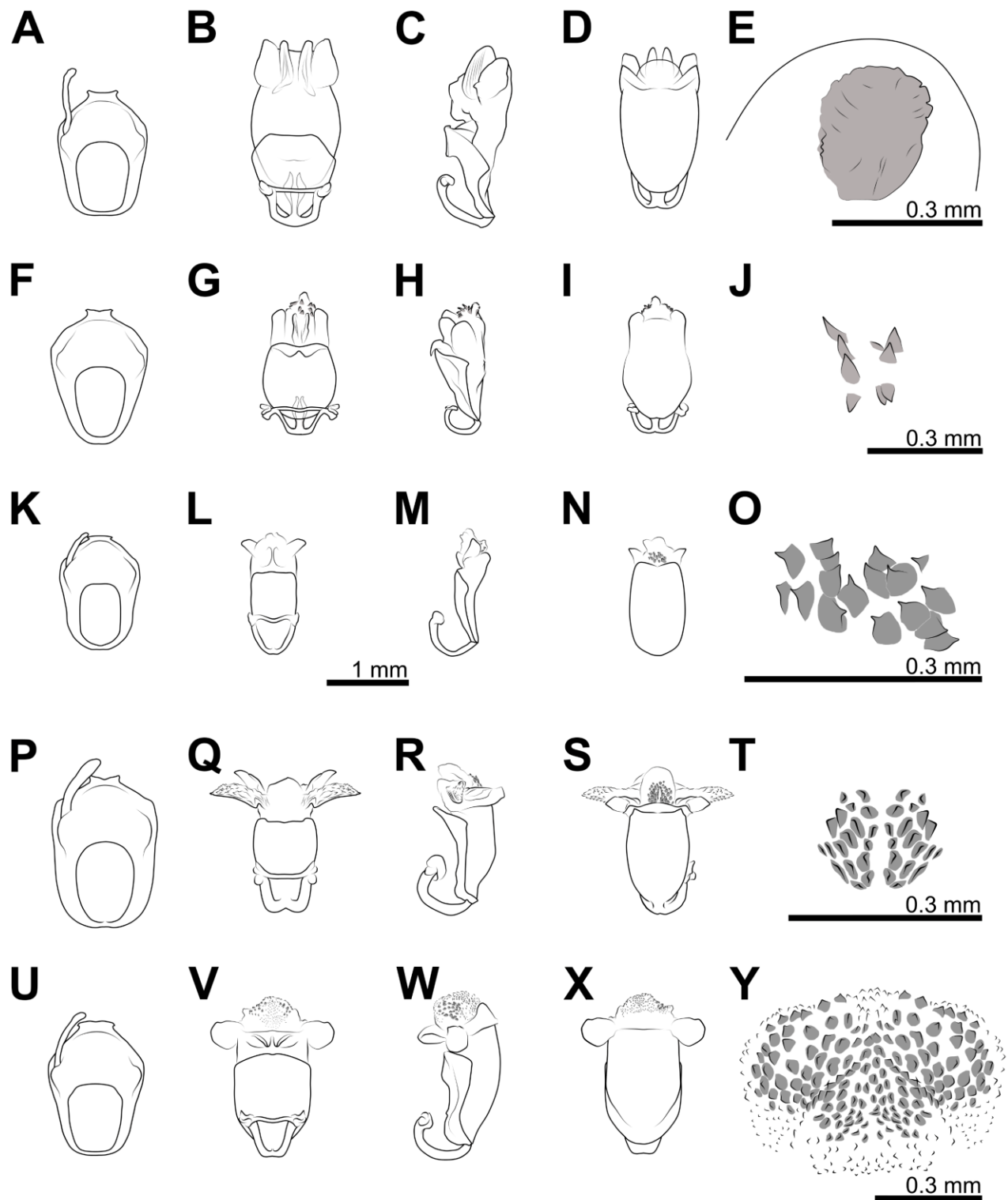


Figure 4.6. Genital morphology of male-based morphospecies of *Biasticus* (cont.). **A–E**, AD2022-005, ♂, *B. sp. M14*; **F–J**, HEM-TH-1998-002, ♂, *B. sp. M15*; **K–O**, AD2021-001, ♂, *B. sp. M22*; **P–T**, HEM-TH-2002-022, ♂, *B. sp. M23*; **U–Y**, NDD2022-015, ♂, *B. sp. M25*. **A, F, K, P, U**, pygophore in dorsal view; **B, G, L, Q, V**, phallus in dorsal view; **C, H, M, R, W**, phallus in lateral view; **D, I, N, S, X**, phallus in ventral view; **E, J, P, T, Y**, distal dorsal lobe of endosoma (ddl).

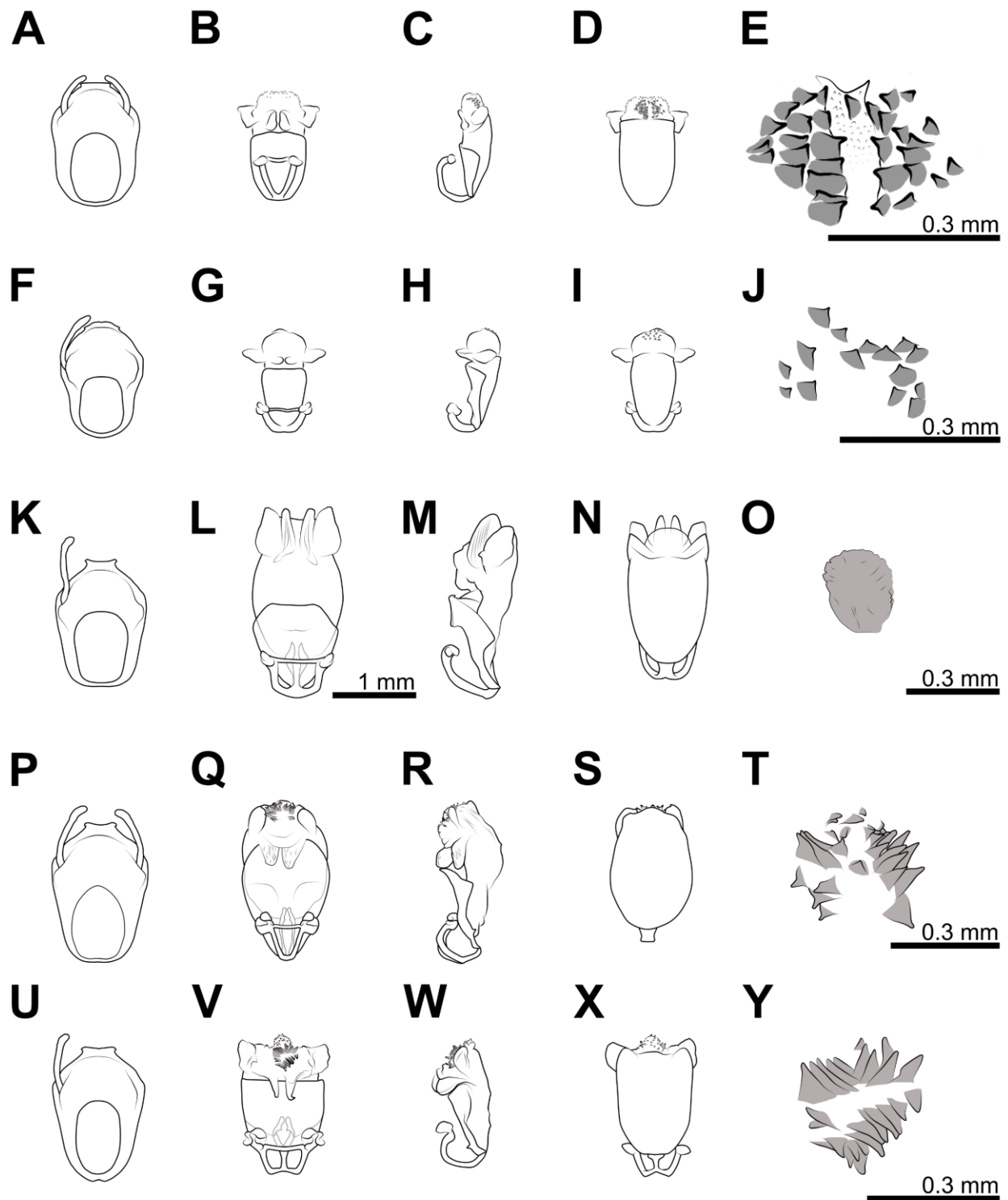


Figure 4.7. Genital morphology of male-based morphospecies of *Biasticus* (cont.). **A–E**, NDD2022-022, ♂, *B. sp.* M26; **F–J**, LA-Redu-2011-006, ♂, *B. sp.* M32; **K–O**, LA-Redu-2004-011, ♂, *B. sp.* M33; **P–T**, TXL2004-001, ♂, *B. sp.* M1; **U–Y**, TXL2016-088, ♂, *B. sp.* M10. **A, F, K, P, U**, pygophore in dorsal view; **B, G, L, Q, V**, phallus in dorsal view; **C, H, M, R, W**, phallus in lateral view; **D, I, N, S, X**, phallus in ventral view; **E, J, P, T, Y**, distal dorsal lobe of endosoma (ddl).

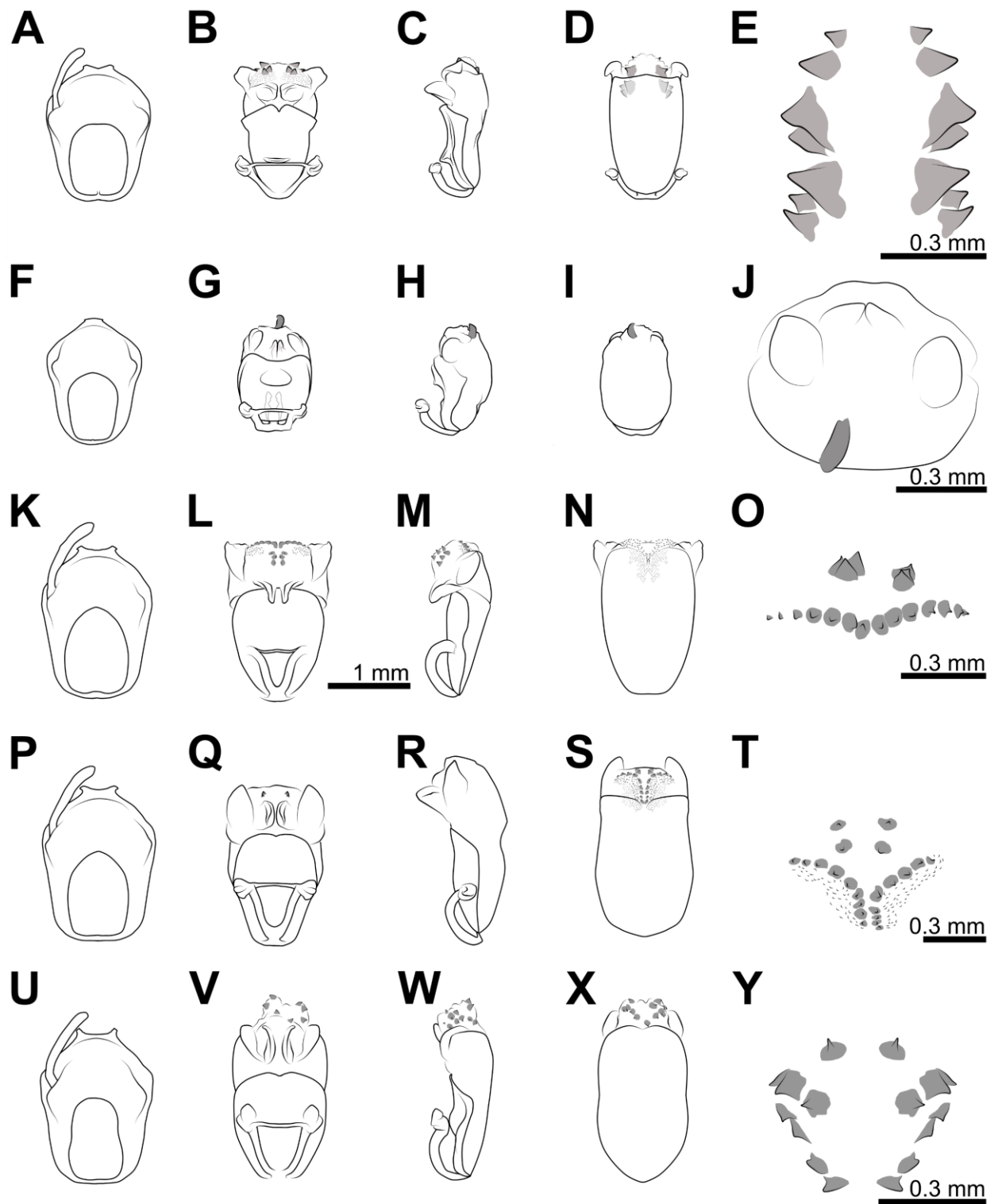


Figure 4.8. Genital morphology of male-based morphospecies of *Biasticus* (cont.). **A–E**, TXL2000-004, ♂, *B. sp.* M13; **F–J**, HEM-TH-2000-004, ♂, *B. sp.* M16; **K–O**, LA-Redu-2004-008, ♂, *B. sp.* M19; **P–T**, VN-Hem-1997-001, ♂, *B. sp.* M20; **U–Y**, La-Redu-2004-015, ♂, *B. sp.* M21. **A, F, K, P, U**, pygophore in dorsal view; **B, G, L, Q, V**, phallus in dorsal view; **C, H, M, R, W**, phallus in lateral view; **D, I, N, S, X**, phallus in ventral view; **E, J, P, T, Y**, distal dorsal lobe of endosoma (ddl).

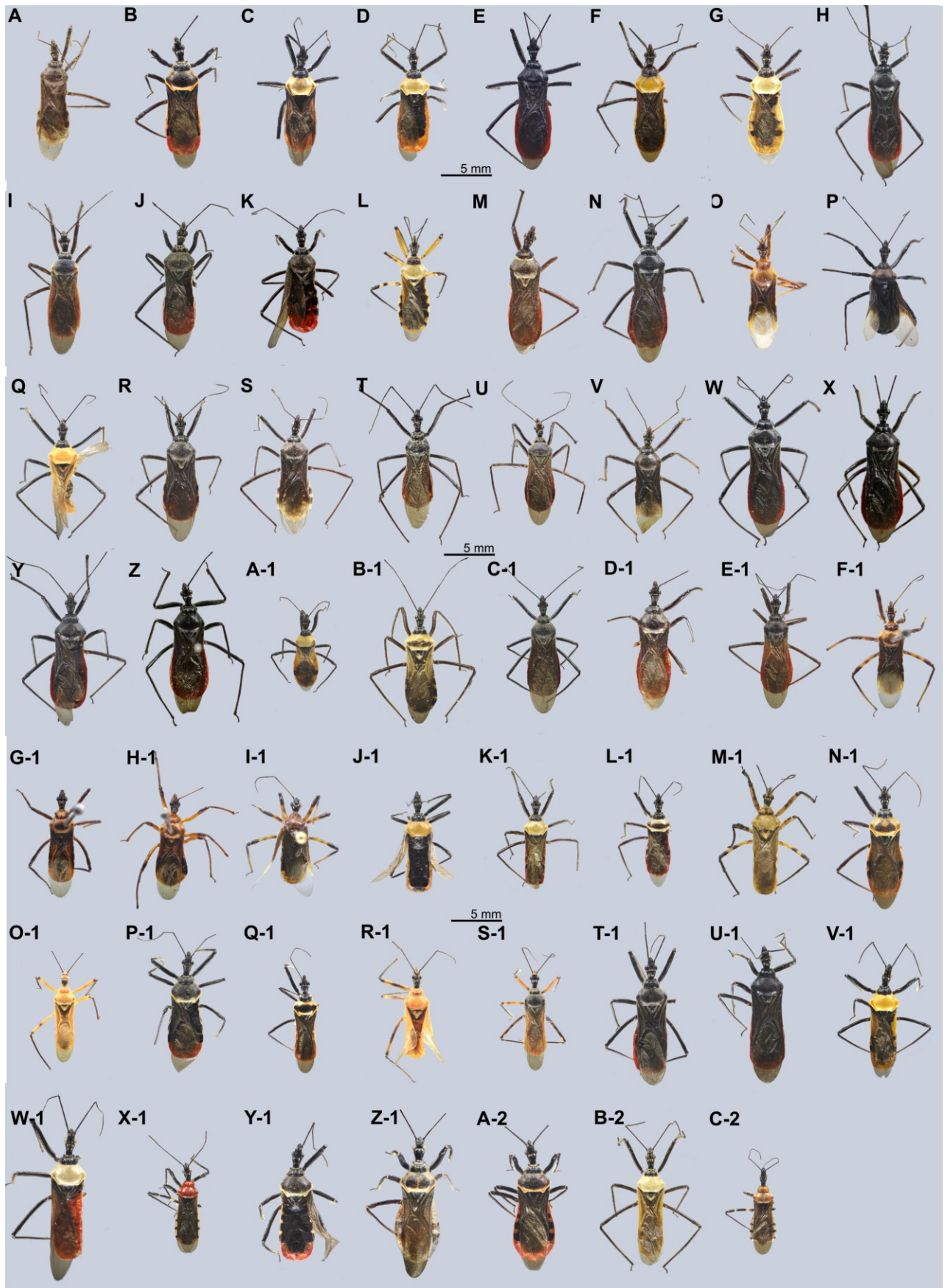


Figure 4.9. Body in dorsal view of female-based morphospecies. **A**, TXL2004-002, ♀, *Biasticus* sp. F1; **B**, TXL2017-839, ♀, *B. sp.* F2; **C**, TXL2018-067, ♀, *B. sp.* F3; **D**, HNL2019-061, ♀, *B. sp.* F4; **E**, VN-Hem-1998-003, ♀, *B. sp.* F5; **F**, TW-Redu-2014-001, ♀, *B. sp.* F6; **G**, HNL2019-092, ♀, *B. sp.* F7; **H**, TXL2019-012, ♀, *B. sp.* F8; **I**, VN-Hem-2011-010, ♀, *B. sp.* F9; **J**, HNL2018-073, ♀, *B. sp.* F10; **K**, HNL2018-038, ♀, *B. sp.* F11; **L**, HNL2018-024, ♀, *B. sp.* F12; **M**, TXL2018-077, ♀, *B. sp.* F13; **N**, VN-Hem-1998-008, ♀, *B. sp.* F14; **O**, ZRC.HEM.50, ♀, *B. sp.* F15; **P**, ZRC.ENT00012353, ♀, *B. sp.* F16; **Q**, AD2020-001, ♀, *B. sp.* F18; **R**, HEM-TH-2000-001, ♀, *B. sp.* F19; **S**, VN-Hem-2004-001, ♀, *B. sp.* F20; **T**, MMR-Hem-1987-001, ♀, *B. sp.* F21; **U**, HEM-TH-2002-005, ♀, *B. sp.* F22; **V**, HEM-TH-2004-023, ♀, *B. sp.* F23; **W**, La-Redu-2004-012, ♀, *B. sp.* F24; **X**, VN-Hem-1997-002, ♀, *B. sp.* F25; **Y**, VN-Hem-2000-008, ♀, *B. sp.* F26; **Z**, VN-Hem-1999-001, ♀, *B. sp.* F27; **A-1**, HEM-TH-2002-004, ♀, *B. sp.* F28; **B-1**, HEM-TH-2000-002, ♀, *B. sp.* F29; **C-1**, VN-Hem-2011-002, ♀, *B. sp.* F30; **D-1**, LA-Redu-2010-001, ♀, *B. sp.* F31; **E-1**, VN-Hem-1998-012, ♀, *B. sp.* F32; **F-1**, ZRC.HEM.55, ♀, *B. sp.* F34; **G-1**, ZRC.HEM.49, ♀, *B. sp.* F35; **H-1**, ZRC.HEM.218, ♀, *B. sp.* F36; **I-1**, ZRC.ENT00012352, ♀, *B. sp.* F37; **J-1**, HNL2018-117, ♀, *B. sp.* F38; **K-1**, HEM-TH2004-022, ♀, *B. sp.* F39; **L-1**, TXL BX2, ♀, *B. sp.* F40; **M-1**, HEM-TH-2004-020, ♀, *B. sp.* F41; **N-1**, TXL BX18, ♀, *B. sp.* F42; **O-1**, TXL2016-547, ♀, *B. sp.* F43; **P-1**, NDD2022-062, ♀, *B. sp.* F44; **Q-1**, NDD2022-014, ♀, *B. sp.* F45; **R-1**, NDD2022-017, ♀, *B. sp.* F46; **S-1**, NDD2022-005, ♀, *B. sp.* F47; **T-1**, LA-Redu-2008-003, ♀, *B. sp.* F48; **U-1**, VN-HEM-2011-015, ♀, *B. sp.* F49; **V-1**, TXL BX16, ♀, *B. sp.* F50; **W-1**, TXL2021-009, ♀, *B. sp.* F51; **X-1**, LA-Redu-2011-005, ♀, *B. sp.* F54; **Y-1**, HNL2018-008, ♀, *B. sp.* F55; **Z-1**, TXL2016-558, ♀, *B. sp.* F56; **A-2**, TXL2016-671, ♀, *B. sp.* F57; **B-2**, HEM-TH2004-017, ♀, *B. sp.* F58; **C-2**, TXL2002-064, ♀, *B. sp.* F59.

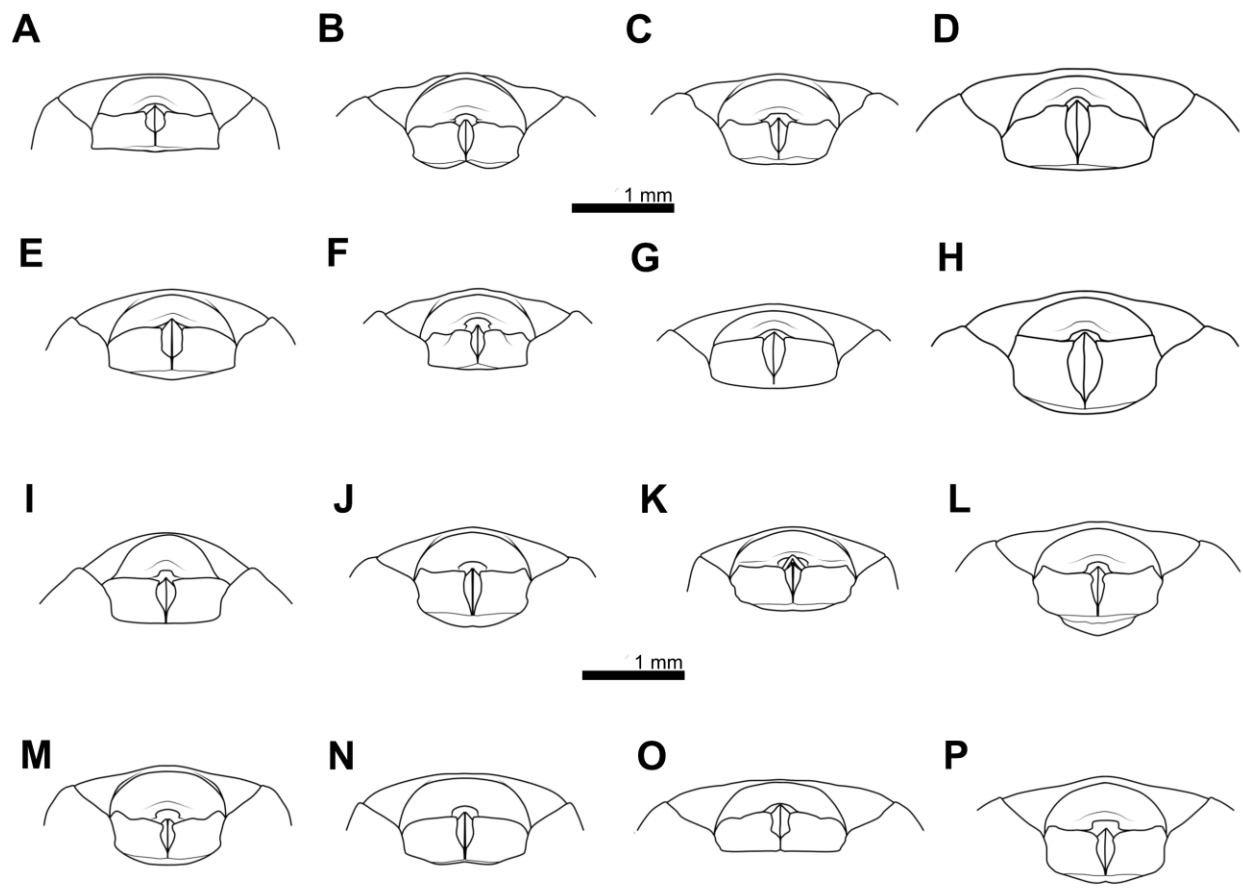


Figure 4.10. Genital morphology of female-based morphospecies. **A–P**, female genitalia in ventral view. **A**, TXL2016-670, ♀, *B. sp.* F2; **B**, TXL2018-067, ♀, *B. sp.* F3; **C**, HNL2019-061, ♀, *B. sp.* F4; **D**, VN-Hem-1998-003, ♀, *B. sp.* F5; **E**, TW-Redu-2014-001, ♀, *B. sp.* F6; **F**, HNL2019-092, ♀, *B. sp.* F7; **G**, TXL2019-012, ♀, *B. sp.* F8; **H**, VN-Hem-1998-004, ♀, *B. sp.* F14; **I**, VN-Hem-2004-001, ♀, *B. sp.* F20; **J**, TXL2018-117, ♀, *B. sp.* F38; **K**, HEM-TH2004-022, ♀, *B. sp.* F39; **L**, NDD2022-062, ♀, *B. sp.* F44; **M**, NDD2022-014, ♀, *B. sp.* F45; **N**, TXLBX16, ♀, *B. sp.* F50; **O**, TXL2018-008, ♀, *B. sp.* F55; **P**, TXL2016-671, ♀, *B. sp.* F57.

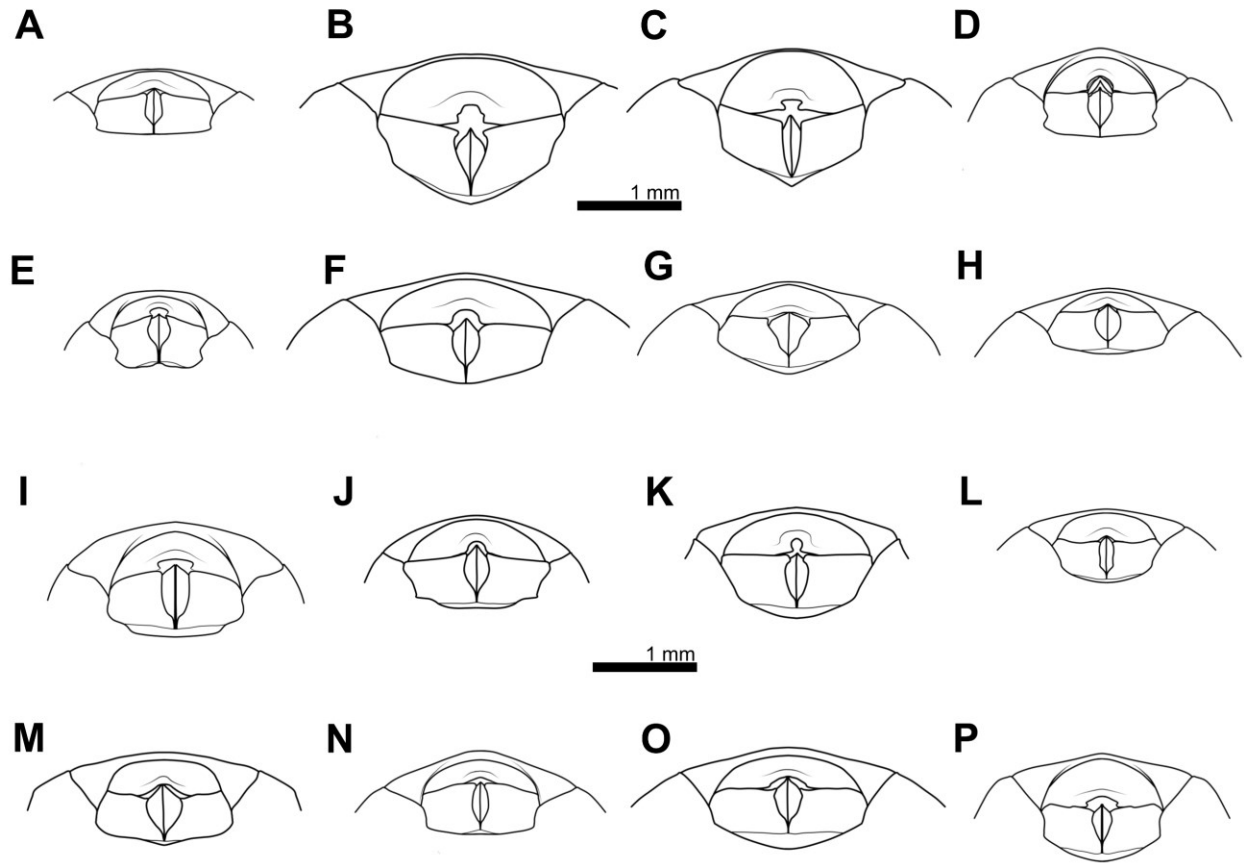


Figure 4.11. Genital morphology of female-based morphospecies (cont). **A–P**, female genitalia in ventral view. **A**, TXL2019-700, ♀, *B. sp.* F9; **B**, HNL2018-073, ♀, *B. sp.* F10; **C**, HNL2018-038, ♀, *B. sp.* F11; **D**, HNL2018-024, ♀, *B. sp.* F12; **E**, AD2022-001, ♀, *B. sp.* F18; **F**, HEM-TH-2000-001, ♀, *B. sp.* F19; **G**, HEM-TH-2002-005, ♀, *B. sp.* F22; **H**, VN-Hem-1998-012, ♀, *B. sp.* F32; **I**, HEM-TH-2004-020, ♀, *B. sp.* F41; **J**, TXL2016-547, ♀, *B. sp.* F43; **K**, NDD2022-017, ♀, *B. sp.* F46; **L**, NDD2022-005, ♀, *B. sp.* F47; **M**, LA-Redu-2011-005, ♀, *B. sp.* F54; **N**, TXL2018-077, ♀, *B. sp.* F13; **O**, ZRC.HEM.50, ♀, *B. sp.* F15; **P**, TW-Redu-1980-001, ♀, *B. sp.* F17.

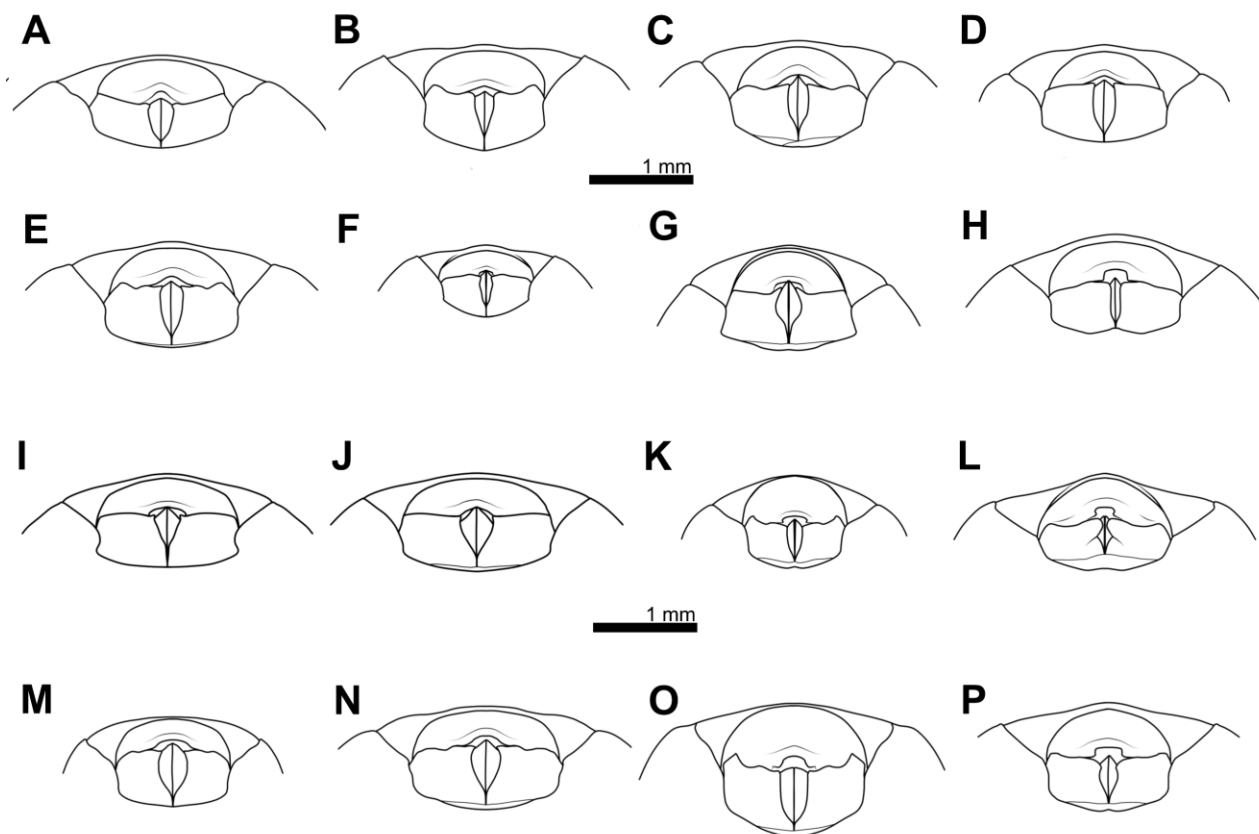


Figure 4.12. Genital morphology of female-based morphospecies (cont). **A–P**, female genitalia in ventral view. **A**, MMR-Hem-1987-001, ♀, *B. sp.* F21; **B**, La-Redu-2004-012, ♀, *B. sp.* F24; **C**, VN-Hem-1997-002, ♀, *B. sp.* F25; **D**, VN-Hem-2000-007, ♀, *B. sp.* F26; **E**, VN-Hem-1999-001, ♀, *B. sp.* F27; **F**, HEM-TH-2002-004, ♀, *B. sp.* F28; **G**, HEM-TH-2000-002, ♀, *B. sp.* F29; **H**, LA-Redu-2010-001, ♀, *B. sp.* F31; **I**, ZRC.HEM.55, ♀, *B. sp.* F34; **J**, ZRC.ENT00012352, ♀, *B. sp.* F37; **K**, TXLBX2, ♀, *B. sp.* F40; **L**, TXLBX18, ♀, *B. sp.* F42; **M**, LA-Redu-2008-002, ♀, *B. sp.* F48; **N**, VN-HEM-2011-015, ♀, *B. sp.* F49; **O**, TXL2021-009, ♀, *B. sp.* F51; **P**, TXLBX19, ♀, *B. sp.* F52.

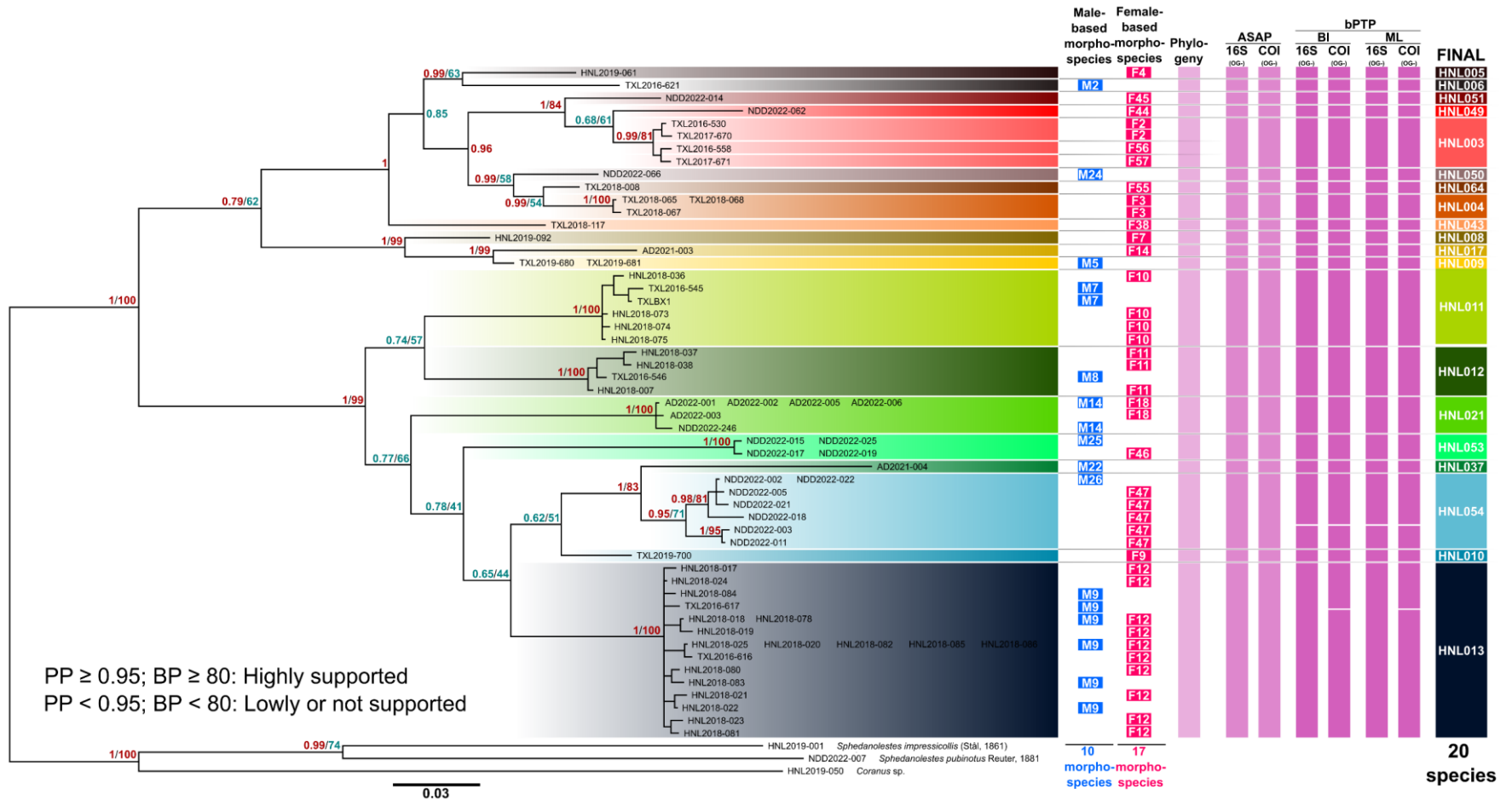


Figure 4.13. Bayesian inference phylogenetic trees based on the concatenated 16S + COI dataset (1085 bp) of the genus *Biasticus*. Supports by posterior probability (PP) and bootstrap value (BP in %) are indicated behind each node. In which red is indicated for a high supporting value (PP \geq 0.95; BP \geq 80) and blue is indicated for a low supporting value (PP < 0.95; BP < 80).

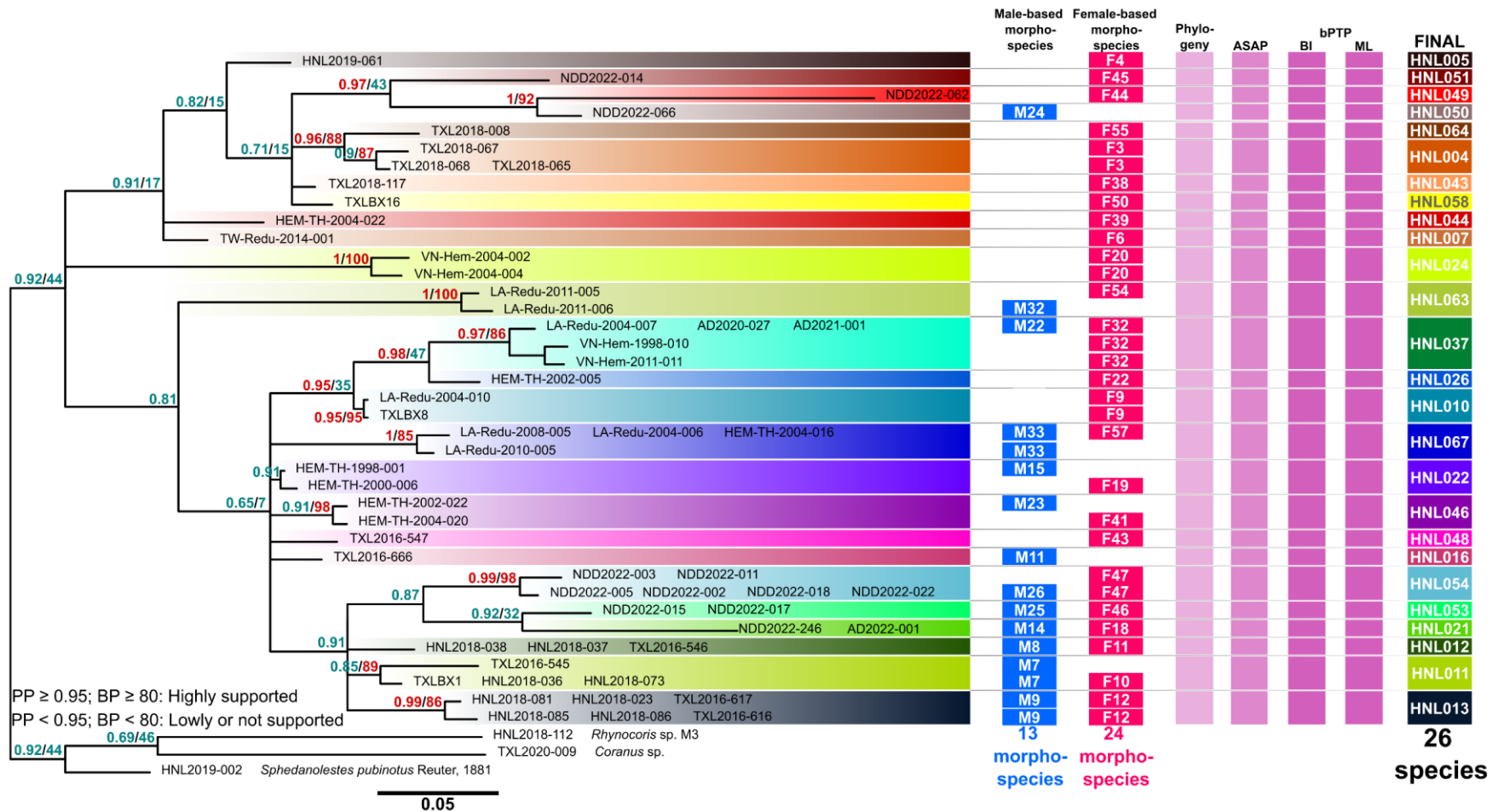


Figure 4.14. Bayesian inference phylogenetic trees based on the Uni-Minibar dataset (177 bp) of the genus *Biasticus*. Supports by posterior probability (PP) and bootstrap value (BP in %) are indicated behind each node. In which, red is indicated for high supporting value (PP \geq 0.95; BP \geq 80), blue is indicated for low supporting value (PP < 0.95; BP < 80).

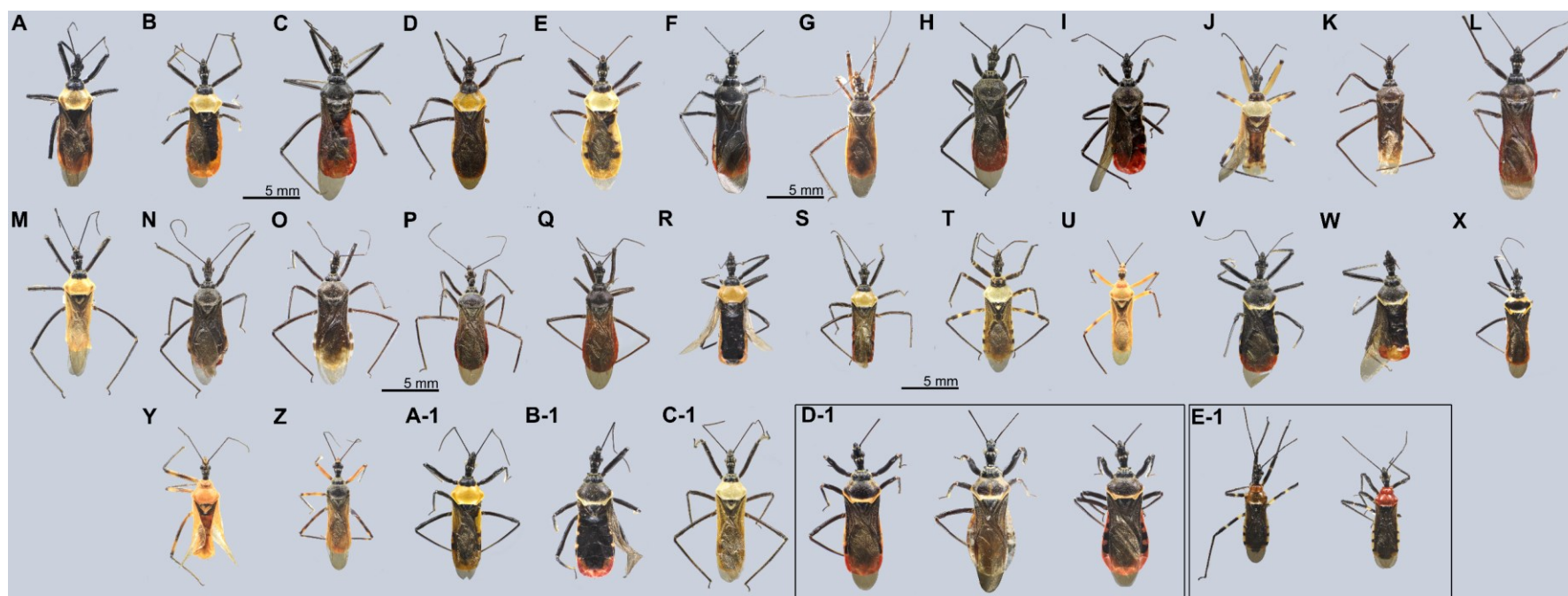


Figure 4.15. Body in dorsal view of fully-recognized species. **A**, *Biasticus* sp. HNL004, TXL2018-067, ♀; **B**, *B.* sp. HNL005, HNL2019-061, ♀; **C**, *B.* sp. HNL006, TXL2016-621, ♂; **D**, *B.* sp. HNL007, TW-Redu-2014-001, ♀; **E**, *B.* sp. HNL008, HNL2019-092, ♀; **F**, *B.* sp. HNL009, TXL2019-680, ♂; **G**, *B.* sp. HNL010, VN-Hem-2011-017, ♂; **H**, *B.* sp. HNL011, HNL2018-073, ♀; **I**, *B.* sp. HNL012, HNL2018-038, ♀; **J**, *B.* sp. HNL013, HNL2018-025, ♂; **K**, *B.* sp. HNL016, TXL2017-666, ♂; **L**, *B.* sp. HNL017, TXL2018-843, ♂; **M**, *B.* sp. HNL021, AD2022-005, ♂; **N**, *B.* sp. HNL022, HEM-TH-2002-003, ♂; **O**, *B.* sp. HNL024, VN-Hem-2004-001, ♀; **P**, *B.* sp. HNL026, HEM-TH-2002-005, ♀; **Q**, *B.* sp. HNL037, VN-Hem-1998-012, ♀; **R**, *B.* sp. HNL043, HNL2018-117, ♀; **S**, *B.* sp. HNL044, HEM-TH2004-022, ♀; **T**, *B.* sp. HNL046, HEM-TH-2002-022, ♂; **U**, *B.* sp. HNL048, TXL2016-547, ♀; **V**, *B.* sp. HNL049, NDD2022-062, ♀; **W**, *B.* sp. HNL050, NDD2022-066, ♂; **X**, *B.* sp. HNL051, NDD2022-014, ♀; **Y**, *B.* sp. HNL053, NDD2022-015, ♂; **Z**, *B.* sp. HNL054, NDD2022-005, ♀; **A-1**, *B.* sp. HNL058, TXL BX16, ♀; **B-1**, *B.* sp. HNL064, HNL2018-008, ♀; **C-1**, *B.* sp. HNL067, HEM-TH2004-018, ♂; **D-1**, *B.* sp. HNL003, TXL2016-670, TXL2016-558, TXL2016-671, ♀; **E-1**, *B.* sp. HNL063, LA-Redu-2011-006, ♂, TXL2002-064, ♀.

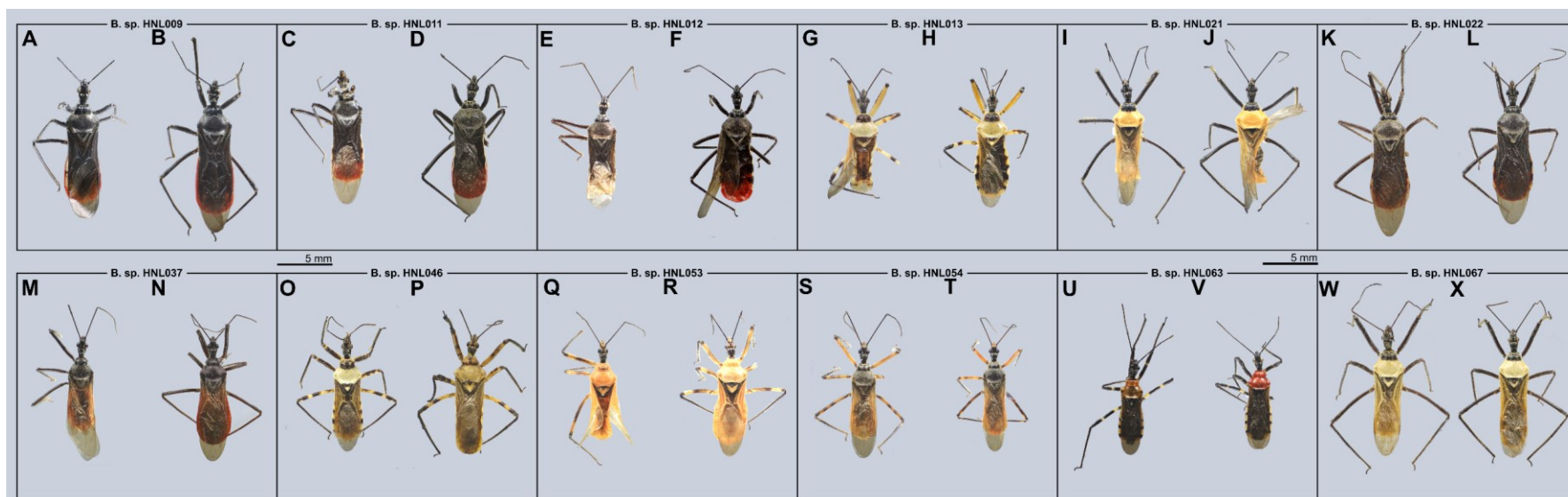


Figure 4.16. Conspecific male-female combinations. **A, B**, *Biastiscus* sp. HNL009; **C, D**, *B. sp.* HNL011; **E, F**, *B. sp.* HNL012; **G, H**, *B. sp.* HNL013; **I, J**, *B. sp.* HNL021; **K, L**, *B. sp.* HNL022; **M, N**, *B. sp.* HNL037; **O, P**, *B. sp.* HNL046; **Q, R**, *B. sp.* HNL053; **S, T**, *B. sp.* HNL054; **U, V**, *B. sp.* HNL063; **W, X**, *B. sp.* HNL067. **A**, *B. sp.* M5, TXL2019-680, ♂; **B**, *B. sp.* F8, VN-HEM-2011-007, ♀; **C**, *B. sp.* M7, TXL2016-545, ♂; **D**, *B. sp.* F10, HNL2018-073, ♀; **E**, *B. sp.* M8, TXL2016-546, ♂; **F**, *B. sp.* F11, HNL2018-038, ♀; **G**, *B. sp.* M9, HNL2018-025, ♂; **H**, *B. sp.* F12, HNL2018-024, ♀; **I**, *B. sp.* M14, AD2022-005, ♂; **J**, *B. sp.* F18, AD2022-001, ♀; **K**, *B. sp.* M15, HEM-TH-2002-003, ♂; **L**, *B. sp.* F19, HEM-TH-2000-001, ♀; **M**, *B. sp.* M22, AD2021-001, ♂; **N**, *B. sp.* F32, VN-Hem-1998-012, ♀; **O**, *B. sp.* M23, HEM-TH-2002-022, ♂; **P**, *B. sp.* F41, HEM-TH-2004-020, ♀; **Q**, *B. sp.* M25, NDD2022-015, ♂; **R**, *B. sp.* F46, NDD2022-017, ♀; **S**, *B. sp.* M26, NDD2022-022, ♂; **T**, *B. sp.* F47, NDD2022-005, ♀; **U**, *B. sp.* M32, LA-Redu-2011-006, ♂; **V**, *B. sp.* F59, TXL2002-064, ♀; **W**, *B. sp.* M33, HEM-TH2004-018, ♂; **X**, *B. sp.* F58, LA-Redu-2004-011, ♀.

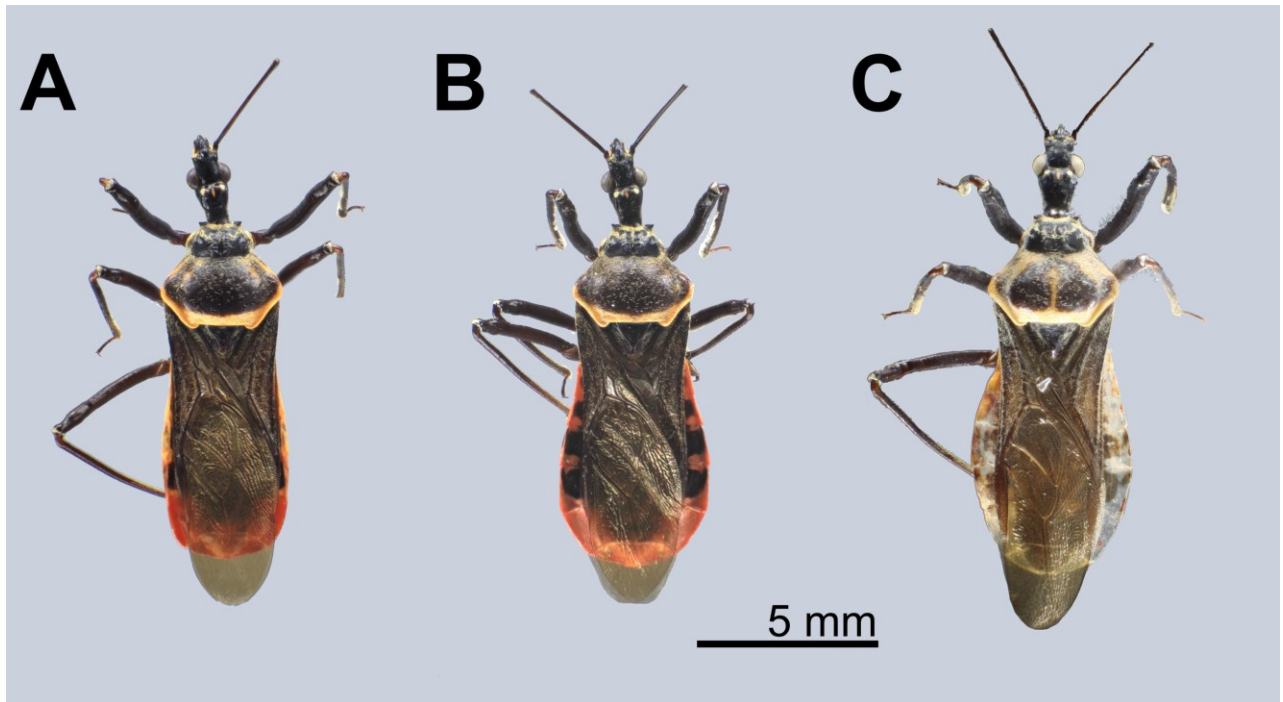


Figure 4.17. Habitus of three morphological forms of *B. sp.* HNL003. **A**, TXL2017-670, ♀, *B. sp.* F2; **B**, TXL2017-671, ♀, *B. sp.* F57; **C**, TXL2016-558, ♀, *B. sp.* F56.

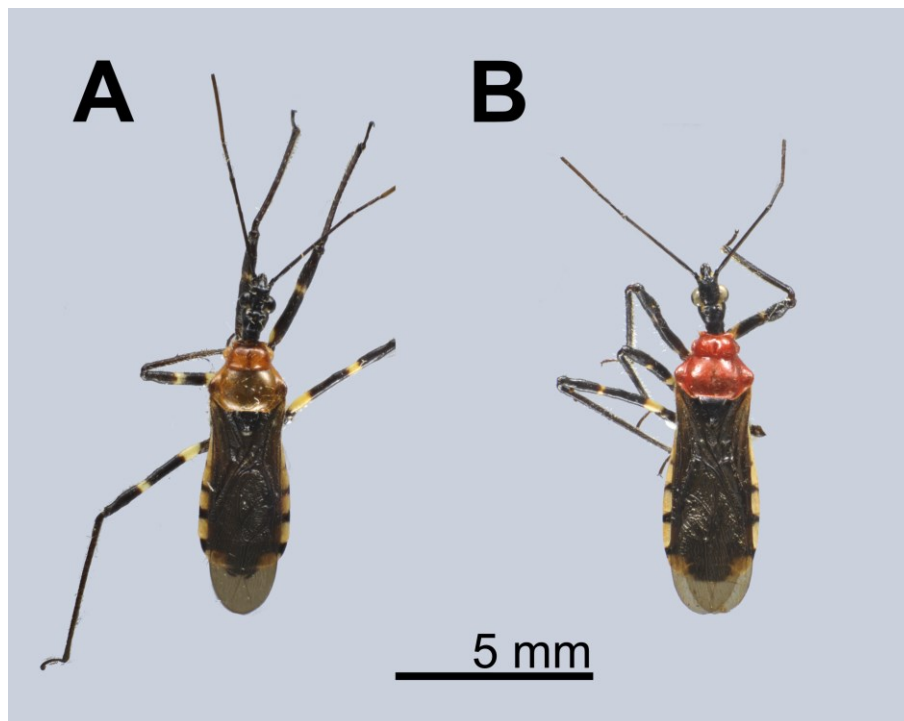


Figure 4.18. Habitus of two morphological form of *B. sp.* HNL063. **A**, LA-Redu-2011-006, ♂, *B. sp.* M32; **B**, LA-Redu-2011-005, ♀, *B. sp.* F54.

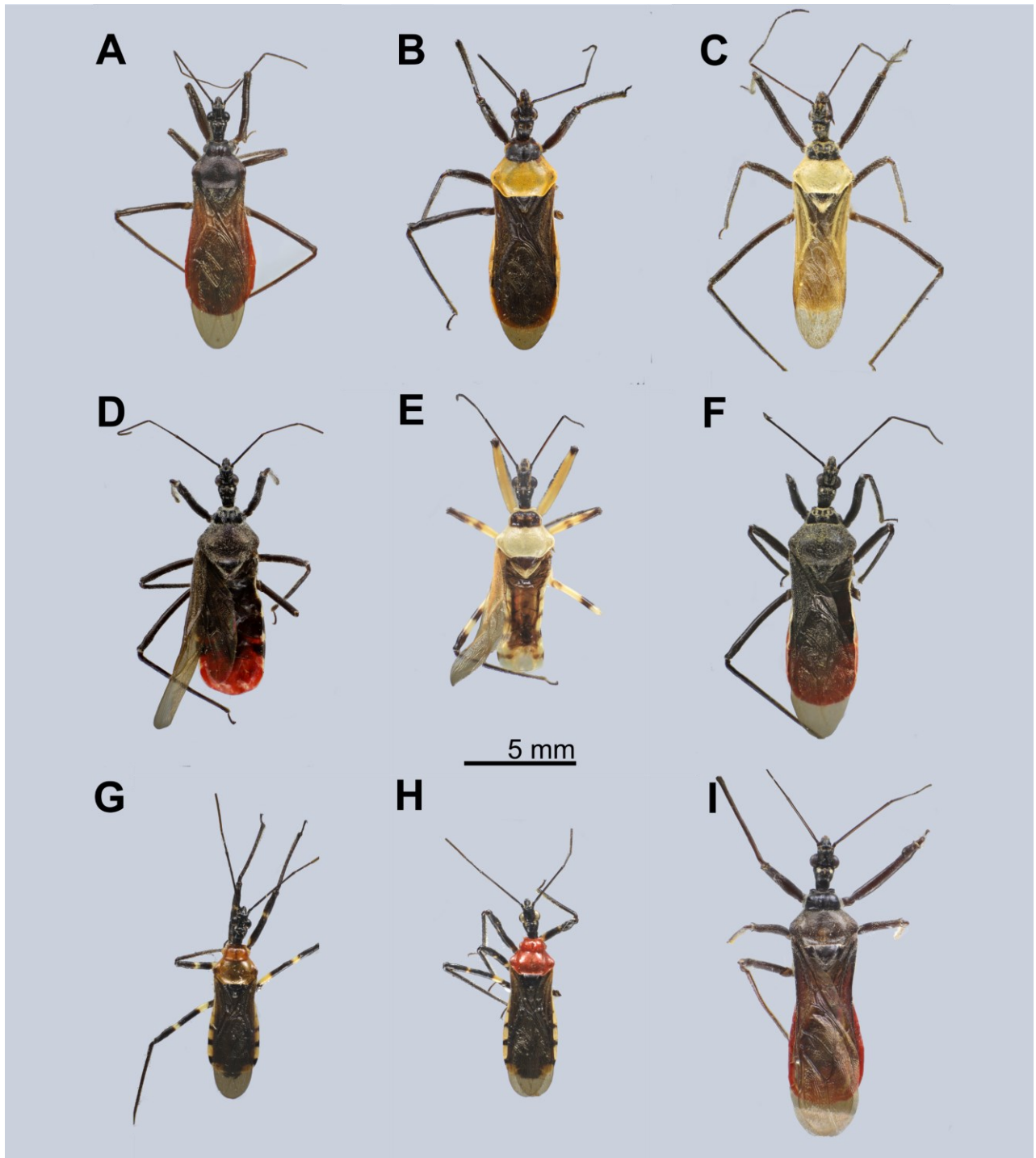


Figure 4.19. Habitus of validly named species recognized in this study. **A**, *Biasticus confusus* Hsiao et al., 1979 (= *B. sp.* HNL037); **B**, *B. flavinotus* (Matsumura, 1913) (= *B. sp.* HNL007); **C**, *B. flavus* (Distant, 1903) (= *B. sp.* HNL067); **D**, *B. griseocapillus* Ha, Truong et Ishikawa, 2022 (= *B. sp.* HNL012); **E**, *B. luteicollis* Ha, Truong et Ishikawa, 2022 (= *B. sp.* HNL013); **F**, *B. taynguyenensis* Ha, Truong et Ishikawa, 2022 (= *B. sp.* HNL011); **G**, **H**, “*Sphedanolestes*” *annulipes* Distant, 1903 (= *B. sp.* HNL063); **I**, “*Sphedanolestes*” *gularis* Hsiao et al., 1979 (= *B. sp.* HNL017).

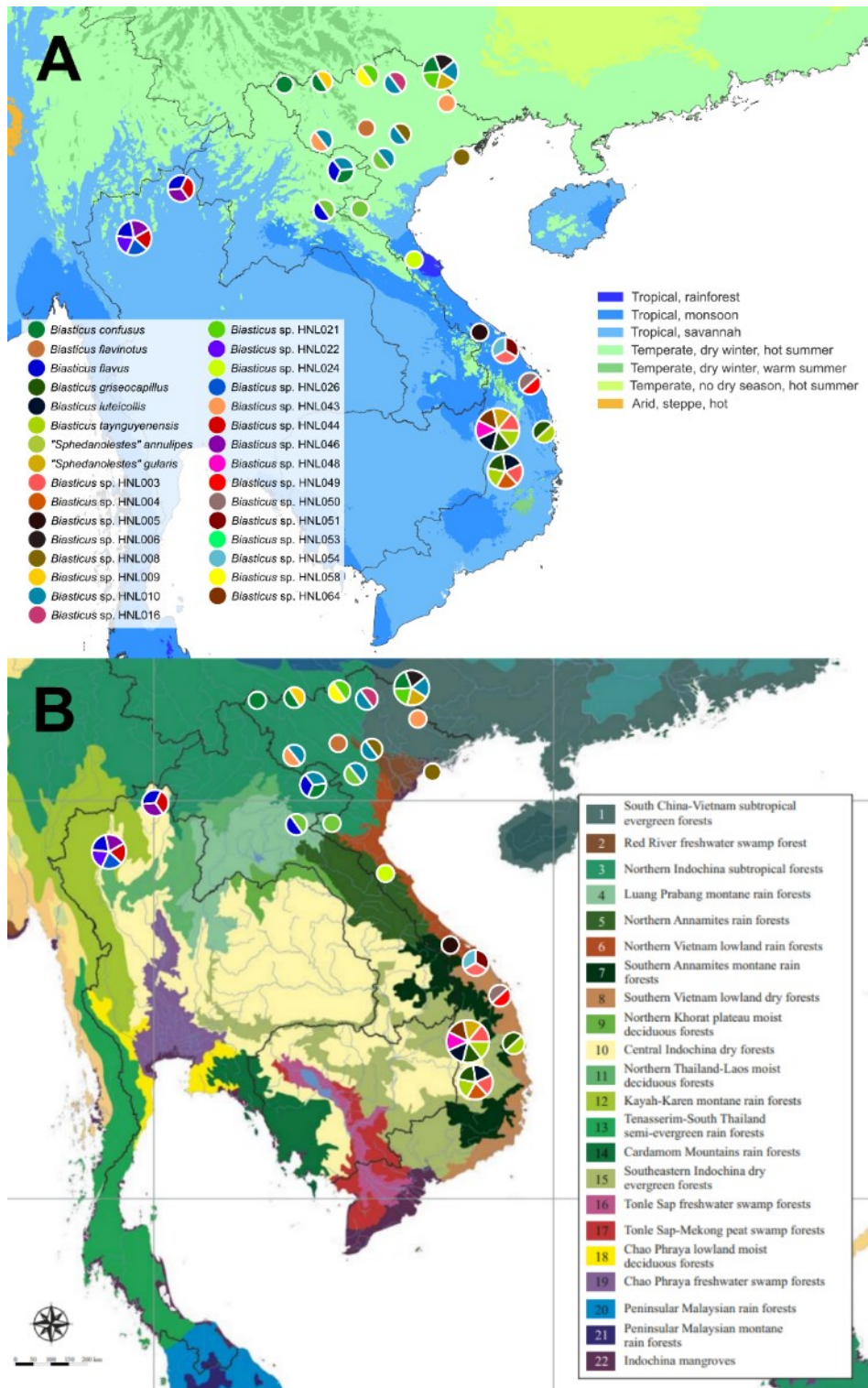


Figure 4.20. Distribution maps of *Biasticus* species in Vietnam and surrounding areas. **A**, combining with climate regions given by Beck et al. (2018); **B**, combining with terrestrial ecoregions given by Poyarkov et al. (2021) following Olson et al. (2001).

Table 4.1. The minimal interspecific distance of *Biasticus* species based on the COI dataset. Upper right diagonal shows the p-distance (%), and the lower left diagonal shows the distance in the K2P model (%). Blue cells indicated the lowest minimal interspecific distance, orange cells indicated the highest minimal interspecific distance.

	<i>B. sp.</i> HNL037	<i>B. sp.</i> HNL012	<i>B. sp.</i> HNL013	<i>B. sp.</i> HNL011	<i>B. sp.</i> HNL017	<i>B. sp.</i> HNL003	<i>B. sp.</i> HNL004	<i>B. sp.</i> HNL005	<i>B. sp.</i> HNL006	<i>B. sp.</i> HNL008	<i>B. sp.</i> HNL009	<i>B. sp.</i> HNL010	<i>B. sp.</i> HNL021	<i>B. sp.</i> HNL043	<i>B. sp.</i> HNL049	<i>B. sp.</i> HNL050	<i>B. sp.</i> HNL053	<i>B. sp.</i> HNL054	<i>B. sp.</i> HNL064
<i>Biasticus confusus</i> (= <i>B. sp.</i> HNL037) (N = 1)		12.9	11.5	10.8	15.9	12.3	14.6	15.0	12.4	13.6	13.1	10.9	11.2	14.1	14.2	15.7	12.2	7.5	14.5
<i>B. griseocapillus</i> (= <i>B. sp.</i> HNL012) (N = 5) (Max K2P = 1.3%; Max p = 1.3%)	14.4		8.9	7.3	12.2	11.5	11.6	12.0	12.3	9.1	7.9	10.7	10.4	12.5	11.9	12.7	8.6	9.4	9.4
<i>B. luteicollis</i> (= <i>B. sp.</i> HNL013) (N = 20) (Max K2P = 1.7%; Max p = 1.7%)	12.6	9.6		8.7	13.3	11.3	11.9	11.2	11.3	10.2	10.6	5.2	9.4	11.9	13.5	12.0	8.7	7.9	11.9
<i>B. taynguyenensis</i> (= <i>B. sp.</i> HNL011) (N = 7) (Max K2P = 0.9%; Max p = 0.9%)	11.7	7.7	9.4		13.3	11.8	11.3	12.2	11.8	10.2	10.4	10.6	9.4	11.9	12.5	13.0	8.7	7.6	11.0
" <i>Sphecanolestes</i> " <i>gularis</i> (= <i>B. sp.</i> HNL017) (N = 1)	18.1	13.4	14.9	14.8		12.7	12.4	12.6	13.2	9.2	5.6	14.0	10.8	13.3	13.2	14.9	14.9	13.1	12.6

<i>B. sp.</i> HNL003 (N = 4) (Max K2P = 1.0%; Max p = 1.0%)	13.5	12.6	12.3	12.9	14.1		9.2	7.2	6.3	10.4	9.1	12.1	11.6	8.6	3.8	9.1	12.2	11.1	8.4
<i>B. sp.</i> HNL004 (N = 3)	16.4	12.9	13.1	12.3	13.7	9.9		5.1	8.3	8.7	8.8	11.6	12.7	6.8	10.3	4.5	12.4	10.1	2.1
<i>B. sp.</i> HNL005 (N = 1)	16.8	13.3	12.3	13.4	14.0	7.6	5.3		6.7	9.2	10.4	11.9	12.7	7.3	10.9	5.8	12.5	10.9	5.0
<i>B. sp.</i> HNL006 (N = 1)	13.6	13.6	12.4	12.9	14.8	6.6	8.9	7.1		11.6	10.7	12.4	11.3	8.1	9.4	8.6	13.9	10.9	7.4
<i>B. sp.</i> HNL008 (N = 1)	15.1	9.8	11.1	11.1	9.9	11.3	9.4	10.0	12.8		5.0	11.4	10.2	9.6	11.7	10.1	11.9	10.6	9.1
<i>B. sp.</i> HNL009 (N = 2) (Identical sequences)	14.6	8.4	11.6	11.3	5.8	9.7	9.5	11.4	11.6	5.2		10.4	9.1	11.1	11.0	11.3	12.2	10.2	9.1
<i>B. sp.</i> HNL010 (N = 1)	11.8	11.7	5.4	11.5	15.8	13.3	12.7	13.1	13.7	12.5	11.3		10.6	13.1	12.5	12.6	10.1	6.2	11.4
<i>B. sp.</i> HNL021 (N = 6) (Max K2P = 0.5% Max p = 0.5%)	12.2	11.4	10.2	10.1	11.8	12.7	14.1	14.1	12.5	11.1	9.7	11.7		12.2	12.7	12.7	9.9	9.1	13.0
<i>B. sp.</i> HNL043 (N = 1)	15.7	13.8	13.0	13.0	14.8	9.3	7.1	7.8	8.7	10.3	12.1	14.5	13.5		9.1	6.9	12.4	11.1	7.3

<i>B. sp.</i> HNL049 (N = 1)	15.8	13.1	14.9	13.7	14.7	3.9	11.1	11.9	10.2	12.8	12.0	13.8	14.0	9.8		8.7	13.3	12.5	10.1
<i>B. sp.</i> HNL050 (N = 1)	17.7	14.0	13.2	14.4	16.9	9.8	4.6	6.1	9.2	10.9	12.4	13.9	14.1	7.4	9.4		13.0	11.9	4.6
<i>B. sp.</i> HNL053 (N = 4) (Max K2P = 0.3%; Max p = 0.3%)	13.5	9.2	9.4	9.3	16.9	13.5	13.7	13.9	15.6	13.1	13.5	11.1	10.8	13.6	14.7	14.5		8.6	12.4
<i>B. sp.</i> HNL054 (N = 7) (Max K2P = 2.4%; Max p = 2.3%)	7.9	10.2	8.4	8.0	14.6	12.1	10.9	11.9	11.9	11.5	11.1	6.5	9.8	12.0	13.7	13.0	9.2		10.1
<i>B. sp.</i> HNL064 (N = 1)	16.2	10.2	13.1	12.0	14.0	9.0	2.2	5.2	7.9	9.8	9.8	12.4	14.5	7.7	10.9	4.8	13.7	10.9	

Table 4.2. Discrimination of *Biasticus* species with results of male-based and female-based morphospecies.

No	Male-based morphospecies	Female-based morphospecies	Final
			Species
		<i>B. sp. F2</i>	
1		<i>B. sp. F56</i>	<i>B. sp. HNL003</i>
		<i>B. sp. F57</i>	
2		<i>B. sp. F3</i>	<i>B. sp. HNL004</i>
3		<i>B. sp. F4</i>	<i>B. sp. HNL005</i>
4	<i>B. sp. M2</i>	<i>B. sp. F5</i>	<i>B. sp. HNL006</i>
5	<i>B. sp. M3</i>	<i>B. sp. F6</i>	<i>B. sp. HNL007</i> (= <i>B. flavinotus</i> (Matsumura, 1913))
6	<i>B. sp. M4</i>	<i>B. sp. F7</i>	<i>B. sp. HNL008</i>
7	<i>B. sp. M5</i>	<i>B. sp. F8</i>	<i>B. sp. HNL009</i>
8	<i>B. sp. M6</i>	<i>B. sp. F9</i>	<i>B. sp. HNL010</i>
9	<i>B. sp. M7</i>	<i>B. sp. F10</i>	<i>B. sp. HNL011</i> (= <i>B. taynguyenensis</i> Ha, Truong & Ishikawa, 2022)
10	<i>B. sp. M8</i>	<i>B. sp. F11</i>	<i>B. sp. HNL012</i> (= <i>B. griseocapillus</i> Ha, Truong & Ishikawa, 2022)
11	<i>B. sp. M9</i>	<i>B. sp. F12</i>	<i>B. sp. HNL013</i> (= <i>B. luteicollis</i> Ha, Truong & Ishikawa, 2022)
12	<i>B. sp. M11</i>		<i>B. sp. HNL016</i>
13	<i>B. sp. M12</i>	<i>B. sp. F14</i>	<i>B. sp. HNL017</i> (= " <i>Sphedanolestes</i> " <i>gularis</i> Hsiao et al., 1979)
14	<i>B. sp. M14</i>	<i>B. sp. F18</i>	<i>B. sp. HNL021</i>
15	<i>B. sp. M15</i>	<i>B. sp. F19</i>	<i>B. sp. HNL022</i>
16		<i>B. sp. F20</i>	<i>B. sp. HNL024</i>
17	<i>B. sp. M18</i>	<i>B. sp. F22</i>	<i>B. sp. HNL026</i>

18	<i>B. sp. M22</i>	<i>B. sp. F32</i>	<i>B. sp. HNL037</i> (= <i>B. confusus</i> Hsiao et al., 1979)
19		<i>B. sp. F38</i>	<i>B. sp. HNL043</i>
20		<i>B. sp. F39</i>	<i>B. sp. HNL044</i>
21	<i>B. sp. M23</i>	<i>B. sp. F41</i>	<i>B. sp. HNL046</i>
22		<i>B. sp. F43</i>	<i>B. sp. HNL048</i>
23		<i>B. sp. F44</i>	<i>B. sp. HNL049</i>
24	<i>B. sp. M24</i>		<i>B. sp. HNL050</i>
25		<i>B. sp. F45</i>	<i>B. sp. HNL051</i>
26	<i>B. sp. M25</i>	<i>B. sp. F46</i>	<i>B. sp. HNL053</i>
27	<i>B. sp. M26</i>	<i>B. sp. F47</i>	<i>B. sp. HNL054</i>
28		<i>B. sp. F50</i>	<i>B. sp. HNL058</i>
29	<i>B. sp. M32</i>	<i>B. sp. F54</i>	<i>B. sp. HNL063</i> (= " <i>Sphedanolestes</i> " <i>annulipes</i> Distant, 1903)
30		<i>B. sp. F55</i>	<i>B. sp. HNL064</i>
31	<i>B. sp. M33</i>	<i>B. sp. F58</i>	<i>B. sp. HNL067</i> (= <i>B. flavus</i> (Distant, 1903))

Appendix: Taxonomic accounts of the genus *Blasticus* found in Vietnam and surrounding areas

1. Fully Recognized and Determined Species

Blasticus confusus Hsiao et al., 1979

(Fig. 4.3S, Fig. 4.6K–O, Fig. 4.9E-1, Fig. 4.11H, Fig. 4.19A; Table 4.1)

Blasticus confusus Hsiao et al., 1979, in Hsiao et al. (1979): 537.

Examined material. Non-type material. 4♂, NSMT-I-He-8263, AD2020-027, AD2021-001, AD2021-004; 7♀, VN-Hem-1998-010, VN-Hem-1998-011, VN-Hem-1998-012, LA-Hem-2004-007, VN-HEM-2011-011, VN-HEM-2011-013, AD2021-002.

Diagnosis. Body shiny black; pronotum dark brown to blackish brown; central disc of scutellum blackish brown, remaining of scutellum dark brown; abdominal mediotergites and sternites luteous to pale sanguineous; connexivum sanguineous; femora and tibiae dark brown to blackish brown.

Distribution. China (Guangdong, Hainan Island); Vietnam (Northern Vietnam); Laos (Houaphan).

Type locality. China (Guangdong, Hainan Island).

Blasticus flavinotus (Matsumura, 1913)

(Figs 4.9F, Fig. 4.10E, Fig. 4.19B; Table 4.1)

Harpactor flavinotum Matsumura, 1913, in Matsumura (1913): 171.

Blasticus minus Hsiao et al., 1979, in Hsiao et al. (1979): 538.

Examined materials. Non-type material. 1♂, HU-TW-1928-001; 2♀, TW-Redu-2014-001, TW-Redu-2019-001.

Diagnosis. Body black; pronotum covered with short bent cream-yellow setae; anterior pronotal lobe black, posterior pronotal lobe luteous; scutellum wholly blackish brown to black; abdominal mediotergites, except lateral margins of mediotergite VII, blackish brown or dark reddish brown, lateral margins of mediotergite VII luteous; abdominal sternites luteous with some blackish brown

or black segmental transverse stripes laterally; connexivum yellow to sanguineous; femora and tibiae black.

Distribution. China (Guangdong, Hainan Island, Yunnan); Taiwan.

Type locality. Taiwan.

***Biasticus flavus* (Distant, 1903)**

(Fig. 4.3D-1, Fig. 4.7K–O, Fig. 4.9B-2, Fig. 4.16W, X, Fig. 4.19C; Table 4.1)

Harpactor flavus Distant, 1903, in Distant (1903a): 206–207.

Examined material. Non-type material. 6♂, LA-Redu-2004-011, LA-Redu-2004-014, HEM-TH2004-016, HEM-TH2004-018, HEM-TH2004-019, LA-Redu-2010-004; 5♀, LA-Redu-2004-006, HEM-TH2004-017, HEM-TH2004-021, LA-Redu-2008-005, LA-Redu-2010-004.

Diagnosis. Body shiny black; pronotum densely covered with long thick yellow erect setae and anterior pronotal lobe blackish brown to black with some rows of short yellow bent setae, posterior pronotal lobe luteous, somewhat anteriorly centrally suffused with blackish brown; scutellum blackish brown to black, except posterior halves of lateral margins and posterior apex luteous; abdominal sternites luteous with some blackish brown or black segmental transverse stripes laterally; connexivum pale luteous to luteous; femora and tibiae blackish brown to black.

Distribution. Hong Kong; Burma; China (Yunnan); Taiwan; Thailand (Chiang Mai, Chiang Rai); Laos (Xieng Khouang, Houaphan); India; Japan; Indonesia (Java); Malaysia.

Type locality. Hong Kong; Burma.

***Biasticus griseocapillus* Ha, Truong et Ishikawa, 2022**

(Fig. 4.3E, Fig. 4.5K–O, Fig. 4.9K, Fig. 4.11C, Fig. 4.16E, F, Fig. 4.19D; Table 4.1)

Biasticus griseocapillus Ha, Truong et Ishikawa, 2022, in Ha et al. (2022): 163–169.

Examined material. Type material. *Holotype*. 1♀, HNL2018-038. ***Paratypes*.** 1♀, HNL2018-037; 1♂, TXL2016-546. **Non-type material.** 1♀, HNL2018-007; 1♂, TXLBX17.

Diagnosis. Body shiny blackish-brown; anterior pronotal lobe black or blackish-brown with some rows of long bent griseous setae; posterior pronotal lobe blackish-brown or brown and densely covered with short bent griseous setae somewhat interspersed with long griseous setae; scutellum black in basal half and dark brown or brown in lateral margin and apical half; abdominal sternites shiny sanguineous; laterotergites II to VI luteous, segmentally suffused with dark brown spots or blackish-brown spots; laterotergite VII sanguineous.

Distribution. Vietnam, Central Highlands (Gia Lai, Dak Lak).

Type locality. Vietnam, Central Highlands, Dak Lak Province, Chu Yang Sin National Park.

***Blasticus luteicollis* Ha, Truong et Ishikawa, 2022**

(Fig. 4.3F, Fig. 4.5P–T, Fig. 4.9L, Fig. 4.11D, Fig. 4.16G, H, Fig. 4.19E; Table 4.1)

Blasticus luteicollis Ha, Truong et Ishikawa, 2022, in Ha et al. (2022): 169–175.

Examined material. Type material. *Holotype*. ♂, HNL2018-025. ***Paratypes*.** 3♂, HNL2018-083, HNL2018-085, HNL2018-086; 4♀, HNL2018-017, HNL2018-020, HNL2018-024, HNL2018-082.

Non-type material. 4♂, TXL2016-617, HNL2018-022, HNL2018-079, HNL2018-084; 8♀, TXL2016-616, HNL2018-018, HNL2018-019, HNL2018-021, HNL2018-023, HNL2018-078, HNL2018-080, HNL2018-081.

Diagnosis. Body shiny luteous; first visible labial segment and base of second visible labial segment luteous; apical 2/3 of second visible labial segment to third visible labial segment yellowish brown or brown; posterior pronotal lobe luteous; scutellum dark brown in basal half and luteous in apical half, with median pale brownish luteous portion; femora luteous with dark brown or yellowish-brown suffusions at apex and sometimes at middle.

Distribution. Vietnam, Central Highlands (Dak Lak, Gia Lai).

Type locality. Vietnam, Central Highlands, Dak Lak Province, Chu Yang Sin National Park.

***Biasticus taynguyenensis* Ha, Truong et Ishikawa, 2022**

(Fig. 4.3D, Fig. 4.5F–J, Fig. 4.9J, Fig. 4.11B, Fig. 4.16C, D, Fig. 4.19F; Table 4.1)

Biasticus taynguyenensis Ha, Truong et Ishikawa, 2022, in Ha et al. (2022): 156–163.

Examined material. Type material. Holotype. ♀, HNL2018-073. **Paratypes.** 1♂, TXL2016-545; 3♀, HNL2018-036, HNL2018-074, HNL2018-075. **Non-type material.** 1♂, TXLBX1; 3♀, HNL2018-072, HNL2018-076, AD2020-002.

Diagnosis. Body shiny blackish-brown; anterior pronotal lobe blackish-brown or black with some rows of short bent cream-yellow setae; posterior pronotal lobe blackish-brown or dark brown, densely covered with short bent cream-yellow setae, interspersed with long erect setae; scutellum black or blackish-brown; abdominal sternites sanguineous; laterotergites II to IV luteous; anterior half of laterotergite V suffused with brown; posterior half of laterotergite V and laterotergites VI and VII sanguineous.

Distribution. Vietnam, Central Highlands (Gia Lai, Dak Lak).

Type locality. Vietnam, Central Highlands, Gia Lai Province, Kon Chu Rang Nature Reserve.

***Biasticus annulipes* (Distant, 1903)**

(Fig. 4.3C-1, Fig. 4.7F–J, Fig. 4.9X-1, Fig. 4.11M, Fig. 4.18; Table 4.1)

Sphedanolestes annulipes Distant, 1903, in Distant (1903a): 75–76.

Examined material. Non-type material. 1♀, LA-Redu-2011-005; 1♂, LA-Redu-2011-006.

Diagnosis. Body shiny blackish-brown; pronotum, prosternum, and anterior and mid coxae sanguineous; scutellum blackish brown or black; femora black with a large luteous suffusion at base

and a smaller suffusion in middle; abdominal sternites pale creamy luteous with marginal areas suffused with tessellate black markings enclosing two series of large luteous spots; connexivum luteous, with anterior margin suffused segmentally with black.

Var. Pronotum, prosternum, anterior and mid coxae brownish yellow, or luteous.

Distribution. China (Yunnan), Burma, Laos (Xieng Khouang), Vietnam.

Type locality. Burma, Karennee, Bhamo.

***Biasticus gularis* (Hsiao et al., 1979)**

(Fig. 4.3I, Fig. 4.4P–T, Fig. 4.19I; Table 4.1)

Sphedanolestes gularis Hsiao et al., 1979, in Hsiao et al., 1979: 535.

Examined material. Non-type material. 1♂, TXL2018-843; 1♂, AD2021-003.

Diagnosis. Body shiny blackish-brown; pronotum and scutellum black or blackish-brown; abdominal sternites sanguineous, reddish-orange, or luteous with a large dark lateral brown or brown suffusion in sternite V and VI; laterotergites sanguineous; coxae, trochanters, femora, and tibia blackish brown or dark brown.

Distribution. Vietnam (Northern Part), China.

Type locality. China.

2. Fully Recognized and Undetermined Species

***Biasticus* sp. HNL003**

(Fig. 4.10A, P, Fig. 4.17; Table 4.1)

Examined material. 5♀, TXL2016-530, TXL2016-558, TXL2016-670, TXL2016-671, TXL2017-839.

Diagnosis. Body shiny blackish-brown; anterior pronotal lobe blackish-brown or black with some

rows of short bent yellow setae; posterior pronotal lobe blackish-brown or dark brown, densely covered with short bent cream-yellow setae; posterior margin, anterolateral margin of posterior pronotal lobe and anterolateral and posterolateral margin of humerus luteous or yellow; anterior and mid acetabulum luteous; scutellum black or blackish-brown; abdominal mediotergites blackish brown or black except mediotergite VIII sanguineous; abdominal sternites II–VI luteous with or without some irregular blackish brown or brown suffusion in each segment; laterotergites II to IV luteous somewhat with blackish brown or brown suffusion segmentally; abdominal sternite VII and laterotergite VII reddish yellow.

Var. posterior pronotal lobe luteous with a large blackish brown suffusion centrally; a longitudinal luteous suffusion in the middle of posterior pronotal lobe; humerus luteous with a blackish brown suffusion in the middle.

Var. posterior pronotal lobe blackish brown with posterior margin luteous.

Unfortunately, the mature male specimen of this morphospecies was unavailable.

Distribution. Vietnam, Central Highland (Gia Lai, Dak Lak).

***Blasticus* sp. HNL004**

(Fig. 4.9C, Fig. 4.10B, Fig. 4.15A, Table 4.1)

Examined material. 3♀, TXL2018-065, TXL2018-067, TXL2018-068.

Diagnosis. Body shiny black; anterior pronotal lobe black or brownish black with some rows of bent pubescence centrally; posterior pronotal lobe pale yellow with long thick erect setae in posterior margin; scutellum black or brownish black except lateral margin dark brown and margin of posterior apex yellowish brown and covered densely with short bent setae except lateral margin of scutellum without setae and posterior apex of scutellum densely covered with short thick erect setae; connexivum and abdominal sternites yellow without transverse stripe.

Unfortunately, the mature male specimen of this morphospecies was unavailable.

Distribution. Vietnam, Central Highland (Dak Lak).

***Blasticus* sp. HNL005**

(Fig. 4.9D, Fig. 4.10C, Fig. 4.15B, Table 4.1)

Examined material. 1♀, HNL2019-061.

Diagnosis. Body shiny black; anterior pronotal lobe black or brownish-black with some rows of bent pubescence centrally; posterior pronotal lobe pale yellow with long thick erect setae in posterior margin; scutellum black and covered densely with short bent setae except lateral margin of scutellum without setae and posterior apex of scutellum densely covered with short bent setae; abdominal mediotergites blackish with marginal area suffused with orange; connexivum and mediotergite VIII orange; abdominal sternites yellow without transverse stripe.

Unfortunately, the mature male specimen of this morphospecies was unavailable.

Distribution. Vietnam, Central Part (Thua Thien - Hue).

***Blasticus* sp. HNL006**

(Fig. 4.3A, Fig. 4.4A–E, Fig. 4.15C, Table 4.1)

Examined material. 1♂, TXL2016-621.

Diagnosis. Body shiny blackish brown; pronotum and scutellum black or blackish-brown; abdominal mediotergite I + II blackish brown; mediotergites III to VI sanguineous with large central blackish brown suffusions; mediotergites VII and VIII sanguineous; abdominal sternites sanguineous or reddish-orange with a large dark lateral brown or brown suffusion in sternites IV, V. and VI; laterotergites sanguineous; coxae, trochanters, femora, and tibia blackish brown or dark brown.

Unfortunately, the mature female specimen of this morphospecies was unavailable.

Distribution. Vietnam, Northern Part (Thanh Hoa).

***Biasticus* sp. HNL008**

(Fig. 4.9G, Fig. 4.10F, Fig. 4.15E, Table 4.1)

Examined material. 1♀, HNL2019-092.

Diagnosis. Body shiny black; anterior pronotal lobe black or brownish black with some rows of bent pubescence centrally; posterior pronotal lobe pale yellow; scutellum blackish brown, paler backward, and covered densely with bent setae except lateral margin of scutellum without setae and posterior apex of scutellum densely covered with short bent setae; lateral margin of scutellum pale luteous and lateral areas of scutellum suffused with pale luteous spot; abdominal mediosternite II blackish brown; mediotergites III to VII luteous with segmentally centrally suffused with blackish brown stripes, especially mediotergites V and VII, blackish brown stripes reach to lateral margin of segments; connexivum and abdominal sternites pale yellow without transverse stripe.

Unfortunately, the mature male specimen of this morphospecies was unavailable.

Distribution. Vietnam, Northern Part (Vinh Phuc).

***Biasticus* sp. HNL009**

(Fig. 4.3B, Fig. 4.4K–O, Fig. 4.9H, Fig. 4.10G, Fig. 4.15F, Table 4.1)

Examined material. 5♂, TXL2019-680, TXL2019-681, TXL2019-011, TXL2019-013, TXL2019-015; 1♀, TXL2019-012.

Diagnosis. Body black; first and second visible labial segment black or brownish black, apical 1/4 of second visible labial segment and third visible labial segment blackish brown or dark reddish brown, tips of first and second labial segments pale luteous; Scape ~ 1.6 × as long as head, ~ 2.4 × as long as pedicel; first and second flagellomeres missing; proportional average length of scape,

pedicel 3.25:1.35; anterior pronotal lobe black or brownish black with some slender erect setae; posterior pronotal lobe blackish brown densely covered with short bent pubescence, and interleaved with long slender erect setae; scutellum blackish brown; abdominal mediotergites I+II dark brown, mediotergites III–VII sanguineous with brown or sometimes darker to dark brown suffusion in center of each segment; abdominal sternites pale luteous; connexivum sanguineous; femora and tibiae blackish brown.

Distribution. Vietnam, Northern Part (Lao Cai).

***Biasticus* sp. HNL010**

(Fig. 4.9I, Fig. 4.11A, Fig. 4.15G, Table 4.1)

Examined material. 1♀, TXL2019-700.

Diagnosis. Body blackish brown; base of first visible labial segment luteous, remaining labium brown and darker toward tip, tips of first and second labial segments pale luteous; anterior pronotal lobe brown or mild blackish brown covered some rows of bent pubescence centrally with very long slender, erect setae; posterior pronotal lobe dark brown, but anterior one-third of humerus blackish brown and the remaining of humerus pale brownish luteous, covered with short bent pubescence and interleaved with long slender, erect setae; scutellum dark brown; abdominal mediotergites I+II dark brown, mediotergite III–VII yellow with brown or sometimes darker to blackish brown suffusion in center of each segment; abdominal sternites and connexivum yellow; femora brown with/without dark brown or blackish brown suffusions at apex and sometimes at middle; tibiae blackish brown.

Unfortunately, the mature male specimen of this morphospecies was unavailable.

Distribution. Vietnam, Northern Part (Vinh Phuc).

***Biasticus* sp. HNL016**

(Fig. 4.3H, Fig. 4.4U–Y, Fig. 4.15K, Table 4.1)

Examined material. 1♂, TXL2017-666.

Diagnosis. Body dark brown; anterior pronotal lobe blackish-brown with some short bent griseous setae; posterior pronotal lobe dark brown, densely covered with short bent griseous setae; scutellum dark brown; abdominal mediotergites dark brown; abdominal sternites pale orange; laterotergites luteous with segmentally suffused with dark brown spots; coxae, trochanters, femora, and tibia dark brown.

Unfortunately, the mature female specimen of this morphospecies was unavailable.

Distribution. Vietnam, Northern Part (Tuyen Quang).

***Biasticus* sp. HNL021**

(Fig. 4.3K, Fig. 4.4A–E, Fig. 4.9Q, Fig. 4.11E, Fig. 4.15M, Table 4.1)

Examined material. 3♂, AD2022-005, AD2022-006, NDD2022-246; 3♀, AD2022-001, AD2022-002, AD2022-003.

Diagnosis. Body shiny black; pronotum densely covered with long thick yellow erect setae and anterior pronotal lobe blackish brown to black with some rows of short yellow bent setae, posterior pronotal lobe luteous, somewhat anteriorly centrally suffused with blackish brown; scutellum blackish brown to black, except posterior halves of lateral margins and posterior apex luteous; abdominal sternites luteous without blackish brown or black segmental transverse stripes laterally; connexivum pale luteous to luteous; femora and tibiae blackish brown to black.

Distribution. Vietnam, Northern Part (Cao Bang, Ha Giang).

***Blasticus* sp. HNL022**

(Fig. 4.3L, Fig. 4.4F–J, Fig. 4.9R, Fig. 4.11F, Fig. 4.15N, Table 4.1)

Examined material. 3♂, HEM-TH-1998-001, HEM-TH-1998-002, HEM-TH-2002-003; 5♀, HEM-TH-2000-001, HEM-TH-2000-006, HEM-TH-2002-002, HEM-TH-2002-006, HEM-TH-2002-007.

Diagnosis. Body dark brown; base of first visible labial segment brown, remaining of labium blackish brown, tips of first and second labial segments bronzy brown; anterior pronotal lobe blackish brown with some rows of short bent setae centrally; posterior pronotal lobe dark brown, densely covered with short bent cream-yellow pubescence interspersed with long slender erect setae; scutellum dark brown; abdominal mediotergites I+II, III–VI brown with irregular blackish brown and dark brown suffusions; mediotergites VII sanguineous with a brown suffusion in median of anterior half; abdominal sternites sanguineous; connexivum pale luteous, laterotergite I+II, III–VI segmentally suffused with dark brown spots; femora dark brown; tibiae brown.

Distribution. Thailand, Northern Part (Chiang Mai).

***Blasticus* sp. HNL024**

(Fig. 4.9S, Fig. 4.10I, Fig. 4.15O, Table 4.1)

Examined material. 4♀, VN-Hem-2004-001, VN-Hem-2004-002, VN-Hem-2004-003, VN-Hem-2004-004.

Diagnosis. Body blackish brown; anterior pronotal lobe blackish-brown with some rows of short bent griseous setae; posterior pronotal lobe dark brown, densely covered with short bent griseous setae, interspersed with long slender setae; scutellum dark brown and densely covered with long slender griseous setae; abdominal mediotergites II to V dark brown; mediotergites VI and VII luteous with a central suffusion of dark brown or brown; abdominal sternites pale orange; laterotergites

luteous with segmentally suffused with dark brown spots; coxae, trochanters, femora, and tibia blackish brown or dark brown.

Unfortunately, the mature male specimen of this morphospecies was unavailable.

Distribution. Thailand, Central Part (Ha Tinh).

***Blasticus* sp. HNL026**

(Fig. 4.9U, Fig. 4.11G, Fig. 4.15P, Table 4.1)

Examined material. 2♀, HEM-TH-2002-005, HEM-TH-2002-008.

Diagnosis. Body blackish-brown; anterior pronotal lobe blackish-brown or black with some rows of short bent cream-yellow setae interleaved with long slender, erect setae; posterior pronotal lobe blackish-brown, rugulose, densely covered with short bent cream-yellow setae, interspersed with long erect setae; scutellum blackish-brown, and densely covered with short bent yellow-cream setae interspersed with long erect setae; abdominal sternites luteous; laterotergites sanguineous; coxae, trochanters, femora, and tibia blackish brown or dark brown.

Unfortunately, the mature male specimen of this morphospecies was unavailable.

Distribution. Thailand, Central Part (Chiang Mai).

***Blasticus* sp. HNL043**

(Fig. 4.9J-1, Fig. 4.10J, Fig. 4.15R, Table 4.1)

Examined material. 1♀, HNL2018-117.

Diagnosis. Body shiny black; anterior pronotal lobe black or brownish black; posterior pronotal lobe yellow; scutellum blackish and lateral margin of scutellum blackish brown; abdominal mediosternites blackish brown; mediotergite VIII blackish brown with posterior margin orange; connexivum brownish yellow or pale orange; abdominal sternites pale yellow with transverse stripe;

abdominal sternite VII luteous with blackish brown horizontal suffusion in sides; legs black or blackish brown.

Unfortunately, the mature male specimen of this morphospecies was unavailable.

Distribution. Vietnam, Northern Part (Lang Son).

***Blasticus* sp. HNL044**

(Fig. 4.9K-1, Fig. 4.10K, Fig. 4.15S, Table 4.1)

Examined material. 2♀, HEM-TH1999-002, HEM-TH2004-022.

Diagnosis. Body shiny black; anterior pronotal lobe black or brownish black with some rows of short bent pubescence; posterior pronotal lobe yellow with some long thick erect setae in posterior margin; scutellum blackish with base blackish brown and covered with short bent pubescence, densely in posterior apex; abdominal mediosternites blackish brown; mediotergite VIII blackish brown with posterior margin orange; connexivum sanguineous with blackish brown suffusion in laterotergites V and VI; abdominal sternites pale yellow with transverse stripes in sternites IV to VI; abdominal sternite VII luteous with blackish brown horizontal suffusion in sides; legs blackish brown.

Unfortunately, the mature male specimen of this morphospecies was unavailable.

Distribution. Thailand, Northern Part (Chiang Mai, Chiang Rai).

***Blasticus* sp. HNL046**

(Fig. 4.3T, Fig. 4.6P–T, Fig. 4.9M-1, Fig. 4.11I, Fig. 4.15T, Table 4.1)

Examined material. 1♂, HEM-TH-2002-022; 1♀, HEM-TH-2004-020.

Diagnosis. Body shiny luteous; first visible labial segment and base of second visible labial segment luteous; apical 2/3 of second visible labial segment to third visible labial segment yellowish brown

or brown; anterior pronotal lobe black with irregular luteous suffusions; posterior pronotal lobe pale luteous; pronotum densely covered with long setae; scutellum dark brown in basal 2/3 and luteous in apical 1/3, with pale brownish luteous intersection; femora luteous with dark brown or yellowish brown suffusions at apex and sometimes at middle.

Distribution. Thailand, Northern Part (Chiang Mai, Chiang Rai).

***Biasticus* sp. HNL048**

(Fig. 4.9O-1, Fig. 4.11J, Fig. 4.15U, Table 4.1)

Examined material. 1♀, TXL2016-547.

Diagnosis. Body shiny turmeric yellow; labium brownish yellow basally, browner and darker to dark brown toward tip; tips of first and second labial segments bronzy brown; anterior pronotal lobe orangish yellow, sometimes with rows of short bent setae; posterior pronotal lobe turmeric yellow with short bent setae; scutellum blackish brown in basal 1/3 and luteous in apical half, with median brown portion and densely covered with short bent setae; connexivum turmeric yellow coated densely with short bent setae; abdominal sternites luteous and coated densely with short bent setae; yellow or turmeric yellow with dark brown or suffusion medially and blackish brown apically; tibiae blackish brown.

Unfortunately, the mature male specimen of this morphospecies was unavailable.

Distribution. Vietnam, Central Highlands (Gia Lai).

***Biasticus* sp. HNL049**

(Fig. 4.9P-1, Fig. 4.11L, Fig. 4.15V, Table 4.1)

Examined material. 1♀, NDD2022-062.

Diagnosis. Body shiny blackish-brown; anterior pronotal lobe blackish-brown or black with some

rows of short bent yellow setae; posterior pronotal lobe blackish brown with posterior margin luteous and densely covered by short yellow bent setae, posteriorly interspersed with long thick erect setae; anterior and mid acetabulum luteous; scutellum black and covered with short bent yellow setae, especially dense at posterior apex; abdominal mediotergites blackish brown or black except mediotergite VIII sanguineous with dark brown suffusion centrally; abdominal sternites II–VI luteous with transverse blackish brown or black stripe in each segment; sternite VII luteous without transverse stripe; laterotergites II to VI luteous with blackish brown suffusion segmentally; laterotergite VII reddish yellow or sanguineous; coxae, trochanters, femora and tibiae blackish brown.

Unfortunately, the mature male specimen of this morphospecies was unavailable.

Distribution. Vietnam, South Central Coast (Binh Dinh).

***Blasticus* sp. HNL050**

(Fig. 4.3U, Fig. 4.4U–Y, Fig. 4.15W, Table 4.1)

Examined material. 1♂, NDD2022-066.

Diagnosis. Body shiny blackish-brown; anterior pronotal lobe blackish-brown or black with some rows of short bent yellow setae; posterior pronotal lobe blackish brown with posterior margin luteous and densely covered by short yellow bent setae, posteriorly interspersed with long thick erect setae; anterior and mid acetabulum luteous; scutellum black and covered with bent yellow setae interleaved with long slender setae, especially dense at posterior apex; abdominal mediotergites blackish brown or black except mediotergites VII and VIII sanguineous with reddish yellow suffusion centrally; abdominal sternites II–VI luteous with transverse blackish brown or black stripe in each segment; sternite VII orange without transverse stripe; laterotergites II to VI luteous with blackish brown suffusion segmentally; laterotergite VII reddish yellow or sanguineous; coxae, trochanters, femora

and tibiae blackish brown.

Unfortunately, the mature female specimen of this morphospecies was unavailable.

Distribution. Vietnam, South Central Coast (Binh Dinh).

***Blasticus* sp. HNL051**

(Fig. 4.9Q-1, Fig. 4.10M, Fig. 4.15X, Table 4.1)

Examined material. 1♀, NDD2022-014.

Diagnosis. Body shiny black; anterior pronotal lobe black; posterior pronotal lobe yellow with a large horizontal blackish brown suffusion in the central; scutellum blackish; abdominal mediosternites blackish brown; mediotergite VIII blackish brown with posterior margin orange; connexivum pale orange; abdominal sternites pale yellow with thin segmental horizontal stripes in lateral areas of sternites IV to VI; legs black or blackish brown.

Unfortunately, the mature male specimen of this morphospecies was unavailable.

Distribution. Vietnam, South Central Coast (Quang Nam).

***Blasticus* sp. HNL053**

(Fig. 4.3V, Fig. 4.6U–Y, Fig. 4.9R-1, Fig. 4.11K, Fig. 4.15Y, Table 4.1)

Examined material. 3♂, NDD2022-015, NDD2022-020, NDD2022-025; 2♀, NDD2022-017, NDD2022-019.

Diagnosis. Body shiny turmeric yellow; labium brownish yellow basally, browner and darker to dark brown toward tip; tips of first and second labial segments bronzy brown; anterior pronotal lobe brownish yellow, sometimes with or without brown suffusion centrally and centrally with rows of short bent setae; posterior pronotal lobe turmeric yellow with very short bent and erect setae; scutellum blackish brown in basal 1/3 and orangish yellow or turmeric yellow in apical half, with

median luteous portion and densely covered with short bent setae, especially in the central triangular, slopes, and posterior apex; abdominal mediotergites orangish brown sometimes with irregular dark brown suffusion; connexivum and abdominal sternites orangish brown or yellowish brown and coated densely with short bent setae; femora brown or slightly dark brown, with dark brown or suffusion medially and blackish brown apically; tibiae blackish brown.

Distribution. Vietnam, South Central Coast (Quang Nam).

***Biasticus* sp. HNL054**

(Fig. 4.3W, Fig. 4.6A–E, Fig. 4.9S-1, Fig. 4.11L, Fig. 4.15Z, Table 4.1)

Examined material. 1♂, NDD2022-022; 6♀, NDD2022-002, NDD2022-003, NDD2022-005, NDD2022-011, NDD2022-018, NDD2022-021.

Diagnosis. Body blackish brown; first visible labial segment brownish yellow and browner posteriorly, remaining of labium blackish brown, tips of first and second labial segments pale luteous; anterior pronotal lobe blackish brown covered centrally with some rows of bent pubescence interleaved with very long slender erect setae; posterior pronotal lobe dark brown but lateral apex luteous or dark luteous, densely covered with short bent cream-yellow pubescence, somewhat interleaved with long slender erect setae; scutellum dark brown except posterior apex with a small yellow suffusion, with long bent slender setae with long thick erect setae; abdominal mediotergites I+II dark brown or blackish brown, mediotergite III–V yellow or orangish yellow with yellowish brown or sometimes darker to blackish brown suffusion centrally, mediotergites VI–VII and connexivum orangish yellow; abdominal sternites luteous; connexivum yellow; femora brownish yellow with/without dark brown or blackish brown suffusions at apex and sometimes at middle; tibiae blackish brown with small brown or dark brown spots basally.

Distribution. Vietnam, South Central Coast (Quang Nam).

***Blasticus* sp. HNL058**

(Fig. 4.9V-1, Fig. 4.10N, Fig. 4.15A-1, Table 4.1)

Examined material. 1♀, TXLBX16.

Diagnosis. Body shiny black; anterior pronotal lobe black; posterior pronotal lobe yellow; scutellum blackish with small luteous suffusion in lateral margin; abdominal mediosternites blackish brown; mediotergites III, IV with lateral margin areas suffused with yellow; mediotergite VII with yellow posterior and lateral margins; mediotergites V and VI with yellow lateral margin; mediotergite VIII yellow; connexivum yellow with blackish brown suffusions in laterotergites V and VI; abdominal sternites pale yellow; legs black or blackish brown.

Unfortunately, the mature male specimen of this morphospecies was unavailable.

Distribution. Vietnam, Northern Part (Ha Giang).

***Blasticus* sp. HNL064**

(Fig. 4.9Y-1, Fig. 4.10O, Fig. 4.15B-1, Table 4.1)

Examined material. 1♀, TXL2018-008.

Diagnosis. Body shiny blackish-brown; anterior pronotal lobe black with some rows of short bent yellow setae; posterior pronotal lobe blackish brown with posterior margin luteous and densely covered by short yellow bent setae, posteriorly interspersed with long thick erect setae; anterior and mid acetabulum luteous; scutellum black and covered with short bent yellow setae, especially dense at posterior apex; abdominal mediotergites blackish brown or black except mediotergite VII orange with dark brown suffusion centrally and mediotergite VIII reddish-orange or sanguineous; abdominal sternites luteous; sternites IV–VI with lateral blackish brown or black stripe in each segment; laterotergites II–V luteous; laterotergites VI to posterior apex of abdomen sanguineous or reddish-orange; laterotergites V and VI with blackish brown suffusion segmentally; coxae,

trochanters, femora and tibiae blackish brown.

Unfortunately, the mature male specimen of this morphospecies was unavailable.

Distribution. Vietnam, Central Highlands (Gia Lai).

3. Morphospecies Species not yet confirmed by the Integrative Taxonomy

3.1. Male-based morphospecies

Blasticus sp. M4

(Fig. 4.4F–J, Table 4.1)

Examined material. 1♂, TXL2003-005.

Diagnosis. Body shiny black; anterior pronotal lobe black or brownish black with some rows of bent pubescence centrally; posterior pronotal lobe pale yellow; scutellum blackish brown, paler backward, and covered densely with bent setae except lateral margin of scutellum without setae and posterior apex of scutellum densely covered with short bent setae; lateral margin of scutellum pale luteous and lateral areas of scutellum suffused with pale luteous spot; abdominal mediosternite II blackish brown; mediotergites III to VII luteous with segmentally centrally suffused with blackish brown stripes, especially mediotergites V and VII, blackish brown stripes reach to lateral margin of segments; connexivum and abdominal sternites pale yellow without transverse stripe.

Distribution. Vietnam, Northern Part (Hai Phong, Cat Ba NP).

Blasticus sp. M6

(Fig. 4.3C, Fig. 4.5A–E, Table 4.1)

Examined material. 1♂, NSMT-I-He-8268; 1♂, TXL2004-003; 2♂, VN-Hem-2011-017, VN-Hem-2011-019.

Diagnosis. Body blackish brown; base of first visible labial segment luteous, remaining labium brown and darker toward tip, tips of first and second labial segments pale luteous; anterior pronotal

lobe brown or mild blackish brown covered some rows of bent pubescence centrally with very long slender, erect setae; posterior pronotal lobe dark brown, but anterior one-third of humerus blackish brown and the remaining of humerus pale brownish luteous, covered with short bent pubescence and interleaved with long slender, erect setae; scutellum dark brown; abdominal mediotergites I+II dark brown, mediotergite III–VII yellow with brown or sometimes darker to blackish brown suffusion in center of each segment; abdominal sternites and connexivum yellow; femora brown with/without dark brown or blackish brown suffusions at apex and sometimes at middle; tibiae blackish brown.

Distribution. Vietnam, Northern Part (Son La, Vinh Phuc).

***Biasticus* sp. M10**

(Fig. 4.3G, Fig. 4.7U–Y, Table 4.1)

Examined material. 1♂, TXL2016-088.

Diagnosis. Body blackish brown; labium black or blackish brown; anterior pronotal lobe blackish brown covered some rows of short bent pubescence; posterior pronotal lobe luteous; scutellum blackish brown with dark brown lateral margins; abdominal mediotergites blackish brown; abdominal sternites luteous with dark brown transverse stripes in sternites IV to VII; connexivum yellow; coxae, trochanters, femora, tibiae blackish brown.

Distribution. Vietnam, Northern Part (Son La).

***Biasticus* sp. M13**

(Fig. 4.3J, Fig. 4.8A–E, Table 4.1)

Examined material. 1♂, TXL2000-004.

Diagnosis. Body blackish brown; labium dark brown; anterior pronotal lobe blackish brown covered some rows of short bent pubescence; posterior pronotal lobe yellow; scutellum dark brown;

abdominal sternites luteous; connexivum yellow; coxae, trochanters, femora, tibiae dark brown.

Distribution. Vietnam, Northern Part (Hoa Binh).

***Biasticus* sp. M16**

(Fig. 4.3M, Fig. 4.8F–J, Table 4.1)

Examined material. 3♂, HEM-TH-2000-003, HEM-TH-2000-004, HEM-TH-2000-005.

Diagnosis. Body blackish brown; labium blackish brown to black, tips of first and second labial segments bronzy; anterior pronotal lobe blackish brown with some rows of short bent setae with long thick erect setae centrally; posterior pronotal lobe dark brown, densely covered with short bent cream-yellow pubescence, somewhat interleaved with long slender erect setae in anterior half, and covered with long thick erect setae in posterior half; central triangular area of scutellum dark brown, remaining of scutellum blackish brown; abdominal mediotergites dark reddish brown, posterior margin of mediotergite VIII sanguineous; abdominal sternites sanguineous; laterotergites sanguineous and segmentally suffused with luteous in posterior 1/3; femora and tibiae black.

Distribution. Thailand, Northern Part (Chiang Mai).

***Biasticus* sp. M19**

(Fig. 4.3P, Fig. 4.8K–O, Table 4.1)

Examined material. 3♂, LA-Redu-2004-005, LA-Redu-2004-008, LA-Redu-2004-013.

Diagnosis. Body blackish brown; labium blackish brown; anterior pronotal lobe black with some rows of bent yellow pubescence with some slender erect setae; posterior pronotal lobe blackish brown and densely covered with short bent yellow setae; scutellum blackish brown and coated by short bent yellow setae, somewhat interleaved with long slender erect setae; abdominal sternites luteous; connexivum sanguineous; coxae, trochanters, femora, and tibiae black.

Distribution. Laos, Northern Part (Houaphan).

***Biasticus* sp. M20**

(Fig. 4.3Q, Fig. 4.8P–T, Table 4.1)

Examined material. 1♂, VN-Hem-1997-001.

Diagnosis. Body blackish brown; base of first visible labial segment dark brown, remaining labium blackish brown and darker toward tip; anterior pronotal lobe blackish brown and covered with some rows of slender setae; posterior pronotal lobe blackish brown and covered with long slender setae; scutellum dark brown with long slender setae; abdominal mediotergites I+II blackish brown; mediotergite III and IV sanguineous with dark brown suffusion in center of each segment; mediotergite V to VII luteous with dark brown suffusion centrally; abdominal sternites luteous; connexivum sanguineous; coxae, trochanters, femora, and tibiae blackish brown.

Distribution. Vietnam, Northern Part (Lao Cai).

***Biasticus* sp. M21**

(Fig. 4.3R, Fig. 4.8U–Y, Table 4.1)

Examined material. 1♂, La-Redu-2004-015.

Diagnosis. . Body blackish brown; labium blackish brown, paler toward tip; anterior pronotal lobe brown or mild blackish brown covered with some rows of bent pubescence with long slender, erect setae; posterior pronotal lobe pale yellow covered with long thick erect setae; scutellum blackish brown coated by long slender bent setae, especially dense at posterior apex; abdominal sternites orange; connexivum reddish-orange or sanguineous; coxae, trochanters, femora, and tibiae blackish brown.

Distribution. Laos, Northern Part (Houaphan).

***Biasticus* sp. M27**

(Fig. 4.3X, Table 4.1)

Examined material. 1♂, LA-Redu-2008-004.

Diagnosis. Body blackish brown; labium blackish brown or black; anterior pronotal lobe black with some rows of bent yellow pubescence; posterior pronotal lobe blackish brown and densely covered with short bent yellow setae; scutellum blackish brown and coated by short bent yellow setae, somewhat interleaved with long slender, erect setae; abdominal sternites luteous; connexivum sanguineous; coxae, trochanters, femora, and tibiae black.

Distribution. Laos, Northern Part (Xieng Khouang).

***Biasticus* sp. M28**

(Fig. 4.3Y, Table 4.1)

Examined material. 1♂, VN-HEM-2011-012.

Diagnosis. Body blackish brown; labium blackish brown or black; anterior pronotal lobe black with some rows of long slender erect griseous pubescence; posterior pronotal lobe blackish brown and densely covered with short bent yellow setae interleaved with long slender erect setae; scutellum blackish brown and coated by short bent yellow setae, somewhat interleaved with long slender, erect setae; abdominal sternites luteous; connexivum sanguineous; coxae, trochanters, femora, and tibiae black.

Distribution. Vietnam, Northern Part (Lao Cai).

***Biasticus* sp. M29**

(Fig. 4.3Z, Table 4.1)

Examined material. 1♂, LA-Redu-2011-003.

Diagnosis. Body blackish brown; labium yellowish brown; anterior pronotal lobe black with some rows of bent yellow pubescence; posterior pronotal lobe blackish brown or black and covered with short and long thick erect black or blackish brown setae; anterior margin of posterior pronotal lobe somewhat with short bent yellow pubescence; scutellum blackish brown, and covered with short bent setae; abdominal mediotergites blackish brown; abdominal sternites dark brown except sternite VII brownish yellow; connexivum blackish brown with small brown suffusion in laterotergites II, III, and IV, somewhat laterotergite V; femora blackish brown with/without dark brown suffusions at middle; basal 1/3 of tibia dark brown, remaining of tibia brown or yellowish brown.

Distribution. Laos, Northern Part (Houaphan).

***Biasticus* sp. M30**

(Fig. 4.3A-1, Table 4.1)

Examined material. 1♂, VN-HEM-2011-016.

Diagnosis. Body blackish brown; first visible labial segment and basal 1/3 of second segment blackish brown; remaining of labium dark brown; anterior pronotal lobe black with some rows of long slender erect griseous pubescence; posterior pronotal lobe blackish brown and densely covered with long slender erect griseous setae; scutellum blackish brown and coated by short bent yellow setae, somewhat interleaved with long slender, erect setae; abdominal sternites luteous; connexivum sanguineous; coxae, trochanters, femora, and tibiae black.

Distribution. Vietnam, Northern Part (Lai Chau).

3.2. Female-based morphospecies

***Biasticus* sp. F1**

(Fig. 4.9A, Table 4.1)

Examined material. 1♀, TXL2004-002.

Diagnosis. Body blackish brown; anterior pronotal lobe blackish-brown with some rows of short bent griseous setae; posterior pronotal lobe dark brown, densely covered with short bent griseous setae, interspersed with long slender setae; scutellum dark brown and densely covered with long slender griseous setae; abdominal mediotergites II to V dark brown; mediotergites VI and VII luteous with a central suffusion of dark brown or brown; abdominal sternites pale orange; laterotergites luteous with segmentally suffused with dark brown spots; coxae, trochanters, femora, and tibia blackish brown or dark brown.

Distribution. Vietnam, Central Part (Ha Tinh).

***Blasticus* sp. F5**

(Fig. 4.9E, Fig. 4.10D, Table 4.1)

Examined material. 1♀, VN-Hem-1998-003.

Diagnosis. Body shiny blackish brown; pronotum and scutellum black or blackish-brown; abdominal mediotergite I + II blackish brown; mediotergites III to VI sanguineous with large central blackish brown suffusions; mediotergites VII and VIII sanguineous; abdominal sternites sanguineous or reddish-orange with a large dark lateral brown or brown suffusion in sternites IV, V. and VI; laterotergites sanguineous; coxae, trochanters, femora, and tibia blackish brown or dark brown.

Distribution. Vietnam, Northern Part (Cao Bang).

***Blasticus* sp. F13**

(Fig. 4.9M, Fig. 4.11N, Table 4.1)

Examined material. 1♀, TXL2018-077.

Diagnosis. Body dark brown; labium blackish brown; anterior pronotal lobe blackish brown and

covered with short bent yellow pubescence and long thick erect setae centrally; posterior pronotal lobe dark brown, covered with short bent yellow pubescence and long thick erect setae; scutellum dark brown covered with short bent yellow pubescence and long thick erect setae; abdominal sternites luteous; connexivum red; coxae, trochanters, femora, and tibiae blackish brown.

Distribution. Vietnam, Central Highlands (Gia Lai).

***Biasticus* sp. F14**

(Fig. 4.9N, Fig. 4.10H, Table 4.1)

Examined material. 2♀, VN-Hem-1998-004, VN-Hem-1998-008; 1♀, TXLBX20-2.

Diagnosis. Body shiny blackish-brown; pronotum and scutellum black or blackish-brown; abdominal sternites sanguineous, reddish-orange, or luteous with a large dark lateral brown or brown suffusion in sternite V and VI; laterotergites sanguineous; coxae, trochanters, femora, and tibia blackish brown or dark brown.

Distribution. Vietnam, Northern Part (Cao Bang).

***Biasticus* sp. F15**

(Fig. 4.9O, Fig. 4.11O, Table 4.1)

Examined material. 1♀, ZRC.HEM.50; 1♀, ZRC.HEM.244.

Diagnosis. Body shiny brown; labium brownish-yellow; scape ~ 1.6 × as long as head, pedicel shorter than first flagellomere, first flagellomere shorter than second flagellomere; proportional average length of scape, pedicel, first and second flagellomeres 3.2:1.1:1.8:2.5; anterior pronotal lobe orangish-brown with a few long thick erect setae; anterior two-thirds of posterior pronotal lobe brownish-yellow; remaining of posterior pronotal lobe brown, covered with black long slender erect setae; scutellum dark brown with centrally suffused with orangish-brown; abdominal mediotergites

dark brown to blackish-brown; abdominal sternites, except sternites V and VI, yellowish-brown; anterior margins of sternites II and III, and center of sternite IV–VI brown; sternites V and VI with transverse blackish-brown stripe; laterotergites II to IV luteous with blackish-brown marginal spots; laterotergite V, VI blackish-brown; laterotergite VII luteous; femora apically brown; remaining of femora and tibiae suffused with yellowish-brown and orangish-brown.

Distribution. Singapore, Malaysia (Kuala Lumpur).

***Blasticus* sp. F16**

(Fig. 4.9P, Table 4.1)

Examined material. 1♀, ZRC.ENT00012353.

Diagnosis. Body shiny brown; labium brownish-yellow; scape ~ 1.6 × as long as head, pedicel ~ 0.6 × as long as first flagellomere and ~ 0.4 × as long as second flagellomere; proportional length of scape, pedicel, first and second flagellomeres 3.1:1.1:1.9:2.8; anterior pronotal lobe dark brown with a few long thick erect setae; anterior half of posterior pronotal lobe brownish-yellow without setae; posterior half of posterior pronotal lobe yellowish-brown and posteriorly covered with long thick erect setae; scutellum dark brown; abdominal mediotergites blackish-brown; laterotergite except laterotergite V and VII and sternite except sternite V, VI and VII yellowish-brown; anterior margin of laterotergite II, III and VI, laterotergite V and VI and sternite IV suffused with blackish-brown; sternite V and VI with blackish-brown transverse suffusion; sternite VII brownish-yellow; femora brown sometimes with yellowish-brown suffusion; basal half of tibiae brown, apical half of tibiae yellowish-brown

Distribution. Singapore.

***Biasticus* sp. F21**

(Fig. 4.9T, Fig. 4.12A, Table 4.1)

Examined material. 1♀, MMR-Hem-1987-001.

Diagnosis. Body blackish brown; labium blackish brown, paler toward tip; anterior pronotal lobe black or blackish brown with a few rows of short bent yellow pubescence interleaved with long thick erect setae; posterior pronotal lobe blackish brown or brownish-black and densely covered with short bent yellowish pubescence and long thick erect setae posteriorly; scutellum blackish brown and densely covered with short bent yellow pubescence; laterotergites red; abdominal sternite luteous; coxae, trochanters, and femora blackish brown; tibiae dark brown.

Distribution. Myanmar (Shan).

***Biasticus* sp. F23**

(Fig. 4.9V, Table 4.1)

Examined material. 1♀, HEM-TH-2004-023.

Diagnosis. Body blackish brown; labium yellowish brown; third visible labial segment brown; anterior pronotal lobe black with some rows of bent yellow pubescence; posterior pronotal lobe blackish brown or black and covered with short thick erect setae; anterior margin of posterior pronotal lobe somewhat with short bent yellow pubescence; scutellum blackish brown, and covered with short bent setae; abdominal sternites dark brown, darker posteriorly except sternite VII brownish yellow; laterotergites II to IV brown or dark brown, with yellowish brown in posterior 1/3; laterotergites V and VI blackish brown or black; femora blackish brown; basal 1/3 of tibia dark brown, middle 1/3 dark brown, and remaining of tibia brown or yellowish brown.

Distribution. Thailand, Northern Part (Chiang Rai).

***Biasticus* sp. F24**

(Fig. 4.9W, Fig. 4.12B, Table 4.1)

Examined material. 1♀, La-Redu-2004-012; 1♀, LA-Redu-2010-002; 1♀, VN-Hem-2011-001.

Diagnosis. Body blackish brown; labium blackish brown; anterior pronotal lobe black with some rows of bent yellow pubescence with some slender erect setae; posterior pronotal lobe blackish brown and densely covered with short bent yellow setae; scutellum blackish brown and coated by short bent yellow setae, somewhat interleaved with long slender erect setae; abdominal sternites luteous; connexivum sanguineous; coxae, trochanters, femora, and tibiae black.

Distribution. Laos, Northern Part (Houaphan); Vietnam, Northern Part (Lao Cai).

***Biasticus* sp. F25**

(Fig. 4.9X, Fig. 4.12C, Table 4.1)

Examined material. 1♀, VN-Hem-1997-002.

Diagnosis. Body blackish brown; base of first visible labial segment dark brown, remaining labium blackish brown and darker toward tip; anterior pronotal lobe blackish brown and covered with some rows of slender setae; posterior pronotal lobe blackish brown and covered with long slender setae; scutellum dark brown with long slender setae; abdominal mediotergites I+II blackish brown; mediotergite III and IV sanguineous with dark brown suffusion in center of each segment; mediotergite V to VII luteous with dark brown suffusion centrally; abdominal sternites luteous; connexivum sanguineous; coxae, trochanters, femora, and tibiae blackish brown.

Distribution. Vietnam, Northern Part (Lao Cai).

***Biasticus* sp. F26**

(Fig. 4.9Y, Fig. 4.12D, Table 4.1)

Examined material. 4♀, VN-Hem-2000-007, VN-Hem-2000-008, VN-Hem-2000-009, VN-Hem-2000-010.

Diagnosis. Body blackish brown; labium blackish brown, slightly paler toward tip; anterior pronotal lobe black; posterior pronotal lobe black or blackish brown, densely covered with short slender erect setae; scutellum blackish-brown; abdominal mediotergites blackish brown, somewhat sanguineous in lateral margin; abdominal sternites luteous; laterotergites sanguineous; coxae, trochanters, femora, and tibiae blackish brown.

Distribution. Vietnam, Northern Part (Lao Cai).

***Blasticus* sp. F27**

(Fig. 4.9Z, Fig. 4.12E, Table 4.1)

Examined material. 1♀, VN-Hem-1999-001.

Diagnosis. Body blackish brown; labium blackish brown; anterior pronotal lobe black; posterior pronotal lobe black or blackish brown, densely covered with short slender oblique setae; scutellum blackish-brown with long slender setae; abdominal sternites luteous; laterotergites sanguineous; coxae, trochanters, femora, and tibiae blackish brown.

Distribution. Vietnam, Northern Part (Lao Cai).

***Blasticus* sp. F28**

(Fig. 4.9A-1, Fig. 4.12F, Table 4.1)

Examined material. 1♀, HEM-TH-2002-004.

Diagnosis. Body blackish brown; first visible labial segment blackish brown; remaining of labium dark brown, paler toward tip; anterior pronotal lobe black; posterior pronotal lobe pale yellow and almost glabrous; scutellum blackish-brown; abdominal sternites brownish yellow with lateral areas

suffused with brown; laterotergites brownish yellow with a dark brown suffusion in laterotergite VI; coxae, trochanters, femora, and tibiae blackish brown.

Distribution. Thailand, Northern Part (Chiang Mai).

***Biasticus* sp. F29**

(Fig. 4.9B-1, Fig. 4.12G, Table 4.1)

Examined material. 1♀, HEM-TH-2000-002.

Diagnosis. Body dark brown; labium dark brown; anterior pronotal lobe black with some rows of short bent cream-yellow setae, somewhat interspersed with long thick erect setae; posterior pronotal lobe pale yellow with a transverse dark brown suffusion medially, densely covered with long thick erect setae, anterior margin densely coated with short bent cream-yellow setae; scutellum blackish-brown at basal 2/3 and luteous at posterior 1/3 and densely covered with bent griseous setae, somewhat interspersed with long thick erect setae; abdominal sternites and laterotergites brownish yellow with transverse blackish-brown stripe segmentally; coxae, trochanters, femora, and tibiae dark brown.

Distribution. Thailand, Northern Part (Chiang Mai).

***Biasticus* sp. F30**

(Fig. 4.9C-1, Table 4.1)

Examined material. 1♀, VN-Hem-2011-002.

Diagnosis. Body blackish-brown; labium blackish brown; anterior pronotal lobe black with some rows of short bent cream-yellow setae; posterior pronotal lobe blackish-brown, densely covered with short bent cream-yellow setae, interspersed with long erect setae; scutellum blackish-brown and densely covered with short bent cream-yellow setae; abdominal sternites and laterotergites

sanguineous; coxae, trochanters, femora, and tibiae blackish brown or black.

Distribution. Vietnam, Northern Part (Lai Chau).

***Biasticus* sp. F31**

(Fig. 4.9D-1, Fig. 4.12H, Table 4.1)

Examined material. 1♀, LA-Redu-2010-001; 1♀, TXL2018-840.

Diagnosis. Body blackish brown; labium blackish brown or black; anterior pronotal lobe black with some rows of bent yellow pubescence with some long thick erect setae; posterior pronotal lobe blackish brown and densely covered with short bent yellow pubescence, somewhat interspersed with long thick erect setae; scutellum blackish brown and coated by short bent yellow setae, especially dense at posterior apex; abdominal mediotergites and laterotergites sanguineous; mediotergite I+II blackish brown; abdominal sternites luteous; coxae, trochanters, femora, and tibiae black.

Distribution. Laos, Northern Part (Xieng Khouang); Vietnam, Northern Part (Lai Chau).

***Biasticus* sp. F34**

(Fig. 4.9F-1, Fig. 4.12I, Table 4.1)

Examined material. 1♀, ZRC.HEM.55.

Diagnosis. Body shiny brown; labium brownish-yellow; scape $\sim 1.6 \times$ as long as head, pedicel $\sim 0.6 \times$ as long as first flagellomere and $\sim 0.4 \times$ as long as second flagellomere; proportional length of scape, pedicel, first and second flagellomeres 3.1:1.1:1.9:2.8; anterior pronotal lobe dark brown with a few long thick erect setae; anterior half of posterior pronotal lobe brownish-yellow without setae; posterior half of posterior pronotal lobe yellowish-brown and posteriorly covered with long thick erect setae; scutellum dark brown; abdominal mediotergites blackish-brown; laterotergite except laterotergite V and VII and sternite except sternite V, VI and VII yellowish-brown; anterior margin

of laterotergite II, III and VI, laterotergite V and VI and sternite IV suffused with blackish-brown; sternite V and VI with blackish-brown transverse suffusion; sternite VII brownish-yellow; femora brown sometimes with yellowish-brown suffusion; basal half of tibiae brown, apical half of tibiae yellowish-brown.

Distribution. Singapore.

***Biasticus* sp. F35**

(Fig. 4.9G-1, Table 4.1)

Examined material. 1♀, ZRC.HEM.49.

Diagnosis. Body shiny orangish-brown; first and second visible labial segments blackish-brown, apical region of second visible labial segment and third visible labial segments brownish-orange; antennae missing; anterior pronotal lobe except center blackish-brown, center of anterior pronotal lobe orange; posterior pronotal lobe orangish-brown with reddish-brown suffusion in center; scutellum blackish-brown; abdominal mediotergites, except posterior margin of mediotergite VI and mediotergite VII, blackish-brown; posterior margin of mediotergite VI and mediotergite VII orange; abdominal sternite II–VI yellowish-brown, sternite IV, V and VI with blackish-brown segmental transverse suffusion, sternite VII orange; anterior two-thirds of laterotergite II brown; anterior half of laterotergite III, anterior two-thirds of laterotergite IV blackish-brown, remaining of laterotergite II, III and IV yellowish-brown; laterotergite V and VI, except posterior margin of laterotergite V and posterior one-fifth of laterotergite VI, blackish-brown; posterior margin of laterotergite V orangish-brown; posterior one-fifth of laterotergite VI and laterotergite VII orange; femora and tibiae dark brown.

Distribution. Malaysia (Pahang).

***Biasticus* sp. F36**

(Fig. 4.9H-1, Table 4.1)

Examined material. 1♀, ZRC.HEM.218.

Diagnosis. Body shiny orangish-brown; labium brown; scape ~ 1.6 × as long as head, pedicel ~ 0.6 × as long as first flagellomere, second flagellomere nearly equal in length to pedicel and first flagellomere together; proportional average length of scape, pedicel, first and second flagellomeres 3.3:1.1:1.8:2.7; anterior and posterior pronotal lobes orangish-brown; center and posterior apex of scutellum orange, lateral margin of scutellum orangish-brown; abdominal mediotergite I+II and III brownish-yellow, mediotergite IV–VII blackish-brown with dark brown irregular patterns; abdominal sternites II–VI orangish-brown, sternites V and VI with blackish-brown segmental transverse suffusion, sternite VII brownish-yellow; laterotergite II–IV orangish-brown, laterotergite V and VI blackish-brown, laterotergite VII brownish-yellow; femora, except apical one-third of femora, brownish-orange; apical one-third of femora, basal one-third of tibiae dark brown; remaining of tibiae brown.

Distribution. Malaysia (Kuala Lumpur).

***Biasticus* sp. F37**

(Fig. 4.9I-1, Fig. 4.12J, Table 4.1)

Examined material. 1♀, ZRC.ENT00012352.

Diagnosis. Body shiny dark brown; labium yellowish-brown; scape ~ 1.6 × as long as head, first flagellomere slightly twice as long as pedicel; second flagellomere slightly shorter than scape; proportional average length of scape, pedicel, first and second flagellomeres 3.2:1.1:2.1:2.9. anterior pronotal lobe dark brown; anterior half of posterior pronotal lobe yellowish-brown to orangish-brown, posterior half of posterior pronotal lobe dark brown; scutellum dark brown to blackish-

brown; abdominal mediotergite , except posterior half of mediotergite VII, blackish-brown; laterotergites brownish-yellow; anterior margin of laterotergites II and III blackish-brown; laterotergite IV and V blackish-brown; sternites II–III yellowish-brown; sternites IV–VI brown with blackish-brown segmental transverse suffusion; sternite VII orangish-brown; basal two-thirds of femora brown, remaining of femora and basal two-fifths of tibiae blackish-brown, remaining of tibiae yellowish-brown.

Distribution. Singapore.

***Biasticus* sp. F40**

(Fig. 4.9L-1, Fig. 4.12K, Table 4.1)

Examined material. 1♀, TXLBX2.

Diagnosis. Body blackish brown; labium blackish brown or black; anterior pronotal lobe black with some rows of bent yellow pubescence; posterior pronotal lobe luteous with a transverse blackish-brown suffusion medially and almost glabrous; scutellum blackish brown with dark brown lateral margin and coated by short bent yellow setae; abdominal mediotergites dark brown; abdominal sternites luteous; connexivum sanguineous; coxae, trochanters, femora, and tibiae black.

Distribution. Vietnam, Central Highlands (Gia Lai).

***Biasticus* sp. F42**

(Fig. 4.9N-1, Fig. 4.12L, Table 4.1)

Examined material. 1♀, TXLBX18.

Diagnosis. Body blackish brown; labium blackish brown or black; anterior pronotal lobe black with some rows of bent yellow pubescence; posterior pronotal lobe yellow with a large blackish-brown suffusion centrally and somewhat small dark brown suffusion in central of humerus; posterior

pronotal lobe densely covered with short bent yellow setae, interspersed with long slender setae; somewhat with long thick erect setae in the posterior margin; scutellum blackish brown with dark brown lateral margin and coated by short bent yellow setae, somewhat interleaved with long slender setae; abdominal sternites luteous with horizontal blackish brown suffusion in lateral areas of sternites IV, V, and VI; connexivum orange, with blackish brown suffusion in laterotergites V and VI; coxae, trochanters, femora, and tibiae black.

Distribution. Vietnam, Central Part (Nghe An).

***Blasticus* sp. F48**

(Fig. 4.9T-1, Fig. 4.12M, Table 4.1)

Examined material. 2♀, LA-Redu-2008-002, LA-Redu-2008-003; 1♀, LA-Redu-2010-003.

Diagnosis. Body blackish brown; labium blackish brown or black; anterior pronotal lobe black with some rows of bent yellow pubescence; posterior pronotal lobe blackish brown and densely covered with short bent yellow setae; scutellum blackish brown and coated by short bent yellow setae, somewhat interleaved with long slender, erect setae; abdominal sternites luteous; connexivum sanguineous; coxae, trochanters, femora, and tibiae black.

Distribution. Laos, Northern Part (Xieng Khouang).

***Blasticus* sp. F49**

(Fig. 4.9U-1, Fig. 4.12N, Table 4.1)

Examined material. 2♀, VN-HEM-2011-014, VN-HEM-2011-015.

Diagnosis. Body blackish brown; labium blackish brown or black; anterior pronotal lobe black with some rows of long slender erect griseous pubescence; posterior pronotal lobe blackish brown and densely covered with short bent yellow setae interleaved with long slender erect setae; scutellum

blackish brown and coated by short bent yellow setae, somewhat interleaved with long slender, erect setae; abdominal sternites luteous; connexivum sanguineous; coxae, trochanters, femora, and tibiae black.

Distribution. Vietnam, Northern Part (Lai Chau).

***Biasticus* sp. F51**

(Fig. 4.9W-1, Fig. 4.12O, Table 4.1)

Examined material. 1♀, TXL2021-009.

Diagnosis. Body shiny blackish brown; labium blackish brown; anterior pronotal lobe black with a few long thick erect setae; posterior pronotal lobe luteous covered with long thick erect setae and somewhat covered with short bent pubescent in the anterior margin areas; scutellum blackish brown with dark brown lateral margin, somewhat covered with short slender setae; posterior apex of scutellum densely covered with erect setae; abdominal mediotergites, sternites, and laterotergites sanguineous; mediotergite I+II dark brown; coxae, trochanters, femora, and tibiae blackish brown.

Distribution. Vietnam, Northern Part (Cao Bang).

CHAPTER 5:
DISCRIMINATION OF THE SPECIES OF
***SPHEDANOLESTES* SENSU LATO**
(HEMIPTERA: HETEROPTERA: REDUVIIDAE)
KNOWN FROM VIETNAM AND SURROUNDING AREAS

Notification. The formal taxonomic actions will not be done in this thesis (disclaiming of taxonomic actions declared in the concerning work is supported by the International Code of Zoological Nomenclature: Article 8.3)

5.1. Introduction

Sphedanolestes Stål, 1867 was established for *Reduvius impressicollis* Stål, 1861, and has been assigned to the tribe Harpactorini of the subfamily Harpactorinae in the current classification of the family Reduviidae (Stål 1861a, 1867; Maldonado 1990).

The present integrative approach (Chapter 3) did not support the monophyly of *Sphedanolestes* and subdivided it into at least three independent genera, *Sphedanolestes* sensu stricto, genera C, and D, with revised morphological definitions of the three genera (see Appendix of Chapter 3). The three genera are collectively referred to as *Sphedanolestes* sensu lato.

Sphedanolestes sensu lato currently comprises 185 valid named species distributing exclusively from the Afrotropical, Palearctic, Sino-Japanese, Oriental, and Oceanic Realms (Maldonado 1990; Livingstone and Ravichandran 1990; Cai and Yang 2002; Cai et al. 2004; Zhao et al. 2015) (Fig. 2.4). Among them, ten species have been recorded and described from Indo-China, i.e., *S. annulipes* Distant, 1903, *S. femoralis* Distant, 1919, *S. flaviventris* Distant, 1919, *S. gularis* Hsiao, 1979, *S. impressicollis* (Stål, 1861), *S. marginiventris* Distant, 1919, *S. pubinotus* Reuter, 1881, *S. sericatus* Breddin, 1903, *S. trichrous* Stål, 1874, and *S. xiongi* Cai et al., 2004 (Breddin 1903; Distant 1919; Truong et al. 2015).

In the present study, the species-level classification of the Indo-Chinese species of *Sphedanolestes* sensu stricto, genera C and D are revised by the integrative approach, as explained in Chapter 2.

5.2. Material and Methods

The definitions of the three genera *Sphedanolestes* sensu stricto, C, and D follow the Appendix of Chapter 3. General information on sampling sites (Fig. 5.1), specimen depositories, and analytical

methods (imaging, DNA sequencing, sequencing, and phylogenetic analyses) were given in Chapter 2. Additional information for this chapter is given below.

This study included 59 *Sphedanolestes* and *Sphedanolestes*-like specimens (26 male and 32 female adults), of which 36 specimens were from Vietnam, 2 specimens from Singapore, and 6 specimens from Japan. Among 59 *Sphedanolestes* specimens, there were 15 type specimens from the Swedish Museum of Natural History (NRM) (Table 2.1).

The following type specimens were also examined for identifying the species: *Sphedanolestes impressicollis* (Stål, 1861) (a type specimen, NRM), *S. bicolor* Schouteden, 1910 (a type, NRM), *S. dromedarius* Reuter, 1881 (a type, NRM), *S. fasciventris* (Stål, 1855) (a type specimen, NRM), *S. gulo* (Stål, 1863) (a type, NRM), *S. hemiochrus* (Stål, 1871) (a type, NRM), *S. indicus* Reuter, 1881 (a type, NRM), *S. jucundus* (Stål, 1866) (a type, NRM), *S. nanus* (Stål, 1855) (a holotype, NRM), *S. politus* (Stål, 1870) (a holotype, NRM), *S. pubinotus* Reuter, 1881 (a holotype, NRM), *S. pulchellus* (Klug, 1830) (a holotype, NRM), *S. saucius* (Stål, 1861) (a holotype, NRM), *S. sjostedti* Villiers, 1948 (a holotype, NRM), and *S. verecundus* (Stål, 1863) (a holotype, NRM) (Table 2.1).

Furthermore, specimens of *Biasticus luteicollis* Ha, Truong & Ishikawa, 2022, “*Sphedanolestes*” *gularis* Hsiao et al., 1979, *Coranus* sp., and “*Rhynocoris*” *mendicus* (Stål, 1867) collected from Vietnam were used as outgroups in molecular phylogenetic analyses (Table 2.1). It is noted that “*Sphedanolestes*” *gularis* Hsiao et al., 1979 is one of the two *Sphedanolestes* species which was proposed to move to the genus *Biasticus* in Chapter 4.

Morphological examination of the validly named species of the genus was conducted by referring to the original descriptions, other taxonomic publications, and type specimens where available (Stål 1861, 1863, 1870, 1874; Reuter 1881; Jakovlev 1893; Breddin 1903, 1904; Distant 1903, 1904, 1909, 1919; Bergroth 1908; Schouteden 1910; Miller 1941, 1954; Hsiao and Ren 1981; Livingstone and Ravichandran 1990; Cai and Yang 2002; Cai et al. 2004; Ishikawa et al. 2007; Zhao

et al. 2015; Dioli et al. 2020) of the following congeners known from Vietnam and adjacent areas: *Sphedanolestes albigula* Breddin, 1905, type location: Indonesia; *S. albipilosus* Ishikawa, Cai and Tomokuni, 2007, Japan (Ryukyu islands); *S. anellus* Hsiao, 1979, China (Yunnan); *S. annulatus* Linnavuori, 1961, Israel; *S. annulipes* Distant, 1903, Myanmar (see also Table 4.1, 4.3); *S. aurescens* Distant, 1919, India; *S. avidus* Miller, 1941, Borneo; *S. badgleyi* Distant, 1909, India; *S. bellus* Stål, 1874, Indonesia; *S. bicolor* Schouteden, 1910, Tanzania; *S. bicolorous* Livingstone and Ravichandran, 1990, India; *S. bituberculatus* (Jakovlev, 1893), China and Korea; *S. bowringi* Distant, 1909, India; *S. cameronicus* Miller, 1941, Malaysia; *S. compressipes* Stål, 1874, Indonesia; *S. discifer* Reuter, 1881, Malaysia; *S. discopygus* Miller, 1954, Indonesia; *S. dives* Distant, 1904, Myanmar; *S. fallax* Miller, 1941, Borneo; *S. femoralis* Distant, 1919, Laos and Vietnam; *S. flaviventris* Distant, 1919, Vietnam; *S. funeralis* Distant, 1903, India; *S. gestuosus* (Stål, 1861), Indonesia; *S. nodilipes* Hsiao and Ren, 1981, China; *S. gularis* Hsiao, 1979, China (see also Table 4.1, 4.3); *S. gulo* (Stål, 1863), Indonesia; *S. hemiochrus* (Stål, 1870), Philippines; *S. himalayensis* Distant, 1909, East Himalaya; *S. impressicollis* (Stål, 1861), Hongkong (see also Table 2.1, 5.1); *S. indicus* Reuter, 1881, India; *S. lucorum* Miller, 1941, Malaysia; *S. marginiventris* Distant, 1919, Vietnam; *S. melanocephalus* (Stål, 1863), Indonesia; *S. minusculus* Bergroth, 1908, India; *S. modestus* Miller, 1941, Borneo; *S. nigrocephala* Livingstone and Ravichandran, 1990, India; *S. pilosus* Hsiao, 1979, China (Yunnan); *S. politus* (Stål, 1870), Philippines; *S. pubinotus* Reuter, 1881, India and Myanmar (see also Table 2.1, 5.1); *S. pulchriventris* (Stål, 1863), India; *S. quadrinotatus* Cai et al., 2004, China (Yunnan); *S. rubecula* Distant, 1909, Myanmar; *S. rubripes* Cai et al., 2004, China (Yunnan); *S. sarawakensis* Miller, 1941, Malaysia; *S. saucius* (Stål, 1861), Indonesia; *S. scandens* Miller, 1941, Borneo; *S. sericatus* Breddin, 1903, Vietnam; *S. shelfordi* Miller, 1941, Malaysia; *S. signatus* Distant, 1903, India; *S. sinicus* Cai and Yang, 2002, Taiwan; *S. stigmatellus* Distant, 1903, India; *S. subtilis* (Jakovlev, 1893), China; *S. trichrous* Stål, 1874, India; *S. variabilis*

Distant, 1904, India; *S. vesbioides* Breddin, 1903, Indonesia; *S. xanthogaster* (Stål, 1863), Malaysia; *S. xiongi* Cai et al., 2004, China (Yunnan) (see also Table 2.1, 5.1); *S. zhengi* Zhao, Ren, Wang and Cai, 2015, China (Guizhou).

Similar to the genus *Blasticus*, the sexual dimorphism in external morphology of male and female adults is usually not very clear in the genera *Sphedanolestes* sensu stricto, C, and D, while female adults commonly showed larger body size, more prominent abdomen, and more horizontally expanded connexivum than male adults (Kwadjo et al. 2010; Forthman 2017; Gil-Santana 2017; Weirauch et al. 2017; Chen et al. 2021) (Fig. 5.2). However, in order to take account of the importance of the sexual dimorphism, morphospecies recognition was made separately for males and females, and the male-based and female-based morphospecies are hereafter specified with unique codes such as *S. sp. M1* and *S. sp. F1*, “gen. C” sp. M1 and “gen. C” sp. F1, or “gen. D” sp. M1 and “gen. D” sp. F1, in which M and F mean the male and female-based morphospecies, respectively. Each morphospecies was characterized by the external and genitalia morphology of its sex.

The mitochondrial 16S dataset (480 bp; 31 ingroup OTUs, 5 outgroup OTUs) and the COI dataset (603 bp; 29 ingroup OTUs, 3 outgroup OTUs) were successfully obtained (as listed in Table 5.1). Molecular phylogenetic analyses were done based on the concatenated 16S + COI dataset. The substitution models, TPM3 + F + I + G4, TIM2 + F + G4, and (TPM3 + F + I + G4, TIM2 + F + G4), were selected respectively for the 16S^(OG+), COI^(OG+), and the concatenated 16S + COI datasets by Model Finder (Kalyaanamoorthy et al. 2017) executed in IQ-TREE 2.1.2 (Minh et al. 2020). Maximum likelihood (ML) examinations were then carried out using IQ-TREE 2.1.2 (Chernomor et al. 2016; Minh et al. 2020); bootstrap values (BP) were estimated from 1,000 replications. The generalized time-reversible (GTR) + Gama model was chosen for the 16S + COI dataset using Model Finder (Kalyaanamoorthy et al. 2017) under the Bayesian information criterion. The Bayesian

inference (BI) evaluations were then executed for the data using MrBayes v.3.2.7 (Ronquist and Huelsenbeck 2003) with 20,000,000 production and statutory parameter configuration (examining every 500 generations and tuning constraints every 100 generations, with a burn-in of 25 %). The effective sampling size (ESS) of each constraint was verified to be > 200 using Tracer 1.7.2 (Rambaut et al. 2018). The nodes were designated as “well supported” when posterior probability (PP) ≥ 0.95 and BP ≥ 80 .

5.3. Results

5.3.1. Morphological Examination in the Male and Female Adults

Thirteen male specimens were grouped into five male-based morphospecies (*Sphedanolestes* sp. M1, *S.* sp. M2, “gen. C” sp. M1, “gen. C” sp. M2, and “gen. D” sp. M1) based on characteristics presenting in external morphology, for example, body coloration, anterior and posterior pronotal lobes, and scutellum (Fig. 5.3) and characteristics presenting in male genitalia, e.g., distal margin of median process of pygophore (mpp), and spinulose process of distal dorsal lobe of endosoma (ddl) (Fig. 5.4–5.5).

On the other hand, sixteen female specimens were grouped into four female-based morphospecies (*Sphedanolestes* sp. F1, *S.* sp. F2, “gen. C” sp. F1, and “gen. D” sp. F1) based on characteristics presenting in external morphology, for example, body coloration, setation, anterior and posterior pronotal lobes, and scutellum (Fig. 5.6) and features presenting in female genitalia, for instance, the posterior margin of abdominal sternite VII, the shape and structure of gonocoxa VIII, and the inner margin of abdominal laterotergite VIII (Fig. 5.7).

5.3.2. Identities of the Morphospecies Based on the 16S + COI Phylogenetic Trees

For five male-based morphospecies and four female-based morphospecies, mitochondrial 16S

and COI sequences were successfully obtained.

In both ML and BI trees, four putative species were recovered as independent monophyletic lineages with high supporting values (PP = 1; BP \geq 87) or singleton lineage and deeply divergent well from each other with long basal branches (Fig. 5.8). However, similar to results of chapter 3, the monophyly of the clade consisting of three genera *Sphedanolestes* sensus stricto, C, and D were not supported with low supporting value in ML analysis.

The phylogenetic independencies of four putative species were also supported consistently by ASAP and bPTP based on the COI^(OG⁻) and 16S^(OG⁻) datasets (Fig. 5.8).

5.4. Discussion

5.4.1. Full Recognition of the Species and Identification

It is reasonable that the following four OTUs, which were consistently recovered by the integrative approach, are treated as fully recognized species (or herein simply referred to as species; abbreviation of each species is given as *Sphedanolestes* sp. HNL001, “gen. C” sp. HNL001, or “gen. D” sp. HNL001, in which HNL is the initials of Ha Ngoc Linh) (Table 5.1; Figs 5.9–5.10).

The four species are listed below, with the species of which both male and female were found being highlighted in bold: ***Sphedanolestes* sp. HNL001** (= *S.* sp. M1 + *S.* sp. M2 + *S.* sp. F1 + *S.* sp. F2); **“gen. C” sp. HNL001** (= “gen. C” sp. M1 + “gen. C” sp. F1); “gen. C” sp. HNL002 (= “gen. C” sp. M2); **“gen. D” sp. HNL001** (= “gen. D” sp. M1 + “gen. D” sp. F1).

However, there is only one incompatible case between morphological and molecular phylogenetic results. The color forms “*S.* sp. M1 + *S.* sp. F1” (Fig. 5.10A–B) and “*S.* sp. M2 + *S.* sp. F2” (Fig. 5.10C–D), which were discriminated from each other by the body coloration, were not discriminated by the present integrative approach, and so the two male-based and two female-based morphospecies are herein treated as intraspecific morphological phenotypes of a single species coded

as *Sphedanolestes* sp. HNL001 (Fig. 5.10A–D). It is noted that the color form “*S.* sp. M1 + *S.* sp. F1” is recorded in Japan, while the color form “*S.* sp. M2 + *S.* sp. F2” is distributed widely in Vietnam. The genetic divergence corresponding to the two color forms was, however, not observed (Fig. 5.8).

By examining type material and taxonomic articles (including the original descriptions) of the validly named species of the genus *Sphedanolestes* and species of some closed related genera (*Biasticus* and *Rhynocoris*), the following three species can be reasonably identified: *S.* sp. HNL001 = *S. impressicollis* (Stål, 1861); “gen. C” sp. HNL001 = “*Sphedanolestes*” *pubinotus* Reuter, 1881; and “gen. D” sp. HNL001 = *S. xiongi* Cai et al., 2004 (Table 5.1).

For another male-based morphospecies of the genus C (“gen. C” sp. M3), which was unable to involve in DNA sequencing, the status of the species and the conspecific male and female combination were not confirmed in the present study. Future studies based on further comprehensive sampling are necessary to solve the issues.

The morphological diagnosis and taxonomic remarks for each fully recognized species, the remaining morphospecies, and the synonymic list for the three species identified above will be provided in the Appendix of this chapter. These may be useful as the prior working hypotheses (= operational taxonomic units) in future integrative taxonomic studies. The formal taxonomic actions will not be done in this thesis (disclaiming of taxonomic actions declared in the concerning work is supported by the International Code of Zoological Nomenclature: Article 8.3).

In three fully recognized species of which the conspecific male-female combination was revealed (i.e., *Sphedanolestes* sp. HNL001, “gen. C”. sp. HNL001 and “gen. D”. sp. HNL001), external morphology shows no remarkable conspecific sexual dimorphism. Therefore, in *Sphedanolestes* sensu lato, external morphology has particular usefulness as supporting evidence to infer conspecific male-female combinations when the molecular phylogenetic approach is not applicable.

5.4.2. Distribution and Biogeographical Criteria

Among four fully recognized species, three were only recorded widely along Vietnam (Fig. 5.11). The remaining species, “gen. C” sp. HNL002, were recorded with a single specimen, so the distribution of this species was not discussed in this study. Moreover, the two morphological forms of *Sphedanolestes impressicollis* were recorded in two far-distance regions, i.e., Vietnam and Japan. Therefore, further studies with more sample sizes from larger geographical scales should be conducted to reveal the distribution patterns and background factors of *Sphedanolestes* sensu lato.

5.4.3. The Future Prospect of This Study

Similar to Chapter 4, the present study highlighted that the assassin bug genera, such as *Sphedanolestes*, still remained many unknown hidden, for example, intraspecific polymorphism. Therefore, the species-level discrimination of the genus *Sphedanolestes* sensu lato and other reduviid genera should be appraised again by integrated taxonomy.

Due to the limitation of specimens and species involved in this study, the usefulness of male genitalia for discriminating species of genus *Sphedanolestes*, C and D, was not confirmed.

Furthermore, mostly validly-named species of the genus *Sphedanolestes* sensu lato were only discriminated by morphological examination, and there has been no available DNA barcode database of the genus yet. Thus, studies on larger collections of fresh or relatively newly collected specimens suitable for DNA sequencing should be done in the future.

References

1. Bergroth E (1908) Neue indische Hemiptera. Deutsche Entomologische Zeitschrift 1908: 589–595.
2. Breddin G (1903) Neue Raubwanzen. Societas Entomologica 17: 169, 170, 177, 178.

3. Breddin G (1904) Rhynochota Heteroptera aus Java gesammelt von Prof. K. Kraepelin. Mitteilungen aus dem Naturhistorischen Museum in Hamburg, 22: 109–159.
4. Cai W, Yang S (2002) Insect from Maolan landscape. Guizhou Science and Technology Publishing House, Guiyang, 208–230.
5. Cai W, Cai X, Wang Y (2004) Notes on the genus *Sphedanolestes* Stål (Heteroptera: Reduviidae: Harpactorinae) from China, with the description of three new species. The Raffles bulletin of Zoology 2004, 52(2): 379–388.
6. Chen Z, Liu Y, Cai W (2021). Taxonomic review of *Xenorhyncocoris* Miller (Heteroptera: Reduviidae: Ectrichodiinae), with description of *X. attractivus* sp. nov. and notes on sexual dimorphism of the genus. European Journal of Taxonomy 746(1): 26–49. <https://doi.org/10.5852/ejt.2021.746.1315>
7. Chernomor O, Haeseler von A, and Minh BQ (2016) Terrace aware data structure for phylogenomic inference from supermatrices. Syst. Biol., 65: 997–1008. <https://doi.org/10.1093/sysbio/syw037>
8. Dioli P, Moulet P, Ghahari H (2020) New genus and species record of *Sphedanolestes annulatus* Linnavuori (Hemiptera: Reduviidae) for Iran and Jordan. Heteroptera Poloniae - Acta Faunistica 14: 213–215. <http://dx.doi.org/10.5281/zenodo.4307848>
9. Distant WL (1903) Rhynchotal notes. XVI. Heteroptera: Family Reduviidae (continued). Apiomerinae, Harpactorinae and Nabidae. Ann. Mag. Nat. Hist., (7)11: 203–213.
10. Distant WL (1904) Rhynchota – Vol. II: The Fauna of British India, including Ceylon and Burma. London: Taylor and Francis.
11. Distant WL (1909) Rhynochota (Heteroptera) from British India. Annales de la Société entomologique de Belgique 53: 360–376.
12. Distant WL (1919) The Heteroptera of Indo-China. The Entomologist 52: 207–211.

13. Forthman M, Weiwauch C (2017) Millipede assassins and allies (Heteroptera: Reduviidae: Ectrichodiinae, Tribelocephalinae): total evidence phylogeny, revised classification and evolution of sexual dimorphism. *Systematic Entomology* 42(3):575–595. <https://doi.org/10.1111/syen.12232>
14. Gil-Santana HR, Salomão AT, Oliveira J (2017) First description of the male and redescription of the female of *Parahiranetis salgadoi* Gil-Santana (Hemiptera, Reduviidae, Harpactorinae). *ZooKeys* 671: 19–48. <https://doi.org/10.3897/zookeys.671.11985>
15. Hsiao TY, Ren SZ (1981) Reduviidae. In: Hsiao, T.Y. (Eds.), *A Handbook for the Determination of the Chinese Hemiptera-Heteroptera*. Vol. II. Science Press, Beijing: 390–538.
16. Ishikawa T, Cai W, Tomokuni M (2007) *Sphedanolestes albipilosus* (Hemiptera: Heteroptera: Reduviidae), a new harpactorine species from the Ryukyus and Taiwan. *Zootaxa* 1388 (1): 45. <http://dx.doi.org/10.11646/zootaxa.1388.1.3>
17. Jakovlev BE (1893) Reduviidae Palaearcticae novae. *Horae Societatis Entomologicae Rossicae* 27: 319–325 (1–17).
18. Kalyaanamoorthy S, Minh BQ, Wong T, Haeseler von A, Jermin LS (2017) ModelFinder: fast model selection for accurate phylogenetic estimates. *Nat Methods* 14, 587–589. <https://doi.org/10.1038/nmeth.4285>
19. Kwadjo KE, Doumbia M, Haubruge E, Kra KD, Tano Y (2010) Sexual dimorphism in adults of *Rhynocoris albopilosus* Signoret (Heteroptera: Reduviidae). *Journal of Applied Biosciences* 2010 Vol.30: 1873–1877.
20. Livingstone D, Ravichandran G (1990) Two new species of Harpactoraria from Southern India (Heteroptera: Reduviidae: Harpactorinae). *Journal of Bombay Natural History Society* 86: 422–424.

21. Maldonado J (1990) Systematic catalogue of the Reduviidae of the World. Caribbean Journal of Science, Special publication No. 1: 171–172.
22. Miller NCE (1941) New genera and species of Malaysian Reduviidae (continued). Part II. Journal of the Federated Malay States Museums, 18: 601–773.
23. Miller NCE (1954) New genera and species of Reduviidae from Indonesia and the description of a new subfamily (Hemiptera – Heteroptera). Tijdschrift Voor Entomologie 97: 75–114.
24. Minh BQ, Schmidt HA, Chernomor O, Schrempf D, Woodhams MD, von Haeseler A, Lanfear R (2020) IQ-TREE 2: new models and efficient methods for phylogenetic inference in the genomic era. Mol Biol Evol 37:1530–1534. <https://doi.org/10.1093/molbev/msaa015>
25. Rambaut A, Drummond AJ, Xie D, Baele G, Suchard MA (2018) Posterior summarization in Bayesian phylogenetics using Tracer 1.7. Systematic Biology. Syy032. <https://doi.org/10.1093/sysbio/syy032>
26. Reuter OM (1881) Ad cognitionem Reduviidarum mundi antique. Acta Societatis Scientiarum Fennicae 12: 269–339.
27. Ronquist F, Huelsenbeck JP (2003) MrBayes: Bayesian Phylogenetic Inference under Mixed Models. Bioinformatics, 19 (12), 1572–1574. <https://doi.org/10.1093/bioinformatics/btg180>
28. Schouteden H (1910) Hemiptera 9. Reduviidae, Pyrrhocoridae and Coreidae. Sjostedts Kilimandjaro-Meru expedition 12: 145–160.
29. Stål C (1861) Miscellanea hemipterologica - Entomologische Zeitung entomologischen Vereine zu Stettin, 22 Jahrgang, 4–6: 147.
30. Stål C (1863) Formae speciesque novae Reduviidum. Annales de la Société entomologique de France 3: 38.
31. Stål C (1870) Hemiptera insularum Philipinarum. Öfversigt af Kongl. Vetenskaps-akademiens forhandlingar 27: 607–776.

32. Stål C (1874) Enumeratio Reduviidarum Europae, Africa, Asiae, et Australiae. In: Ennumeratio Hemipterorum, IV. Kongl. Svenska Vetenskaps-Akademiens Handlingar 4:3–97.
33. Weirauch C, Forthman M, Grebennikov V, Baňář P (2017) From Eastern Arc Mountains to extreme sexual dimorphism: systematics of the enigmatic assassin bug genus *Xenocaucus* (Hemiptera: Reduviidae: Tribelocephalinae). *Organisms Diversity & Evolution* 17: 421–445. <https://doi.org/10.1007/s13127-016-0314-2>
34. Zhao P, Ren S, Wang B, Cai W (2015) A new species of the genus *Sphedanolestes* Stål 1866 (Hemiptera: Reduviidae: Harpactorinae) from China, with a key to Chinese species. *Zootaxa* 3985 (4): 591–599. <http://dx.doi.org/10.11646/zootaxa.3985.4.8>

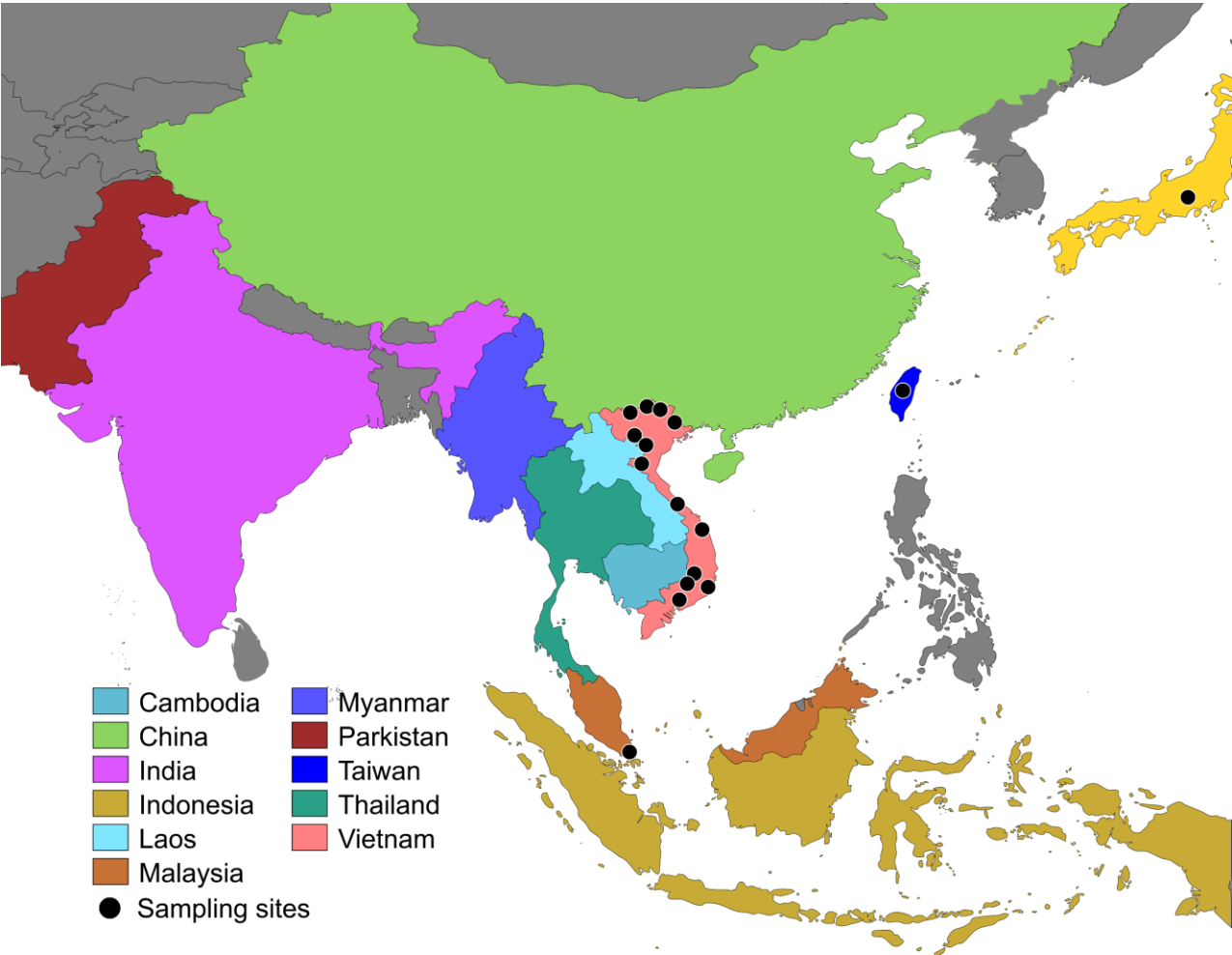


Figure 5.1. Sampling sites.

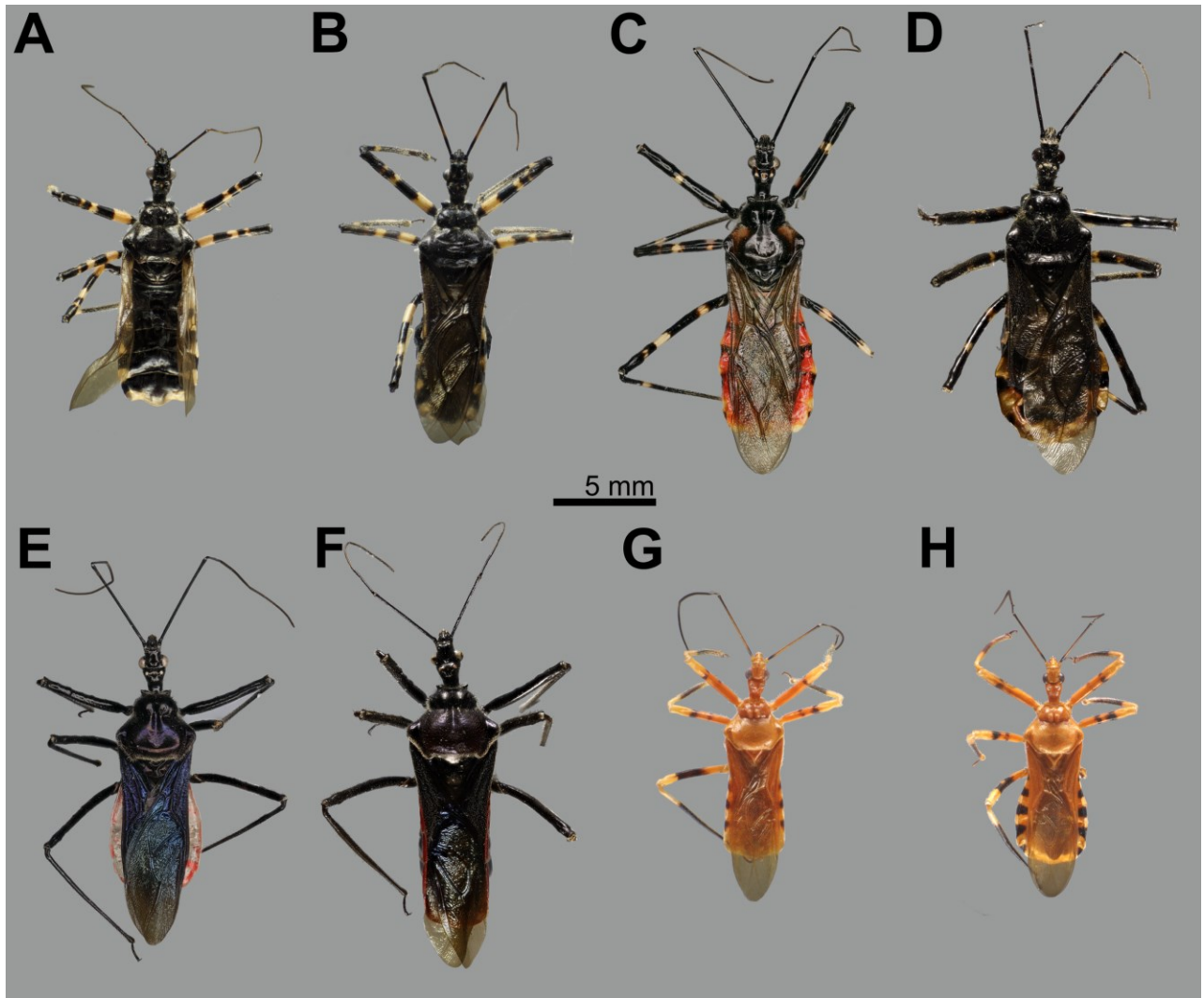


Figure 5.2. Sexual dimorphism in external morphology of male and female adults of *Sphedanolestes* sensu lato species. **A–H**, body in dorsal view. **A, B, C, D**, *Sphedanolestes* sp. HNL001 (*S. impressicollis* (Stål, 1861)); **E, F**, “gen. C” sp. HNL001 (“*Sphedanolestes*” *pubinotus* Reuter, 1881); **G, H**, “gen. D” sp. HNL001 (“*Sphedanolestes*” *xiongi* Cai et al. 2004). **A**, EG2020-001, ♂; **B**, EG2019-002, ♀; **C**, NDD2022-075, ♂; **D**, TXL2021-007, ♀; **E**, NDD2022-007, ♂; **F**, TXL2021-006, ♀; **G**, NDD2019-292, ♂; **H**, NDD2019-314, ♀.

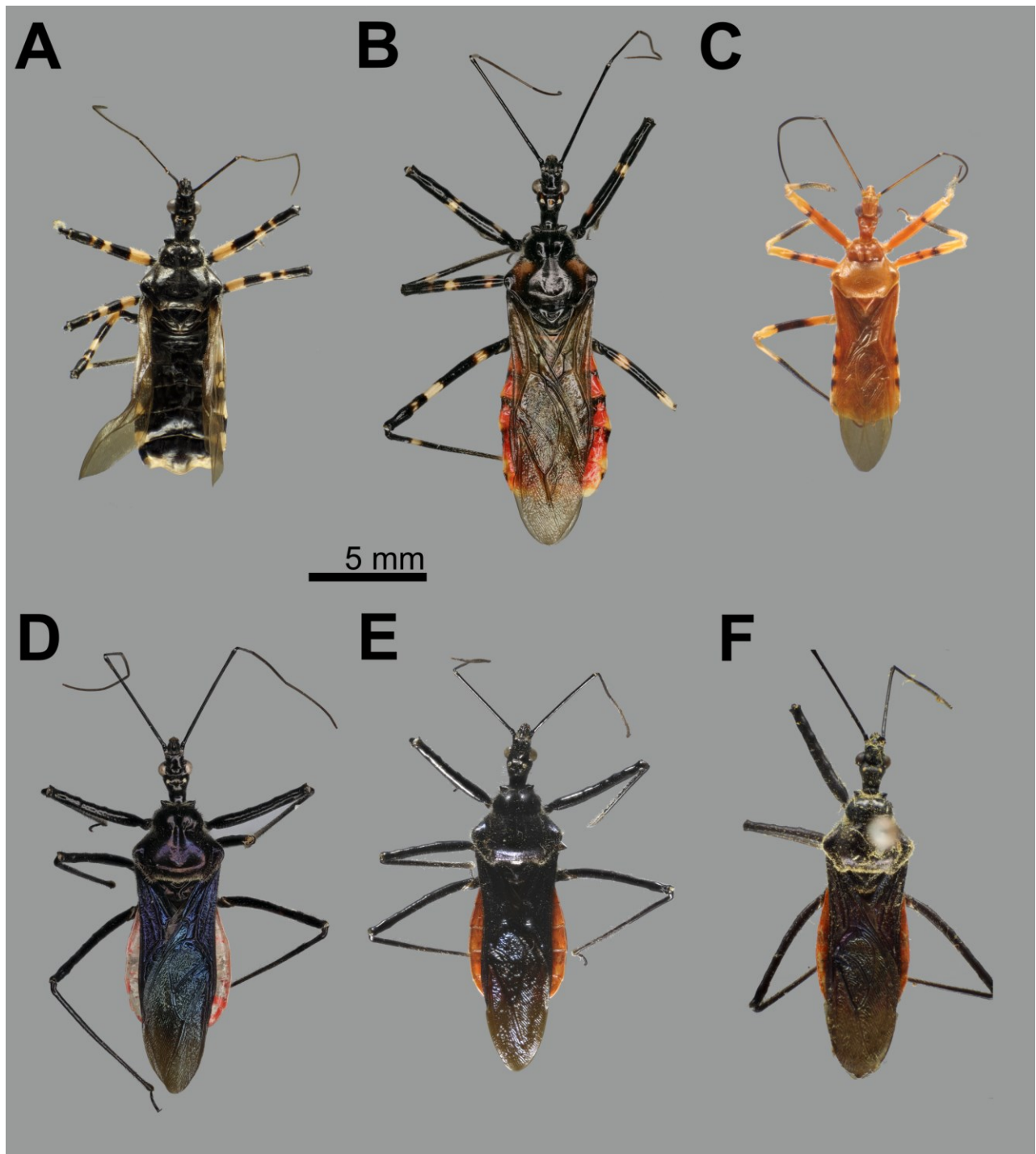


Figure 5.3. Male-based morphospecies. **A–E**, body in dorsal view. **A**, EG2020-001, ♂, *Sphedanolestes* sp. M1; **B**, NDD2022-075, ♂, *S.* sp. M2; **C**, NDD2022-007, ♂, “gen. C” sp. M1; **D**, TXLBX6, ♂, “gen. C” sp. M2; **E**, TXL2000-063, ♂, “gen. C” sp. M3; **F**, NDD2019-292, ♂, “gen. D” sp. M1.

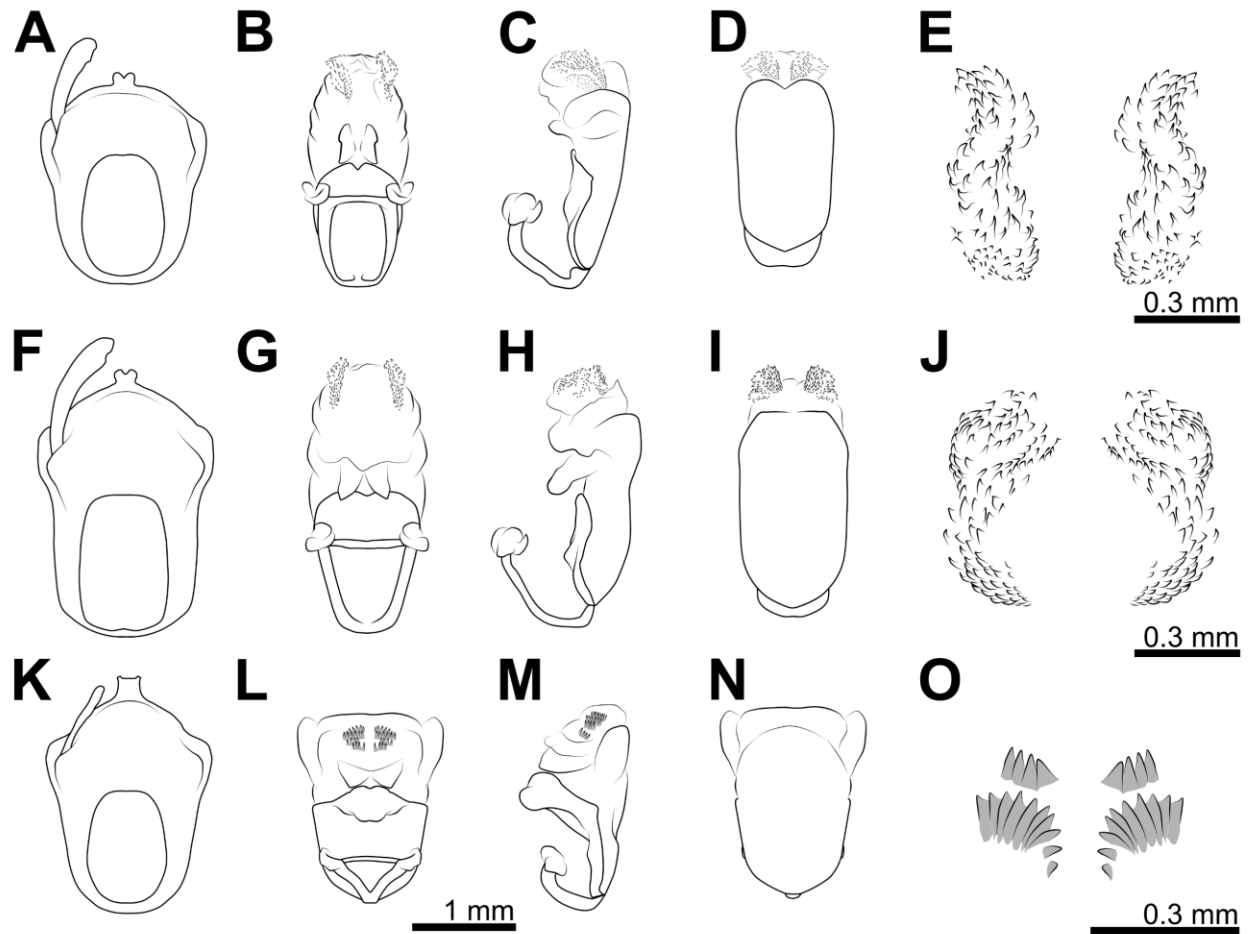


Figure 5.4. Genital morphology of male-based morphospecies of *Sphedanolestes* and genus D. **A–E**, EG2020-001, ♂, *S. sp. M1*; **F–J**, TXL2018-842, ♂, *S. sp. M2*; **K–O**, NDD2019-282, ♂, “gen. D” sp. M1. **A, F, K**, pygophore in dorsal view; **B, G, L**, phallus in dorsal view; **C, H, M**, phallus in lateral view; **D, I, N**, phallus in ventral view; **E, J, P**, distal dorsal lobe of endosoma (ddl).

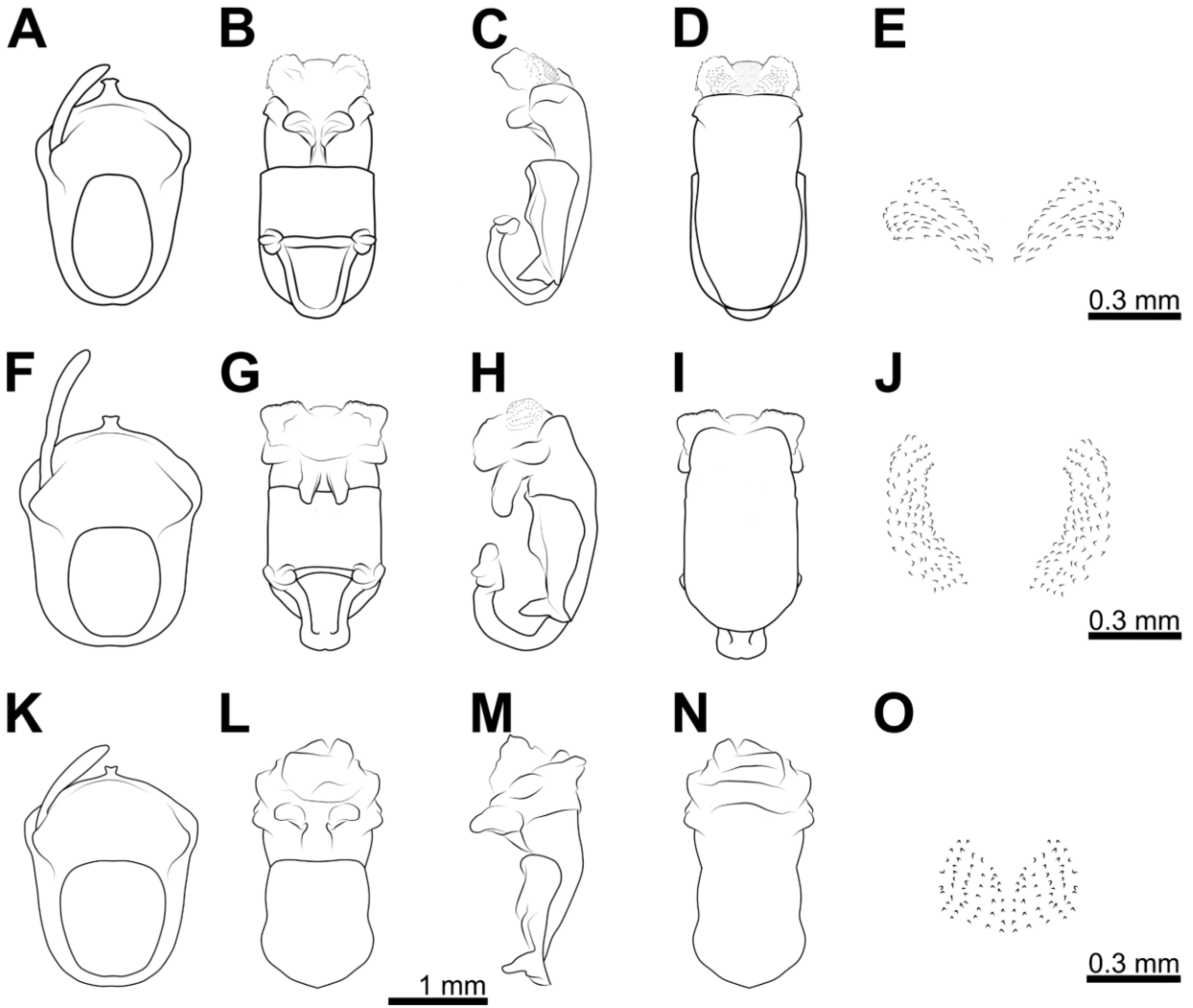


Figure 5.5. Genital morphology of male-based morphospecies of genus *C*. **A–E**, TXLBX11, ♂, “gen. *C*” sp. M1; **F–J**, TXLBX6, ♂, “gen. *C*” sp. M2; **K–O**, TXL2000-063, ♂, “gen. *C*” sp. M3. **A, F, K**, pygophore in dorsal view; **B, G, L**, phallus in dorsal view; **C, H, M**, phallus in lateral view; **D, I, N**, phallus in ventral view; **E, J, P**, distal dorsal lobe of endosoma (ddl).

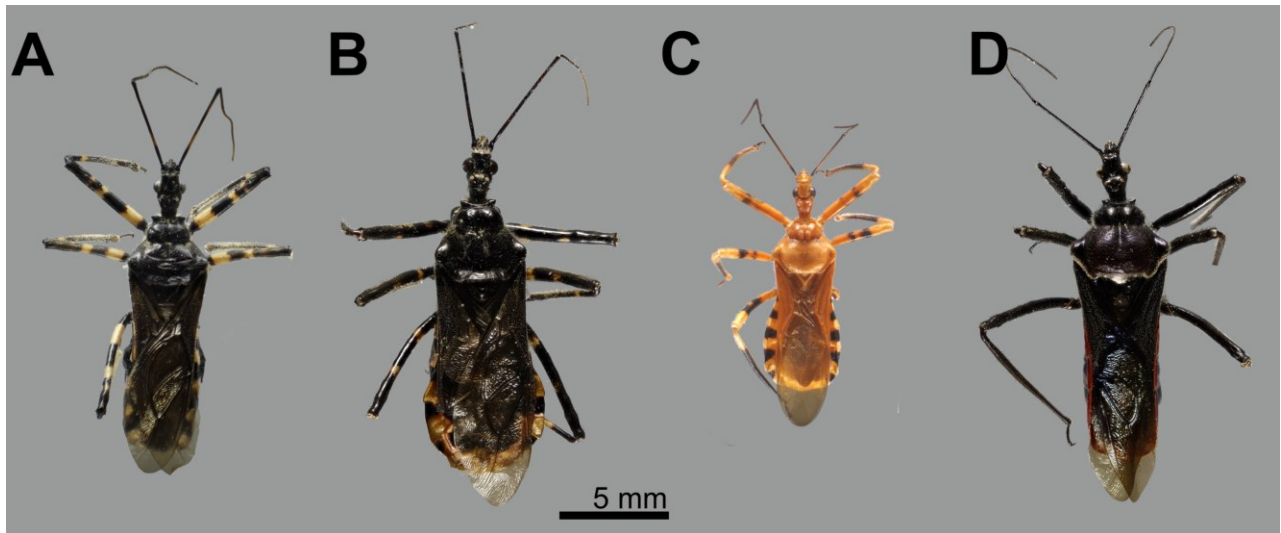


Figure 5.6. Female-based morphospecies of the three genera. **A–D**, Body in dorsal view. **A**, EG2019-002, ♀, *S.* sp. F1; **B**, TXL2021-007, ♀, *S.* sp. F2; **C**, NDD2019-314, ♀, “gen. D” sp. F1; **D**, TXL2021-006, ♀ “gen. C” sp. F1.

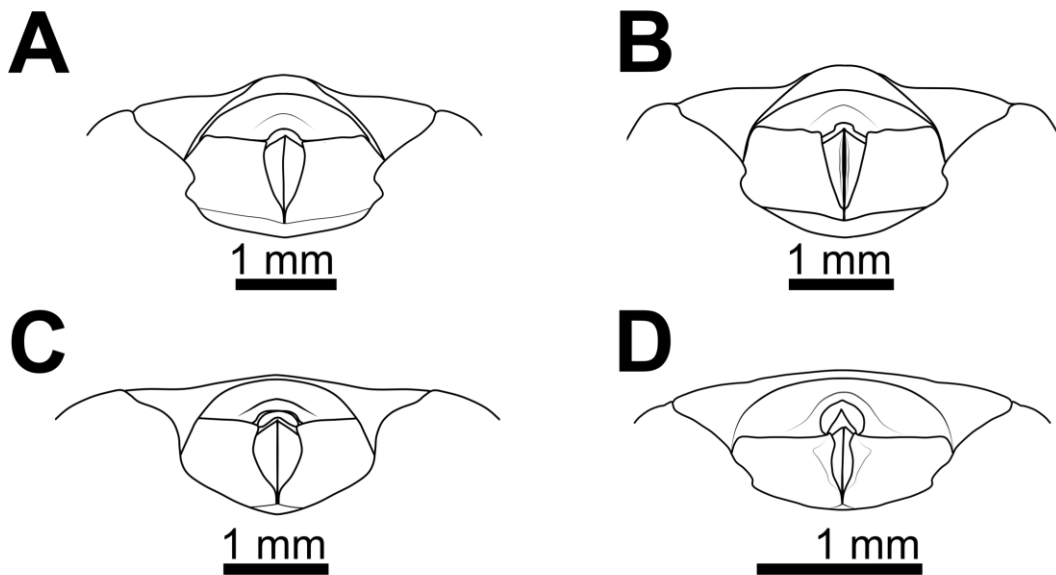


Figure 5.7. Female genital structure of female-based morphospecies of the three genera. Female-based morphospecies of the three genera. **A–D**, External female genitalia in ventral view. **A**, EG2019-002, ♀, *S.* sp. F1; **B**, AD2020-030, ♀, *S.* sp. F2; **C**, TXL2021-006, ♀, “gen. C” sp. F1; **D**, NDD2019-314, ♀, “gen. D” sp. F1.

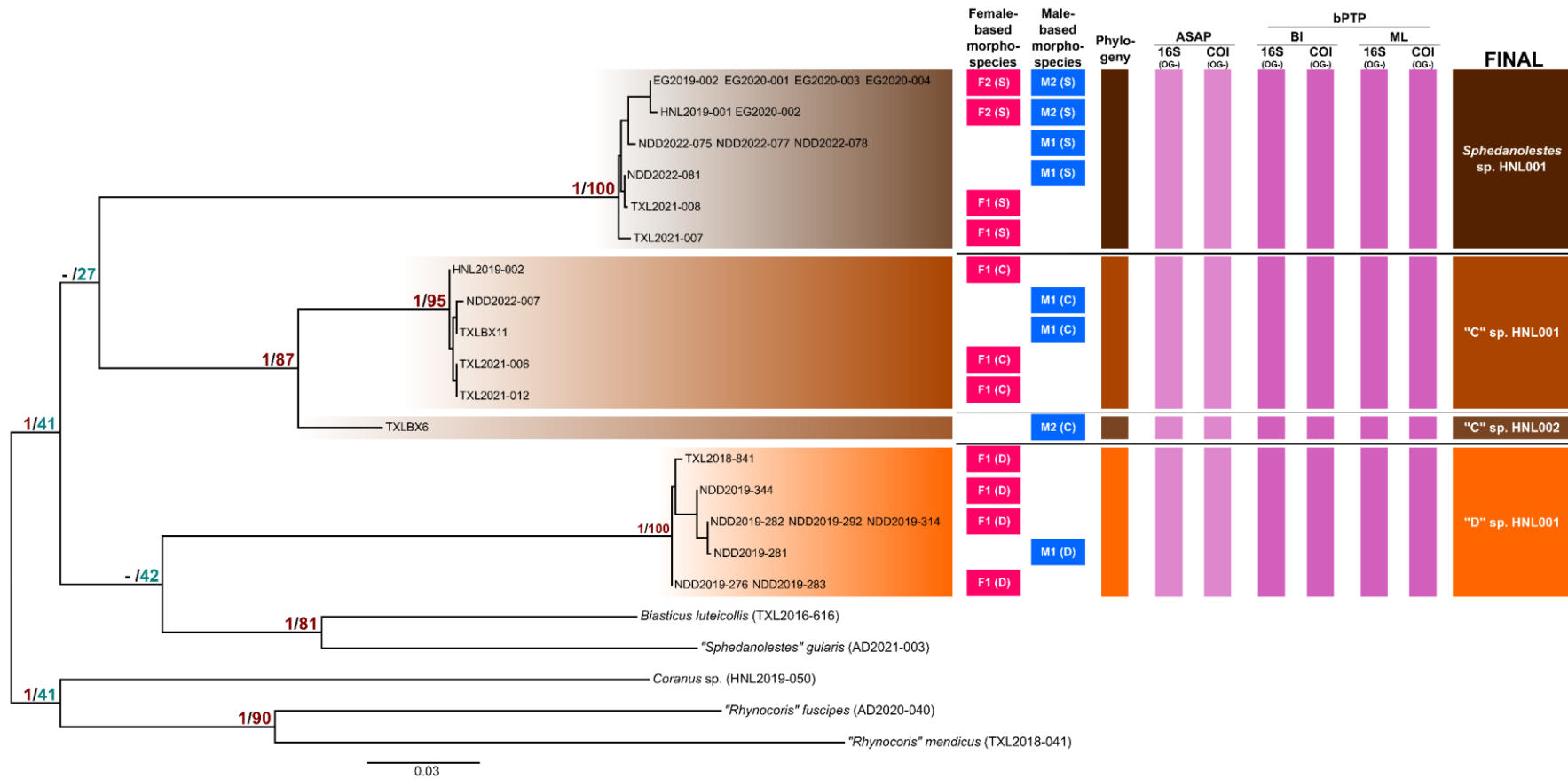


Figure 5.8. Bayesian inference phylogenetic trees based on the concatenated 16S + COI dataset (1085 bp) of the genera *Sphedanolestes*, C and D. Supports by posterior probability (PP) and bootstrap value (BP in %) are indicated behind each node. In which, red is indicated for a high supporting value (PP \geq 0.95; BP \geq 80), and blue is indicated for a low supporting value (PP $<$ 0.95; BP $<$ 80).

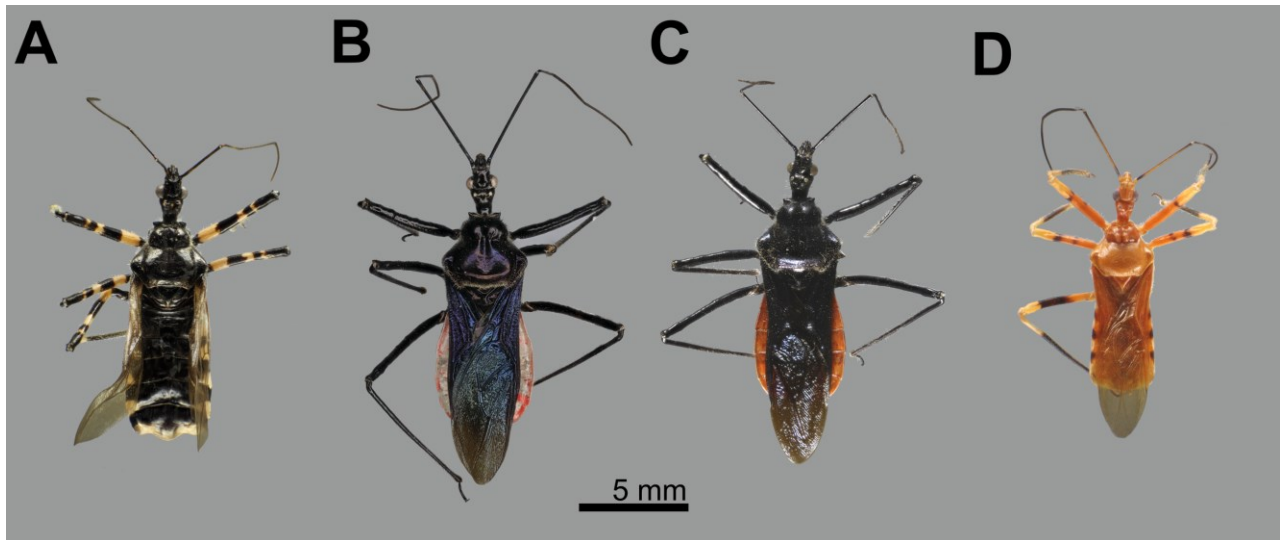


Figure 5.9. Habitus images of fully recognized species of the three genera. **A–D**, body in dorsal view. **A**, *Sphedanolestes* sp. HNL001, EG2020-001, ♂; **B**, “gen. C” sp. HNL001, NDD2022-007, ♂; **C**, “gen. C” sp. HNL002, TXLBX6, ♂; **D**, “gen. D” sp. HNL001, NDD2019-292, ♂.

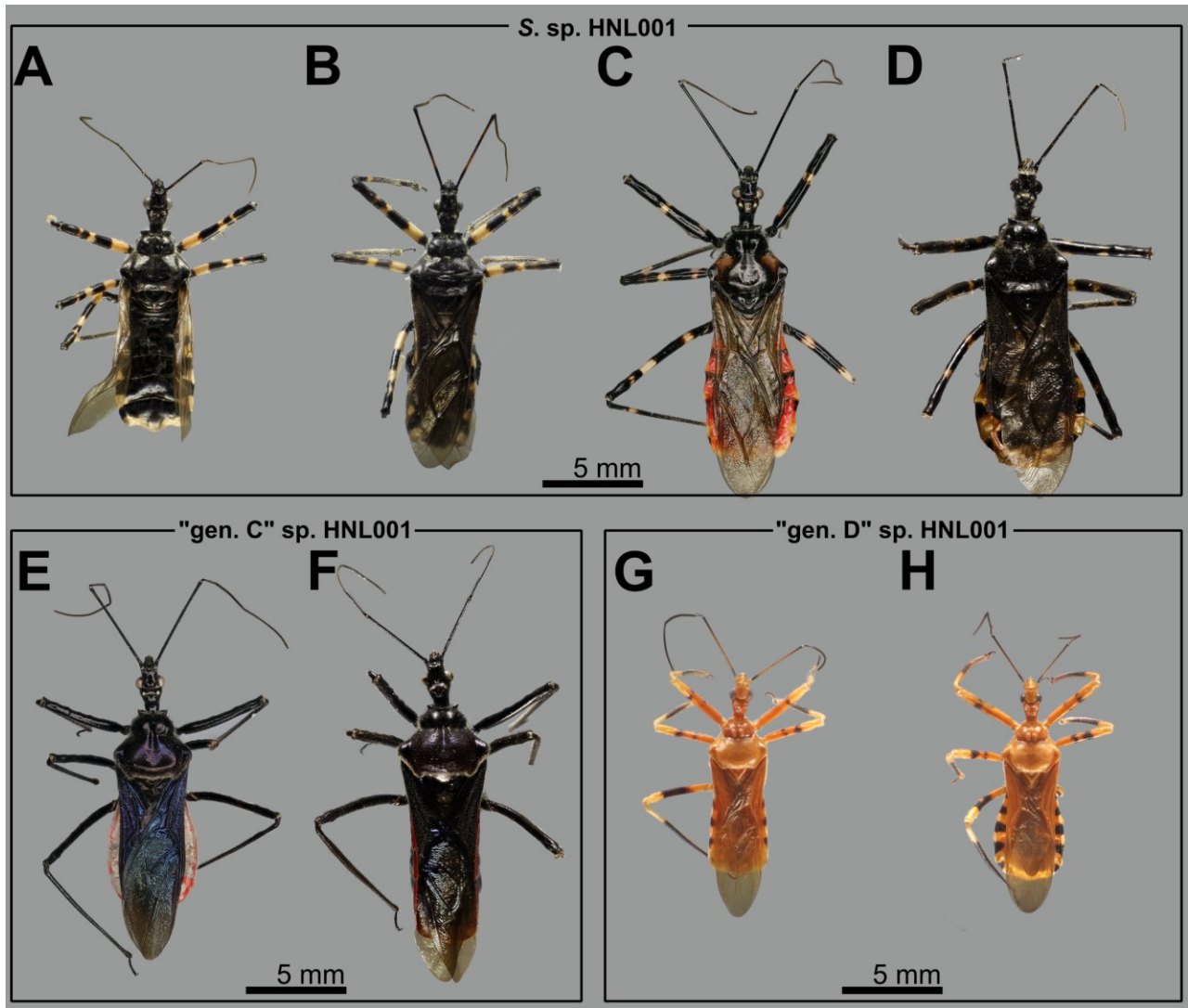


Figure 5.10. Male-female combinations of the three genera. **A–H**, body in dorsal view. **A, B, C, D**, *Sphedanolestes* sp. HNL001; **E, F**, “gen. C” sp. HNL001; **G, H**, “gen. D” sp. HNL001 (“*Sphedanolestes*” *xiongi* Cai et al. 2004). **A**, EG2020-001, ♂; **B**, EG2019-002, ♀; **C**, NDD2022-075, ♂; **D**, TXL2021-007, ♀; **E**, NDD2022-007, ♂; **F**, TXL2021-006, ♀; **G**, NDD2019-292, ♂; **H**, NDD2019-314, ♀.

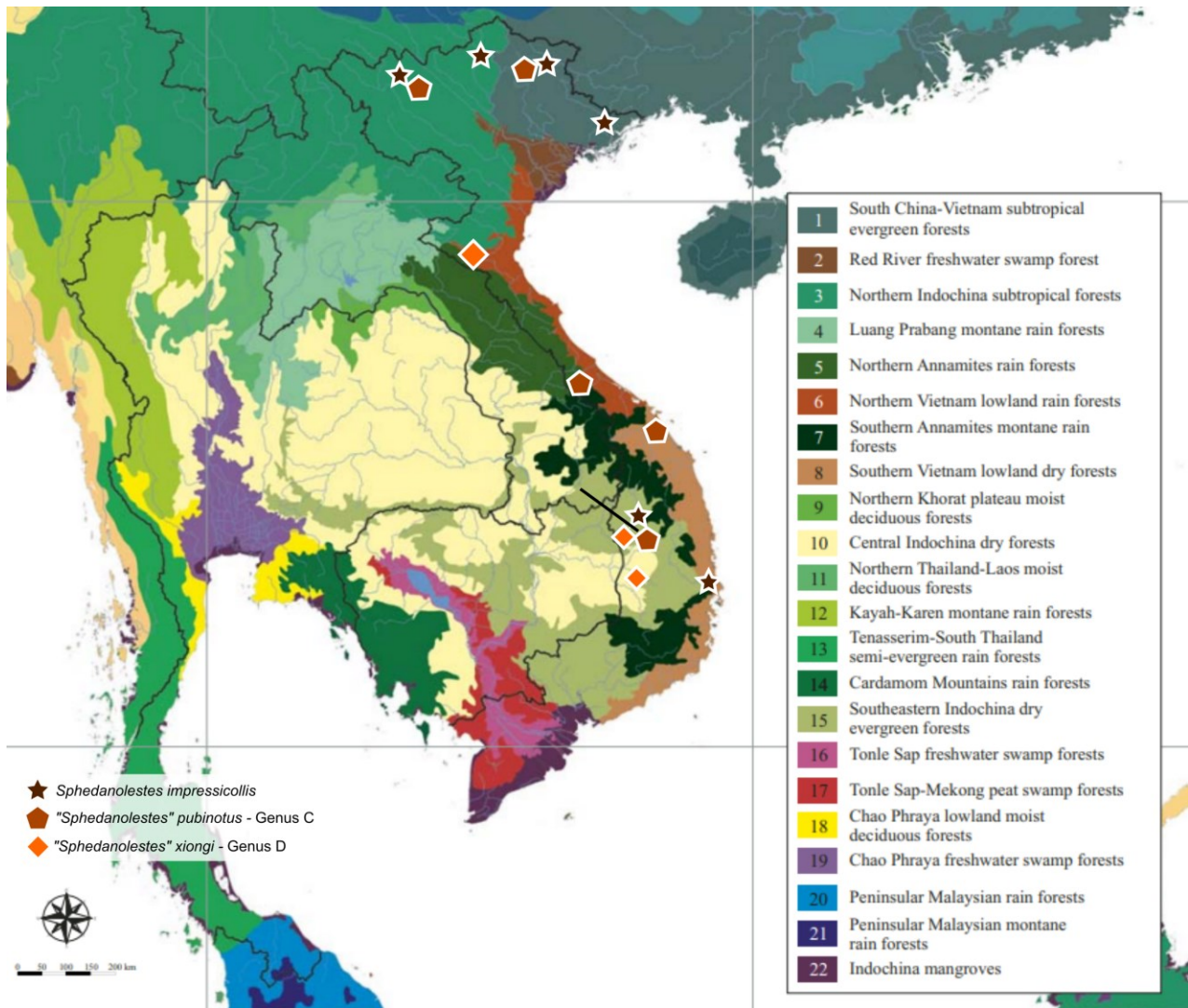


Figure 5.11. Distribution of genera *Spedanolestes*, C and D in Vietnam and surrounding areas compared to the vegetation of Indo-China (Poyarkov et al., 2021).

Table 5.1. Discrimination of species of the three genera with results of male-based and female-based morphospecies.

No	Male-based morphospecies	Female-based morphospecies	Final
			Species
1	<i>Sphedanolestes</i> sp. M1	<i>S.</i> sp. F1	<i>S.</i> sp. HNL001 (= <i>S. impressicollis</i> (Stål, 1861))
	<i>S.</i> sp. M2	<i>S.</i> sp. F2	
2	“gen. C” sp. M1	“gen. C” sp. F1	“gen. C” sp. HNL001 (= “ <i>Sphedanolestes</i> ” <i>pubinotus</i> Reuter, 1881)
3	“gen. C” sp. M2		“gen. C” sp. HNL002
4	“gen. D” sp. M1	“gen. D” sp. F1	“gen. D” sp. HNL001 (= “ <i>Sphedanolestes</i> ” <i>xiongi</i> Cai et al., 2004)

Appendix: Taxonomic accounts of *Sphedanolestes* sensu lato found in Vietnam and surrounding areas

1. Taxonomic accounts of the genus *Sphedanolestes* Stål, 1867, sensu stricto found in Vietnam and surrounding areas

Fully Recognized and Determined Species

***Sphedanolestes impressicollis* (Stål, 1861)**

(Fig. 5.3A, B, Fig. 5.4A–J, Fig. 5.6A, B, Fig. 5.7A, B, Fig. 5.9A, Fig 5.10A–D; Table 5.1)

Sphedanolestes impressicollis (Stål, 1861), in Stål (1861): 147.

Examined material. Non-type material. 4♂, HNL2019-001, Eg2020-001, Eg2020-003, Eg2020-004; 7♂, TXL2018-842, TXL2004-068, TXL2008-081, NDD2022-075, NDD2022-077, NDD2022-078, NDD2022-081; 2♀, Eg2019-002, Eg2020-002; 7♀, NDD2013-001, TXL2011-509, TXL2004-069, AD2020-033, TXL2021-007, TXL2021-008, AD2022-004.

Diagnosis. Body medium to large-sized, elongated, and somewhat robust, shiny black; base of first visible labial segment black; remaining of first visible segment pale brown or luteous; second visible labial segment dark brown, with a pale brown suffusion ventrally; remaining of labium dark brown or blackish brown; anterior pronotal lobe black with a few short slender, erect setae; posterior pronotal lobe black and covered with short slender, erect setae, especially dense in anterior margin; scutellum black with slender, erect setae in lateral areas and densely at posterior apex; abdominal mediotergites black; anterior half of each laterotergite black; posterior half of each laterotergite luteous; abdominal sternites luteous with lateral margin areas black; femora luteous and black annulated; tibiae black, paler and browner toward tip, with a luteous suffusion near basal.

Var. Body large-sized; posterior pronotal lobe black, sometimes suffused with brown; abdominal mediotergites red; laterotergites red, anterior 1/3 of lateral margin of each laterotergite black or brown; posterior 1/3 of lateral margin of each laterotergite luteous.

Distribution. China, Japan, Korea, Vietnam.

Type locality. Hong Kong.

2. Taxonomic accounts of the genus C found in Vietnam and surrounding areas

Fully Recognized and Determined Species

***“Sphedanolestes” pubinotus* Reuter, 1881**

(Fig. 5.3D, Fig. 5.5A–E, Fig. 5.6D, B, Fig. 5.7C, Fig. 5.9B, Fig 5.10E, F; Table 5.1)

“Sphedanolestes” pubinotus Reuter, 1881, in Reuter (1881): 289.

Examined material. Non-type material. 3♂, VN-HEM-2011-009, NDD2022-007, TXLBX11; 5♀, HNL2019-002, TXL2021-006, TXL2021-012, TXL2004-070, AD2020-003.

Diagnosis. Body large-sized, elongated, and somewhat robust, shiny black; labium black; anterior pronotal lobe black and covered with black thick erect setae; posterior pronotal lobe black and densely covered with black thick erect setae; posterior and lateral margins of posterior pronotal lobe densely covered with short griseous bent setae; scutellum black with black erect setae in lateral areas and densely at posterior apex; laterotergites red or sanguineous; abdominal sternites red or sanguineous with lateral areas of sternites IV to VI with black or blackish brown horizontal suffusion; coxae, trochanters, femora, and tibiae black.

Distribution. India, Myanmar, China, Laos, Vietnam, Indonesia, Malaysia.

Type locality. India.

Fully Recognized and Undetermined Species

“gen. C” sp. HNL002

(Fig. 5.3E, Fig. 5.5F–J, Fig. 5.9C; Table 5.1)

Examined material. Non-type material. 1♂, TXLBX6.

Diagnosis. Body large-sized, elongated, and somewhat robust, shiny black; labium black; anterior pronotal lobe black and covered with black thick erect setae; posterior pronotal lobe black and densely covered with black thick erect setae; posterior and lateral margins of posterior pronotal lobe densely covered with short griseous bent setae; scutellum black with black erect setae in lateral areas and densely at posterior apex; laterotergites red or sanguineous; abdominal sternites reddish-orange with lateral areas of sternites III to VI with luteous suffusion; coxae, trochanters, femora, and tibiae black.

Distribution. Vietnam.

Morphospecies Species not yet confirmed by the Integrative Taxonomy

“gen. C” sp. M3

(Fig. 5.3F, Fig. 5.5K–O; Table 5.1)

Examined material. Non-type material. 1♂, TXL2000-063.

Diagnosis. Body large-sized, elongated, and somewhat robust, shiny black; labium black; anterior pronotal lobe black and covered with black thick erect setae; posterior pronotal lobe black and densely covered with black thick erect setae; posterior and lateral margins of posterior pronotal lobe densely covered with short griseous bent setae; scutellum black with black erect setae in lateral areas and densely at posterior apex; laterotergites red or sanguineous; abdominal sternites reddish-orange; coxae, trochanters, femora, and tibiae black.

Distribution. Vietnam.

3. Taxonomic accounts of the genus D found in Vietnam and surrounding areas

Fully Recognized and Determined Species

“*Sphedanolestes*” *xiongi* Cai et al., 2004

(Fig. 5.3C, Fig. 5.4K–O, Fig. 5.6C, B, Fig. 5.7D, Fig. 5.9D, Fig 5.10G, H; Table 5.1)

“*Sphedanolestes*” *xiongi* Cai et al., 2004, in Cai et al. (2004): 385–387.

Examined material. Non-type material. 3♂, NDD2019-282, NDD2019-292, TXL2003-067; 8♀, NDD2019-276, NDD2019-281, NDD2019-283, NDD2019-313, NDD2019-314, NDD2019-344, TXL2018-841, TXL2003-066.

Diagnosis. Body medium-sized, elongated, and somewhat robust, shiny orangish brown; labium brownish orange; anterior pronotal lobe orangish brown with a few short thick erect setae; posterior pronotal lobe orangish brown and covered with short thick erect black setae; posterior and lateral margins of posterior pronotal lobe densely covered with short griseous bent setae; scutellum orangish brown with short erect setae and densely covered with short bent pubescence at posterior apex; laterotergites orangish brown, anterior half of lateral margin of each laterotergite blackish brown; posterior half of lateral margin of each laterotergite pale luteous; abdominal sternites orangish brown or brown; coxae, trochanters brown; femora, and tibiae black except for base of femora and tibia and apical area of femora pale brown.

Distribution. China, Vietnam.

Type locality. China.

CHAPTER 6:
DISCRIMINATION OF THE SPECIES OF
RHYNOCORIS SENSU LATO
(HEMIPTERA: HETEROPTERA: REDUVIIDAE)
KNOWN FROM VIETNAM AND SURROUNDING AREAS

Notification. The formal taxonomic actions will not be done in this thesis (disclaiming of taxonomic actions declared in the concerning work is supported by the International Code of Zoological Nomenclature: Article 8.3)

6.1. Introduction

Rhynocoris Hahn, 1834 is a reduviid genus, established with *Cimex iracundus* Poda, 1761 (syn. *Reduvius cruentus* Fabricius, 1787) as the type species of the genus. The genus has been allocated currently to the tribe Harpactorini, subfamily Harpactorinae of the family Reduviidae (Fabricius 1787; Hahn 1834; Maldonado 1990).

The present integrative approach (Chapter 3) did not support the monophyly of *Rhynocoris* and subdivided it into at least two independent genera, E and F, with revised morphological definitions of the two genera (see Appendix of Chapter 3). The two genera are collectively referred to as *Rhynocoris* sensu lato.

Rhynocoris sensu lato currently comprises 144 validly named species distributing widely in Afrotropical, Palearctic, Sino-Japanese, Oriental, and Nearctic Realms (Stål 1867; Distant 1903; Ambrose and Livingstone 1986; Maldonado 1990; Truong et al. 2015) (Fig. 2.6). Among them, three species have been recorded and described from Vietnam, i.e., *R. fuscipes* (Fabricius, 1787), *R. marginellus* (Fabricius, 1803), *R. mendicus* (Stål, 1867).

In the present study, the species-level classification of the Indo-Chinese species of *Rhynocoris* sensu lato (genera E and F) is revised by the integrative approach, as explained in Chapter 2.

6.2. Material and methods

The definitions of the two genera, E and F, follow the Appendix of Chapter 3. General information on sampling sites (Fig. 6.1), specimen depositories, and analytical methods (imaging, DNA sequencing, sequencing, and phylogenetic analyses) were given in Chapter 2. Additional information for this chapter is given below.

This study included 96 *Rhynocoris* and *Rhynocoris*-like specimens (65 male and 30 female adults and an immature specimen), of which 90 specimens were from Vietnam, 5 specimens from

Laos, and 1 specimen from Taiwan. Besides the above-mentioned 96 specimens, there were 23 type specimens from the Swedish Museum of Natural History (NRM) and the British Natural History Museum collection (BNHM) (Table 2.1).

The following type specimens were also examined for identifying the species: *Rhynocoris albopunctatus* (Stål, 1855) (a type specimen, NRM), *R. aulicus* (Stål, 1866) (a type specimen, NRM), *R. bellicosus* (Stål, 1865) (a type specimen, NRM), *R. carmelita* (Stål, 1859) (a type specimen, NRM), *R. cinctorius* (Stål, 1865) (a type specimen, NRM), *R. discoidalis* (Reuter, 1881) (a type specimen, NRM), *R. erythrocnemis* (Germar, 1837) (a type specimen, NRM), *R. illotus* Miller, 1941 (a holotype and a paratype, BNHM), *R. kiritshenkoi* Popov, 1964 (a type specimen, NRM), *R. latro* (Stål, 1855) (a type specimen, NRM), *R. leucospilus* (Stål, 1859) (a type specimen, NRM), *R. longifrons* (Stål, 1874) (a type specimen, NRM), *R. mendicus* (Stål, 1867) (a type specimen, NRM), *R. monachus* Miller, 1941 (a holotype and a paratype, BNHM), *R. nigripes* (Reuter, 1881) (a type specimen, NRM), *R. nigronitens* (Reuter, 1881) (a type specimen, NRM), *R. rapax* (Stål, 1855) (a type specimen, NRM), *R. suspectus* Schouteden, 1910 (a type specimen, NRM), *R. tristicolor* (Reuter, 1881) (a type specimen, NRM), *R. tristis* (Stål, 1855) (a type specimen, NRM), *R. venustus* (Stål, 1855) (a type specimen, NRM), *R. vicinus* (Schouteden, 1910) (a type specimen, NRM), and *R. vittiventris* (Stål, 1859) (a type specimen, NRM), (Table 2.1).

Furthermore, specimens of *B. luteicollis* Ha, Truong & Ishikawa, 2022, "*Sphedanolestes*" *pubinotus* Reuter, 1881, and *Coranus* sp. collected from Vietnam were used as outgroups in molecular phylogenetic analyses (Table 2.1).

Morphological examination of the validly named species of the genus was conducted by referring to the original descriptions, other taxonomic publications, and type specimens where available (Fabricius 1794, 1803; Stål 1867, 1874; Reuter 1881; Distant 1903, 1904, 1909; Schouteden 1910; Bergroth 1915; Miller 1941, 1948, 1954; Ambrose & Livingstone 1986; Dioli

1990) of the following congeners known from Vietnam and adjacent areas: *Rhynocoris aulicus* (Stål, 1866), type location: Malaysia; *R. cruralis* Bergroth, 1915, India; *R. fimbriatus* Miller, 1948, Indonesia; *R. fuscipes* (Fabricius, 1787), India (see also Table 2.1, 6.2); *R. illotus* Miller, 1941, Malaysia; *R. incertis* (Distant, 1903), China and Japan; *R. iracundus* (Poda, 1761), Greece; *R. kedahensis* Miller, 1941, Malaysia; *R. kumarii* Ambrose and Livingstone, 1986, India; *R. longifrons* (Stål, 1874), India; *R. maeandrus* Distant, 1909, Myanmar; *R. marginatus* (Fabricius, 1794), India and Sri Lanka; *R. marginellus* (Fabricius, 1803), Indonesia (see also Table 2.1, 6.2); *R. mendicus* (Stål, 1867), Malaysia (see also Table 2.1, 6.2); *R. milvus* Miller, 1948, Indonesia; *R. monachus* Miller, 1941, Indonesia; *R. niasensis* Miller, 1941, Indonesia; *R. nilgiriensis* Distant, 1903, India; *R. pygmaeus* (Distant, 1903), India; *R. rathjensi* Miller, 1954, Yemen; *R. reuteri* (Distant, 1879), India; *R. rubricus* (Germar in Ahrens, 1816), Iran; *R. rubrizonatus* Miller, 1954, Yemen; *R. suspectus* Schouteden, 1910, Tanzania; *R. tristicolor* (Reuter, 1881), India.

Similar to the genera *Biasticus* and *Sphedanolestes* sensu lato, the sexual dimorphism in external morphology of male and female adults is usually unclear in the genera E and F, while female adults commonly showed larger body size, more prominent abdomen, and more horizontally expanded connexivum than male adults (Kwadjo et al. 2010; Forthman 2017; Gil-Santana 2017; Weirauch et al. 2017; Chen et al. 2021) (Fig. 6.2). However, in order to take account of the importance of the sexual dimorphism, morphospecies recognition was made separately for males and females, and the male-based and female-based morphospecies are hereafter specified with unique codes such as “gen. E” sp. M1, “gen. E” sp. F1, “gen. F” sp. M1 or “gen. F” sp. F1, in which M and F mean the male and female-based morphospecies, respectively. Each morphospecies was characterized by the external and genitalia morphology of its sex.

The mitochondrial 16S dataset (480 bp; 75 ingroup OTUs, 3 outgroup OTUs) and the COI dataset (603 bp; 68 ingroup OTUs, 3 outgroup OTUs) were successfully obtained (as listed in Table

6.1). Molecular phylogenetic analyses were done based on the concatenated 16S + COI dataset. The substitution models, TPM3 + F + G4, TIM2 + F + I + G4, and (TPM3 + F + G4, TIM2 + F + I + G4), were selected respectively for the 16S^(OG+), COI^(OG+), and the concatenated 16S + COI datasets by Model Finder (Kalyaanamoorthy et al. 2017) executed in IQ-TREE 2.1.2 (Minh et al. 2020). Maximum likelihood (ML) examinations were then carried out using IQ-TREE 2.1.2 (Chernomor et al. 2016; Minh et al. 2020); bootstrap values (BP) were estimated from 1,000 replications. The generalized time-reversible (GTR) + Gama model was chosen for the 16S + COI dataset using Model Finder (Kalyaanamoorthy et al. 2017) under the Bayesian information criterion. The Bayesian inference (BI) evaluations were then executed for the data using MrBayes v.3.2.7 (Ronquist and Huelsenbeck 2003) with 20,000,000 production and statutory parameter configuration (examining every 500 generations and tuning constraints every 100 generations, with a burn-in of 25 %). The effective sampling size (ESS) of each constraint was verified to be > 200 using Tracer 1.7.2 (Rambaut et al. 2018). The nodes were designated as “well supported” when posterior probability (PP) ≥ 0.95 and BP ≥ 80 .

6.3. Results

6.3.1. Morphological Examination in the Male and Female Adults

Forty-seven male specimens were grouped into eight male-based morphospecies (“gen. E” sp. M1–M7 or “gen. F” sp. M1) based on characteristics presenting in external morphology, for example, body coloration, anterior and posterior pronotal lobes, and scutellum (Fig. 6.3). However, no remarkable distinct characteristics were found in the genital morphology of male-based morphospecies of genus E (Figs 6.4–6.5).

On the other hand, twenty female specimens were grouped into five female-based morphospecies (“gen. E” sp. F1–F4 or “gen. F” sp. F1) based on characteristics presenting in external

morphology, for example, body coloration, setation, anterior and posterior pronotal lobes, and scutellum (Fig. 6.6) and features presenting in female genitalia, for instance, the posterior margin of abdominal sternite VII, the shape and structure of gonocoxa VIII, and the inner margin of abdominal laterotergite VIII (Fig. 6.7).

6.3.2. Identities of the Morphospecies Based on the 16S + COI Phylogenetic Trees

For six male-based morphospecies, five female-based morphospecies, and a nymph, mitochondrial 16S and COI sequences were successfully obtained.

In both ML and BI trees, five putative species were recovered as independent monophyletic lineages with high supporting values ($PP \geq 0.99$; $BP \geq 95$), or singleton lineages were recovered by deep divergence from each other with long basal branches (Fig. 6.8). Among them, the lineage consisting of “gen. E” sp. M1, M2, and “gen. E” sp. F1, F4 was highly supported in the BI analysis ($PP = 0.99$) but was lowly supported in the ML analysis ($BP = 65$).

On the other hand, the lineage consisting of “gen. E” sp. M3 and “gen. E” sp. F2 was subdivided into four sub-lineages in the ML tree. Therefore, the male-based morphospecies “gen. E” sp. M3 was temporarily divided into four morphospecies, named “gen. E” sp. M3a–M3d, and the female-based morphospecies “E” sp. F2 will be temporarily separated to two morphospecies, i.e., “gen. E” sp. F2a–F2b. Three of the four sub-lineages, except the sub-lineage of “gen. E” sp. M3a and F2a, were recovered as lineages in both BI and ML trees with high supporting values ($PP \geq 0.99$; $BP \geq 95$). The sub-lineage consisting of “gen. E” sp. M3a and F2a was not supported in the ML tree ($BP = 55$) and not recovered as a lineage in the BI tree. Furthermore, the minimum interspecific distances in COI among each putative sub-lineage was 1.9–3.3 % in K2P and 1.8–3.2 % in p-distance, and the maximum intraspecific distance in COI of the lineage was 4.5 % in K2P and 4.3 % in p-distance (Table 6.1).

The phylogenetic independencies of the above five lineages were also supported consistently by ASAP and bPTP based on the COI^(OG⁻) and 16S^(OG⁻) datasets (Fig. 6.8). The four sub-lineages mentioned above were subdivided into four lineages in phylogenetic analyses (BI and ML trees) and bPTP based on both ingroup datasets of 16S and COI, but not subdivided in ASAP based on the ingroup datasets of 16S and COI (Fig. 6.8).

6.4. Discussion

6.4.1. Full Recognition of the Species and Identification

It is reasonable that the following eight OTUs, which were consistently recovered by the integrative approach, are treated as fully recognized species (or herein simply referred to as species): “gen. E” sp. HNL001 (= “gen. E” sp. M1 + “gen. E” sp. M2 + “gen. E” sp. F1 + “gen. E” sp. F5); “gen. E” sp. HNL002 (= “gen. E” sp. M3a + “gen. E” sp. F2a); “gen. E” sp. HNL003 (= “gen. E” sp. M3b + “gen. E” sp. F2b); “gen. E” sp. HNL004 (= “gen. E” sp. M3c); “gen. E” sp. HNL005 (= “gen. E” sp. M4); “gen. E” sp. HNL006 (= “gen. E” sp. M3d); “gen. E” sp. HNL007 (= “gen. E” sp. M6 + “gen. E” sp. F3); “gen. E” sp. HNL008; and “gen. F” sp. HNL001 (= “gen. F” sp. M1 + “gen. F” sp. F1).

However, there is only one incompatible case between morphological and molecular phylogenetic results. The color forms “gen. E” sp. M1 + “gen. E” sp. F1 (Fig. 6.10A–B) and “gen. E” sp. M2 + “gen. E” sp. F4 (Fig. 6.10C–D), which were discriminated from each other by the body coloration, were not discriminated by the present integrative approach, and so the two male-based and two female-based morphospecies are herein treated as intraspecific morphological phenotypes of a single species coded as “gen. E” sp. HNL001 (Fig. 6.10A–D). It is noted that the two color forms were recorded exclusively in Central Highlands of Vietnam, but the color form “gen. E” sp. M1 + “gen. E” sp. F1 was recorded mainly in May, while the color form “gen. E” sp. M2 + “gen. E”

sp. F4 was recorded exclusively in September. The genetic divergence corresponding to the two color forms was, however, not observed (Fig. 6.8).

Moreover, the lineage, consisting of “gen. E” sp. M3 and “gen. E” sp. F2, which is correlated to four sub-lineages, “gen. E” sp. M3a + “gen. E” sp. F2a, “gen. E” sp. M3b + “gen. E” sp. F2b, “gen. E” sp. M3c, and “gen. E” sp. M3d, was then treated as a species complex due to the controversial minimum interspecific distances in COI among each putative lineage (Min K2P = 1.9–3.3 %; Min p = 1.8–3.2 %; the speciation of Heteroptera might be considered if the minimum interspecific distance about 3 % in COI (Park et al., 2011)), but a high maximum intraspecific distance if assuming they are an independent lineage (Max K2P = 4.5 %, Max p = 4.3 % in COI) (Table 6.1). Moreover, their external and genital morphology were highly similar to each other (Figs 6.4–6.5, 6.11), and it is noted that it is difficult to discriminate the species of the genus E recognized in this study by examining male genitalia morphology (Figs 6.4–6.5). The species complex comprises four species, “gen. E” sp. HNL002 (= “gen. E” sp. M3a + “gen. E” sp. F2a); “gen. E” sp. HNL003 (= “gen. E” sp. M3b + “gen. E” sp. F2b); “gen. E” sp. HNL004 (= “gen. E” sp. M3c); and “gen. E” sp. HNL006 (= “gen. E” sp. M3d) (Fig. 6.11).

By examining type material and taxonomic articles (including the original descriptions) of the validly named species of the genus *Rhynocoris* and species of some closed related genera (*Sphedanolestes* and *Biasticus*), the following two species can be reasonably identified: “gen. E”. sp. HNL001 = “*Rhynocoris*” *mendicus* (Stål, 1867) and “gen. F”. sp. HNL001 = “*Rhynocoris*” *fuscipes* (Fabricius, 1787). Furthermore, the species complex of four species “gen. E”. sp. HNL002, HNL003, HNL004, and HNL006 were determined as “*Rhynocoris*” *marginellus* (Fabricius, 1803).

For the other two male-based morphospecies of the genus E (“gen. E” sp. M5 and “gen. E” sp. M7) and the other “*Rhynocoris*” *marginellus*-liked specimens, which were unable to involve in DNA sequencing, the status of the species and the conspecific male and female combination were not

confirmed in the present study. Future studies based on further comprehensive sampling are necessary to solve the issues.

The morphological diagnosis and taxonomic remarks for each fully recognized species, the remaining morphospecies, and the synonymic list for the three species identified above will be provided in the Appendix of this chapter. These may be useful as the prior working hypotheses (= operational taxonomic units) in future integrative taxonomic studies. The formal taxonomic actions will not be done in this thesis (disclaiming of taxonomic actions declared in the concerning work is supported by the International Code of Zoological Nomenclature: Article 8.3).

6.4.2. The Problem of Using Morphological Examination in Discrimination of Genus E

The conspecific male and female were revealed for four of the eight species of genus E, which were confirmed as being independent in this study. In these species, external morphology shows no remarkable conspecific sexual dimorphism. However, among the eight species, a polymorphic species and a species complex comprising four species have been recognized. Therefore, the morphological examination based on external and genital morphology might not be a reasonable approach for discriminating species of genus E.

6.4.3. Distribution and Biogeographical Criteria

Among eight fully recognized species, four were widely distributed in Indo-China, “gen. E” sp. HNL001, “gen. E” sp. HNL002, “gen. E” sp. HNL003, and “gen. F” sp. HNL001 (Fig. 6.13). Two other species were recorded in the Northern Part of Vietnam, i.e., “gen. E” sp. HNL004, “gen. E” sp. HNL006. The remaining two species, “gen. E” sp. HNL005 and “gen. E” sp. HNL007, were recorded with a single specimen or identical specimens, so the distribution of these species was not discussed in this study. Therefore, further studies with more sample sizes from larger geographical

scales should be conducted to reveal the distribution patterns and background factors of *Rhynocoris* sensu lato.

Moreover, the two color forms of “*Rhynocoris*” *mendicus* (= “gen. E” sp. HNL001) occurred sympatrically, but the color form “gen. E” sp. M1 + “gen. E” sp. F1 was recorded mainly in May, while the color form “gen. E” sp. M2 + “gen. E” sp. F4 was recorded exclusively in September. It is worth noted that the genetic divergence corresponding to the two color forms was, however, not observed.

6.4.4. The Future Prospect of This Study

Similar to Chapters 4 and 5, the present study highlighted that the assassin bug genera, such as *Rhynocoris*, still remained many unknown hidden, especially in cases of intraspecific polymorphism and cryptic species. Therefore, the species-level discrimination of the genus *Rhynocoris* sensu lato and other reduviid genera should be appraised again by integrated taxonomy.

The use of male genitalia was highlighted in this study for discriminating species of *Blasticus* but was unsuccessful in delimitating the species of genus E. Therefore, in order to reveal the species level of some genera, such as genus E, molecular phylogenetic approaches are required. Moreover, due to the limitation of specimens and species involved in this study, the usefulness of male genitalia for discriminating species of genus F, was not confirmed.

Furthermore, mostly validly-named species of the genus *Rhynocoris* sensu lato were only discriminated by morphological examination, and there has been no available DNA barcode database of the genus yet. Thus, studies on more extensive collections of fresh or relatively newly collected specimens suitable for DNA sequencing should be done in the future.

References

1. Ambrose DP, Livingstone D (1986) A new species of *Rhynocoris* (Fabricius) from Southern India (Heteroptera-Reduviidae-Harpactorinae). *The Journal of the Bombay Natural History Society* 83: 173–177.
2. Bergroth E (1915) Hemiptera from the Bombay Presidency. *The Journal of the Bombay Natural History Society* 24: 170–179.
3. Chen Z, Liu Y, Cai W (2021). Taxonomic review of *Xenorhynocoris* Miller (Heteroptera: Reduviidae: Ectrichodiinae), with description of *X. attractivus* sp. nov. and notes on sexual dimorphism of the genus. *European Journal of Taxonomy* 746(1): 26–49. <https://doi.org/10.5852/ejt.2021.746.1315>
4. Chernomor O, Haeseler von A, and Minh BQ (2016) Terrace aware data structure for phylogenomic inference from supermatrices. *Syst. Biol.*, 65: 997–1008. <https://doi.org/10.1093/sysbio/syw037>
5. Dioli P (1990) *Rhinocoris irancundus* (Poda, 1761) e *Rhinocoris rubricus* (Germar, 1816) in Valtellina. (Insecta, Heteroptera, Reduviidae). *Il Naturalista Valtellinese – Atti del Museo civico di Storia naturale di Morbegno*. 1: 55–60.
6. Distant WL (1903) Rhynchotal notes. XVI. Heteroptera: Family Reduviidae (continued). Apiomerinae, Harpactorinae and Nabidae. *The Annals and Magazine of Natural History* (7)11: 203–213.
7. Distant WL (1904) Rhynchota – Vol. II: The Fauna of British India, including Ceylon and Burma. London: Taylor and Francis.
8. Distant WL (1909) Rhynchota (Heteroptera) from British India. *Annales de la Société entomologique de Belgique* 53: 360–376.
9. Fabricius JC (1794) *Entomologia Systematica*. Hafniae IV: 197–198.

10. Fabricius JC (1803) *Systema Rhyngotorum. Brunsvigae*: Apud Carolum Richard. 314 pp.
11. Forthman M, Weiwauch C (2017) Millipede assassins and allies (Heteroptera: Reduviidae: Ectrichodiinae, Tribelocephalinae): total evidence phylogeny, revised classification and evolution of sexual dimorphism. *Systematic Entomology* 42(3):575–595.
<https://doi.org/10.1111/syen.12232>
12. Gil-Santana HR, Salomão AT, Oliveira J (2017) First description of the male and redescription of the female of *Parahiranetis salgadoi* Gil-Santana (Hemiptera, Reduviidae, Harpactorinae). *ZooKeys* 671: 19–48. <https://doi.org/10.3897/zookeys.671.11985>
13. Kwadjo KE, Doumbia M, Haubruge E, Kra KD, Tano Y (2010) Sexual dimorphism in adults of *Rhynocoris albopilosus* Signoret (Heteroptera: Reduviidae). *Journal of Applied Biosciences* 2010 Vol.30: 1873–1877.
14. Kalyaanamoorthy S, Minh BQ, Wong T, Haeseler von A, Jermin LS (2017) ModelFinder: fast model selection for accurate phylogenetic estimates. *Nat Methods* 14, 587–589.
<https://doi.org/10.1038/nmeth.4285>
15. Maldonado J (1990) Systematic catalogue of the Reduviidae of the World. *Caribbean Journal of Science*, Special publication No. 1: 171–172.
16. Miller NCE (1941) New genera and species of Malaysian Reduviidae (continued). Part II. *Journal of the Federated Malay States Museums*, 18: 601–773.
17. Miller NCE (1948) New genera and species of Reduviidae from the Philippines, Celebes, and Malaysia. *Transactions of the Entomological Society of London*, 99: 411–473.
18. Miller NCE (1954) New genera and species of Reduviidae from Indonesia and the description of a new subfamily (Hemiptera – Heteroptera). *Tijdschrift Voor Entomologie* 97: 75–114.

19. Minh BQ, Schmidt HA, Chernomor O, Schrempf D, Woodhams MD, von Haeseler A, Lanfear R (2020) IQ-TREE 2: new models and efficient methods for phylogenetic inference in the genomic era. *Mol Biol Evol* 37:1530–1534. <https://doi.org/10.1093/molbev/msaa015>
20. Rambaut A, Drummond AJ, Xie D, Baele G, Suchard MA (2018) Posterior summarization in Bayesian phylogenetics using Tracer 1.7. *Systematic Biology*. Syy032. <https://doi.org/10.1093/sysbio/syy032>
21. Ronquist F, Huelsenbeck JP (2003) MrBayes: Bayesian Phylogenetic Inference under Mixed Models. *Bioinformatics*, 19 (12), 1572–1574. <https://doi.org/10.1093/bioinformatics/btg180>
22. Park DS, Footitt R, Maw E, Hebert PDN (2011) Barcoding Bugs: DNA-Based Identification of the True Bugs (Insecta: Hemiptera: Heteroptera). *PLoS One*. 2011; 6(4): e18749. <https://doi.org/10.1371/journal.pone.0018749>
23. Reuter OM (1881) Ad cognitionem Reduviidarum mundi antique. *Acta Societatis Scientiarum Fennicae* 12: 269–339.
24. Schouteden H (1910) Hemiptera 9. Reduviidae, Pyrrhocoridae and Coreidae. *Sjostedts Kilimandjaro-Meru expedition* 12: 145–160.
25. Stål C (1867) Bidrag till Reduviidarnas kaennedom. *Öfversigt af Kongl. Vetenskaps-akademiens forhandlingar* 23, 235–302.
26. Stål C (1874) Enumeratio Reduviidarum Europae, Africa, Asiae, et Australiae. In: *Enumeratio Hemipterorum*, IV. *Kongl. Svenska Vetenskaps-Akademiens Handlingar* 4:3–97.
27. Truong XL, Cai WZ, Tomokuni M, Ishikawa T (2015) The assassin bug subfamily Harpactorinae (Hemiptera: Reduviidae) from Vietnam: an annotated checklist of species. *Zootaxa*, ISSN: 1175-5326:101–116. <https://doi.org/10.11646/zootaxa.3931.1.7>
28. Weirauch C, Forthman M, Grebennikov V, Baňář P (2017) From Eastern Arc Mountains to extreme sexual dimorphism: systematics of the enigmatic assassin bug genus *Xenocaucus*

(Hemiptera: Reduviidae: Tribelocephalinae). *Organisms Diversity & Evolution* 17: 421–445.

<https://doi.org/10.1007/s13127-016-0314-2>

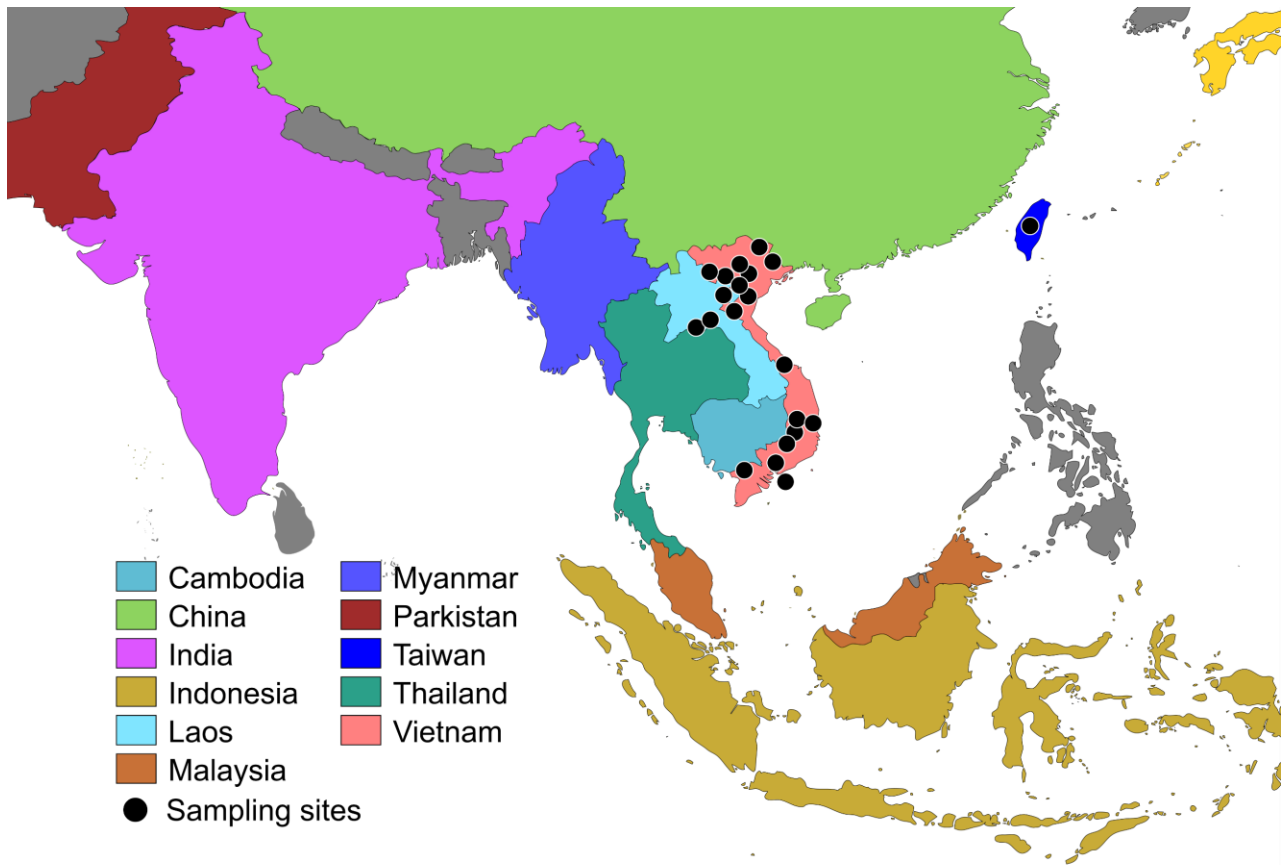


Figure 6.1. Sampling sites.

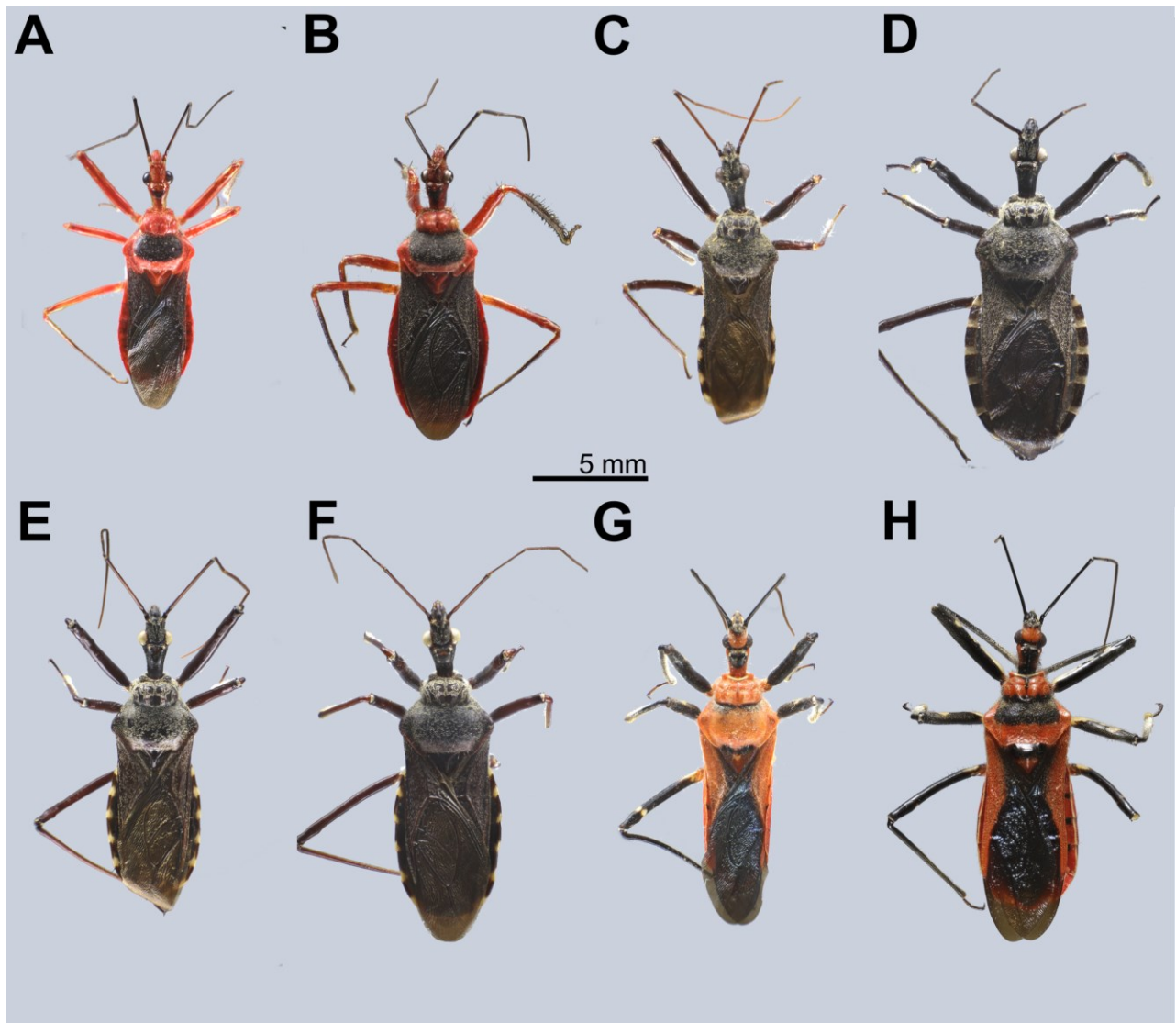


Figure 6.2. Male-female conspecific dimorphisms among species of genus E and F. **A, B**, “gen. E” sp. HNL001; **C, D**, “gen. E” sp. HNL002; **E, F**, “gen. E” sp. HNL003; **G, H**, “gen. F” sp. HNL001. **A**, AD2019-001, ♂; **B**, TXL2018-041, ♀; **C**, HNL2018-112, ♂; **D**, TXL2017-650, ♀; **E**, TXL2016-625, ♂; **F**, TXL2016-623, ♀; **G**, TXL2019-692, ♂; **H**, AD2020-040, ♀.

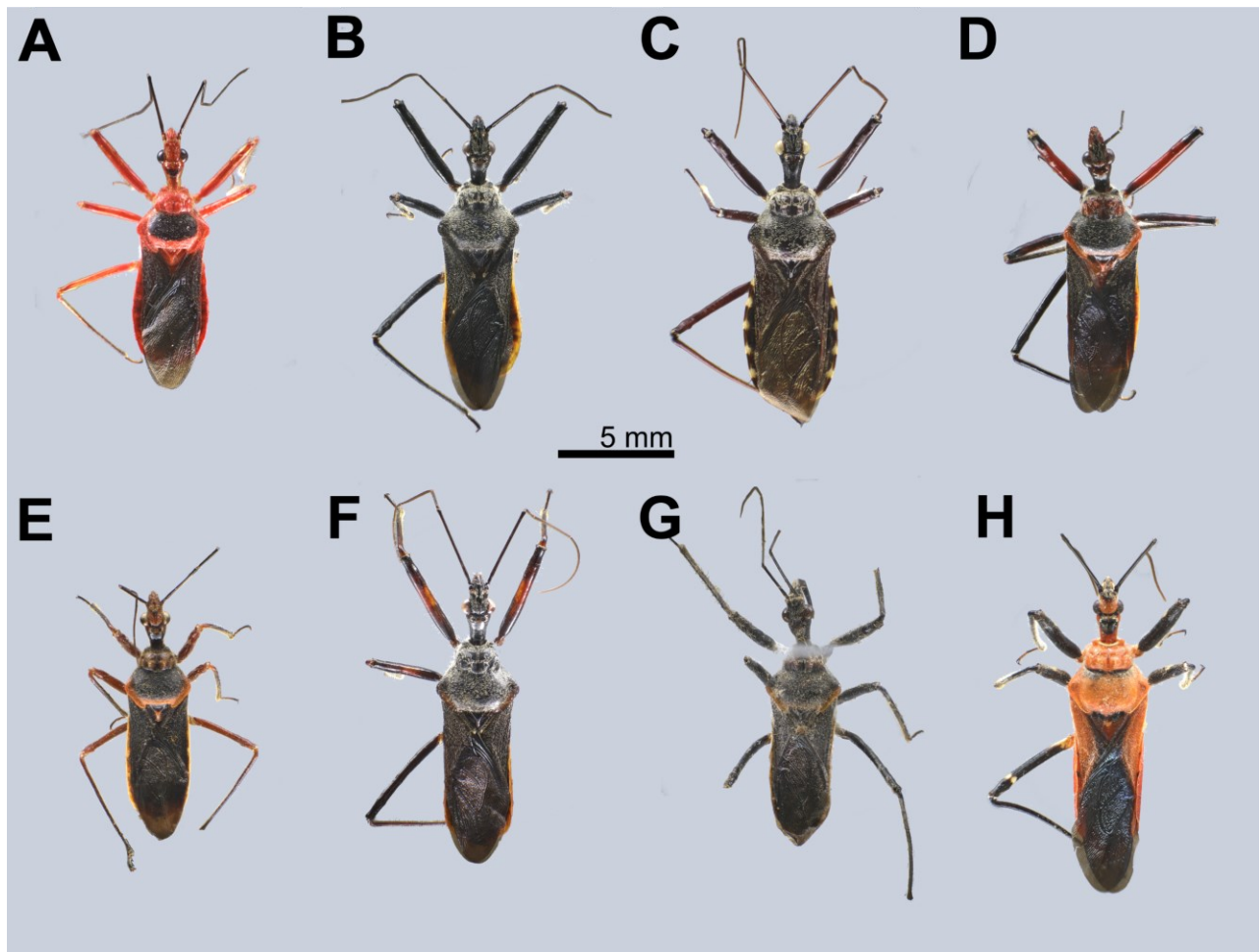


Figure 6.3. Body in dorsal view of male-based morphospecies. **A**, AD2019-001, ♂, “gen. E” sp. M1; **B**, NDD2019-245, ♂, “gen. E” sp. M2; **C**, TXL2016-625, ♂, “gen. E” sp. M3; **D**, NDD2019-277, ♂, “gen. E” sp. M3B; **E**, LA-Redu-2010-006, ♂, “gen. E” sp. M5; **F**, TXLBX24b, ♂, “gen. E” sp. M6; **G**, LA-Redu-2016-001, ♂, “gen. E” sp. M7; **H**, TXL2019-692, ♂, “gen. F” sp. M1.

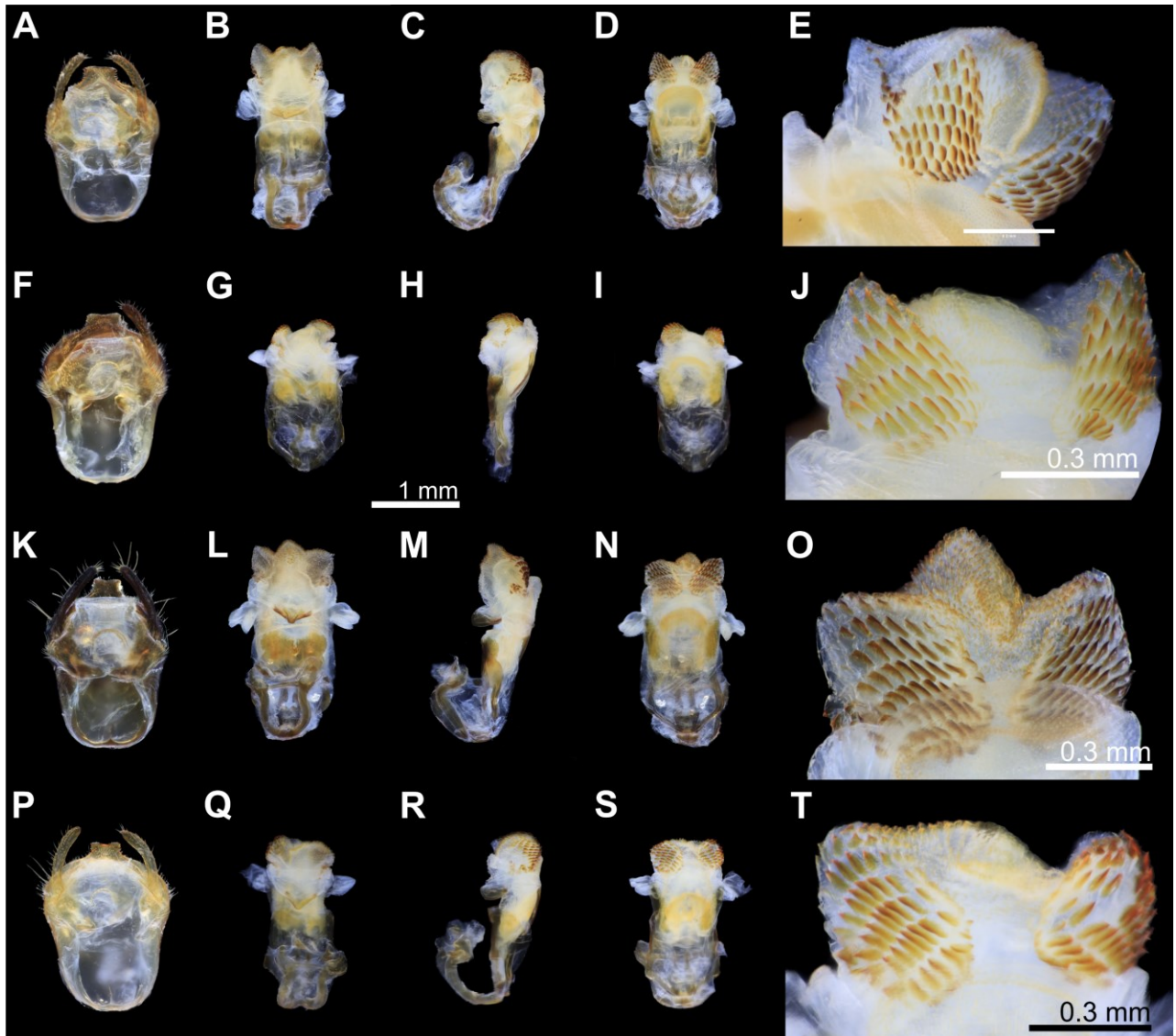


Figure 6.4. Genital morphology of male-based morphospecies. **A–E**, TXL2016-594, ♂, “gen. E” sp. M1; **F–J**, TXL2016-663, ♂, “gen. E” sp. M2; **K–O**, TXL2021-001, ♂, “gen. E” sp. M3; **P–T**, NDD2019-277, ♂, “gen. E” sp. M4. **A, F, K, P**, pygophore in dorsal view; **B, G, L, Q**, phallus in dorsal view; **C, H, M, R**, phallus in lateral view; **D, I, N, S**, phallus in ventral view; **E, J, O, T**, distal dorsal lobe of endosoma (ddl).

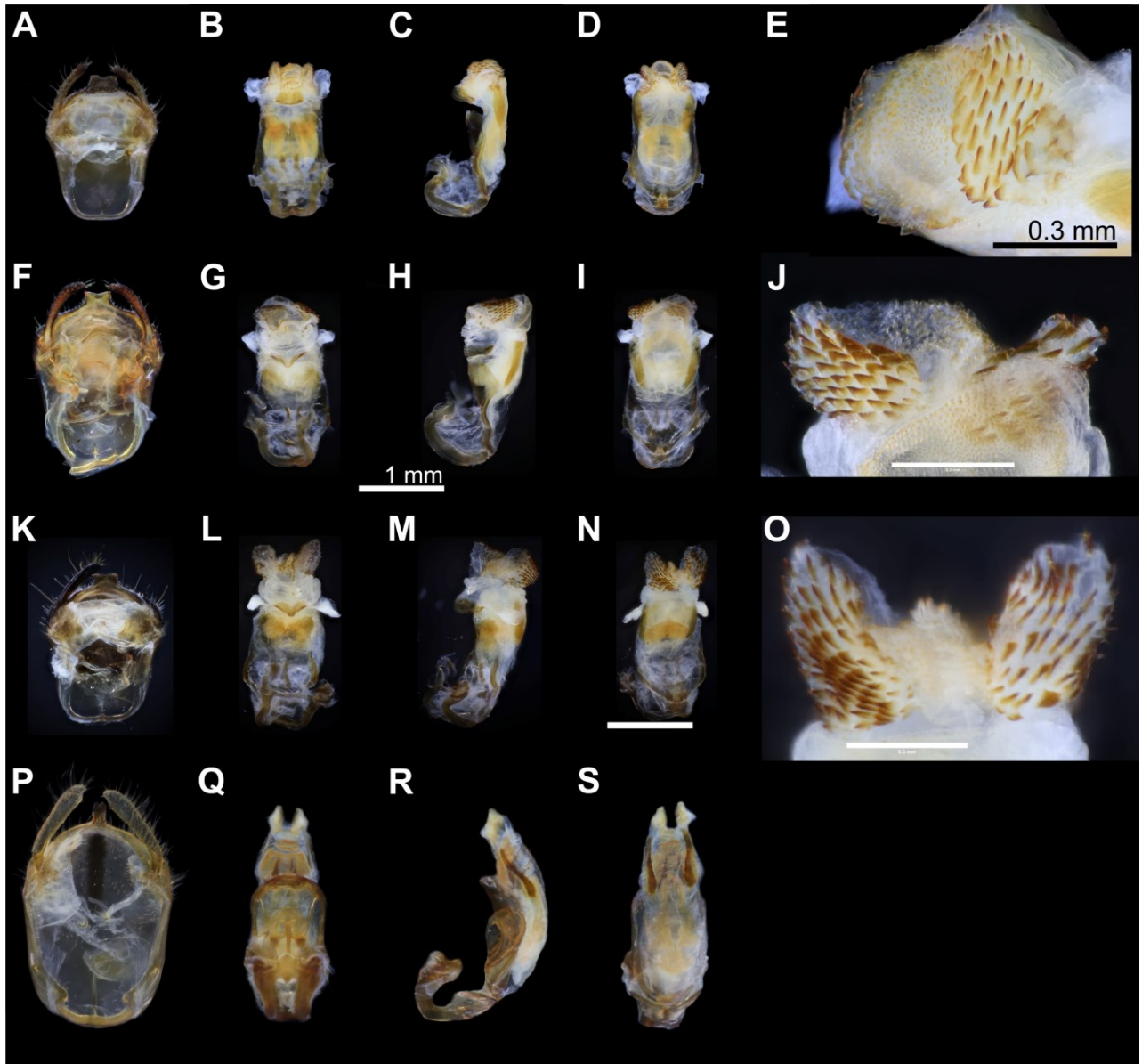


Figure 6.5. Genital morphology of male-based morphospecies. **A–E**, LA-Redu-2016-001, ♂, “gen. E” sp. M5; **F–J**, TXLBX24c, ♂, “gen. E” sp. M6; **K–O**, LA-Redu-2016-001, ♂, “gen. E” sp. M7; **P–S**, TXL2018-127, ♂, “gen. D” sp. M1. **A, F, K, P**, pygophore in dorsal view; **B, G, L, Q**, phallus in dorsal view; **C, H, M, R**, phallus in lateral view; **D, I, N, S**, phallus in ventral view; **E, J, P**, distal dorsal lobe of endosoma (ddl).

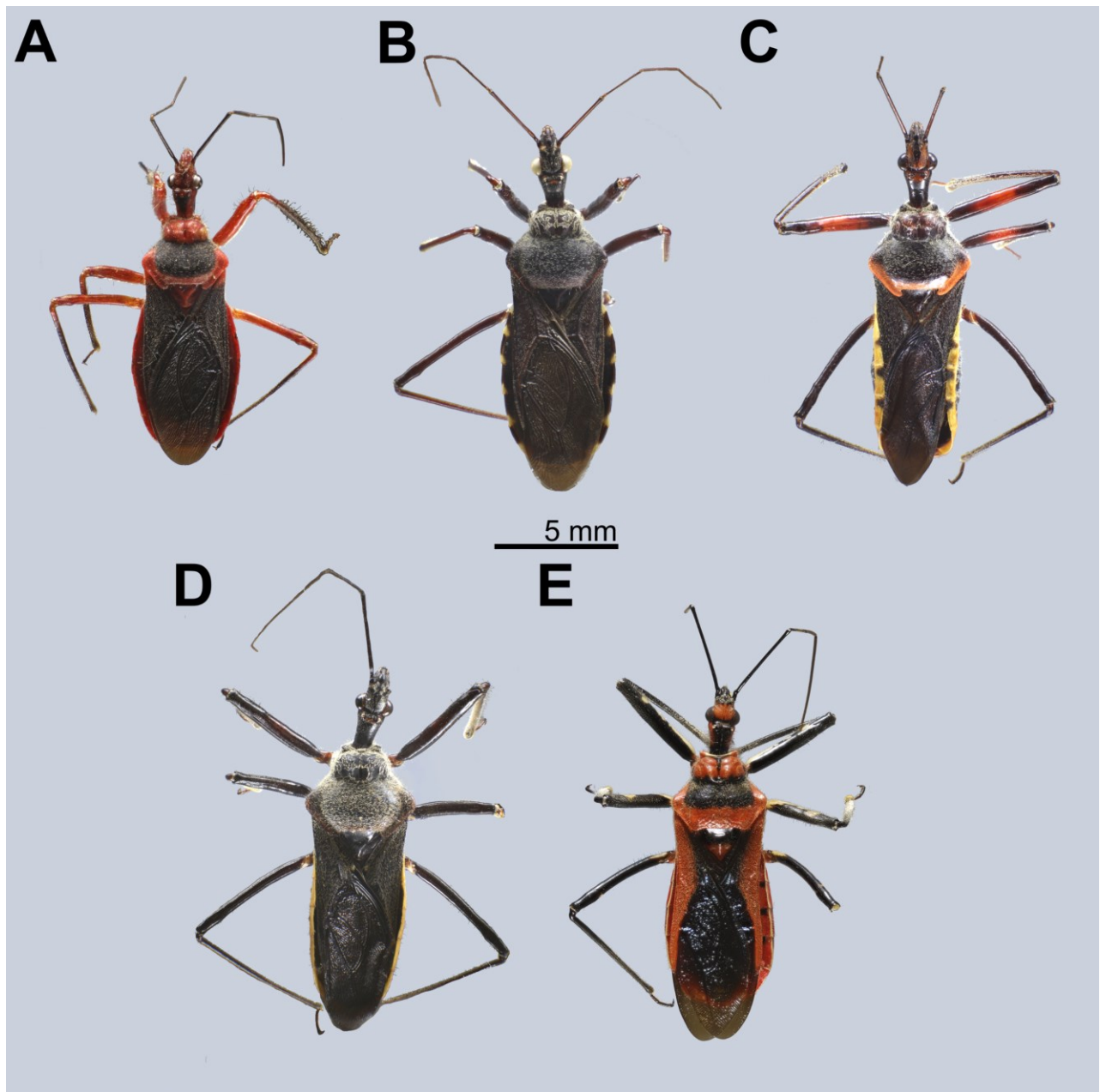


Figure 6.6. Body in dorsal view of female-based morphospecies. **A**, TXL2018-041, ♀, “gen. E” sp. F1; **B**, TXL2016-623, ♀, “gen. E” sp. F2; **C**, TXLBX24a, ♀, “gen. E” sp. F3; **D**, TXLBX23, ♀, “gen. E” sp. F4; **E**, AD2020-040, ♀, “gen. F” sp. F1.

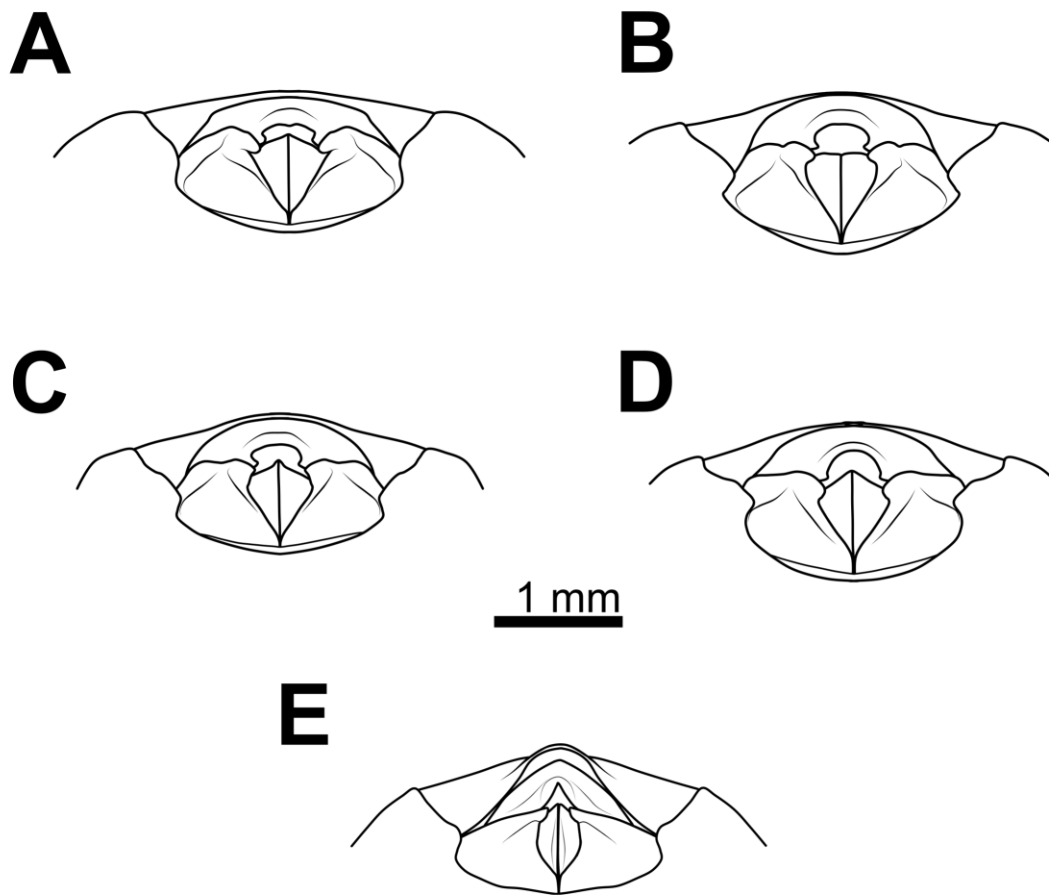


Figure 6.7. Genital morphology of female-based morphospecies. **A–E**, female genitalia in ventral view. **A**, TXL2018-041, ♀, “gen. E” sp. F1; **B**, HNL2019-136, ♀, “gen. E” sp. F2; **C**, TXL BX24a, ♀, “gen. E” sp. F3; **D**, TXL BX23, ♀, “gen. E” sp. F4; **E**, LA-Redu-2008-001, ♀, “gen. F” sp. F1.

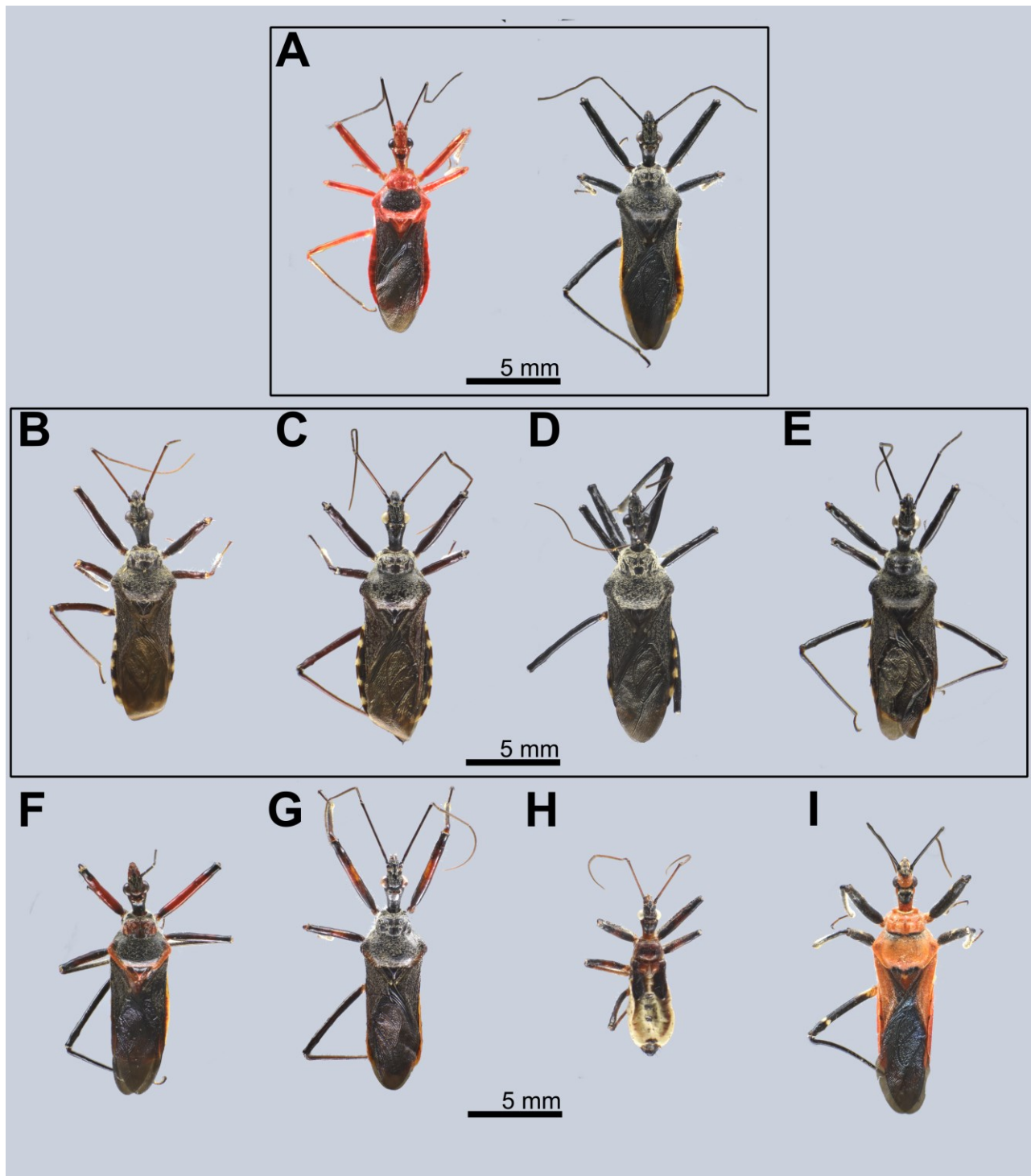


Figure 6.9. Body in dorsal view of fully-recorded species of genus E and F. **A**, “gen. E” sp. HNL001, AD2019-001, ♂, NDD2019-245, ♂; **B**, “gen. E” sp. HNL002, HNL2018-112, ♂; **C**, “gen. E” sp. HNL003, TXL2016-625, ♂; **D**, “gen. E” sp. HNL004, TTN2020-002, ♂; **E**, “gen. E” sp. HNL006, TXLBX7, ♂; **F**, “gen. E” sp. HNL005, NDD2019-277, ♂; **G**, “gen. E” sp. HNL007, TXLBX24b, ♂; **H**, “gen. E” sp. HNL008, AD2021-035, ♂; **I**, “gen. F” sp. HNL001, TXL2019-692, ♂.

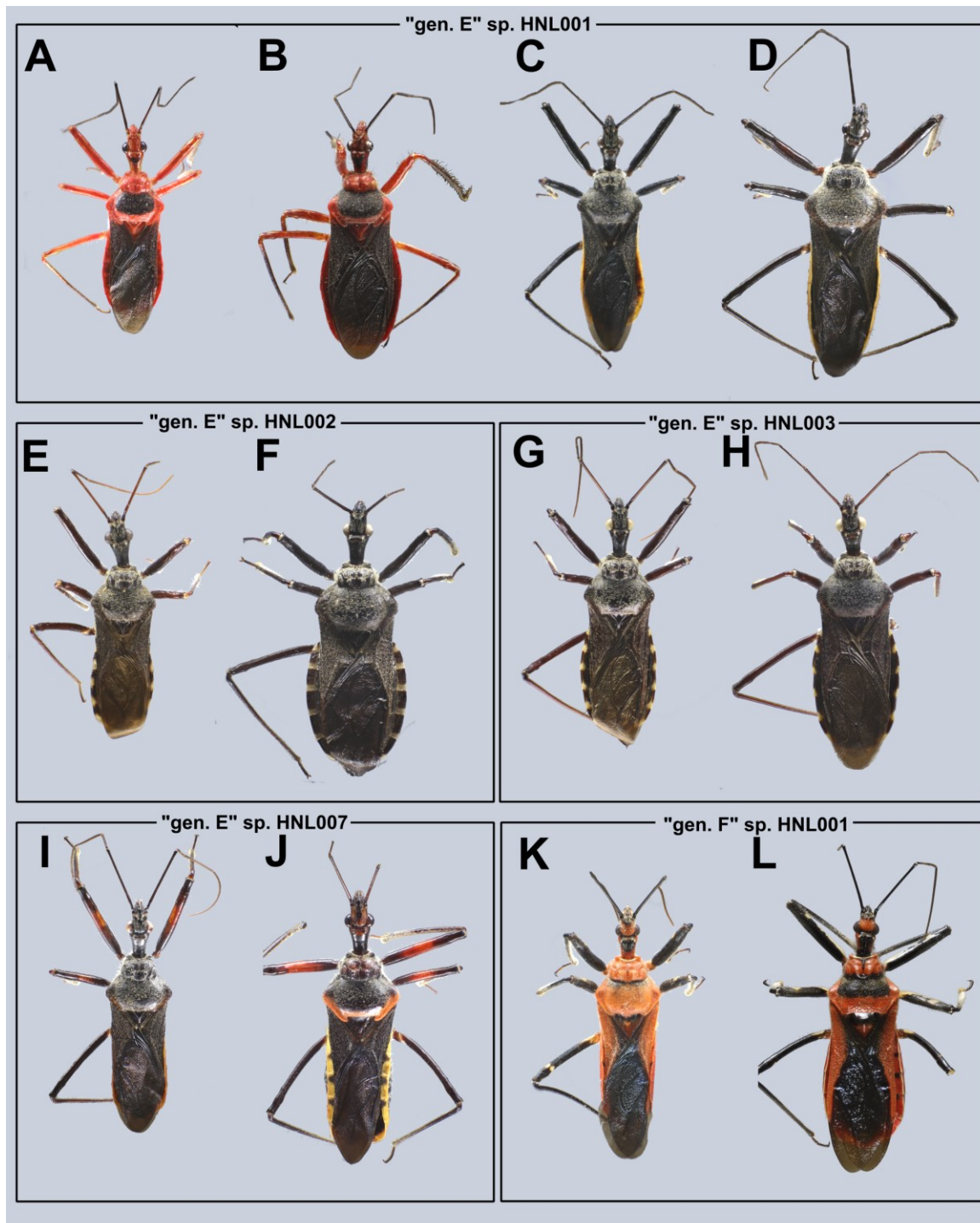


Figure 6.10. Conspecific male-female combinations of genus E and F. **A**, AD2019-001, ♂, “gen. E” sp. M1; **B**, TXL2018-041, ♀, “gen. E” sp. F1; **C**, NDD2019-245, ♂, “gen. E” sp. M2; **D**, TXL BX23, ♀, “gen. E” sp. F4; **E**, HNL2018-112, ♂, “gen. E” sp. M3a; **F**, TXL2017-650, ♀, “gen. E” sp. F2a; **G**, TXL2016-625, ♂, “gen. E” sp. M3b; **H**, TXL2016-623, ♀, “gen. E” sp. F2b; **I**, TXL BX24b, ♂, “gen. E” sp. M6; **J**, TXL BX24a, ♀, “gen. E” sp. F3; **K**, TXL2019-692, ♂, “gen. F” sp. M1; **L**, AD2020-040, ♀, “gen. F” sp. F1.

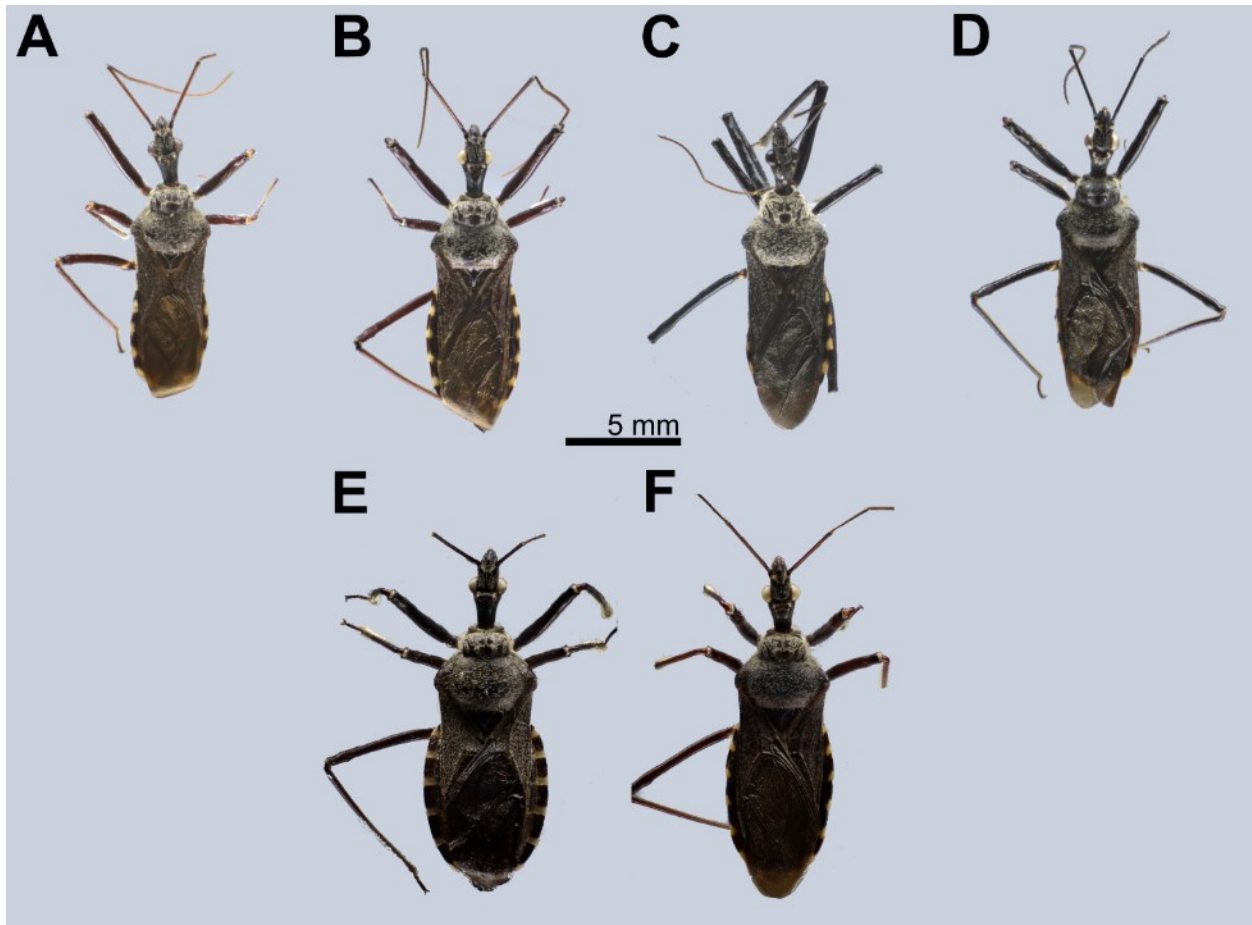


Figure 6.11. Species complex of *Rhynocoris marginellus* (= “gen. E” sp. HNL002–HNL004, HNL006). **A**, “gen. E” sp. HNL002, HNL2018-112, ♂; **B**, “gen. E” sp. HNL003, TXL2016-625, ♂; **C**, “gen. E” sp. HNL004, TTN2020-002, ♂; **D**, “gen. E” sp. HNL006, TXLBX7, ♂; **E**, “gen. E” sp. F2, TXL2017-650, ♀; **F**, “gen. E” sp. F3, TXL2016-623, ♀.

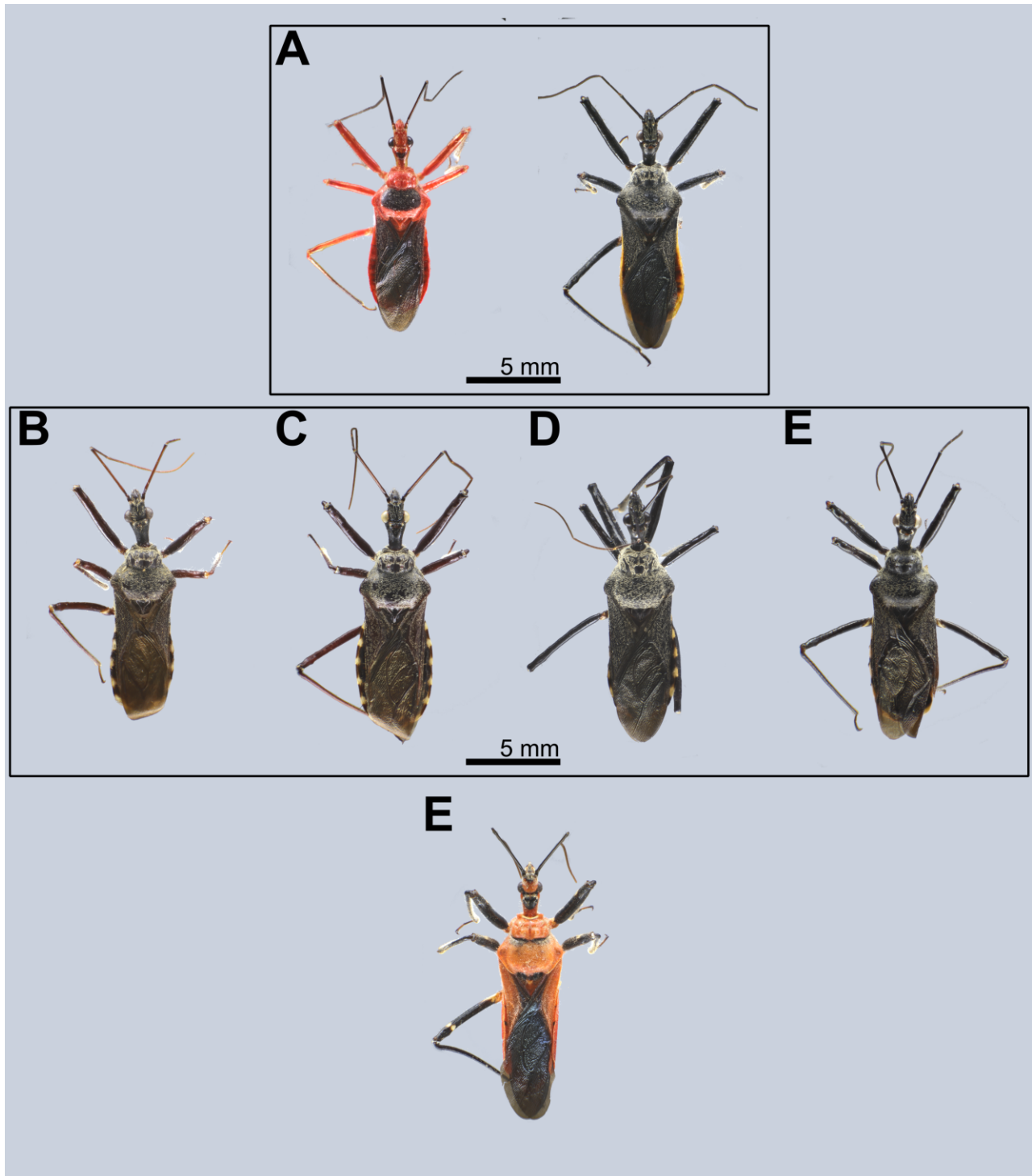


Figure 6.12. Identification of species of genus E and F. **A**, “*Rhynocoris*” *mendicus* (Stål, 1867) (= “gen. E” sp. HNL001); **B–E**, “*Rhynocoris*” *marginellus* (Fabricius, 1803) complex (= “gen. E” sp. HNL002–HNL004, HNL006); **F**, “*Rhynocoris*” *fuscipes* (Fabricius, 1787) (= “gen. F” sp. HNL001).

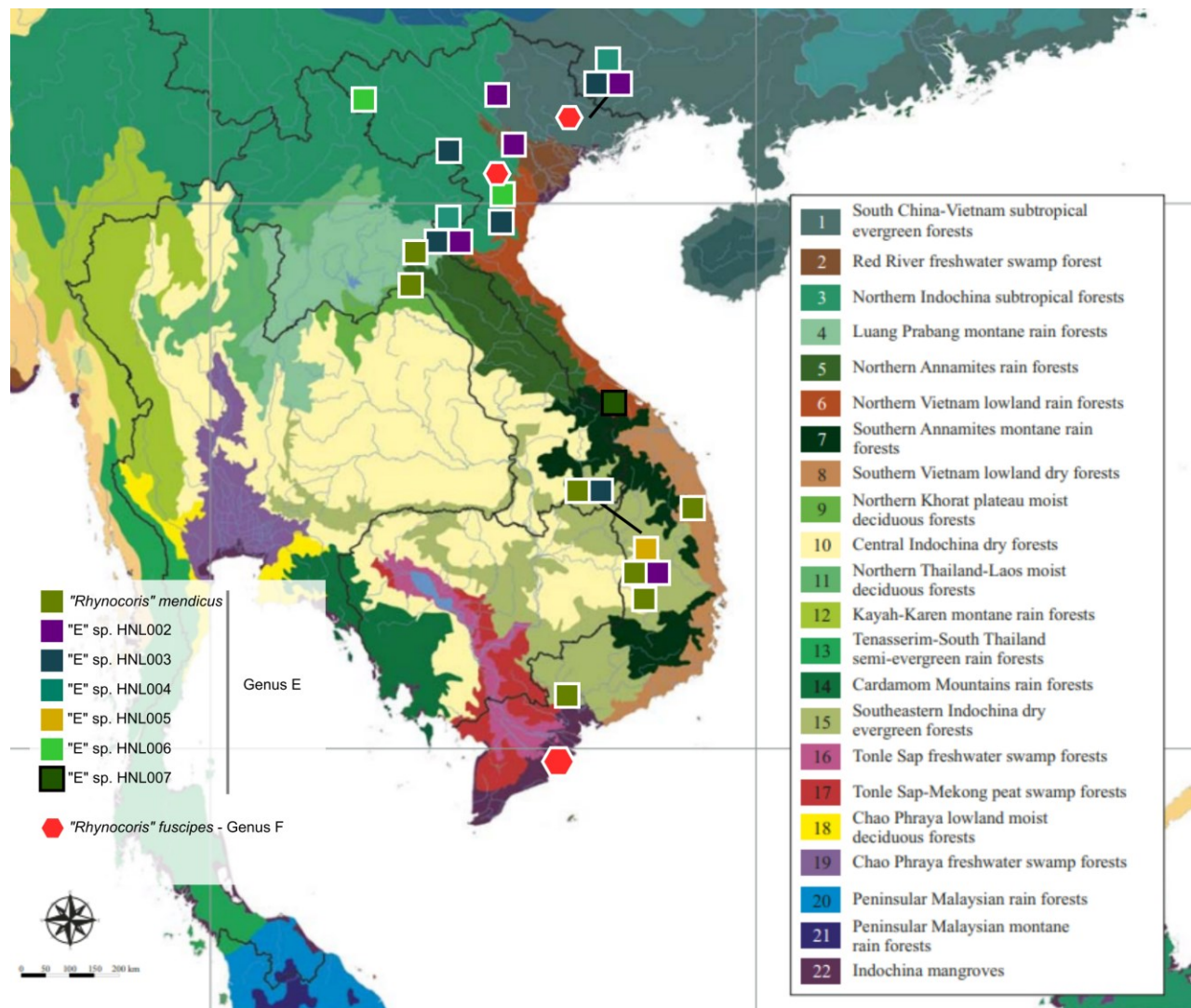


Figure 6.13. Distribution of genera E and F in Vietnam and surrounding areas compared to the vegetation of Indo-China (Poyarkov et al., 2021).

Table 6.1. The minimal interspecific distance of species of genus E based on the COI dataset. Upper right diagonal shows the p-distance (%), and the lower left diagonal shows the distance in the K2P model (%). Blue cells indicated the lowest minimal interspecific distance, orange cells indicated the highest minimal interspecific distance.

	“gen. E” sp. HNL001	“gen. E” sp. HNL002	“gen. E” sp. HNL003	“gen. E” sp. HNL004	“gen. E” sp. HNL006	“gen. E” sp. HNL005	“gen. E” sp. HNL007	“gen. E” sp. HNL008
“ <i>Rhynocoris</i> ” <i>mendicus</i> (= “gen. E” sp. HNL001) (N = 19) (Max K2P = 2.5%; Max p = 2.5%)		7.8	9.3	8.5	8.1	4.8	3.3	4.6
“gen. E” sp. HNL002 (N = 16) (Max K2P = 1.3%; Max p = 1.3%) (“ <i>Rhynocoris</i> ” <i>marginellus</i> complex)	8.3		3.2	2.2	2.0	9.0	8.0	8.5
“gen. E” sp. HNL003 (N = 14) (Max K2P = 0.5%; Max p = 0.5%) (<i>Rhynocoris</i> ” <i>marginellus</i> complex)	10.2	3.3		2.9	3.2	9.8	9.5	9.6
“gen. E” sp. HNL004 (N = 3) (Max K2P = 0.2%; Max p = 0.2%) (<i>Rhynocoris</i> ” <i>marginellus</i> complex)	9.2	2.2	2.9		1.8	10.1	8.8	9.6
“gen. E” sp. HNL006 (N = 2) (Max K2P = 0.6%; Max p = 0.6%) (<i>Rhynocoris</i> ” <i>marginellus</i> complex)	8.8	2.0	3.2	1.9		9.3	8.0	9.1
“gen. E” sp. HNL005 (N = 1)	5.0	9.7	10.7	11.1	10.1		5.1	4.6
“gen. E” sp. HNL007 (N = 3) (Identical sequences)	3.4	8.5	10.4	9.6	8.6	5.4		5.3
“gen. E” sp. HNL008 (N = 1)	4.8	9.1	10.5	10.5	9.9	4.9	5.6	

Table 6.2. Discrimination of *Rhynocoris* sensu lato species and morphospecies with results of male-based, female-based, external-morphology-based examinations.

No	Male-based morphospecies	Female-based morphospecies	Final
			Species
1	“gen. E” sp. M1	“gen. E” sp. F1	“gen. E” sp. HNL001 (= “ <i>Rhynocoris</i> ” <i>mendicus</i> (Stål, 1867))
	“gen. E” sp. M2	“gen. E” sp. F5	
2	“gen. E” sp. M3a	“gen. E” sp. F2a	“gen. E” sp. HNL002 (= “ <i>Rhynocoris</i> ” <i>marginellus</i> (Fabricius 1803) species complex)
3	“gen. E” sp. M3b	“gen. E” sp. Fb	“gen. E” sp. HNL003 (= “ <i>Rhynocoris</i> ” <i>marginellus</i> (Fabricius 1803) species complex)
4	“gen. E” sp. M3c		“gen. E” sp. HNL004 (= “ <i>Rhynocoris</i> ” <i>marginellus</i> (Fabricius 1803) species complex)
5	“gen. E” sp. M3d		“gen. E” sp. HNL006 (= “ <i>Rhynocoris</i> ” <i>marginellus</i> (Fabricius 1803) species)
6	“gen. E” sp. M6		“gen. E” sp. HNL005
7	“gen. E” sp. M9	“gen. E” sp. F4	“gen. E” sp. HNL007
8	Nymphal specimen		“gen. E” sp. HNL008
9	“gen. F” sp. M1	“gen. F” sp. F1	“gen. F” sp. HNL001 (= “ <i>Rhynocoris</i> ” <i>fuscipes</i> (Fabricius, 1787))

Appendix: Taxonomic accounts of the genus *Rhynocoris* sensu lato found in Vietnam and surrounding areas

1. Taxonomic accounts of the genus E found in Vietnam and surrounding areas

Fully Recognized and Determined Species

“Rhynocoris” mendicus (Stål, 1867)

(Fig. 6.3A, B, Fig. 6.4A–J, Fig. 6.6A, D, Fig. 6.7A, D, Fig 6.10A–D; Table 6.1)

“Rhynocoris” mendicus (Stål, 1867), in Stål (1867): 286.

Examined material. Non-type material. 10♂, HNL2018-040, TXL2016-592, TXL2016-593, TXL2016-594, TXL2016-595, TXL2016-596, TXL2016-597, TXL2016-598, TXL2016-599, AD2019-001; 9♂, TXL2011-663, HNL2019-174, NDD2019-229, NDD2019-233, NDD2019-234, NDD2019-239, NDD2019-244, NDD2019-245, NDD2019-246; 3♀, TXL2004-051, LA-Redu-2011-004, TXL2018-041; 1♀, TXL BX23.

Diagnosis. Body medium to large-sized, elongated, and somewhat robust, shiny orangish-brown, reddish-orange or red; labium reddish-orange to red; anterior pronotal lobe orange or red with short bent pubescence, interleaved with erect setae; posterior pronotal lobe orange or red with centrally suffused with blackish brown, and covered with short bent pubescence, interleaved with erect setae; scutellum orangish brown or red with long thick erect setae; abdominal mediotergites, laterotergites, and sternites orangish brown or sanguineous; abdominal sternites with or without dark brown suffusion; coxae, trochanters, and femora orange or red; basal 1/3 of tibiae red; remaining of tibia dark brown.

Var. Body black; labium black or blackish brown, paler toward tip; anterior pronotal lobe black with some rows of short bent pubescence, interleaved with erect setae; posterior pronotal lobe black and densely covered with short bent pubescence, interleaved with erect setae; scutellum black with long thick erect setae; abdominal mediotergites and sternites black; laterotergites yellow or luteous with

anterior half of lateral margin of each laterotergite dark brown; coxae, trochanters, femora and tibiae black.

Distribution. India, Myanmar, China, Laos, Vietnam, Malaysia.

Type locality. Malaysia.

“Rhynocoris” marginellus (Fabricius, 1803) species complex

“Rhynocoris” marginellus (Fabricius, 1803), in Fabricius (1803): 271.

Distribution. India, Myanmar, China, Vietnam, Malaysia, Indonesia, New Guinea.

Type locality. Indonesia and New Guinea.

“gen. E” sp. HNL002

(Fig. 6.3C, Fig. 6.4K–O, Fig. 6.6B, Fig. 6.7B, Fig. 6.9B, Fig 6.10E, F; Table 6.1)

Examined material. Non-type material. 8♂, HNL2018-112, TXL2018-115, HNL2018-181, HNL2018-185, TTN2020-004, TXL2021-001, TXL2021-002, TXL2021-003; 9♀, HNL2018-113, HNL2019-113, HNL2019-136, TXL2017-650, TXL2017-652, TXL2019-676, TXL2021-004, TXL2021-005.

Diagnosis. Body medium to large-sized, elongated, and somewhat robust, blackish brown; labium black or blackish brown, paler toward tip; anterior pronotal lobe black with some rows of short bent pubescence, interleaved with erect setae; posterior pronotal lobe black or blackish brown and densely covered with short bent pubescence, interleaved with erect setae; black with long thick erect setae; laterotergites yellow or luteous with anterior half of lateral margin of each laterotergite dark brown; abdominal sternites blackish brown or dark brown with lateral areas black; coxae, trochanters, femora, and tibiae slightly dark brown, blackish brown or black, basal and apical region of femora and tibiae sometimes suffused with blackish brown.

Distribution. Vietnam.

“gen. E” sp. HNL003

(Fig. 6.9C, Fig 6.10G, H; Table 6.1)

Examined material. Non-type material. 16♂, HNL2018-129, TXL2016-622, TXL2016-624, TXL2016-625, TXL2016-626, TXL2016-627, TXL2016-628, TXL2016-629, TXL2016-632, TXL2016-636, TXL2016-641, TXL BX15b, TXL BX15c, TXL2017-665, TXL2018-836, TTN2020-003; 8♀, TXL2016-623, TXL2016-630, TXL2016-631, TXL2016-635, TXL2016-637, TXL2016-643, TXL BX15, TTN2020-011.

Diagnosis. Body medium to large-sized, elongated, and somewhat robust, blackish brown; labium black or blackish brown, paler toward tip; anterior pronotal lobe black with some rows of short bent pubescence, interleaved with erect setae; posterior pronotal lobe black or blackish brown and densely covered with short bent pubescence, interleaved with erect setae; scutellum black with long thick erect setae; laterotergites yellow or luteous with anterior half of lateral margin of each laterotergite dark brown; abdominal sternites blackish brown or dark brown with lateral areas black; coxae, trochanters, femora, and tibiae slightly dark brown, blackish brown or black, basal and apical region of femora and tibiae sometimes suffused with blackish brown.

Distribution. Vietnam.

“gen. E” sp. HNL004

(Fig. 6.9D; Table 6.1)

Examined material. Non-type material. 3♂, TXL2017-656, TTN2020-002, TTN2020-008.

Diagnosis. Body medium-sized, elongated, and somewhat robust, black; labium black or blackish brown, second visible labial segment blackish brown, somewhat suffused with brown spot; anterior pronotal lobe black with some rows of short bent pubescence, interleaved with erect setae; posterior pronotal lobe black and densely covered with short bent pubescence, interleaved with erect setae;

scutellum black with long thick erect setae; abdominal mediotergite black; laterotergites yellow or luteous with anterior half of lateral margin of each laterotergite dark brown; abdominal sternites blackish brown or dark brown with lateral areas black; coxae, trochanters, femora, and tibiae slightly dark brown, blackish brown or black, basal and apical region of femora and tibiae sometimes suffused with blackish brown.

Distribution. Vietnam.

“gen. E” sp. HNL006

(Fig. 6.9E; Table 6.1)

Examined material. Non-type material. 2♂, DTH2022-001, TXLBX7.

Diagnosis. Body medium-sized, elongated, and somewhat robust, black; labium black or blackish brown, second visible labial segment blackish brown, somewhat suffused with brown spot; anterior pronotal lobe black with some rows of short bent pubescence, interleaved with erect setae; posterior pronotal lobe black and densely covered with short bent pubescence, interleaved with erect setae; scutellum black with long thick erect setae; abdominal mediotergite black; laterotergites yellow or luteous with anterior half of lateral margin of each laterotergite dark brown; abdominal sternites blackish brown or dark brown with lateral areas black; coxae, trochanters, femora, and tibiae slightly dark brown, blackish brown or black, basal and apical region of femora and tibiae sometimes suffused with blackish brown.

Distribution. Vietnam.

Fully Recognized and Undetermined Species

“gen. E” sp. HNL005

(Fig. 6.3D, Fig. 6.4P–T, Fig. 6.9F; Table 6.1)

Examined material. Non-type material. 1♂, NDD2019-277.

Diagnosis. Body medium-sized, elongated, and somewhat robust, reddish brown; first visible labial segment red; remaining labium blackish red, darker toward tip; anterior pronotal lobe reddish brown with some rows of short bent pubescence, interleaved with erect setae; posterior pronotal lobe black and densely covered with short bent pubescence, interleaved with erect setae; posterior margin and posterior half of humerus orangish brown or brown; basal half of scutellum blackish brown or dark brown, posterior half of scutellum reddish brown or brown with some long thick erect setae; abdominal mediotergites red with irregularly extensive black suffusion except mediotergite I+II brown; laterotergites yellow; abdominal sternites red with lateral areas black; anterior femora red with basal and apical region suffused with black; mid femora black with a blackish red suffusion in the middle; posterior femora black; tibiae black.

Distribution. Vietnam.

“gen. E” sp. HNL007

(Fig. 6.3F, Fig. 6.5F–J, Fig. 6.6C, Fig. 6.7C, Fig. 6.9G; Table 6.1)

Examined material. Non-type material. 2♂, TXLBX24b, TXLBX24c; 1♀, TXLBX24a.

Diagnosis. Body medium-sized, elongated, and somewhat robust, blackish brown; labium brown; anterior pronotal lobe black or blackish red with some rows of short bent pubescence, interleaved with erect setae; posterior pronotal lobe black and densely covered with short bent pubescence, interleaved with erect setae; posterior half of humerus brown or orange, posterior margin of posterior pronotal lobe orange or black; scutellum black; laterotergites yellow and segmentally suffused with blackish brown suffusion in apical lateral margin; abdominal sternites black; anterior and mid femora black with a brown or dark brown suffusion in the middle; posterior femora black; tibiae dark brown or blackish brown.

Distribution. Vietnam.

Morphospecies Species not yet confirmed by the Integrative Taxonomy

“gen. E” sp. M5

(Fig. 6.3E, Fig. 6.5A–E; Table 6.1)

Examined material. 1♂, LA-Redu-2010-006.

Diagnosis. Body medium-sized, elongated, and somewhat robust, black and brown; head and labium brown or dark brown; anterior pronotal lobe dark brown with some rows of short bent pubescence, interleaved with erect setae; posterior pronotal lobe black and densely covered with short bent pubescence, interleaved with erect setae; posterior margin of posterior pronotal lobe and posterior half of humerus orange; scutellum black except apical central area orange or brown, margin of posterior apex brown; laterotergites yellowish brown; abdominal sternites black; femora and tibiae reddish brown.

Distribution. Laos.

“gen. E” sp. M7

(Fig. 6.3G, Fig. 6.5K–O; Table 6.1)

Examined material. 1♂, LA-Redu-2016-001.

Diagnosis. Body medium-sized, elongated, and somewhat robust, black; head and labium black; anterior pronotal lobe black with some irregular dark brown suffusions, covered with some rows of short bent pubescence, interleaved with erect setae; posterior pronotal lobe black and densely covered with short bent pubescence, interleaved with erect setae; posterior margin of posterior pronotal lobe and posterior half of humerus brown; scutellum black; laterotergites yellowish brown; abdominal sternites black; femora and tibiae black.

Distribution. Laos.

2. Taxonomic accounts of the genus *F* found in Vietnam and surrounding areas

Fully Recognized and Determined Species

“Rhynocoris” fuscipes (Fabricius, 1787)

(Fig. 6.3H, Fig. 6.5P–S, Fig. 6.6E, Fig. 6.7E, Fig. 6.9I, Fig 6.10K–L; Table 6.1)

“Rhynocoris” fuscipes (Fabricius, 1787), in Fabricius (1787): 312.

Examined material. Non-type material. 7♂, TW-Redu-1982-001, TXL1999-044, TXL1999-046, TXL2018-127, TXL2019-692, TXL2019-693, AD2020-041; 3♀, TXL1999-045, LA-Redu-2008-001, AD2020-040.

Diagnosis. Body large-sized, elongated, and somewhat robust, orange or red; head orange or red; labium blackish brown except first visible labial segment brown, somewhat suffused with blackish brown or dark brown; anterior pronotal lobe orangish brown or red with some rows of short bent pubescence, interleaved with erect setae; posterior pronotal lobe orange or red, somewhat suffused with blackish brown, and densely covered with short bent pubescence, interleaved with erect setae; scutellum black except lateral areas and posterior apex orange or red; lateral areas of scutellum with some short bent pubescence; posterior apex of scutellum laterally reflexed; laterotergites orange or red with lateral margin white; abdominal sternites orange or red, with lateral areas of each sternite with white and small black horizontal suffusions; femora and tibiae black; femora suffused white basally and medially.

Distribution. India, Sri Lanka, China, Taiwan, Laos, Vietnam, Myanmar, Indonesia, Malaysia.

Type locality. India.

CHAPTER 7:

GENERAL DISCUSSION

7.1. The Validity of the Three Genera *Biasticus*, *Sphedanolestes*, and *Rhynocoris*

The validity of the genus *Biasticus* is strongly supported by morphological and phylogenetic evidence. The Indo-China specimens of the genus *Biasticus* have shared characteristics in external and male genitalia morphology, and all of them were recovered as a monophyletic clade with high supporting value in Bayesian Inference analysis.

On the other hand, *Sphedanolestes* sensu lato and *Rhynocoris* sensu lato, two of the most speciose genera in the tribe Harpactorini, were not supported to be monophyletic. The present molecular phylogenetic analyses and morphological examination suggest that *Sphedanolestes* sensu lato can be subdivided into three independent genera, genus *Sphedanolestes* sensu stricto, genus C, and genus D, and *Rhynocoris* sensu lato two independent genera, genus E and genus F.

However, the specimens of *Sphedanolestes* sensu lato and *Rhynocoris* sensu lato used in this research were limited. Therefore, further comprehensive examination of the external and genitalia morphology and molecular phylogenetic analyses based on regionwide or hopefully worldwide datasets (including the specimens of the type species of relevant genera) might confirm the status of the unidentified genera C, D, E, and F.

7.2. Morphological Characters Useful in the Classification of Harpactorinae

The conventional taxonomy of the subfamily Harpactorinae has been primarily based on external morphology such as the head and hemelytron and general body shapes and coloration which can be observed without dissection or destruction of specimens. However, a high similarity in such morphology was found in some close-related genera, such as *Biasticus*, *Sphedanolestes* sensu lato, and *Rhynocoris* sensu lato. On the other hand, the six different genera recognized in the present study can be defined with a combination of several external and genital morphology as explained below. These diagnostic characters are likely useful for revising the generic boundaries of other harpactorine

genera too.

The structure of the anterior pronotal lobe. The prolongation of the middle longitudinal sulcus (reaching or not reaching the anterior margin of the posterior lobe), and the presence or absence of tubercle in the center of the lateral bulge of the anterior pronotal lobe are the diagnostic features separating the three genera and their potentially newly separated genera.

The structure of the anteromedial region of the posterior pronotal lobe. Structural differences, e.g., swollen and elevated, shallowly sulcate, or distinctly sulcate, are found among the genus-level taxa.

The structure of the posterolateral margin of the humerus. Although the posterolateral margin and the posterior apex of the humerus are almost similar among the targeted genera, *Rhynocoris fuscipes*, which have a posterolateral margin and posterior apex slightly reflexed, is unique among the examined species.

The structure of the scutellum. The general structure of the scutellum is almost similar among the targeted taxa with a triangular shape, triangularly depressed basally, apically produced, and sloping downward. However, some features are often useful for discriminating some taxa in the genus level, e.g., reflex or not reflex posterior margin and posteriorly produced or not produced posterior apex. The reflex posterior margin of the scutellum is found in *Rhynocoris fuscipes*, and the posteriorly produced posterior apex of the scutellum is observed in *Sphedanolestes impressicollis*.

The median process of the male pygophore, male. Median process (mpp) might be one of the most reliable features for discriminating genus-level taxa. For example, *Biasticus* is characterized by broad mpp with a convex or concave distal margin; *Sphedanolestes* sensu lato is featured by narrow mpp which is posteriorly produced with bifurcate

projection in the distal margin; *Rhynocoris* sensu lato is characterized by broad mpp which is posteriorly produced with slightly concave distal margin.

The structure of Gonocoxa VIII (Gc8), female. External morphology of female genitalia is somewhat poorly characterized, but in some special cases, the shape and structure of the posterior apex of Gc8 might be helpful for discriminating at the species level. For example, *Rhynocoris fuscipes* was recognized with a reflexed and slightly produced posterior apex, or *Rhynocoris* clade was characterized by Gc8 with a bolded inner posterolateral margin and elevated and posteriorly produced posterior apex.

The posterior margin of abdominal laterotergite VIII (AL8). The posterior margin of AL8 might be a valuable feature in some specific taxa. For example, *Sphedanolestes impressicollis* and genus F is characterized by posterior produced and elevated posterior margin of AL8, while *Biasticus*, genera C, D, and E have a thin and narrow posterior margin of AL8.

The importance of male genital morphology in discriminating species of the genus *Biasticus* has been proved in Chapter 4. The male genitalia also illustrated distinction among species of genus C. However, the species of genus E have shown a high similarity in male genitalia characteristics, i.e., the medial process of male pygophore and spinulous processes on the distal dorsal lobe of the endosoma. Therefore, depending on the specific target genus or taxon, the usefulness of male genital morphology in discriminating at the species level might vary.

7.3. Notes on the Diversification of Genital Morphology in the Examined Genera

Furthermore, while the diversity of male genitalia structures was commonly seen in genera of Harpactorinae as well as genera of Reduviidae, the species of genus E showed very few distinctions among the species. In this section, it takes work to precisely answer this unusual phenomenon.

However, I attempted to come up with a few hypotheses to explain as follows.

If multiple related species sympatrically exist and their habitats and breeding seasons largely overlap, the reinforcement of the prezygotic isolation among the species may occur to avoid interspecific hybridization. Diversification of male and female genital structures is one of the possible modes of the reinforcement that has been reported in insects (Masly 2012).

For example, in *Biasticus* of which the species diversity in Indochina is quite high (as concluded in Chapter 4, Fig. 4.20), situations in which adults of many closely related species coexist in the same locality at the same season are likely to occur, which can promote the morphological diversification of genital organs among the species. On the other hand, the species diversity of genus E in Indochina is much smaller than in *Biasticus* (Chapter 6, Fig. 6.13), adults of multiple species are less likely to coexist at the same time. Such a situation may not induce the reinforcement above-mentioned.

Another possibility is that prezygotic isolation mechanisms (e.g., pheromone-based mate recognition) without morphological complementarity of genital organs between the conspecific male and female may have developed in genus E.

Ecological studies are needed to determine which theory is correct, or if another theory is correct altogether.

7.4. Distribution Pattern of Indo-Chinese Species of the Three Genera *Biasticus*, *Sphedanolestes*, and *Rhynocoris*

Of the 39 species of *Biasticus*, *Sphedanolestes* (including *Sphedanolestes* sensu stricto, genus C, and genus D), and *Rhynocoris* (including genus E and genus F) recognized from Indo-China, seven species and a morphospecies have an Oriental and Sino-Japanese distribution, consisting of *Biasticus confusus* (= *B.* sp. HNL037), *B. flavinotus* (= *B.* sp. HNL021), *B. flavus* (= *B.* sp. HNL007),

“*Sphedanolestes*” *anullipes* (= *B.* sp. HNL063), “*Sphedanolestes*” *gularis* (= *B.* sp. HNL017), *Sphedanolestes impressicollis* (= *S.* sp. HNL001), and “*Rhynocoris*” *fuscipes* (= “gen. F” sp. HNL001). The other 32 species are only known from the Oriental realm.

Among seven species distributed in the Oriental and Sino-Japanese realms, *B. confusus* is recorded on the border of the two realms, which covers Northern Vietnam and Southern China (Hsiao 1979, Truong et al. 2015, Ha et al. 2022, the present study). *Biasticus flavinotus* was reported as distributed in Taiwan (type locality), China, and Northern Vietnam (Matsumura 1913, Hsiao 1979, Cai and Yang 2002, Truong et al. 2015). However, no Vietnamese specimen of this species was found in this study. *Biasticus flavus* was reported in Northern Vietnam, Northern Laos, Northern Thailand, China Mainland including Hong Kong, and Taiwan as well as Myanmar and Pakistan (Hsiao 1979, Cai and Yang 2002, Truong et al. 2015, Ha et al. 2022, the present study). “*Sphedanolestes*” *anullipes*, “*Sphedanolestes*” *gularis* were documented as distributed in China and Vietnam (Hsiao 1979, Truong et al. 2015). *Sphedanolestes impressicollis* is widespread in Indo-China (Vietnam) and the Sino-Japanese realm (China and Japan) (Hsiao 1979, Truong et al. 2015, the present study). *Rhynocoris fuscipes* is widely distributed in Indo-China (Vietnam, Laos), mainland China, and Taiwan.

Despite the lack of distribution of *Biasticus* species in the western part of the Oriental realm, by accumulating distribution data of the genus *Biasticus* in previous publications and reports, the genus *Biasticus* is likely to be widespread in Oriental and Sino-Japanese realms (Fig. 7.1).

As mentioned in Section 4.4.3, 11 species were only recognized in Northern Indochina (Northern Vietnam and Northern Laos), characterized by temperate climates, while 14 species were only recorded in Middle and Southern Vietnam, mainly characterized by tropical climates, primarily tropical monsoon and savannah with some tropical rainforests and temperate climates (high elevation areas of Truong Son Mountain Range). Three other species were only found in Northern Thailand,

which was characterized by a tropical savannah climate (Fig. 7.2). Besides the species mentioned above were only recorded in certain regions, *Biasticus flavus* is widespread in East, Southeast and South Asia as mentioned above and another species, “*Sphedanolestes*” *confusus*, was founded in both Northern Vietnam and Southern Vietnam (Fig. 7.2).

The distribution patterns of *Biasticus* species in the study area suggest that, except in a few exceptional cases, the distribution of these species may be influenced by climatic factors (Fig. 4.20A) rather than broad-scale vegetation types (Fig. 4.20B) types. *Biasticus* species are generally adapted to forest edges and open vegetation types, where they tend to select specific herbs as ambush sites for hunting their prey. In other words, this may be the reason for the discrepancy with the broad-scale vegetation types. However, this does not exclude the possibility of the bias of this study and the limitation of collecting surveys.

No survey in Middle and Southern Indochina (Southern Laos, Southern Thailand, and Cambodia) was conducted during this study. Therefore, the overlap of species composition of Northern Thailand and Middle and Southern Vietnam was not confirmed in this study, even though the two regions have tropical climates. The further question is whether *Biasticus* species can overcome geographical distances in the same climatic range to have a wider distribution. More comprehensive studies on the species composition and diversity of *Biasticus* in the region are needed to answer this question.

The distribution of *Sphedanolestes* and *Rhynocoris* species has not yet been concluded. Further study on the distribution of the two genera should be conducted for a more accurate distributional pattern.

7.5. The Male and Female Imbalance among Harpactorinae Species

Previous studies pronounced the popularity of female bias in Harpactorinae as well as Reduviidae. This biological feature can be viewed as a result of local mating competition (LMC).

When brothers compete with each other for mating opportunities, local mate competition (LMC) can occur and results in selection for a female-biased sex ratio within a local breeding population (Somjee et al. 2011). The female-biased sex ratio may ensure higher reproduction in nature and reared conditions, thus increasing their potential use as a biocontrol agent.

However, the genus *E* recorded in this study was a rare case of a male-biased ratio. Although I have not yet conducted quantitative surveys, one possibility was recalled from my field-collecting experiences. In this genus, males seem to be more active than females not only in foraging but also in searching for mates and to exist more conspicuously and frequently on the surface of vegetation, which means that they are more likely to be collected than females, while females tend to hide in the bushes.

7.6. Prospects of the Taxonomy of Harpactorinae and Other Reduviids

One of the outstanding achievements of the present study is the discovery of 31 species of the genus *Biasticus*, of which 22 species are distinct from the 23 validly-named species of the genus and are herein considered to be new to science. Furthermore, three of the 23 validly-named species were also described and named as a part of the present study (Linh et al., 2022) prior to the completion of this thesis: *Biasticus taynguyenensis* Ha, Truong & Ishikawa, sp. nov., *B. griseocapillus* Ha, Truong & Ishikawa, sp. nov., and *B. luteicollis* Ha, Truong & Ishikawa, sp. nov. Therefore, the number of species involved in *Biasticus* has increased from 20 named species to 48 species or even more than seventy species if the independence of the 18 male-based and 30 female-based morphospecies is fully confirmed by future DNA-based species discrimination analyses. This result demonstrates that the species diversity of the genus *Biasticus* in Indo-China and Indo-Malay is very high and suggests that there is a considerable number of species waiting to be discovered and named.

Moreover, among the 31 *Biasticus* species recognized in the present study, two species have

been known as “*Sphedanolestes*” *annulipes* and “*Sphedanolestes*” *gularis*. Thus, it is suggested that there should be other cases in *Biasticus* species but now being erroneously treated as members of other genera. Besides, the usefulness of integrated taxonomy in discriminating species of the genus as well as *Sphedanolestes* and *Rhynocoris* has been remarked. The future extensive use of integrative approaches for Harpactorinae and other redviids will improve our understanding of their species diversity and ecological diversity and encourage the discovery of potential natural enemies of pests in agriculture and forestry.

As mentioned in Chapter 3 and Section 7.1, the morphologically and genetically heterogeneous statuses of the two genera *Sphedanolestes* and *Rhynocoris* were revealed by integrated taxonomy, with a revised diagnosis for the two genera and a proposal of three potentially new genera. DNA sequences were given, and male genitalia morphology of some representative of these genera are illustrated in this study. Such information may work as the working hypothesis in future taxonomic studies of the genera.

Interspecific and intraspecific divergences calculated based on the COI dataset of *Biasticus* species remarked a clear gap so-called “DNA barcode gap”: maximum intraspecific divergence rate of *Biasticus* species is 0–1.7% in both Kimura 2-parameter model (K2P) and in p-distance; minimum interspecific divergence ranges 2.2–18.1% in K2P model (2.1–15.9% in p-distance) (Table 4.1). While the maximum intraspecific divergence calculated based on the COI dataset of Vietnamese *Rhynocoris* species ranges from 0–2.5% in both K2P and p-distance, and the minimum interspecific divergence among those species, except for the complex of “*Rhynocoris*” *marginellus* (“gen. E” sp. HNL002, HNL003, HNL004, and HNL006), are from 3.4–11.2% in the K2P model (3.3–10.1% in p-distance) (Table 6.1). Among the complex of *Rhynocoris marginellus*, the maximum intraspecific p-distances vary from 0.2–1.3% in both the K2P model and p-distance, and the minimum interspecific p-distances vary from 1.9–3.3% in the K2P (1.8%–3.2% in p-distance) (Table 6.1). The

maximum intraspecific divergence among Vietnamese and Japanese representatives of *Sphedanolestes impressicollis* calculated based on the COI dataset is 0.8%. Unfortunately, since the other congeners of the genus *Sphedanolestes* are unavailable in this study, there is no interspecific divergence calibrated.

Jung *et al.* (2010) calculated that the average maximum intraspecific distance of 139 Sino-Japanese and Palearctic heteropteran species based on COI sequences was 1.8%, and the average minimum interspecific distance of compared congeners was 3.5%. Furthermore, Park *et al.* (2011) revealed that the intraspecific divergence is less than 2% in almost all of the Heteropteran taxa examined in that study, while the minimum interspecific p-distances is higher than 3% in 77% of congeneric paired taxa.

The results of the present study are mostly consistent with the previous studies on species of the suborder Heteroptera, except for the case of *Rhynocoris mendicus* (maximum intraspecific distance is 2.5%), the case of *Biasticus* sp. HNL004 and *B.* sp. HNL064 (minimum interspecific distance is 2.2% in K2P, 2.1% in p-distance), and the case of *Rhynocoris marginellus* group.

Consequently, in the subfamily Harpactorinae or the family Reduviidae, the species-level divergence can usually be confirmed if the COI divergence among lineages is more than 3% and the COI diversity within each lineage is less than 2%. On the other hand, if there is no clear barcode gap in the 2-3% range in the frequency distribution of COI distances, the species boundary should be carefully examined using multiple other lines of evidence.

References

1. Cai W, Yang S (2002) Insect from Maolan landscape. Guizhou Science and Technology Publishing House, Guiyang, 208–230.

2. Ha NL, Truong XL, Ishikawa T, Jaitrong W, Lee CF, Chouangthavy B, Eguchi K (2022) Three new species of the genus *Biasticus* Stål, 1867 (Insecta, Heteroptera, Reduviidae, Harpactorinae) from Central Highlands, Vietnam. *ZooKeys* 1118: 133–180. <https://doi.org/10.3897/zookeys.1118.83156>
3. Hsiao TY (1979) New species of Harpactorinae from China. II. (Hemiptera: Reduviidae). *Acta Zootaxonomica Sinica* 4: 238–295.
4. Jung S, Duwal RK, Lee S (2011) COI barcoding of true bugs (Insecta, Heteroptera). *Molecular Ecology Resources* 11: 266–270. <https://doi.org/10.1111/j.1755-0998.2010.02945.x>
5. Masly JP (2012) "170 Years of “Lock-and-Key”: Genital Morphology and Reproductive Isolation". *International Journal of Evolutionary Biology*, vol. 2012, Article ID 247352, 10 pages, 2012. <https://doi.org/10.1155/2012/247352>
6. Matsumura S (1913) *Additions to Thousand Insects of Japan*. 1: 1–184.
7. Park DS, Footitt R, Maw E, Hebert PDN (2011) Barcoding Bugs: DNA-Based Identification of the True Bugs (Insecta: Hemiptera: Heteroptera). *PLoS ONE* 6(4): e18749. <https://doi.org/10.1371/journal.pone.0018749>
8. Somjee U, Ablard K, Crespi B, Schaefer PW, Gries G (2011) Local mate competition in the solitary parasitoid wasp *Ooencyrtus kuvanae*. *Behavioral Ecology and Sociobiology* 65: 1071–107. <https://doi.org/10.1007/s00265-010-1114-x>
9. Truong XL, Cai WZ, Tomokuni M, Ishikawa T (2015) The assassin bug subfamily Harpactorinae (Hemiptera: Reduviidae) from Vietnam: an annotated checklist of species. *Zootaxa*, ISSN: 1175-5326:101–116. <https://doi.org/10.11646/zootaxa.3931.1.7>

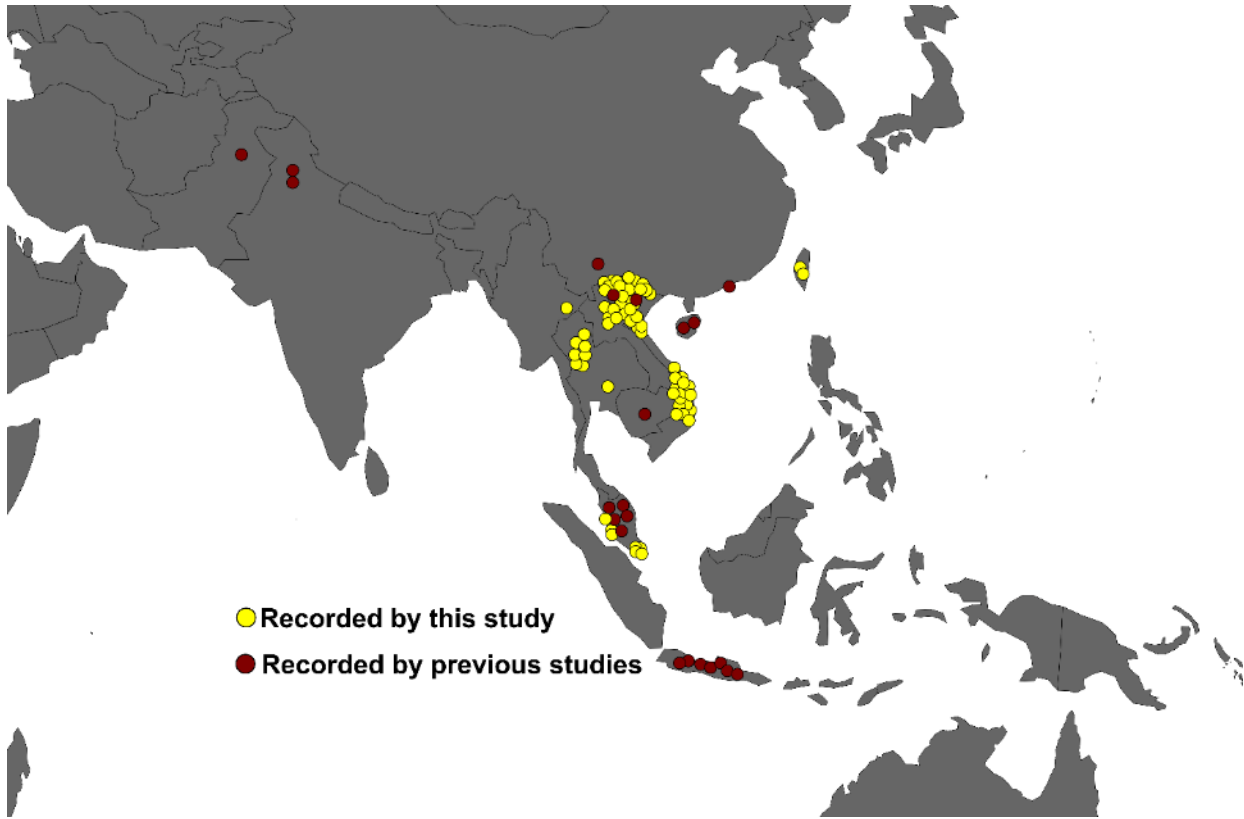
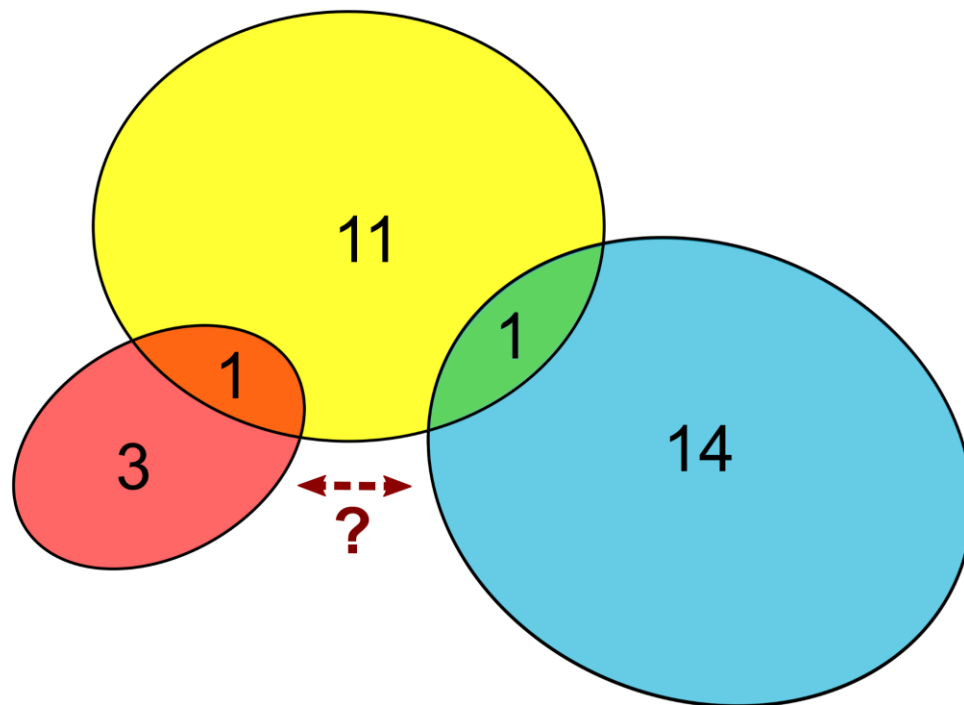


Figure 7.1. Distribution of *Biasticus* in Oriental realm.



- Northern Vietnam and Northern Laos (Temperate climate)
- Middle and Southern Vietnam (Tropical climate)
- Northern Thailand (Tropical savannah climate)

Figure 7.2. Number of *Biasticus* species in three main climatic regions of Indochina.